Universidad de Valladolid

FACULTAD DE CIENCIAS

DEPARTAMENTO DE QUIMICA FISICA Y QUIMICA INORGANICA

TESIS DOCTORAL:

FUNCIONALIZACIÓN DE COMPLEJOS DE METALES DE TRANSICIÓN CON LIGANDOS POLIAROMÁTICOS NO PLANOS Y OTROS GRUPOS

Presentada por Luis Ángel García Escudero
para optar al grado de
doctor por la Universidad de Valladolid

Dirigida por:
Dr. Daniel Miguel San José
Dr. Celedonio Manuel Álvarez González

Esta Memoria se presenta para su consideración como Tesis Doctoral como compendio de publicaciones. La normativa de la Universidad de Valladolid, establece lo siguiente:

> *REQUISITOS PARA LA PRESENTACIÓN DE TESIS DOCTORALES COMO COMPENDIO DE PUBLICACIONES (PhD Thesis by compendium of research publications)*
> *1. Las tesis doctorales presentadas como compendio de publicaciones deberán contener:*
> *a) Una síntesis general de al menos veinte páginas, donde se justifique la unidad temática de los trabajos y se presenten los objetivos perseguidos, la metodología empleada, los resultados obtenidos y su discusión, y las conclusiones alcanzadas.*
> *b) Una copia completa de las publicaciones, con el nombre y filiación de todos los autores y la referencia completa de la publicación.*
> *2. Deberá adjuntarse por escrito la conformidad de los coautores a la presentación de los trabajos como parte de la tesis y su renuncia a que formen parte de otra tesis doctoral.*
> *3. Los trabajos que se presenten como parte de la tesis doctoral consistirán en tres artículos en revistas científicas con factor de impacto, de los cuales al menos dos estarán publicados o aceptados, lo que deberá documentarse. Los artículos en periodo de revisión podrán formar parte de la tesis como documentación complementaria a los artículos publicados o aceptados.*
> *4. Los trabajos que formen parte de la tesis estarán publicados o aceptados para la publicación con posterioridad al inicio de los estudios de Doctorado.*

De acuerdo con la normativa, en la presente memoria se incluyen cinco artículos, dos de los cuales, en el momento de la presentación de la Memoria ante la Comisión de Doctorado, han sido aceptados y publicados:

Artículo I.- **η^6-Hexahelicene Complexes of Iridium and Ruthenium. Running along the Helix.**
Publicado en *Inorganic Chemistry* DOI: 10.1021/ic300462z

Artículo V.- **Beyond click chemistry: spontaneous C-triazolyl transfer from copper to rhenium and transformation into mesoionic C-triazolylidene carbene.**
Publicado en *Chemical Communications*, 2012, **48**, 7209-7211

Además, se ha enviado:

Artículo III.- **How Metals Can Induce the Right Geometry as Hosts for Fullerenes.**
Enviado a *Journal of the American Chemical Society*, con fecha 17 de julio de 2012.

Se incluyen además otros dos artículos que serán enviados en fechas próximas:

Artículo II.- **Assembling Nonplanar Polyaromatic Units by Click Chemistry. Study of Multicorannulene Systems as Host for Fullerenes.**
Para ser enviado a *Organic Letters*

Artículo IV.- **Schiff plus Click: One-pot Preparation of Triazole- Substituted Iminopyridines and Ring Opening of the Triazole Ring.**
Para ser enviado a *Dalton Transactions*

Por último, se incluye como anexo, o material suplementario, el artículo:

Artículo VI.- **Carbonyl complexes of manganese, rhenium and molybdenum with ethynyliminopyridine ligands.**
Publicado en *Journal of Organometallic Chemistry*, 2006, **691**, 3434-3444.
que fue realizado por el autor antes de comenzar los estudios de doctorado y que contiene la síntesis de algunos complejos que se utilizan como sustratos de partida.

Índice

SÍNTESIS GENERAL

El núcleo de esta memoria que se presenta como compendio de publicaciones es la funcionalización de compuestos poliaromáticos no planos orientada fundamentalmente a la preparación de derivados con complejos de metales de transición. Dichos trabajos se presentan en el Capitulo 1 de esta tesis y se dividen en tres subapartados que corresponden a cada una de las publicaciones. En el primero de ellos (Artículo I) se describe la síntesis de una serie de complejos de rutenio e iridio coordinados η^6 a hexahelicenos. En el Artículo II se presenta el estudio como receptores de fulerenos de varios compuestos multicoranuleno sintetizados usando la reacción conocida como *click chemistry*, y en el Artículo III se sintetiza una novedosa familia de complejos planocuadrados de platino con ligandos poliarénicos con objeto de evaluar sus interacciones no covalentes con fulerenos. Todos estos estudios englobados bajo el título de "Funcionalización de compuestos poliarómaticos no planos" presentan el denominador común de describir la síntesis de derivados de coranuleno o heliceno. Ambos, son compuestos

poliarénicos con peculiares estructuras tridimensionales de las que derivan interesantes propiedades como más adelante detallaremos. En este contexto, el objetivo de nuestros estudios se ha enfocado principalmente en la evaluación de sus interacciones no covalentes con fulerenos.

Paralelamente a estos estudios y englobado en el Capitulo 2 se profundizará en la reactividad que deriva del uso de la *click chemistry* en metales de transición con ligandos iminopiridina. Así, se presentan otras dos publicaciones (Artículos IV y V) donde se describe la preparación de una familia de compuestos que se obtienen de estas cicloadiciones 3+2 en derivados carbonílicos de renio, manganeso o molibdeno. Este segundo capítulo titulado "Funcionalización de complejos con ligandos iminopiridina mediante *click chemistry*", viene a completar los estudios de la reacción de cicloadición 3+2 de Huisgsen entre azidas metálicas y acetilenos previamente descritos en nuestro grupo de investigación.

En los epígrafes que siguen se presenta el estado del campo en cada uno de los capítulos que componen la tesis.

1. INTRODUCCIÓN

1.1. Funcionalización de compuestos poliaromáticos no planos.

Dentro de la gran variedad de hidrocarburos policíclicos aromáticos (PAHs), también denominados poliarenos, cuya característica común es la presencia de anillos de benceno fusionados, se encuentran los compuestos poliaromáticos no planos. En éstos la fusión entre los anillos aromáticos se produce de tal modo que no permite mantener la planaridad en toda la molécula, adoptando una geometría tridimensional.

Dentro de esta familia de compuestos, los denominados helicenos presentan un interés especial. Los helicenos están formados por anillos aromáticos fusionados que adoptan una estructura general de forma helicoidal. En 1956 Newman y Lednicer publicaron la preparación del primer carboheliceno, al que denominaron hexaheliceno o [6]-heliceno haciendo referencia al número de anillos bencénicos que forman dicho compuesto (Figura 1).[1] Después de las relativamente tempranas primeras síntesis, basadas en reacciones fotoquímicas,[2] no fue hasta la década de los 90 donde se produjo un avance significativo gracias a una nueva metodología basada en reacciones de tipo Diels-Alder[3], que permitió la preparación de una amplia variedad de helicenos a gran escala.[4]

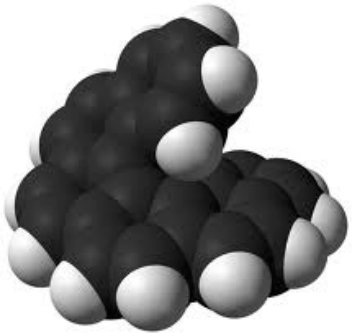

Figura 1. Hexaheliceno

(1) M. S. Newman, D. Lednicer *J. Am. Chem. Soc.* **1956**, *78*, 4765.
(2) R. H. Martin *Angew. Chem., Int. Ed. Engl.* **1974**, *13*, 649.
(3) L. B. Liu, T. J. Katz Tetrahedron Lett. **1990**, *31*, 3983.
(4) (a) N. D. Willmore, D. A. Hoic, T. J. Katz *J. Org. Chem.* **1994**, *59*, 1889. (b) T. J. Katz, L. B. Liu, N. D. Willmore, J. M. Fox, A. L. Rheingold, S. H. Shi, C. Nuckolls, B. H. Rickman *J. Am. Chem. Soc.* **1997**, *119*, 10054. (c) J. M. Fox, N. R. Goldberg, T. J. Katz *J. Org. Chem.* **1998**, *63*, 7456. (d) M. C. Carreño, R. Hernández-Sánchez, J. Mahugo, A. Urbano *J. Org. Chem.* **1999**, *64*, 1387. (e) C. Nuckolls, T. J. Katz, G. Katz, P. J. Collings, L. Castellanos *J. Am. Chem. Soc.* **1999**, *121*, 79. (f) S. D. Dreher, K. Paruch, T. J. Katz *J. Org. Chem.* **2000**, *65*, 806. (g) K. Paruch, T. J. Katz, C. Incarvito, K. C. Lam, B. Rhatigan, A. L. Rheingold *J. Org. Chem.* **2000**, *65*, 7602. (h) K. Paruch, L. Vyklicky, D. Z. Wang, T. J. Katz, C. Incarvito, L. Zakharov, A. L. Rheingold *J. Org. Chem.* **2003**, *68*, 8539.

Estos exóticos compuestos poseen relevantes propiedades ópticas[5] y electrónicas[6]. Quizás, la más llamativa de sus características sea que se trata de compuestos quirales. Aunque no presentan centros estereogénicos sí que poseen un eje quiral y así, dependiendo del sentido del giro que describen estos compuestos alrededor de este eje, podemos hablar de enantiomero M (minus) o P (plus).[7] Los helicenos, además, son compuestos con buenas propiedades como π-dadores y se ha publicado la formación de complejos de transferencia de carga con los π-aceptores apropiados.[8] En este sentido, las interacciones π-π pueden condicionar de forma relevante sus propiedades[9] siendo relativamente común la formación de aductos supramoleculares por procesos de autoensamblaje.[10] Todas estas características hacen de los helicenos compuestos que han sido utilizados como cristales líquidos, sensores o en campos tan diversos como síntesis asimétrica, reconocimiento molecular o en otras muchas áreas de la ciencia de los materiales.[11]

Como ya hemos mencionado el objeto de estudio de la primera publicación de esta memoria es la coordinación η^6 de metales de transición a helicenos. Hasta ahora, la incorporación de metales de transición a helicenos estaba únicamente reducida a la coordinación sobre heterohelicenos, fundamentalmente azahelicenos,[12] mientras que la coordinación en helicenos puramente

(5) (a) T. J. Wigglesworth, D. Sud, T. B. Norsten, V. S. Lekhi, N. R. Branda *J. Am. Chem. Soc.* **2005**, *127*, 7272. (b) E. Botek, B. Champane, M. Turki, J. M. André *J. Chem. Phys.* **2004**, *120*, 2042. (c) C. Nuckolls, T. J. Katz, T. Verbiest, S. Van Elshotch, H. G. Kuball, S. Kiesewalter, A. J. Lovinger, A. Persoons *J. Am. Chem. Soc.* **1998**, *120*, 8656.

(6) (a) F. Furche, R. Ahlrichs, C. Wachsmann, E. Weber, A. Sobanski, F. Vögtle, S. Grimme *J. Am. Chem. Soc.* **2000**, *122*, 1717. (b) G. Treboux, P. Lapstun, Z. Wu, K. Silverbrook *Chem. Phys. Lett.* **1999**, 301, 493. (c) D. Beljonne, Z. Shuai, J. L. Brédas, M. Kauranen, T. Verbiest, A. Persoons *J. Chem. Phys.* **1998**, *108*, 1301.

(7) D. B. Amabilino "*Chirality at the Nanoscale"*, Wiley-VCH: Weinheim, Germany, 2009.

(8) (a) O. Ermer, J. Neudörfl *Helv. Chim. Acta* **2001**, *84*, 1268. (b) J. M. Brown, I. P. Field, P. J. Sidebottom *Tetrahedron Lett.* **1981**, *22*, 4867. (c) F. Mikes, G. Boshart, E. Gilav *J. Chem. Soc., Chem. Commun.* **1976**, 99.

(9) (a) B. Busson, M. Kauranen, C. Nuckolls, T. J. Katz, A. Persoons *Phys. Rev. Lett.* **2000**, *84*, 79. (b) T. Verbiest, S. Van Elshocht, M. Kauranen, L. Hellemans, J. Snauwaert, C. Nuckolls, T. J. Katz, A. Persoons *Science* **1998**, *282*, 913.

(10) (a) R. Amemiya, M. Yamaguchi *Chem. Rec.* **2008**, *8*, 116. (b) R. Amemiya, M. Yamaguchi, *Org. Biomol. Chem.* **2008**, *6*, 26.

(11) Y. Shen, C.-F. Chen, *Chem. Rev.* **2012**, 112, 1463.

(12) (a) E. Anger, M. Rudolph, C. Shen, N. Vanthuyne, L. Toupet, C. Roussel, J. Autschbach, J. Crassous, R. Réau *J. Am. Chem. Soc.* **2011**, *133*, 3800. (b) S. Graule, M. Rudolph, W. T. Shen, J. A. G. Williams, C. Lescop, J. Autschbach, J. Crassous, R. Reau *Chem. Eur. J.* **2010**, *16*, 5976. (c) L. Norel, M. Rudolph, N. Vanthuyne, J. A. G. Williams, C. Lescop, C. Roussel, J. Autschbach, J. Crassous, R. Reau *Angew. Chem., Int. Ed.* **2010**, *49*, 99. (d) S. Graule, M. Rudolph, N. Vanthuyne,; J. Autschbach, C. Roussel, J. Crassous, R. Reau, *J. Am. Chem. Soc.* **2009**, *131*, 3183. (e) F. Aloui, B. B. Hassine, *Tetrahedron Lett.* **2009**, *50*, 4321. (f) M. H. Garcia, P. Florindo, M. D. M. Piedade, S. Maiorana, Licandro, E. *Polyhedron* **2009**, *28*, 621. (g) W. T. Shen, S. Graule, J. Crassous, C. Lescop, H. Gornitzka, R. Reau *Chem. Commun.* **2008**, 850. (h) R. El Abed, F. Aloui,; J. P. Genet, B. Ben Hassine, A. Marinetti *J. Organomet. Chem.* **2007**, *692*, 1156.

carboaromáticos sólo había sido descrita en unos pocos derivados que presentan grupos ciclopentadienilo (Cp) en los extremos del heliceno.[13] En concreto, estos complejos presentan una coordinación η^5 sobre los anillos aniónicos Cp de los ciclopentadienilhelicenos. Es importante por tanto resaltar que la coordinación de metales de transición sobre helicenos carboaromáticos no sustituidos permanecía totalmente inexplorada.

Sin embargo, existen algunos antecedentes que describen la coordinación η^6 de fragmentos metálicos a compuestos poliaromáticos no planos. Se trata de una familia de complejos de rodio, rutenio e iridio enlazados a varios poliarenos geodésicos abiertos (Figura 2).[14]

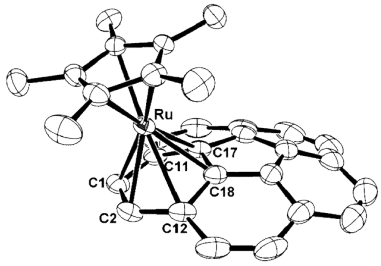

Figura 2. Ejemplo de coordinación η^6 sobre coranuleno.

Los poliarenos geodésicos constituyen otra variedad de compuestos poliaromáticos no planos cuyo interés ha crecido muy rápidamente y que se asemejan a las formas que presentan las obras del arquitecto americano Buckminster Fuller. Son estructuras curvadas cuya forma se parece a la que presenta la superficie de la tierra (de ahí el término geodésico). Los poliarenos geodésicos pueden ser cerrados o abiertos, haciendo notar con esto si las estructuras poliédricas generadas pueden considerarse tridimensionalmente completas, refiriéndonos en este caso a los cerrados; o si bien pueden considerarse incompletas, es decir, si pueden ser fragmentos constitutivos de las cerradas, refiriéndonos en este último caso a los poliarenos geodésicos abiertos.

(13) (a) A. Sudhakar, T. J. Katz, B. W. Yang *J. Am. Chem. Soc.* **1986**, *108*, 2790. (b) A. Sudhakar, T. J. Katz *J. Am. Chem. Soc.* **1986**, *108*, 179. (c) J. C. Dewan *Organometallics* **1983**, *2*, 83. (d) T. J. Katz, J. Pesti *J. Am. Chem. Soc.* **1982**, *104*, 346.

(14)(a) A. S. Filatov, M. A. Petrukhina *Coord. Chem. Rev.* **2010**, *254*, 2234. (b) M. A. Petrukhina *Angew. Chem. Int. Ed.* **2008**, *47*, 1550. (c) B. Zhu, A. Ellern, A. Sygula, R. Sygula, R. J. Angelici *Organometallics* **2007**, *26*, 1721. (d) J. S. Siegel, K. K. Baldridge, A. Linden, R. Dorta *J. Am. Chem. Soc.* **2006**, *128*, 10644. (e) P. A. Vecchi, C. M. Álvarez, A. Ellern, R. J. Angelici, A. Sygula, R. Sygula, P. W. Rabideau, *Organometallics* **2005**, *24*, 4543. (f) T. J. Seiders, K. K. Baldridge, J. M. O'Connor, J. S. Siegel *Chem. Commum.* **2004**, 950. (g) P. A. Vecchi, C. M. Álvarez, A. Ellern, R. J. Angelici, A. Sygula, R. Sygula, P. W. Rabideau *Angew. Chem. Int. Ed.* **2004**, *43*, 4497. (h) C. M. Álvarez, R. J. Angelici, A. Sygula, R. Sygula, P. W. Rabideau, *Organometallics* **2003**, *22*, 624. (i) T. J. Seiders, K. K. Baldridge, J. M. O'Connor, J. S. Siegel *J. Am. Chem. Soc.* **1997**, *119*, 4781.

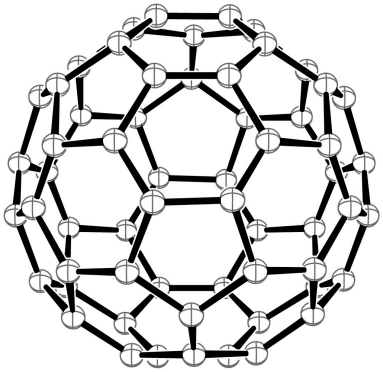

Figura 3. Fulereno o C_{60}.

El fulereno (C_{60}) es una de las formas alotrópicas elementales del carbono. Descubierta por Kroto, Curl y Smalley en 1985 a partir de sus estudios de nucleación de un plasma de carbono formado por la evaporación mediante láser de láminas de grafito.[15] Por este hallazgo consiguieron el premio Nobel de Química en 1996. Nombrada como molécula del año en 1991, ha tenido una creciente e innegable repercusión desde su descubrimiento e innumerables son las investigaciones que actualmente involucran a este compuesto.[16] El C_{60} está formado por 60 átomos de carbono, que se disponen formando pentágonos y hexágonos de forma alternativa, de manera que cada pentágono está rodeado de cinco anillos hexagonales. El fulereno fue el pionero de los poliarenos geodésicos cerrados y supuso el punto de partida para la investigación y el descubrimiento de todos sus congéneres mayores. Estas especies, denominadas también *buckyballs* por su forma de balón, poseen estructuras que aumentan en tamaño siguiendo el teorema de Euler[17] según este orden: C60, C70, C74, C76, C78, C80, C82, C84,...

Dentro de este tipo de estructuras es necesario mencionar a los nanotubos de carbono que, desde una visión simplificada, se consideran fulerenos alargados donde el número de átomos de carbono que constituyen la estructura aumenta de forma muy significativa. Dependiendo de la forma en la que se disponen los anillos bencénicos en la pared del nanotubo, éstos se pueden clasificar en: zig-zag, *armchair* o quirales. Además, dependiendo del número de capas que constituyen el nanotubo podemos hablar de SWNT (nanotubos de pared única) o de MWNT (nanotubos de pared múltiple).

(15) H. W. Kroto, J. R. Heath, S. C. O'Brian, R. F. Curl, R. E. Smalley *Nature* **1985**, *318*, 162.
(16) (a) R. F. Curl *Angew. Chem., Int. Ed. Engl.*, **1997**, *36*, 1566. (b) R. Kroto, *Angew. Chem., Int. Ed. Engl.,* **1997**, *36*, 1578-1593. (c) R. E. Smalley, *Angew. Chem., Int. Ed. Engl.,* **1997**, *36*, 1594-1603.
(17) La teoría de poliedros de Euler indica el número de caras, aristas y vértices permitidos para un poliedro convexo.

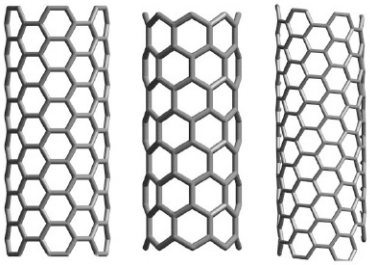

Figura 4. Representación de nanotubos de carbono con forma de zig-zag (izquierda), *armchair* (centro) y quiral (derecha).

Tanto fulerenos como nanotubos, embebidos de lleno en la nanociencia o ciencia de los materiales, poseen propiedades tan diversas y significativas que hacen de ellos candidatos óptimos para su uso en infinidad de aplicaciones.[18] Así, es importante mencionar que el fulereno C_{60} ha sido usado con éxito como aceptor de electrones en la construcción de sistemas fotosintéticos debido a sus destacadas propiedades fotofísicas, electroquímicas y químicas.[19] En este sentido la transferencia electrónica fotoinducida entre un dador y el C_{60} puede tener lugar a través de interacciones no covalentes. En los últimos años, son abundantes los estudios de formación de complejos supramoleculares con fulerenos, convirtiéndose en una de las áreas donde se han obtenido los avances más significativos.[20] La presencia de fragmentos aromáticos en la molécula receptora parece permitir asociarse al huésped (fulereno) de forma muy eficaz. Así, los compuestos poliaromáticos poseen una especial tendencia a asociarse formando estructuras supramoleculares gracias a interacciones no covalentes de apilamiento □ (□ *stacking*).

Las interacciones □-□ estudiadas muy habitualmente tanto en química, biología o ciencias de los materiales son interacciones no covalentes que aunque de carácter débil influyen de forma muy significativa en la estructura supramolecular que adquiere la molécula. Se cree que el fundamento de estas interacciones se debe al aumento de estabilidad que se genera entre moléculas vecinas gracias a la polarización que sufre la nube de densidad electrónica □ en este tipo de hidrocarburos aromáticos. Cuanto mayor es el número de átomos o grupos involucrados en la deslocalización de la nube electrónica, más favorable es esta

(18) M. Dresselhaus, G. Dresselhaus, P. Eklund "Science of Fullerenes and Carbon Nanotubes. Their Properties and Applications" Academic Press **1996**.
(19) (a) A. Hirsch "The Chemistry of Fullerenes" Thieme, New York **1994**. (b) F. Diederich, C. Thilgen, *Science* **1996**, *271*, 317. (c) A. Hirsch "Fullerenes and Related Structures", Topics in Current Chemistry, **1999** , vol. 199 , Springer, Berlin. (d) D. M. Guldi , N. Martín "Fullerenes: From Synthesis to Optoelectronic Properties", Kluwer Academic Publishers, Dordrecht, **2002**.
(20) N. Martin, J.-F. Nierengarten "Supramolecular Chemistry of Fullerenes and Carbon Nanotubes" Wiley-VCH, Weinheim **2012**.

estabilización por dispersión. En estos casos, la contribución de las fuerzas de van der Waals a la energía de estabilización intermolecular es mucho mayor que para los análogos que no poseen anillos aromáticos con deslocalización □. Pero además de ésta, existe una contribución electrostática a la estabilización intermolecular que es la que genera direccionalidad en el empaquetamiento. En esta memoria, se ha puesto un especial énfasis en el diseño de moléculas poliaromáticas susceptibles de actuar como receptores de fulerenos, focalizando nuestra atención en la preparación de compuestos que poseen fragmentos coranuleno.

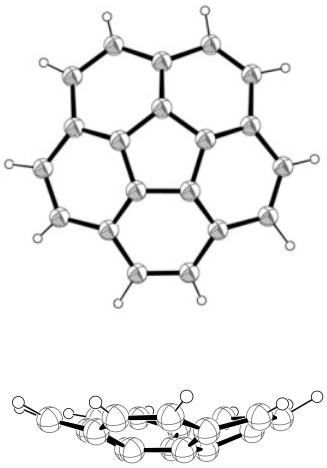

Figura 5. Coranuleno

El coranuleno o [5]-circuleno fue el primer poliareno sintetizado con forma geodésica. Este compuesto está constituido por cinco anillos hexagonales que rodean a un único anillo pentagonal. La forma tridimensional que presenta se debe a que el borde exterior está demasiado tensionado como para permitir que todos los anillos adopten una geometría totalmente plana. Para asumir esta tensión la molécula adopta forma de cuenco con una profundidad de 0.87 Å. Este tipo de compuestos, denominados *buckybowls* por su forma de cuenco, pueden presentar un interesante proceso dinámico de inversión en el que se interconvierten las caras cóncava y convexa. Esta inversión conocida como *bowl to bowl* es muy rápida en el caso del coranuleno. La energía necesaria para este proceso fue calculada para un derivado monosustituido de coranuleno, el coranulenildimetilcarbinol. El proceso de coalescencia de las señales de los metilos diasterotópicos de este compuesto permite estimar una barrera energética de ΔG = 10 kcal/mol. Sin embargo, para el derivado de coranuleno que posee un ciclopentadieno fusionado al coranuleno, es

decir, para el ciclopentadienilcoranuleno, este proceso está frenado a temperatura ambiente.[21]

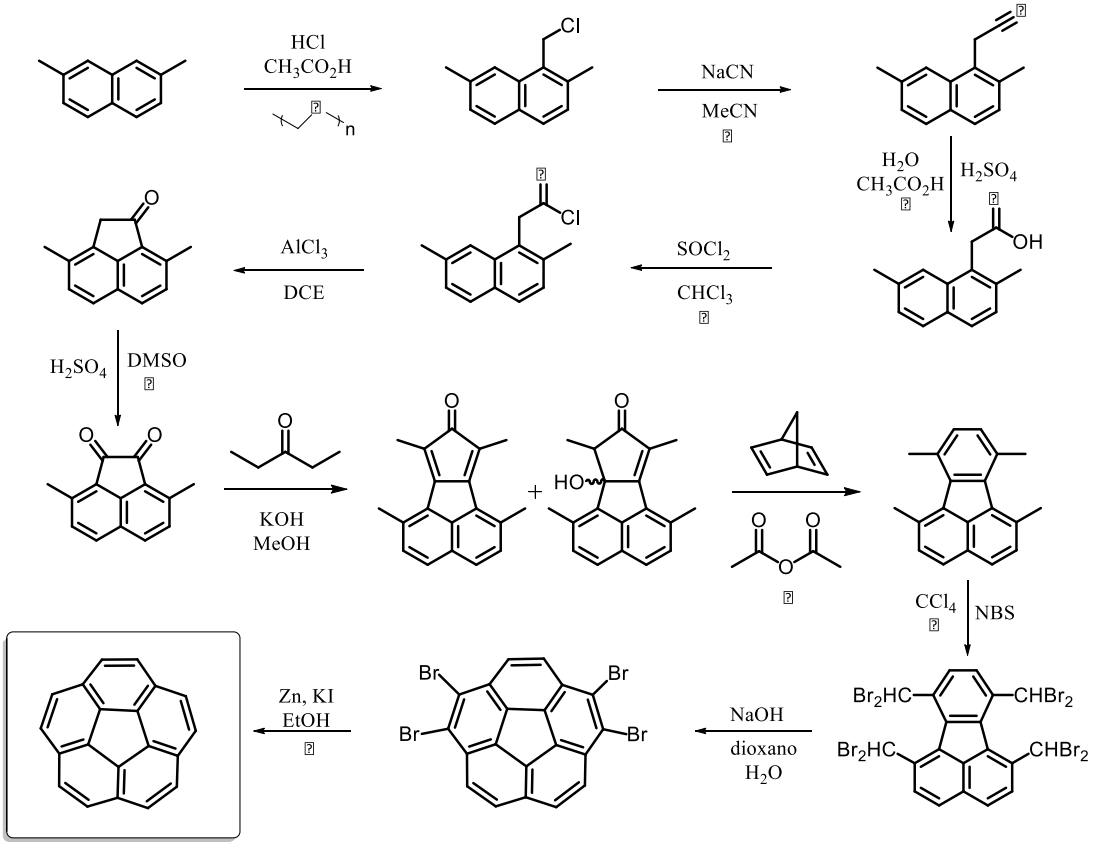

Esquema 1. Ruta desarrollada por Sygula *et al.* para la síntesis completa del coranuleno.

Richard Lawton publicó el descubrimiento del coranuleno en una comunicación en 1966, aunque debido a la gran complejidad sintética no pudo dar los detalles completos de la preparación hasta cinco años después.[22] Tras la primera preparación del coranuleno se desarrollaron varias metodologías sintéticas, todas ellas basadas en FVP (*Flash Vacuum Pyrolysis*),[23] con estos procedimientos que se realizan en fase gas a muy alta temperatura (~1000ºC), se consiguió mejorar el rendimiento global de su obtención. Además, los procedimientos basados en FVP sirvieron para obtener otra serie de *buckybowls* de mayor tamaño, incluyendo en ellos el fragmento $C_{30}H_{12}$ o "semibuckmisnterfulereno" e incluso el fulereno. Sin embargo, el avance más significativo se produjo en el año 2000 cuando Sygula *et al.*

(21) L. T. Scott, M. M. Hashemi, M. S. Bratcher. *J. Am. Chem. Soc.* **1992**, *114,* 1920.
(22) (a) W. E. Barth, R. G. Lawton *J. Am. Chem. Soc.* **1966**, *88*, 380. (b) W. E. Barth, R. G. Lawton *J. Am. Chem. Soc.* **1971**, *93*, 1730.
(23) V. M. Tsefrikas, L. T. Scott *Chem. Rev.* **2006,** *106*, 4868.

consiguieron obtener de forma casual 1,2,5,6-tetrabromocoranuleno con un 80% de rendimiento a partir de 1,6,7,10-tetrakis(dibromometilen)fluoranteno, penúltima etapa del esquema 1.[24] Para conseguir el cierre final tan sólo utilizó un reflujo de 15 minutos en presencia de pequeñas cantidades de NaOH utilizando como disolvente una mezcla de dioxano y agua. La síntesis completa consta de 11 pasos y se inicia partiendo del 2,7-dimetilnaftaleno y fue elegida por nosotros para la preparación del coranuleno, compuesto de partida que usaremos para la síntesis de muchos de los derivados que presentamos en esta memoria. Ésta y algunas otras posteriores metodologías supusieron un impulso definitivo para el desarrollo de la reactividad del coranuleno e incentivaron las esperanzas de conseguir una síntesis racional de otros poliarenos geodésicos de mayor tamaño incluyendo también entre ellos al fulereno o C_{60}.[25]

En el coranuleno, la densidad electrónica de sus dos caras (cóncava y convexa) es diferente, generándose por ello un momento dipolar global en la molécula.[26] Esta propiedad, junto a la especial estructura en forma de cuenco que se complementa de forma casi ideal con la superficie esférica del C_{60}, ha promovido durante años el interés de los investigadores en encontrar derivados de coranuleno que produzcan complejos supramoleculares por interacciones de tipo □-□ con fulerenos. Dicha asociación se ha demostrado insuficiente o apenas significativa en aquellos derivados que poseen una única unidad de coranuleno. Así, en la literatura encontramos una pequeña familia de compuestos monocoranuleno en los que se han observado, en general, moderadas constantes de asociación, calculadas mediante estudios de valoración por RMN de ^{1}H en tolueno-d^8.[27] Además de estos estudios en disolución, el grupo de Fasel ha publicado la deposición de moléculas de aductos coranuleno/C_{60} (1:1) sobre una superficie de Cu(110)[28] y muy recientemente se ha obtenido la estructura por Rayos X de la co-cristalización entre ambos compuestos (coranuleno y fulereno).[29] Muy probablemente hasta ahora la mayor evidencia que demostraba el enlace y por tanto la asociación cóncavo-convexa entre un derivado de coranuleno y fulereno se debía a los estudios

(24) (a) A. Sygula, P. W. Rabideau *J. Am. Chem. Soc.* **2000**, *122,* 6323. (b) G. Xu, A. Sygula, Z. Marcinow, P. W. Rabideau, *Tetrahedron Lett.* **2000**, *41*, 9931.
(25) Y.-T. Wu, J. S. Siegel *Chem. Rev.* **2006,** 106, 4843.
(26) L. T. Scott, M. M. Hashemi, M. S. Bratcher *J. Am. Chem. Soc.* **1992**, *114*, 1920.
(27) (a) S. Mizyed, P. E. Georghiou, M. Bancu, B. Cuadra, A. K. Rai, P. Cheng and L. T. Scott *J. Am. Chem. Soc.* **2001**, *123*, 12770. (b) P. E. Georghiou, A. H. Tran, S. Mizyed, M. Bancu, L. T. Scott *J. Org. Chem.* **2005**, *70*, 6158.
(28) W. Xiao, D. Passerone, P. Ruffieux, K. Ait-Mansour, O. Groning, E. Tosatti, J. S. Siegel, R. Fasel *J. Am. Chem. Soc.* **2008**, *130*, 4767.
(29) L. N. Dawe, T. A. AlHujran, H.-A. Tran, J. I. Mercer, E. J. Jackson, L. S. Scott, P. E. Georghiou *Chem. Commum.*, **2012**, 48, 5563.

realizados por Sygula *et al.*[30] En dicho trabajo se describe la síntesis de una pinza molecular constituida formalmente por dos unidades coranuleno. La cavidad formada en este compuesto es la óptima para acomodar una molécula huésped de C_{60} (Figura 6). Cabe mencionar que dicho aducto supramolecular posee la mayor constante de asociación calculada hasta la fecha para éste tipo de derivados.

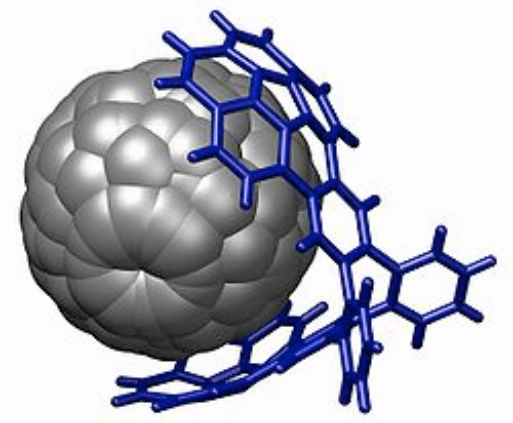

Figura 6. Estructura del aducto $C_{60}H_{28}\subset C_{60}$ descrito por el grupo de Sygula.

En las Artículos II y III de esta memoria se ha centrado la atención en el diseño y síntesis de arquitecturas moleculares que dispusieran como mínimo de dos fragmentos de coranuleno. En ellos se ha estudiado la formación de enlaces supramoleculares con fulerenos. En estos estudios se evalúa la acción sinérgica de dos o tres fragmentos coranuleno enlazados bien a través de cicloadiciones 3+2 (Artículo II) o bien a través de la geometría favorable que adoptan estas unidades en complejos planocuadrados de platino (Artículo III).

(30) A. Sygula, F. R. Fronczek, R. Sygula, P. W. Rabideau, M. M. Olmstead, *J. Am. Chem. Soc.* **2007**, *129*, 3842.

1.2. Funcionalización de complejos con ligandos iminopiridina mediante *Click Chemistry*.

La reacción de cicloadición 3+2 de Huisgen entre azidas orgánicas y alquinos ha generado una considerable atención en estos últimos años.[31] Esto se debe en gran medida a la introducción en dicha reacción de cobre(I) como catalizador. Así, en el año 2002 los grupos de Medal[32] y Sharpless[33] publicaron de manera independiente la formación regioselectiva de triazoles 1,4-disustituidos mediante catálisis con cobre con excelentes rendimientos. A partir de entonces esta metodología conocida como CuAAC (*Copper catalyzed azide–alkyne cycloaddition*) o denominada comúnmente como *Click Chemistry* ha sido exitosamente utilizada para la funcionalización de materiales en prácticamente todas las áreas de la química.[34]

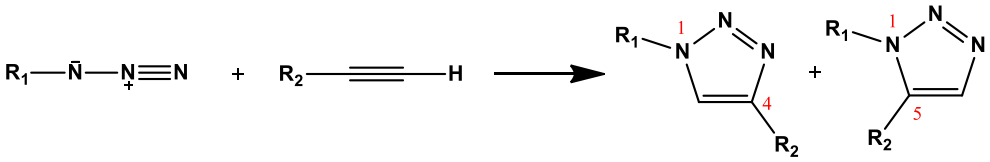

Esquema 2. Reacción de Huisguen entre azidas orgánicas y alquinos terminales.

Dicho procedimiento se ha usado para la preparación de una gran variedad de ligandos que contienen un anillo de triazol.[35] Este fragmento se puede coordinar al complejo metálico tanto por un átomo de nitrógeno como por un átomo de carbono. En este sentido mientras la utilización del ligando triazol como nitrógeno dador se ha detallado para una amplia familia de compuestos organometálicos, la coordinación como triazolilo, a través del carbono, apenas tiene unos pocos precedentes.[36] Dentro de este contexto en nuestro grupo de investigación se había

(31) (a) R. Huisgen *Pure Appl. Chem.* **1989**, *61*, 613. (b) R. Huisgen, G. Szeimies, L. Moebius, *Chem. Ber.* **1967**, *100*, 2494.
(32) C.W. Tornoe, C. Christensen, M. Meldal *J. Org. Chem.* **2002**, *67*, 3057.
(33) V. V. Rostovstsev, L. G. Green, V. V. Fokin, B. K. Sharpless *Angew. Chem., Int. Ed.* **2002**, *41*, 2596.
(34) Joerg Lahann "Click Chemistry for Biotechnology and Materials Science" John Wiley & Sons, **2009**.
(35) (a) H. Struthers, T. L. Mindt, R. Schibli *Dalton Trans.* **2010**, *39*, 675. (b) T. Romero, R. A. Orenes, A. Espinosa, A. Tárraga, P. Molina *Inorg. Chem.* **2011**, *50*, 8214. (c) G. F. Manbeck, W. W. Brennessel, C. M. Evans, R. Eisenberg *Inorg. Chem.* **2010**, *49*, 2834. (d) C. Cote, R. U. Kirss *Inorg. Chim. Acta* **2010**, *363*, 2520. (e) M. Obata, A. Kitamura, A. Mori, C. Kameyama, J. A. Czaplewska, R. Tanaka, I. Kinoshita, T. Kusumoto, H. Hashimoto, M. Harada, Y. Mikata, T. Funabiki, S. Yano *Dalton Trans.* **2008**, 3292. (f) H. Struthers, B. Spingler, T. L. Mindt, R. Schibli, *Chem.–Eur. J.* **2008**, *14*, 6173. (g) D. V. Partika, J. B. Updegraff III, M. Zeller, A. D. Hunter, T. D. Gray *Organometallics* **2007**, *26*, 183. (h) D. Urankan, B. Pinter, A. Pevec, F. De Proft, I. Turel, J. Kosmrlj *Inorg. Chem.* **2010**, *49*, 4820.
(36) (a) D. V. Partika, L. Gao, T. S. Teets, J. B. Updegraff III, N. Deligonul, T. G. Gray *Organometallics* **2009**, *28*, 6171. (b) E. M. Schuster, M. Botoshansky, M. Gandelman *Angew. Chem., Int. Ed.* **2008**, *47*, 4555. (c) E. M. Schuster, M. Botoshansky, M. Gandelman *Organometallics*, **2009**, *28*, 7001. (d) M.

sintetizado una serie de complejos organometálicos de manganeso con fragmentos triazol coordinados por el nitrógeno central.[37] Estos derivados se obtienen al hacer reaccionar a altas temperaturas (en reflujo de THF o DME) azidas metálicas y acetilenos activados con grupos extractores de carga (Esquema 3).

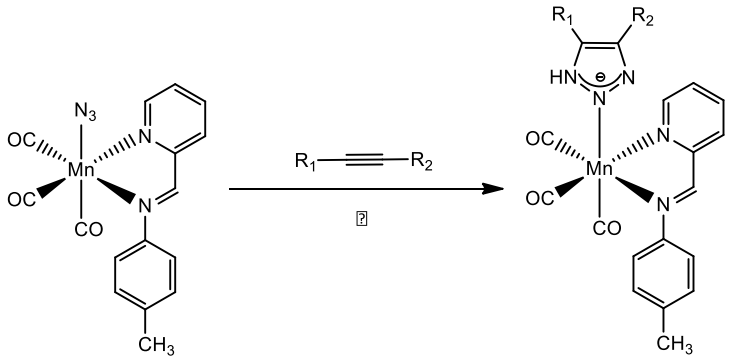

Esquema 3. Reacción de cicloadición entre azidas de manganeso y alquinos activados.

Además, en trabajos precedentes se había abordado la reactividad que deriva de la coordinación del ligando piridín-2-carboxaldehído (pyca) a centros metálicos,[38] estudiando de forma intensiva la formación de complejos de metales de transición con ligandos iminopiridina formados a partir de la reacción de condensación entre los pyca complejos y aminas primarias (reacción de Schiff) tal como se muestra en el esquema 4.[39] En tales estudios se ha conseguido condensar una extensa variedad de aminas primarias incluyendo la incorporación de diferentes moléculas biológicas como aminoácidos, aminoésteres, péptidos, dipéptidos y tripéptidos.[40] En este contexto y previamente a esta memoria ya habíamos descrito la preparación de una familia de complejos carbonílicos coordinados a ligandos iminopiridina que están funcionalizados con grupos alquino terminales.[41] El trabajo se adjunta a esta memoria como anexo (Artículo VI).

En este capítulo se pretende explorar la reactividad que deriva del uso de la *click chemistry* en la funcionalización de complejos carbonílicos de manganeso (I), renio (I) y molibdeno (II) con ligandos iminopiridina. Estos complejos con ligandos

Schuster, G. Nisnevich, M. Botoshansky, M. Gandelman, Organometallics **2009**, *28*, 5025. (e) C. Nolte, P. Mayer and B. F. Straub *Angew. Chem.,Int. Ed.* **2007**, *46*, 2101.

(37) Trabajos realizados por José Ángel Turiel Hernández en su tesis doctoral: "Síntesis y reactividad de complejos de manganeso, renio y molibdeno con ligandos iminopiridina".

(38) C. M. Álvarez, R. García-Rodríguez, D. Miguel *Dalton Trans.* **2007**, 3546.

(39) C. M. Álvarez, R. Carrillo, R. García-Rodríguez, D. Miguel *Chem. Commun.* **2011**, *47*, 12765.

(40) (a) R. García-Rodríguez, D. Miguel *Dalton Trans.* **2006**, 1218. (b) C. M. Álvarez, R. García-Rodríguez, D. Miguel *J. Organomet. Chem.* **2007**, *692*, 5717 (c) C. M. Álvarez, R. García-Rodríguez, D. Miguel *Inorg. Chem.* **2012**, *51,* 2984. (d)

(41) L. A. García-Escudero, D. Miguel, J. A. Turiel *J. Organomet. Chem.* **2006**, *691*, 3434.

iminopiridina que poseen restos azida o grupos alquino terminales son susceptibles de reaccionar con acetilenos o azidas orgánicas, respectivamente. En concreto se ha explorado el uso sucesivo de la reacción de Schiff y CuAAC como una metodología efectiva para la funcionalización de esta familia de complejos. De esta reactividad se deriva la preparación de algunos complejos inesperados con ligandos tridentados (N,N,N) o (N,N,C) coordinados por los dos nitrógenos dadores del ligando iminopiridina y por un átomo de nitrógeno o carbono del anillo de triazol.

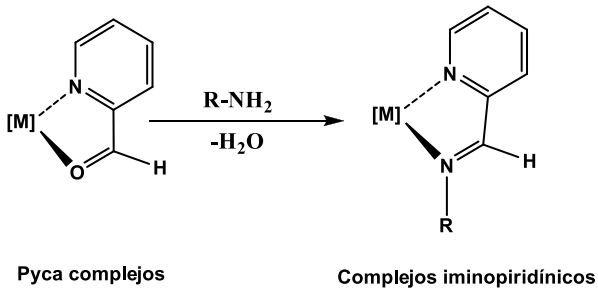

Esquema 4. Síntesis de complejos iminopiridínicos mediante la condensación de Shiff.

2. OBJETIVOS.

Objetivo general

Desarrollar una metodología sintética para funcionalizar complejos con grupos poliaromáticos no planos.

Durante el desarrollo del trabajo, y en línea con el objetivo general, se han ido concretando diversos

Objetivos específicos

1. Poner a punto un procedimiento sintético que permita incorporar fragmentos metálicos a helicenos.

2. Encontrar una arquitectura molecular con la geometría adecuada para poder formar aductos supramoleculares con fulerenos. En concreto, diseñar y preparar compuestos con ligandos poliaromáticos no planos susceptibles de actuar como eficientes receptores de fulerenos. Enfocar el diseño en la síntesis de derivados que posean varios fragmentos coranuleno con objeto de evaluar la sinergia de estas unidades.

3. Evaluar el uso de la reacción denominada *click chemistry* como un adecuado procedimiento para funcionalizar compuestos susceptibles de ser utilizados como receptores de fulerenos.

4. Expandir el uso de la *click chemistry* para la funcionalización de complejos organometálicos con ligandos iminopiridina que posean una cadena lateral con grupos azida o acetileno.

3. METODOLOGÍA EMPLEADA

3.1. Metodología sintética.

Gran parte de las reacciones que se describen en esta memoria han sido efectuadas en atmósfera de nitrógeno siguiendo las técnicas convencionales de Schlenk. Además, los disolventes se han purificado de acuerdo con los procedimientos convencionales.[42] La gran mayoría de los reactivos, salvo que se indique lo contrario, fueron adquiridos de fuentes comerciales y utilizados sin posterior purificación.

Síntesis de precursores.

Algunos de los compuestos de partida han sido preparados siguiendo procedimientos descritos en la bibliografía. Muchos de los precursores poliaromáticos tuvieron que ser sintetizados. Los compuestos hexaheliceno[43], 2,15-dimetilhexaheliceno[44] y 2,15-dibromohexaheliceno[45] se prepararon a través de procedimientos de fotociclación. El coranuleno se sintetizó siguiendo la metodología descrita por el grupo de Sygula y previamente mencionada en la introducción.[24] Mediante reacciones de bromación se prepararon los compuestos (bromometil)-coranuleno[46] (partiendo de metilcoranuleno)[47] y 9-bromoheptaheliceno.[48] Además, el (trimetilsililetinil)coranuleno se preparó mediante una secuencia sintética de dos pasos que transcurre a través del bromocoranuleno.[49] Siguiendo una metodología análoga a la síntesis del 1-(trimetilsililetinil)pireno[50] (mediante reacciones de acoplamiento C-C tipo Sonogashira) se obtuvieron los derivados [(trimetilsililetinil)-metil]coranuleno y 9-(trimetilsililetinil)-[7]-heliceno. Todos los derivados alquílicos de azida (α,α,α-tris(azidometil)etano,[51] 2,15-bis(azidometil)hexaheliceno, 1,3,5-tris-

(42) D. D. Perrin, W. L. F. Armarego, *Purification of Laboratory Chemicals*; 3rd ed.; Pergamon Press: Oxford, **1988**.
(43) (a) F. B.Mallory, C. W. Mallory "*Photocyclation of stilbenes and related molecules" Organic Reactions* Hoboken, NJ, United States, **1984**, 30. (b) D. A. Lightner, D. T. Hefelfinger, T. W. Powers, G. W. Frank, K. N. Trueblood *J. Am. Chem. Soc.* **1972**, *94*, 3492.
(44) (a) M. Sato, K. Yamamoto, H. Sonobe, K. Yano,; H. Matsubara, H. Fujita, T. Sugimoto, K. Yamamoto *J. Chem. Soc., Perkin Trans. 2* **1998**, 1909. (b) K. Yamamoto, H. Sonobe, H. Matsubara, M. Sato, S. Okamoto, K. Kitaura *Angew. Chem. Int. Ed.* **1996**, *35*, 69.
(45) (a) K. Yamamoto, T. Ikeda, T. Kitsudi, Y. Okamoto, H. Chikamatsu, M. Nakazaki *J. Chem. Soc., Perkin Trans. 1* **1990**, 271.
(46) M. C. Stuparu *Tetrahedron* **2012**, *68*, 3527.
(47) T. J. Seiders, E. L. Elliott, G. H. Grube, J. S. Siegel *J. Am. Chem. Soc.* **1999**, *34*, 7804.
(48) A. Sudhakar, T. J. Katz *Tetrahedron Lett.* **1986**, *20*, 2231.
(49) (a) J. Mack, P. Vogel, D. Jones, N. Kaval, A. Sutton *Org. Biomol. Chem.* **2007**, *5*, 2448. (b) C. S. Jones, E. Elliott, J. S. Siegel *Synlett*, **2004**, *1*, 187.
(50) H. Maeda, T. Maeda, K. Mizuno,; K. Fujimoto, H. Shimizu, M. Inouye *Chem. Eur. J.* **2006**, *12*, 824.
(51) L. Beaufort, L. Delaude, A. F.Noels *Tetrahedron* **2007**, *63*, 7003.

(azidometilbenceno),[52] benzilazida,[53] p-toluensulfonilazida,[54] hexadecilazida,[55] 1,6-diazidohexano[56] y 3-aminopropilazida)[57] se prepararon siguiendo una metodología similar. Por otro lado los complejos *fac*-[ReBr(CO)$_3$(pyca)],[38] *fac*-[MnBr(CO)$_3$(pyca)],[38] [MoCl(η^3-C$_3$H$_4$Me-2)(CO)$_2$(pyca)],[38] *fac*-[ReBr(CO)$_3${py-2-CH=N-C$_6$H$_4$-m-(C≡CH)}],[41] *fac*-[ReBr(CO)$_3${py-2-CH=N-C$_6$H$_4$-p-(C≡CH)}],[41] *fac*-[MnBr(CO)$_3${py-2-CH=N-C$_6$H$_4$-m-(C≡CH)}][41] y [MoCl(η^3-C$_3$H$_4$Me-2)(CO)$_2${py-2-CH=N-C$_6$H$_4$-m-(C≡CH)}][41] han sido sintetizados siguiendo los procedimientos descritos en la bibliografía.

Métodos de funcionalización.

En este sentido, la metodología conocida como *click chemistry* es el procedimiento más comúnmente usado para la síntesis de gran parte de los derivados que se presentan en esta memoria. Como ya hemos mencionado en la introducción este procedimiento presenta un amplio abanico de ventajas. Así, se trata de un reacción general, muy robusta, regioselectiva y en la mayoría de los casos virtualmente cuantitativa. Además, dado que es insensible a la presencia de la gran mayoría de grupos funcionales posee las características óptimas para utilizarse en una gran variedad de secuencias ortogonales.

Cabe reseñar además que la metodología sintética usada para coordinar de forma η^6 los fragmentos metálicos a los ligandos heliceno es un procedimiento análogo al descrito en la bibliografía para la incorporación de fragmentos metálicos de iridio al coranuleno, donde se utiliza un disolvente polar poco coordinante como el nitrometano para favorecer este tipo de coordinación.[14h]

3.2. Caracterización.

La metodología empleada para la caracterización de los compuestos que se describen en esta memoria implica la utilización de una gran variedad de técnicas instrumentales que se describe a continuación.

Espectroscopia de infrarrojo.

El seguimiento de la reacción para aquellos complejos que poseen ligandos carbonilo se ha llevado a cabo mediante espectroscopia infrarroja en disolución, mediante la observación de las bandas de tensión CO. Los espectros de IR se han

(52) A. Granzhan, C. Schowey, T. Riis-Johannessen, R. Scopelliti, K. Severin *J. Am. Chem. Soc.* **2011**, *133*, 7106.
(53) H. Zheng, R. McDonald, D. G. Hall, *Chem. Eur. J.* **2010**, *16*, 5454.
(54) M. P.Cassidy, J. Rauschel, V. V. Fokin *Angew. Chem. Int. Ed.* **2006**, *45*, 3154.
(55) M. Lamani, K. R. Prabhu *Angew. Chem. Int. Ed.* **2010**, *49*, 6622.
(56) C. Romuald, E. Busseron, F. Coutrot *J. Org. Chem.* **2010**, *75*, 6516.
(57) V. Novakova, P. Zimcik, M. Miletin, K. Kopecky, J. Ivincova *Tetrahedron Lett.* **2010**, *51*, 1016.

registrado en un aparato Perkin-Elmer RX I FT-IR con una resolución de 4 cm^{-1}. Para los espectros en disolución se ha utilizado una celda de CaF_2 de 0.1 mm de espesor.

Espectroscopia de resonancia magnética nuclear.

Los espectros de resonancia magnética nuclear (RMN) se han registrado en instrumentos Bruker AC-300, ARX-300, AV-400, Varian MR 400 ó Varian VNMRS 500 empleando en todos los casos la señal del deuterio para el mantenimiento y homogeneidad del campo. Los valores de los desplazamientos químicos (δ) se expresan en partes por millón (ppm) siendo valores positivos los que indican desplazamientos a frecuencias más altas o campos más bajos. Las constantes de acoplamiento (j) se expresan en hercios (Hz). Todos los espectros de ^{1}H y $^{13}C\{^{1}H\}$ RMN están referidos a la señal del TMS, utilizándose como referencia una disolución acuosa al 85% de H_3PO_4 para los espectros de $^{31}P\ \{^{1}H\}$ RMN.

Análisis elemental de C, H y N.

Los análisis elementales de C, H y N se han realizados en un microanalizador Perkin Elmer 2400B del área de Química Inorgánica de la Universidad de Valladolid.

Difracción de rayos X.

Para la determinación estructural por difracción de rayos X, los monocristales se han medido en un difractómetro Bruker AXS SMART 1000, o bien Oxford Diffraction Super Nova, provistos de detector CCD, usando radiación Mo-Kα monocromada mediante un cristal de grafito. Los datos se han integrado con el programa SAINT,[58] o CrysAlisPro[59] y para la resolución de las estructuras se ha usado SHELXTL[60] o SIR2002[61] bajo WINGX.[62] En general se ha aplicado una corrección de absorción semi-empírica con el programa SADABS,[63] y en algunos casos se ha usado una corrección analítica mediante indexación de caras, con el

(58) *SAINT+*. SAX area detector integration program. Version 6.02. Bruker AXS, Inc. Madison, WI, **1999**.
(59) CrysAlisPro-Data collection and integration software. Oxford Diffraction Ltd. **2009**.
(60) G. M. Sheldrick *Acta Cryst.* **2008**, *A64,* 112. SHELXTL, An integrated system for solving, refining, and displaying crystal structures from diffraction data. Version 5.1. Bruker AXS, Inc. Madison, WI, **1998**.
(61) M. C.Burla, M. Camalli, B. Carrozzini, G. L. Cascarano, C. Giacovazzo, G. Polidory, R. Spagna, *SIR2002, A program for automatic solution and refinement of crystal structures. J. Appl. Cryst.* **2003**, *36*, 1103.
(62) L. J. Farrugia *J. Appl. Cryst.*, **1999**, *32*, 837.
(63) G. M. Sheldrick; *SADABS*, Empirical Absorption Correction Program. University of Göttingen, Germany, **1997**.

programa CrysAlisPro. Los cálculos de parámetros geométricos se han hecho con SHELXTL y PARST [64] y los gráficos se han hecho con SHELXTL y Mercury. [65]

Espectrometría de masas (EM).

Los análisis de masas se realizaron mediante la técnica de MALDI-TOF. La relación masa carga se expresa como *m/z*.

Cálculos computacionales.

Los cálculos teóricos recogidos en esta memoria han sido realizados por Héctor Barbero y por los doctores Jose Martín y Victor Rayón mediante los programas GAUSSIAN 09 y ADF 2010.

En el artículo I las estructuras se optimizaron con el programa GAUSSIAN 09[66] usando el funcional B3LYP.[67] Se utilizaron las funciones de base SVP (con funciones de polarización añadidas) para los átomos C, H y Br,[68] mientras que para el Ir se usó SDD con los correspondientes pseudo-potenciales incluyendo efectos relativistas.[69] Tanto los mínimos como los estados de transición encontrados fueron confirmados por análisis vibracional. Se consideraron los efectos del disolvente mediante cálculos puntuales sobre las estructuras optimizadas en fase gas usando el algoritmo PCM con nitrometano (ε = 36.562).

En el artículo II se utilizó la misma metodología que para el artículo I, usando las funciones de base 6-31G(d,p) para los átomos de C, H y N.

Para el artículo III, los cálculos teóricos se realizaron usando el nivel de teoría BLYP/TZP incluyendo correcciones de dispersión de Grimme DFT-D3,[70] implementado en ADF 2010.[71] Los efectos relativistas han sido incluidos usando el

(64) (a) M. Nardelli, *Comput. Chem.,* **1983**, 7, 95. (b) M. Nardelli, *J. Appl. Crystallogr.*, **1995**, *28*, 659.
(65) MERCURY: (a) I. J. Bruno, J. C. Cole, P. R. Edgington, M. K. Kessler, C. F. Macrae, P. McCabe, J. Pearson, R. Taylor *Acta Crystallogr.* **2002**, *B58*, 389. (b) C. F. Macrae, P. R. Edgington, P. McCabe, E. Pidcock, G. P. Shields, R. Taylor, M. Towler, J. van de Streek *J. Appl. Crystallogr.*, **2006**, *39*, 453.
(66) *Gaussian 09, Revision A.1*, M. J. Frisch, G. W. Trucks, H. B. Schlegel, G. E. Scuseria, M. A. Robb, J. R. Cheeseman, G. Scalmani, V. Barone, B. Mennucci, G. A. Petersson, H. Nakatsuji, M. Caricato, X. Li, H. P. Hratchian, A. F. Izmaylov, J. Bloino, G. Zheng, J. L. Sonnenberg, M. Hada, M. Ehara, K. Toyota, R. Fukuda, J. Hasegawa, M. Ishida, T. Nakajima, Y. Honda, O. Kitao, H. Nakai, T. Vreven, J. A. Montgomery Jr., J. E. Peralta, F. Ogliaro, M. Bearpark, J. J. Heyd, E. Brothers, K. N. Kudin, V. N. Staroverov, R. Kobayashi, J. Normand, K. Raghavachari, A. Rendell, J. C. Burant, S. S. Iyengar, J. Tomasi, M. Cossi, N. Rega, N. J. Millam, M. Klene, J. E. Knox, J. B. Cross, V. Bakken, C. Adamo, J. Jaramillo, R. Gomperts, R. E. Stratmann, O. Yazyev, A. J. Austin, R. Cammi, C. Pomelli, J. W. Ochterski, R. L. Martin, K. Morokuma, V. G. Zakrzewski, G. A. Voth, P. Salvador, J. J. Dannenberg, S. Dapprich, A. D. Daniels, Ö. Farkas, J. B. Foresman, J. V. Ortiz, J. Cioslowski, D. J. Fox *Gaussian, Inc.*, Wallingford CT, **2009**.
(67) (a) A. D. Becke *J. Chem. Phys.* **1993**, *98*, 5648. (b) C. Lee, W. Yang, R. G. Parr *Phys. Rev. B* **1988**, *37*, 785.
(68) A. Schaefer, H. Horn, R. Ahlrichs *J. Chem. Phys.* **1992**, *97*, 2571.
(69) D. Andrae, U. Haeussermann, M. Dolg, H. Stoll *Preuss, Theor. Chem. Acc.* **1990**, *77*, 123.
(70) S. Grimme, J. Anthony, S. Ehrlich, H. Krieg *J. Chem. Phys.* **2010**, *132*, 154104.
(71) ADF2010.02, Theoretical Chemistry, Vrije Universiteit, SCM, Amsterdam, The Netherlands; http://www.scm.com.

formalismo de ZORA.[72] Los gradientes han sido suavizados y convergen a 0.01 Hartree/angstrom. El análisis de la descomposición de la energía (EDA) se realizó al mismo nivel de teoría.

3.3. Evaluación de propiedades.

Estudios de complejación con fulerenos.

El estudio de las interacciones supramoleculares con fulerenos que se describen en esta memoria se basan en la utilización de la técnica de RMN de ^{1}H.

La metodología utilizada para la determinación de la estequiometria supramolecular se fundamenta en un método de variaciones continuas desarrollado por P. Job y comúnmente conocido como *Job plot*.[73]

Además, la determinación de las constantes de asociación supramolecular entre receptor y huésped se basa en métodos de ajuste no lineal para datos obtenidos a través de experimentos de valoraciones por RMN de ^{1}H.[74] El cálculo de dichas constantes se ha realizado a través de una hoja de cálculo de libre acceso desarrollada por el Prof. J. M. Sanderson y que se encuentra disponible en la dirección: http://www.dur.ac.uk/j.m.sanderson/science/downloads.html.

(72) ver: E. van Lenthe, A. E. Ehlers, E. J. Baerends *J. Chem. Phys*. **1999**, *110*, 8943. y referencias internas.
(73) L. Fielding *Tetrahedron* **2000**, *56*, 6151.
(74) P. Job *Ann. Chim.* **1928**, *9*, 113.

4. RESUMEN DE LOS RESULTADOS OBTENIDOS.

4.1. Funcionalización de compuestos poliaromáticos no planos.

Artículo I.

η^6-Hexahelicene Complexes of Iridium and Ruthenium. Running along the Helix.

En este artículo se describe la preparación y caracterización estructural de una familia de complejos de iridio y rutenio coordinados η^6 a hexahelicenos. La reacción de hexaheliceno (**1**), 2,15-dimetilhexaheliceno (**2**) o 2,15-dibromo-hexaheliceno (**3**) con $[Cp^*IrCl_2]_2$ y $AgBF_4$ utilizando como disolvente nitrometano-d_3 permite obtener cuantitativamente los complejos **4A**, **5A** o **6A** que poseen los fragmentos metálicos enlazados η^6 a los ligandos hexaheliceno (Esquema 5).

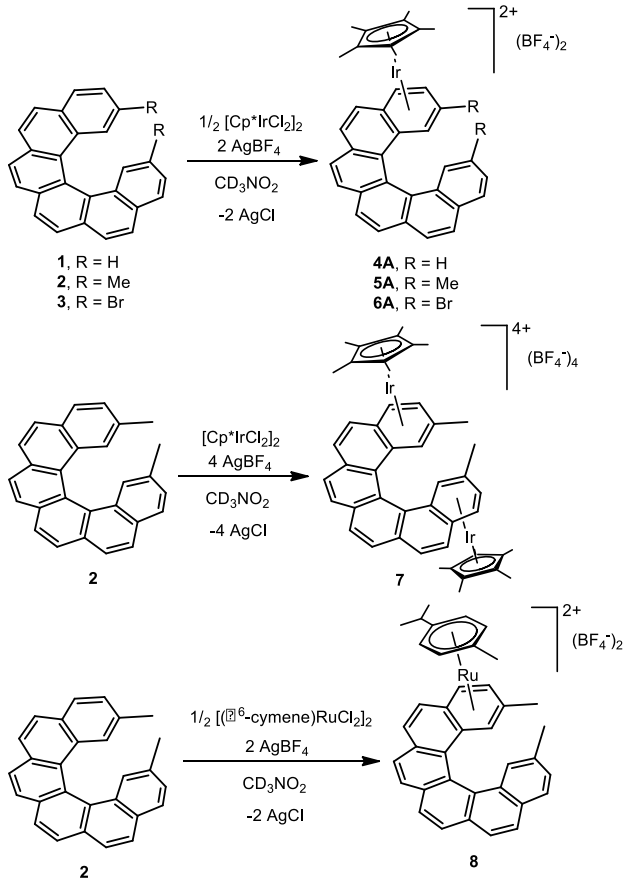

Esquema 5. Reación de coordinación de los fragmentos metálicos a los ligandos hexaheliceno.

Siguiendo las anteriormente mencionadas condiciones se ha sintetizado además el complejo bimetálico **7** formado por la coordinación de dos fragmentos metálicos de iridio al heliceno **2**. En todos los casos los productos finales obtenidos son similares y presentan la coordinación del metal sobre un anillo terminal del hexaheliceno. El seguimiento de la reacción por RMN de ^{1}H demostró la presencia de intermedios, alguno de los cuales fueron totalmente caracterizados en disolución (Esquema 6).

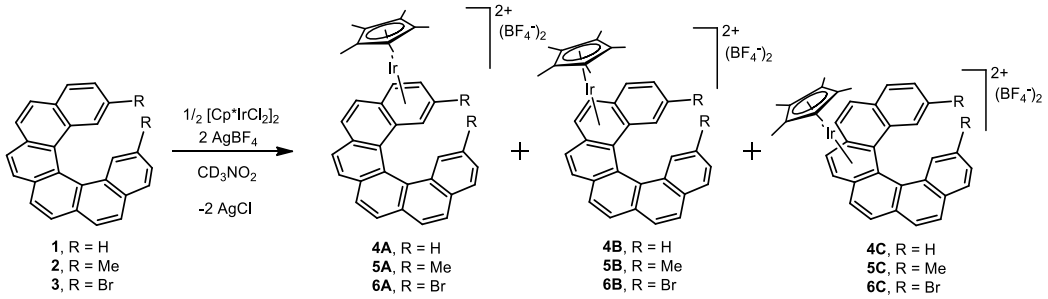

Esquema 6. Isómeros derivados de la reacción de los helicenos **1**-**3** con $[Cp^*IrCl_2]_2$ y $AgBF_4$.

Estos intermedios poseen el fragmento metálico coordinado sobre alguno de los anillos internos del heliceno. Así, al comienzo de la reacción, se encontró una clara preferencia por el enlace entre el iridio y el anillo central del hexaheliceno (complejos **4C**, **5C** y **6C**). Además, durante el seguimiento de la reacción no se observó la presencia de las señales de protón del ligando hexaheliceno libre demostrándose que dicha coordinación es extremadamente rápida. Sin embargo, la formación de los productos termodinámicos finales ocurre después de varios días a temperatura ambiente, lo que evidencia una lenta isomerización.

Siguiendo una metodología análoga se preparó el derivado de rutenio **8**, el cual pudo ser sometido a un estudio de rayos X que confirmó que el producto termodinámico presenta una coordinación η^6 entre el metal y al anillo aromático terminal del hexaheliceno.

Por último cabe destacar que se han realizado cálculos computacionales para obtener un perfil de reacción de la secuencia migratoria del fragmento de iridio sobre los anillos del ligando hexaheliceno (**1**). Los resultados obtenidos parecen indicar que este movimiento se produce a través de una transposición haptotrópica en un proceso de deslizamiento global sobre la superficie, apoyando también los datos experimentales que demuestran que esta migración comienza en el anillo central y acaba en el anillo terminal de la hélice.

Artículo II.

Assembling Nonplanar Polyaromatic Units by Click Chemistry. Study of Multicorannulene Systems as Host for Fullerenes.

En este artículo se describe la preparación y caracterización estructural de tres nuevos derivados poliaromáticos no planos con objeto de estudiar sus interacciones supramoleculares con el fulereno C_{60}. La caracterización de los compuestos fundamentalmente por RMN permite determinar de forma inequívoca que los compuestos sintetizados presentan las estructuras que se muestran en la figura 7. Así, mientras que en los compuestos trípodes **5** y **6** se observa la presencia de tres unidades coranuleno, el compuesto **7** posee dos fragmentos coranuleno enlazados a un esqueleto de hexaheliceno.

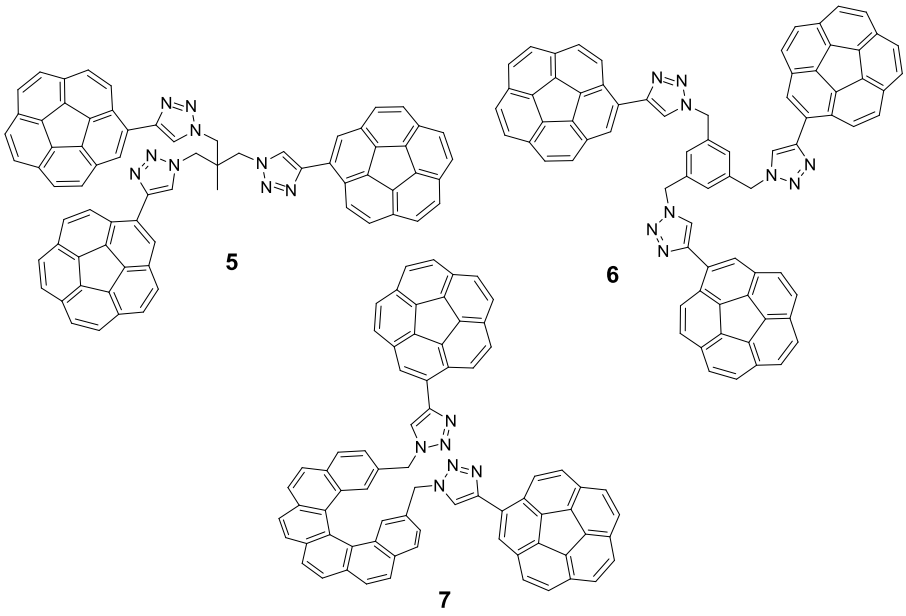

Figura 7. Estructura de los derivados de coranuleno **5**, **6** y **7**.

La síntesis de todos estos nuevos compuestos comienza con el etinilcoranuleno como reactivo común. Así, al mezclar etinilcoranuleno y el adecuado derivado de azida y utilizando las condiciones de la cicloadición catalizada por cobre (I) (CuAAC) se obtuvieron los compuestos multicoranuleno **5**-**7** en altos rendimientos.

Se efectuaron una serie de estudios en disolución mediante RMN de ^1H que demostraron el comportamiento como receptores moleculares de estos tres compuestos. En estos estudios se observó el cambio en el desplazamiento químico de algunas de las señales de protón de los derivados de coranuleno al aumentar de

forma gradual la concentración de fulereno. Además, se realizaron estudios por el método de variaciones continuas (*Job plots*) entre el C_{60} y los derivados **5**-**7** y para todos los casos los resultados obtenidos respaldan una estequiometría 1:1 entre el fulereno y los receptores.

Por último, se determinaron las constantes de asociación de estos aductos supramoleculares mediante estudios de valoración por RMN de ^{1}H utilizando como disolvente tolueno-d^{8}. Así, la constante de asociación para C_{60}⊂**5**, C_{60}⊂**6** y C_{60}⊂**7** fueron respectivamente 2152, 2192 y 2547 M^{-1}.

Artículo III.

How Metals Can Induce the Right Geometry as Hosts for Fullerenes.

En estos estudios se describe la síntesis y caracterización estructural de una familia de complejos planocuadrados de platino con ligandos poliarénicos (Figura 8). En concreto, se han preparado complejos con ligandos que poseen fragmentos coranuleno (compuestos **1** y **4**), pireno (compuesto **2**) y heliceno (compuesto **3**) con estructuras moleculares en forma de pinza. Estos ligandos, que se coordinan como acetiluros al metal, se disponen describiendo un ángulo aproximado de 90 grados.

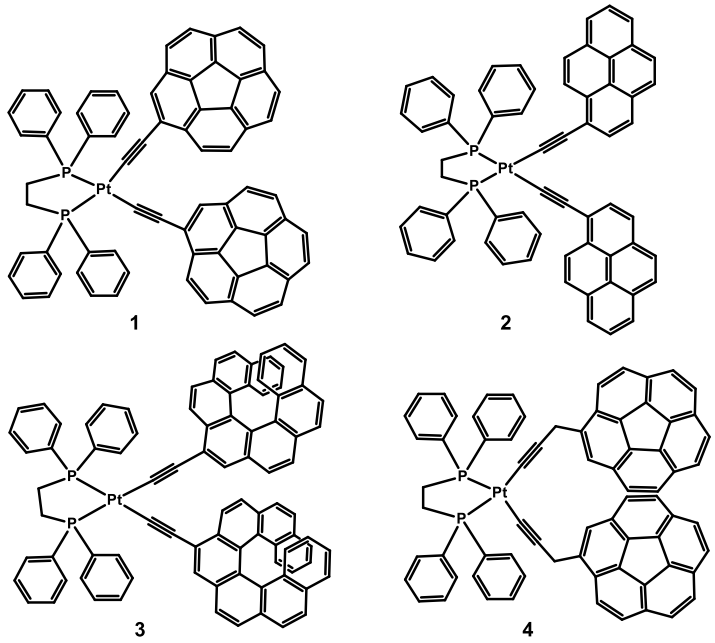

Figura 8. Complejos planocuadrados de platino usados como pinzas moleculares.

En este sentido, la geometría que les otorga el metal promueve la disposición espacial adecuada de las unidades poliaromáticas para que éstos puedan comportarse como receptores eficientes de fulerenos. Por este motivo, se evaluó en todos los casos su probable interacción con C_{60} mediante estudios realizados en disolución a través de valoraciones por RMN de ^1H, encontrando que únicamente el complejo **1** presenta interacciones supramoleculares con fulerenos.

Esta asociación fue confirmada en estado sólido mediante la obtención de la estructura por difracción de rayos X para el aducto $C_{60}\subset$**1** y en fase gas por la presencia de picos en el espectro de masa MALDI-TOF con la relación *m/z* correspondiente a los cationes $[C_{60}\subset\mathbf{1}]^+$ y $[C_{60}\subset\mathbf{1}\text{-H}]^+$. Además, también se estudió la interacción entre este receptor **1** y el fulereno C_{70}. Se calcularon las constantes de

asociación para ambos fulerenos. Dichas constantes tienen un valor de 4665 M^{-1} para el aducto $C_{60}\subset$**1** y de 20708 M^{-1} para el complejo $C_{70}\subset$**1**.

Todos estos resultados ponen de manifiesto que el derivado coranulénico **1** presenta una asociación muy eficiente con fulerenos. Sin embargo, los estudios de complejación con fulerenos de los derivados **2**, **3** y **4** demostraron que el incremento de grados de libertad y la carencia de complementariedad son factores críticos que impiden una buena asociación.

4.2. Funcionalización de complejos con ligandos iminopiridina mediante "Click Chemistry".

Artículo IV.

Schiff plus Click: One-pot Preparation of Triazole- Substituted Iminopyridines and Ring Opening of the Triazole Ring.

En este artículo se describe la síntesis y caracterización de una nueva familia de compuestos de manganeso, molibdeno y renio con ligandos iminopiridina que poseen anillos de triazol en la cadena lateral. Estas especies se pueden preparar de forma muy eficiente por reacción sucesiva de la condensación de Schiff y de la cicloadición CuAAC. Así, la adición secuencial y *one pot* de etinilanilina y bencilazida sobre los complejos **1** (figura 9) en presencia de cantidades catalíticas de cobre (I) permite obtener los derivados **3** sin necesidad de aislar los complejos **2**. Para los derivados **3a** y **3c** se obtuvieron cristales válidos para el análisis por difracción de rayos X confirmando las estructuras de la figura 9.

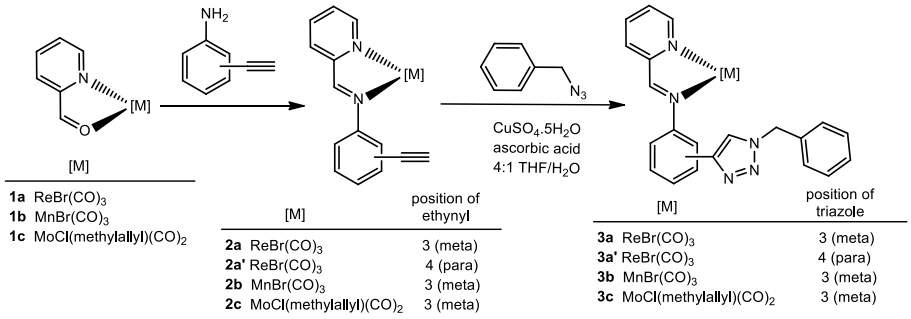

Figura 9. Reacción de formación de los complejos **3**.

Dados los resultados obtenidos por esta metodología nos resultó interesante la preparación de otros derivados de triazol por reacción con la apropiada azida. Así, la reacción entre **2a** y 1,6-diazohexano o hexadecilazida permite obtener respectivamente el esperado complejo homobimetálico o el derivado de renio con el fragmento de triazol enlazado a la cadena alquílica.

Al extender el estudio de la reacción de cicloadición de los compuestos **2a** o **2a'** con p-toluensulfonilazida cabría esperar que la reacción transcurriera de un modo análogo al descrito para las anteriores azidas. Sin embargo, en la caracterización de los complejos **6a** y **6a'** por RMN, se observó la ausencia de la señal de protón asignable al triazol, y no fue hasta que se pudieron obtener cristales válidos para una determinación estructural por difracción de rayos X del

derivado **6a** cuando, inequívocamente, se observó la presencia de un grupo N-acilsulfonamida en lugar del anillo de triazol. Aunque esta apertura del ciclo de triazol ha sido ya detallada para muchos derivados puramente orgánicos,[75] hasta donde nosotros conocemos estos son los primeros ejemplos de apertura de anillos de triazol en ligandos coordinados a metales de transición.

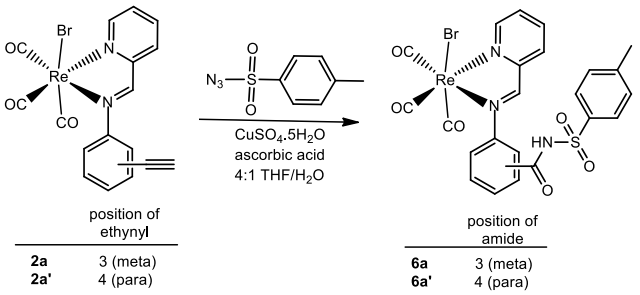

Figura 10. Reacción de etiniliminopiridinas con p-toluensulfonilazida.

Así, se ha puesto a punto una metodología adecuada para permitir la formación de triazoles en la cadena lateral de ligandos iminopiridina cordinados a metales de transición.

El Artículo VI "*Carbonyl complexes of manganese, rhenium and molybdenum with ethynyliminopyridine ligands*" fue publicado con anterioridad al comienzo de mis estudios de doctorado y por tanto no puede ser considerado como parte de la tesis según la normativa. Sin embargo, dado que en él se describe la preparación de los complejos con etinilfeniliminopiridinas **2** que sirven de precursores para los complejos descritos en este artículo, se incluye al final de esta memoria como anexo o información complementaria.

(75) (a) S. H. Cho, E. J. Yoo, I. Bae, S. Chang *J. Am. Chem. Soc.* **2005**, *127*, 16406. (b) M. P. Cassidy, J. Rauschel, V. V. Fokin *Angew. Chem. Int. Ed.* **2006**, *45*, 3154.

Artículo V.

Beyond click chemistry: spontaneous C-triazolyl transfer from copper to rhenium and transformation into mesoionic C-triazolylidene carbene.

En esta comunicación se describe la síntesis y caracterización de una familia de complejos de renio que se preparan a partir de la reactividad que deriva del uso de la cicloadición CuAAC. Se ha explorado la excepcional versatilidad en el modo de coordinación del anillo de triazol en una serie de derivados tridentados de renio (figura 11).

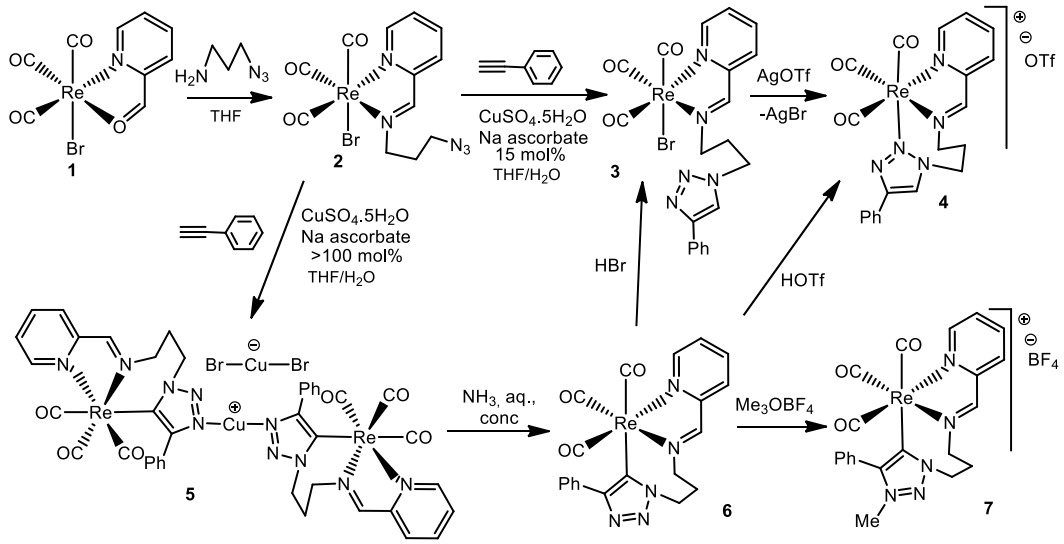

Figura 11. Rutas sintéticas para la preparación de los nuevos complejos.

Éstos se preparan gracias a la espontánea transmetalación del cobre al renio que se produce al hacer reacionar el complejo iminopiridínico **2** y fenilacetileno en condiciones estequiométricas de cobre (I), lo que da lugar a la formación inesperada del dimero **5**, que posee un átomo de cobre actuando como puente entre los dos anillos de triazol. La reacción de **5** con una disolución acuosa de amoniaco produce la eliminación del cobre para formar el derivado **6**, y la posterior reacción de **6** con tetrafluoroborato de trimetiloxonio adiciona un grupo metilo a uno de los nitrógenos del triazol para formar el carbeno mesoiónico **7**.

Por otra parte, la misma reacción entre **2** y fenilacetileno pero con cantidades catalíticas de cobre (I) forma el complejo esperado con el anillo de triazol sin coordinar. La posterior reacción con un extractor de haluros forma el complejo catiónico **4**, donde se observa el anillo de triazol coordinado a través del nitrogeno

central. Es relevante mencionar que la conversión de **6** a **3** y de **6** a **4** se puede realizar respectivamente por el tratamiento con ácido bromídrico o ácido tríflico.

Esto abre nuevas vías para la preparación de carbenos mesoiónicos, hasta ahora poco frecuentes, y para el estudio de la reactividad de estas interesante especies.

5. CONCLUSIONES

A continuación se describen una serie de conclusiones globales que a nuestro juicio pueden ser las más interesantes. La totalidad de conclusiones particulares extraídas de cada trabajo se detallan en el artículo correspondiente.

1. Se ha puesto a punto un método que permite la coordinación η^6 de fragmentos metálicos de iridio y rutenio a ligandos hexaheliceno con excelentes rendimientos.

2. Mediante estudios por RMN se han podido caracterizar procesos de migración del fragmento metálico sobre los anillos de los helicenos.

3. Se ha sintetizado una familia de compuestos planocuadrados de platino que poseen ligandos poliaromáticos. El derivado que presenta dos unidades de coranuleno posee una de las mayores constantes de asociación con fulerenos estimadas hasta la fecha.

4. Se han sintetizado compuestos poliaromáticos no planos que poseen dos o tres unidades de coranuleno utilizando la cicloadición denominada *click chemistry*. Estos derivados resultaron ser receptores eficientes de fulerenos.

5. El uso sucesivo de la reacción de Schiff y de la cicloadición catalizada por cobre (CuAAC) demostró ser una metodología efectiva para preparar complejos con ligandos iminopiridina que poseen un anillo de triazol en la cadena lateral.

6. Cuando se realiza la cicloadición de fenilacetileno a complejos que contienen una iminopiridina funcionalizada con azida, usando cantidades estequiométricas de reactivo de cobre, se observa la transmetalación del anillo de triazolilo a un átomo de renio, lo que abre la puerta para la preparación de complejos con ligandos triazolideno carbeno mesoiónicos.

CAPÍTULO 1

FUNCIONALIZACIÓN DE COMPUESTOS POLIAROMÁTICOS NO PLANOS

Artículo I.

η^6-Hexahelicene Complexes of Iridium and Ruthenium. Running along the Helix.

Inorganic Chemistry

Article

pubs.acs.org/IC

η^6-Hexahelicene Complexes of Iridium and Ruthenium: Running along the Helix

Celedonio M. Álvarez,* Héctor Barbero, Luis A. García-Escudero, Jose M. Martín-Alvarez, Cristina Martínez-Pérez, and Daniel Miguel

IU CINQUIMA/Química Inorgánica, Facultad de Ciencias, Universidad de Valladolid, E-47005, Valladolid, Spain

Supporting Information

ABSTRACT: The first η^6-complexes of iridium and ruthenium coordinated to helicenes have been obtained. Hexahelicene (**1**), 2,15-dimethylhexahelicene (**2**), and 2,15-dibromohexahelicene (**3**) react with $[Cp^*IrCl_2]_2$ and $AgBF_4$ in CD_3NO_2 to afford quantitatively the complexes $[Cp^*Ir(\eta^6\text{-}\mathbf{1})][BF_4]_2$ (**4A**), $[Cp^*Ir(\eta^6\text{-}\mathbf{2})][BF_4]_2$ (**5A**), and $[Cp^*Ir(\eta^6\text{-}\mathbf{3})][BF_4]_2$ (**6A**), respectively. In all cases, the final thermodynamic products are similar, and they exhibit coordination between the 12 e^- metal fragment $[IrCp^*]^{2+}$ and the terminal ring of the helicene. Monitoring the reaction by NMR shows formation of intermediates, some of which have been fully characterized in solution. These intermediates exhibit the metal fragment coordinated to the internal rings. We have also synthesized the bimetallic complex $[(Cp^*Ir)_2(\mu_2\text{-}\eta^6\text{:}\eta^6\text{-}\mathbf{2})][BF_4]_4$ (**7**), achieving coordination between two units $[IrCp^*]^{2+}$ and the helicene **2**. Following an analogous methodology, we have prepared the complex $[(\eta^6\text{-cymene})Ru(\eta^6\text{-}\mathbf{2})][BF_4]_2$ (**8**), which has been studied by X-ray diffraction, confirming the preferential binding to the terminal aromatic ring.

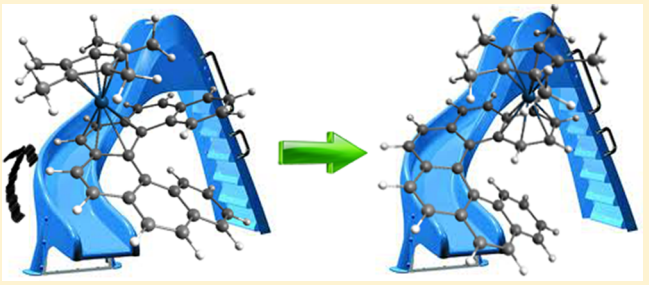

INTRODUCTION

Helicenes are a class of polycyclic aromatic molecules with ortho-fused aromatic rings. These organic compounds were long considered as academic curiosities because of their twisted shape due to repulsive steric interactions between terminal rings.[1] In fact, they represent an attractive class of compounds with a fascinating three-dimensional structure and exceptional optical[2] and electronic[3] properties. Perhaps the most remarkable feature is their inherent chirality; therefore, they have raised attention over the years for their potential use as asymmetric catalysts.[4] This is due to the helicenes having a stereogenic axis that has a left- or right-handed chiral helical structure with M (−) or P (+) configuration, respectively.[5] Additionally, these nonplanar condensed aromatic compounds have been employed for molecular recognition,[6] self-assembly,[7] molecular machines synthesis,[8] biological applications[9] or in several other fields of materials science.[10] The hexahelicene (**1**) was obtained by Newman and Lednicer in 1956,[11] and other helicenes have been prepared by the oxidative photocyclization of bis(stilbene) derivatives[6a,12] or by other nonradiative methodologies.[13] In a recently published work, Shen and Chen[14] provide a comprehensive review of the synthesis and applications of these captivating molecules.

Coordination of the polycyclic aromatic molecules to metal atoms may alter the electronic density distribution and significantly change their properties. Therefore, it has been considered attractive to explore the chemistry of these kinds of complexes. The η^6-bis(arene) complexes of *p*-cymene with ruthenium or η^6-arene complexes of cyclopentadienyl with iridium have been widely studied,[15] and the coordination of the $[Ru(\eta^6\text{-cymene})]^{2+}$ fragment to coronene and other polyaromatic compounds has been described.[16] The preparation of η^6-polyaromatic complexes is simpler when the condensed rings are completely planar, and it is also known that the presence of alkyl substituents on the arene facilitates this coordination. Therefore, only a few exotic examples present this binding type in nonplanar polyaromatic compounds, especially buckybowl derivatives.[17] Particularly interesting are the works of Angelici and co-workers,[17e,g,h] which led to the preparation of η^6-corannulene complexes. In this study, they reported the synthesis and structure of a dimetalated buckybowl that presents the coordination of two 12 e^- metal fragments $[RuCp^*]^+$ to each side of corannulene, thereby increasing the flattening of the molecule. There are several structural differences between coronene, corannulene, and helicenes. Coronene or [6]circulene is a polyaromatic organic molecule formed by the condensation of six benzene rings presenting a totally planar structure, while corannulene and helicenes show a lack of planarity, exhibiting three-dimensional structures (Figure 1). The flattening in nonplanar polyaromatic compounds can be evaluated by the π-orbital axis vector (POAV) analysis,[18] and its value shows that corannulene has a more strained structure than helicenes. Therefore it is reasonable to anticipate that η^6-helicene complexes would be more stable and more robust than their corannulene analogues.

Received: February 29, 2012

   dx.doi.org/10.1021/ic300462z | *Inorg. Chem.* XXXX, XXX, XXX−XXX

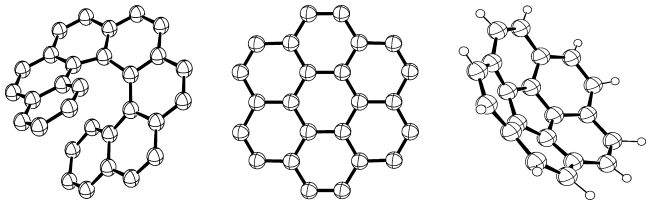

Figure 1. Structures of heptahelicene (left), coronene (middle), and corannulene (right).

However, there are no reported examples of complexes that contain η^6-coordinated helicenes. For all these reasons, we have considered it interesting to study the η^6-coordination between 12 e^- metal fragments $[IrCp^*]^{2+}$ or $[Ru(\eta^6\text{-cymene})]^{2+}$ and [6]helicene (**1**) or 2,15-disubstituted [6]helicenes such as 2,15-dimethylhexahelicene (**2**) and 2,15-dibromohexahelicene (**3**), as a starting point for exploration of the chemistry of η^6-hexahelicene complexes.[19]

EXPERIMENTAL SECTION

General Considerations. Synthetic procedures were carried out under an inert atmosphere of nitrogen, in solvents that had been dried by passage through alumina columns in an IT solvent purification system, and degassed with N_2. Standard Schlenk techniques were used unless otherwise noted. Solution NMR spectra were obtained on a Bruker AV-400 or a Varian MR 400 spectrometer, with CD_3NO_2 as the solvent, internal lock, and internal reference [δ 4.33 (^{1}H) and 62.8 (^{13}C)]. For a correct assignment of NMR signals, one should determine whether the metal fragment is bonded to A, B, or C ring as

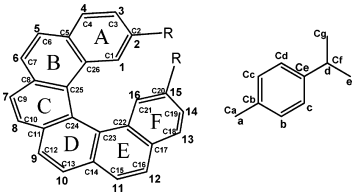

Figure 2. Atom labeling schemes for the cymene and hexahelicene ligands.

shown in Figure 2. Crystal evaluation and data collection of **8** were performed on an Oxford Diffraction Supernova diffractometer, equipped with an Atlas charge-coupled device (CCD) area detector and a four-circle κ goniometer. Elemental analyses were performed on a Perkin-Elmer 2400B CHN analyzer. All reagents and solvents were reagent-grade and were used without further purification unless otherwise specified. Nitromethane-d_3 (CD_3NO_2) was purchased from Aldrich and subjected to three freeze−pump−thaw cycles before use. Hexahelicene (**1**),[20] 2,15-dimethylhexahelicene (**2**),[20a,21] and 2,15-dibromohexahelicene (**3**)[22] were prepared according to literature procedures, and their spectral data were in agreement with those in the literature.

Synthesis. *[Cp*Ir(η^6-**1**)][BF_4]$_2$ (**4A**).* To a flask containing $[Cp^*IrCl_2]_2$ (6.1 mg, 0.008 mmol), **1** (5.0 mg, 0.015 mmol), an excess of $AgBF_4$ (19.5 mg, 0.100 mmol) was added CD_3NO_2 (1 mL). The solution was stirred for 1 h at room temperature, and the AgCl precipitate was removed by filtration. The resulting solution was transferred by cannula to an NMR tube for monitoring. The reaction was completed after 15 days, and the resulting solution was evaporated to dryness under vacuum to give an orange precipitate of **4A**, which was recrystallized from CH_2Cl_2/hexane. This reaction is nearly quantitative by NMR spectroscopy. ^{1}H NMR (400 MHz, CD_3NO_2, 298 K) δ 8.88 [d, ^3J(H,H) = 9.0 Hz, 1H, H6], 8.65 [d, ^3J(H,H) = 8.2 Hz, 1H, H8], 8.39 [d, ^3J(H,H) = 8.2 Hz, 1H, H7], 8.35 [d (AB system), ^3J(H,H) = 8.3 Hz, 1H, H9 or H10], 8.33 [d (AB system), ^3J(H,H) = 8.3 Hz, 1H, H10 or H9], 8.21 [d (AB system), ^3J(H,H) = 8.6 Hz, 1H, H11 or H12], 8.19 [d AB system), ^3J(H,H) = 8.6 Hz, 1H, H12 or H11], 8.11 [dd, ^3J(H,H) = 8.0 Hz and ^5J(H,H) = 1.0 Hz, 1H, H13], 7.97 [d, ^3J(H,H) = 9.0 Hz, 1H, H5], 7.96 [d, ^3J(H,H) = 6.1 Hz, 1H, H4], 7.75 [d, ^3J(H,H) = 8.5 Hz, 1H, H16], 7.51 (m, 1H, H14), 7.43 [d, ^3J(H,H) = 6.7 Hz, 1H, H1], 7.32 (m, 1H, H3), 7.05 (m, 1H, H15), 6.58 (m, 1H, H2), 1.51 (s, 15H, Cp*). ^{13}C{^{1}H} NMR (100 MHz, CD_3NO_2, 298 K) δ 140.80 (C7), 136.30 (C11), 136.03 (C10), 135.97 (C8), 134.79 (C14), 134.29 (C17), 131.92 (C12 or C13), 131.46 (C15 or C16), 130.49 (C18), 129.51 (C22), 129.09 (C9), 128.90 (C12 or C13), 128.45 (C21), 128.43 (C2), 128.37 (C1), 127.92 (C15 or C16), 126.23 (C23), 125.42 (C24), 123.66 (C6), 122.12 (C25), 111.39 (C26), 105.27 (C_5Me_5), 100.32 (C5), 98.14 (C3), 96.50 (C4), 95.03 (C2), 90.48 (C1), 8.91 (C_5Me_5). Anal. Calcd for $C_{36}H_{31}B_2F_8Ir$: C, 52.13; H, 3.77. Found: C, 52.17; H, 3.88.

*Low-Temperature Studies of the Reaction between [Cp*IrCl$_2$]$_2$, AgBF$_4$, and **1**.* Compound **1** (5.0 mg, 0.015 mmol), $[Cp^*IrCl_2]_2$ (6.1 mg, 0.008 mmol), and an excess of $AgBF_4$ (19.5 mg, 0.100 mmol) and CD_3NO_2 (1 mL) were introduced into an NMR tube in a bath at 195 K. The tube containing the frozen reagents and solvent was placed inside the NMR Bruker AV400 spectrometer and allowed to melt and warm to 253 K inside the instrument before measurement. NMR experiments showed the formation of three isomers, **4A**, **4B**, and **4C**. Isomer **4A**: ^{1}H NMR (400 MHz, CD_3NO_2, 253 K) δ 8.85 [d, ^3J(H,H) = 9.0 Hz, 1H, H6], 8.63 [d, ^3J(H,H) = 8.2 Hz, 1H, H8], 8.39 [d, ^3J(H,H) = 8.2 Hz, 1H, H7], 8.34 [s (AB system), 2H, H9 and H10], 8.22 [s (AB system), 2H, H11 and H12], 8.12 [d, ^3J(H,H) = 8.0 Hz, 1H, H13], 7.96 [d, ^3J(H,H) = 9.0 Hz, 1H, H5], 7.95 [d, ^3J(H,H) = 6.1 Hz, 1H, H4], 7.76 [d, ^3J(H,H) = 8.5 Hz, 1H, H16], 7.52 (m, 1H, H14), 7.44 [d, ^3J(H,H) = 6.7 Hz, 1H, H1], 7.30 (m, 1H, H3), 7.05 (m, 1H, H15), 6.57 (m, 1H, H2), 1.47 (s, 15H, Cp*). Isomer **4B**: ^{1}H NMR (400 MHz, CD_3NO_2, 253 K) δ 8.95 [d, ^3J(H,H) = 9.0 Hz, 1H, H6], 8.80 [d, ^3J(H,H) = 8.5 Hz, 1H, H8], 8.64 [d, ^3J(H,H) = 8.2 Hz, 1H, H7], 8.32 [d (AB system), ^3J(H,H) = 8.6 Hz, 1H, H12], 8.31 [d (AB system), ^3J(H,H) = 8.6 Hz, 1H, H9 or H10], 8.29 [d (AB system), ^3J(H,H) = 8.6 Hz, 1H, H10 or H9], 8.22 [d (AB system), ^3J(H,H) = 8.6 Hz, 1H, H11], 8.19 [d, ^3J(H,H) = 8.0 Hz, 1H, H13], 8.18 [d, ^3J(H,H) = 9.0 Hz, 1H, H5], 8.09 [d, ^3J(H,H) = 6.3 Hz, 1H, H4], 7.66 [d, ^3J(H,H) = 8.5 Hz, 1H, H16], 7.62 [d, ^3J(H,H) = 7.0 Hz, 1H, H1], 7.47 (m, 2H, H3 and H14), 6.92 (m, 2H, H2 and H15), 1.53 (s, 15H, Cp*). Isomer **4C**: ^{1}H NMR (400 MHz, CD_3NO_2, 253 K) δ 8.72 [d, ^3J(H,H) = 8.8 Hz, 1H, H10], 8.59 [d, ^3J(H,H) = 8.2 Hz, 1H, H12], 8.57 [d, ^3J(H,H) = 8.5 Hz, 1H, H5], 8.25 [d, ^3J(H,H) = 8.2 Hz, 1H, H11], 8.17 [d, ^3J(H,H) = 8.5 Hz, 1H, H4], 8.16 [d, ^3J(H,H) = 8.8 Hz, 1H, H9], 8.15 [d, ^3J(H,H) = 8.0 Hz, 1H, H13], 8.04 [s (AB system), 2H, H7 and H8], 7.91 [d, ^3J(H,H) = 8.5 Hz, 1H, H6], 7.59 (m, 1H, H3), 7.54 (m, 1H, H14), 7.25 [d, ^3J(H,H) = 7.5 Hz, 1H, H1], 7.20 [d, ^3J(H,H) = 9.0 Hz, 1H, H16], 7.06 (m, 1H, H2), 6.99 (m, 1H, H15), 1.43 (s, 15H, Cp*). ^{13}C{^{1}H} NMR (100 MHz, CD_3NO_2, 253 K): δ 140.7 (C6, **4C**), 139.1 (C7, **4A**), 138.4 (C7, **4B**), 137.3, 136.5 (C16, **4C**), 136.3 (C13, **4C**), 135.7, 135.6 (C10, **4B**), 134.7, 134.5, 134.4 (C10, **4A**), 133.7, 133.2, 132.8, 132.7, 132.0, 131.3 (C3, **4C**), 130.5 (C9, **4B**), 130.2 (C12 or C13, **4A**), 129.9 (C18, **4B**), 129.6 (C15 or C16, **4A**), 129.2, 128.9 (C2, **4C**), 128.8 (C18, **4A**), 128.0, 127.9 (C19, **4C**), 127.7 (C9, **4A**), 127.6 (C12 or C13, **4B**; C16, **4B**), 127.5 (C1, **4C**), 127.4 (C15 or C16, **4A**), 127.3 (C12 or C13, **4A**), 126.9 (C21, **4A**; C15, **4C**), 126.8 (C15, **4B**), 126.7 (C20, **4A**; C12 or C13, **4B**; C20, **4C**), 126.6 (C21, **4B**), 126.5 (C21, **4C**), 126.3 (C19, **4A**), 125.7 (C6, **4B**), 124.8, 123.9, 123.7 (C3 or C19, **4B**), 123.3, 123.1, 122.4 (C6, **4A**), 120.6, 118.8 (C7, **4C**), 118.7, 115.21 (C2 or C15, **4B**), 109.5, 108.3, 104.6 (C_5Me_5, **4B**), 103.6 (C_5Me_5, **4A**), 102.5 (C_5Me_5, **4C**), 99.6, 98.8, 98.1 (C3 or C19, **4B**), 96.7 (C3, **4A**), 95.6 (C4, **4B**; C2 or C20 **4B**), 95.3 (C9 or C10, **4C**), 94.9 (C4, **4A**), 93.5 (C2, **4A**), 91.3 (C9 or C10, **4C**), 88.8 (C1, **4A**), 88.7 (C1, **4B**), 7.6 (C_5Me_5, **4B**), 7.4 (C_5Me_5, **4A**), 6.9 (C_5Me_5, **4C**). Some carbon atoms of isomer **4C** could not be detected.

*[Cp*Ir(η^6-**2**)][BF_4]$_2$ (**5A**).* To a flask containing $[Cp^*IrCl_2]_2$ (5.6 mg, 0.007 mmol), **2** (5.0 mg, 0.014 mmol), and an excess of $AgBF_4$ (19.5 mg, 0.100 mmol) was added CD_3NO_2 (1 mL). The solution was stirred for 1 h at room temperature, and the AgCl precipitate was

dx.doi.org/10.1021/ic300462z | Inorg. Chem. XXXX, XXX, XXX−XXX

removed by filtration. The resulting solution was transferred by cannula to an NMR tube for monitoring. The reaction was completed after 6 days. The solution formed was evaporated to dryness under vacuum to give an orange precipitate of **5A**, which was recrystallized from CH_2Cl_2/hexane. This reaction is nearly quantitative by NMR spectroscopy. ^{1}H NMR (400 MHz, CD_3NO_2, 298 K) δ 8.88 [d, ^3J(H,H) = 8.9 Hz, 1H, H6], 8.68 [d, ^3J(H,H) = 8.2 Hz, 1H, H8], 8.39 [d, ^3J(H,H) = 8.2 Hz, 1H, H7], 8.35 [d (AB system), ^3J(H,H) = 8.3 Hz, 1H, H9 or H10], 8.34 [d (AB system), ^3J(H,H) = 8.3 Hz, 1H, H10 or H9], 8.18 [d (AB system), ^3J(H,H) = 8.6 Hz, 1H, H11 or H12], 8.13 [d (AB system), ^3J(H,H) = 8.6 Hz, 1H, H12 or H11], 8.03 [d, ^3J(H,H) = 8.2 Hz, 1H, H13], 7.93 [d, ^3J(H,H) = 8.9 Hz, 1H, H5], 7.87 [d, ^3J(H,H) = 6.4 Hz, 1H, H4], 7.51 (s, 1H, H16), 7.43 [d, ^3J(H,H) = 8.2 Hz, 1H, H14], 7.31 (s, 1H, H1), 7.20 [d, ^3J(H,H) = 6.4 Hz, 1H, H3], 2.07 (s, 3H, 2-Me), 1.97 (s, 3H, 15-Me), 1.51 (s, 15H, Cp*). Due to the poor solubility of **5** in CD_3NO_2, we were unable to obtain satisfactory $^{13}C\{^1H\}$ NMR spectra. Anal. Calcd for $C_{38}H_{35}B_2F_8Ir$: C, 53.22; H, 4.11. Found: C, 53.05; H, 4.00.

*[Cp*Ir(η^6-**3**)][BF_4]$_2$ (**6A**).* To a flask containing [Cp*$IrCl_2$]$_2$ (4.1 mg, 0.005 mmol), **3** (5.0 mg, 0.010 mmol), and an excess of $AgBF_4$ (19.5 mg, 0.100 mmol) was added CD_3NO_2 (1 mL). The solution was stirred for 1 h at room temperature, and the AgCl precipitate was removed by filtration. The resulting solution was transferred by cannula to an NMR tube for monitoring. The reaction was completed after 14 days and the solution formed was evaporated to dryness under vacuum to afford an orange precipitate of **6A**, which was recrystallized from CH_2Cl_2/hexane. This reaction is nearly quantitative by NMR spectroscopy. ^{1}H NMR (400 MHz, CD_3NO_2, 298 K) δ 8.95 [d, ^3J(H,H) = 9.0 Hz, 1H, H6], 8.72 [d, ^3J(H,H) = 8.2 Hz, 1H, H8], 8.44 [d, ^3J(H,H) = 8.2 Hz, 1H, H7], 8.40 [d (AB system), ^3J(H,H) = 8.4 Hz, 1H, H9 or H10], 8.38 [d (AB system), ^3J(H,H) = 8.4 Hz, 1H, H10 or H9], 8.24 [s (AB system), 2H, H11 and H12], 8.09 [d, ^3J(H,H) = 8.6 Hz, 1H, H13], 8.06 [d, ^3J(H,H) = 6.6 Hz, 1H, H4], 8.04 [d, ^3J(H,H) = 9.0 Hz, 1H, H5], 7.80 [d, ^4J(H,H) = 1.8 Hz, 1H, H16], 7.72 [dd, ^3J(H,H) = 6.6 Hz and ^4J(H,H) = 1.8 Hz, 1H, H3], 7.71 [dd, ^3J(H,H) = 8.6 Hz and ^4J(H,H) = 1.5 Hz, 1H, H14], 7.64 [d, ^4J(H,H) = 1.5 Hz, 1H, H1], 1.54 (s, 15H, Cp*). $^{13}C\{^1H\}$ NMR (100 MHz, CD_3NO_2, 298 K) δ 141.5 (C7), 137.2 (C10), 136.8, 136.5, 135.7, 133.1, 132.7 (C18), 132.2 (C12 or C13), 131.7 (C19), 131.3 (C15 or C16), 131.1 (C21), 130.6, 129.9 (C12 or C13), 129.4 (C9), 128.8 (C15 or C16), 125.5, 124.5, 123.3 (C6), 122.1, 120.4, 112.8, 106.4 (C_5Me_5), 101.6 (C3), 98.9, 97.2, 96.3 (C4), 92.8 (C1), 8.54 (C_5Me_5). Quaternary carbons of helicene could not be assigned. Anal. Calcd for $C_{36}H_{29}B_2Br_2F_8Ir$: C, 43.80; H, 2.96. Found: C, 43.62; H, 3.05.

*Intermediate [Cp*Ir(η^6-**3**)][BF_4]$_2$ (**6C**).* Compound **3** (5.0 mg, 0.010 mmol), [Cp*$IrCl_2$]$_2$ (4.1 mg, 0.005 mmol), and an excess of $AgBF_4$ (19.5 mg, 0.100 mmol) and CD_3NO_2 (1 mL) were introduced into an NMR tube in a bath at 195 K. The tube containing the frozen reagents and solvent was placed inside the NMR Bruker AV400 spectrometer and allowed to melt and warm to 253 K inside the instrument before measurement. Data for **6C**: ^{1}H NMR (400 MHz, CD_3NO_2, 253 K) δ 8.78 [d, ^3J(H,H) = 8.6 Hz, 1H, H10], 8.66 [d, ^3J(H,H) = 8.5 Hz, 1H, H12], 8.62 [d, ^3J(H,H) = 9.0 Hz, 1H, H5], 8.32 [d, ^3J(H,H) = 8.5 Hz, 1H, H11], 8.25 [d, ^3J(H,H) = 8.6 Hz, 1H, H9], 8.19 [d, ^3J(H,H) = 8.6 Hz, 1H, H4], 8.14 [d, ^3J(H,H) = 8.5 Hz, 1H, H13], 8.13 [d (AB system), ^3J(H,H) = 6.5 Hz 1H, H7 or H8], 8.10 [d (AB system), ^3J(H,H) = 6.5 Hz 1H, H8 or H7], 7.99 [d, ^3J(H,H) = 9.0 Hz, 1H, H6], 7.88 [dd, ^3J(H,H) = 8.6 Hz and ^4J(H,H) = 1.7 Hz, 1H, H3], 7.72 [dd, ^3J(H,H) = 8.5 Hz and ^4J(H,H) = 1.5 Hz, 1H, H14], 7.41 (br s, 1H, H16), 7.31 (br s, 1H, H1), 1.51 (s, 15H, Cp*). $^{13}C\{^1H\}$ NMR (100 MHz, CD_3NO_2, 253 K) δ 141.2 (C6), 139.7, 138.6, 137.8 (C13 and C16), 136.0 (C3), 134.4, 133.7 (C4), 132.9, 132.6 (C19), 132.3 (C18), 132.0, 131.0 (C1), 130.5 (C21), 129.8, 129.7, 129.2 (C12), 128.2 (C15), 127.9, 124.2, 121.1 (C7), 110.4, 104.1 (C_5Me_5), 97.5 (C9 or C10), 93.7 (C9 or C10), 93.1, 86.6, 8.2 (C_5Me_5). Quaternary carbons of helicene could not be assigned.

*[(Cp*Ir)$_2$(μ_2-η^6:η^6-**2**)][BF_4]$_4$ (**7**).* To a flask containing [Cp*$IrCl_2$]$_2$ (11.2 mg, 0.014 mmol), **2** (5.0 mg, 0.014 mmol), and an excess of $AgBF_4$ (19.5 mg, 0.100 mmol) was added CD_3NO_2 (1 mL). The solution was stirred for 1 h at room temperature, and the AgCl precipitate was removed by filtration. The resulting solution was transferred by cannula to an NMR tube for monitoring. The reaction was completed after 3 h and the solution formed was evaporated to dryness under vacuum to give an orange precipitate of **7**, which was recrystallized from CH_2Cl_2/hexane. This reaction is nearly quantitative by NMR spectroscopy. ^{1}H NMR (400 MHz, CD_3NO_2, 298 K) δ 8.91 [d, ^3J(H,H) = 9.1 Hz, 2H, H6 and H11], 8.78 [d, ^3J(H,H) = 8.3 Hz, 2H, H8 and H9], 8.60 [d, ^3J(H,H) = 8.3 Hz, 2H, H7 and H10], 8,12 [d, ^3J(H,H) = 9.1 Hz, 2H, H5 and H12], 8.04 [d, ^3J(H,H) = 6.8 Hz, 2H, H4 and H13], 7.38 (s, 2H, H1 and H16), 7.37 [d, ^3J(H,H) = 6.8 Hz, 2H, H3 and H14], 2.29 (s, 6H, Me), 1.50 (s, 30H, Cp*). $^{13}C\{^1H\}$ NMR (100 MHz, CD_3NO_2, 298 K) δ 139.8 (C7 and C15), 139.0, 137.0 (C11 or C24), 136.9 (C10 and C12), 131.9 (C9 and C13), 126.5 (C6 and C16), 125.0 (C11 or C24), 119.5, 113.8, 110.7, 105.9 (C_5Me_5), 100.2 (C3 and C19), 99.2, 96.7 (C4 and C18), 89.9 (C1 and C21), 18.4 (Me), 8.6 (C_5Me_5). Quaternary carbons of helicene could not be assigned. Anal. Calcd for $C_{48}H_{50}B_4F_{16}Ir_2$: C, 42.44; H, 3.71. Found: C, 42.60; H, 3.82.

*[(η^6-Cymene)Ru(η^6-**2**)][BF_4]$_2$ (**8**).* To a flask containing [(η^6-cymene)$RuCl_2$]$_2$ (4.3 mg, 0.007 mmol), **2** (5.0 mg, 0.014 mmol), and an excess of $AgBF_4$ (19.5 mg, 0.100 mmol) was added CD_3NO_2 (1 mL). The solution was stirred for 1 h at room temperature, and the AgCl precipitate was removed by filtration. The resulting solution was transferred by cannula to an NMR tube for monitoring. The reaction was completed after 15 days and the solution formed was evaporated to dryness under vacuum to give a red precipitate of **8**, which was reprecipitated twice from CH_2Cl_2/hexane and vacuum-dried for 24 h. Anal. Calcd for $C_{38}H_{34}B_2F_8Ru$: C, 59.63; H, 4.48. Found: 59.77; H 4.55. This reaction is nearly quantitative by NMR spectroscopy. Red crystals of this complex suitable for an X-ray diffraction study were obtained by layering a methylene chloride solution of the complex with hexane at −20 °C for 1 week. ^{1}H NMR (400 MHz, CD_3NO_2, 298 K) δ 8.630 [d, ^3J(H,H) = 8.2 Hz, 1H, H8], 8.624 [d, ^3J(H,H) = 9.0 Hz, 1H, H6], 8.320 [d (AB system), ^3J(H,H) = 8.4 Hz, 1H, H9 or H10], 8.295 [d, ^3J(H,H) = 8.2 Hz, 1H, H7], 8.292 [d (AB system), ^3J(H,H) = 8.4 Hz, 1H, H10 or H9], 8.159 [d (AB system), ^3J(H,H) = 8.5 Hz, 1H, H11 or H12], 8.118 [d (AB system), ^3J(H,H) = 8.5 Hz, 1H, H12 or H11], 8.010 [d, ^3J(H,H) = 9.0 Hz, 1H, H5], 7.981 [d, ^3J(H,H) = 8.2 Hz, 1H, H13], 7.859 [d, ^3J(H,H) = 6.3 Hz, 1H, H4], 7.355 [d, ^3J(H,H) = 8.2 Hz, 1H, H14], 7.183 (s, 1H, H16), 7.140 (s, 1H, H1), 6.728 [d, ^3J(H,H) = 6.3 Hz, 1H, H3], 6.293 [d, ^3J(H,H) = 6.6 Hz, 1H, Hb], 6.228 [d, ^3J(H,H) = 6.6 Hz, 1H, Hc], 5.822 [d, ^3J(H,H) = 6.6 Hz, 1H, Hc], 5.781 [d, ^3J(H,H) = 6.6 Hz, 1H, Hb], 1.871 (s, 3H, 15-Me), 1.854 (s, 3H, 2-Me), 1.832 (m, 1H, Hd), 1.645 (s, 3H, Ha), 0.902 [d, ^3J(H,H) = 7.0 Hz, 3H, He], 0.622 [d, ^3J(H,H) = 7.0 Hz, 3H, He]). $^{13}C\{^1H\}$ NMR (100 MHz, CD_3NO_2, 298 K) δ 140.2 (C7), 138.5, 136.7, 136.3, 136.1 (C10), 135.0, 132.4, 131.5 (C12 or C13), 130.8 (C15 or C16), 130.1 (C19), 130.0 (C18), 129.8, 129.4 (C9), 128.8 (C12 or C13), 128.7 (C21), 126.8 (C15 or C16), 126.7 (C6), 126.1, 125.9, 122.6, 120.3, 112.0, 111.2, 110.1, 96.4 (*Cc*), 95.2 (C3), 95.1, 94.8 (*Cc*), 94.3 (Cd), 92.7 (C4), 91.7 (Cd), 88.1 (C1), 31.62 (Cf), 23.02 (Cg), 21.4 (15-CH_3), 20.8 (Cg), 19.3 (2-CH_3), 18.2 (Ca).

RESULTS AND DISCUSSION

The pentamethylcyclopentadienyl−iridium(III) complexes exhibiting η^6-coordination to hexahelicenes were obtained in nearly quantitative yield by reaction of [Cp*$IrCl_2$]$_2$, $AgBF_4$, and hexahelicene ligand in CD_3NO_2 solvent at room temperature and under an inert nitrogen atmosphere. Thus, the reaction of hexahelicene (**1**), 2,15-dimethylhexahelicene (**2**), or 2,15-dibromohexahelicene (**3**) with $AgBF_4$ and [Cp*$IrCl_2$]$_2$ led to formation of the complexes [Cp*Ir(η^6-**1**)][BF_4]$_2$ (**4A**), [Cp*Ir(η^6-**2**)][BF_4]$_2$ (**5A**), or [Cp*Ir(η^6-**3**)][BF_4]$_2$ (**6A**), respectively (Scheme 1). These new compounds can be stored in air for several months.

dx.doi.org/10.1021/ic300462z | *Inorg. Chem.* XXXX, XXX, XXX−XXX

Scheme 1

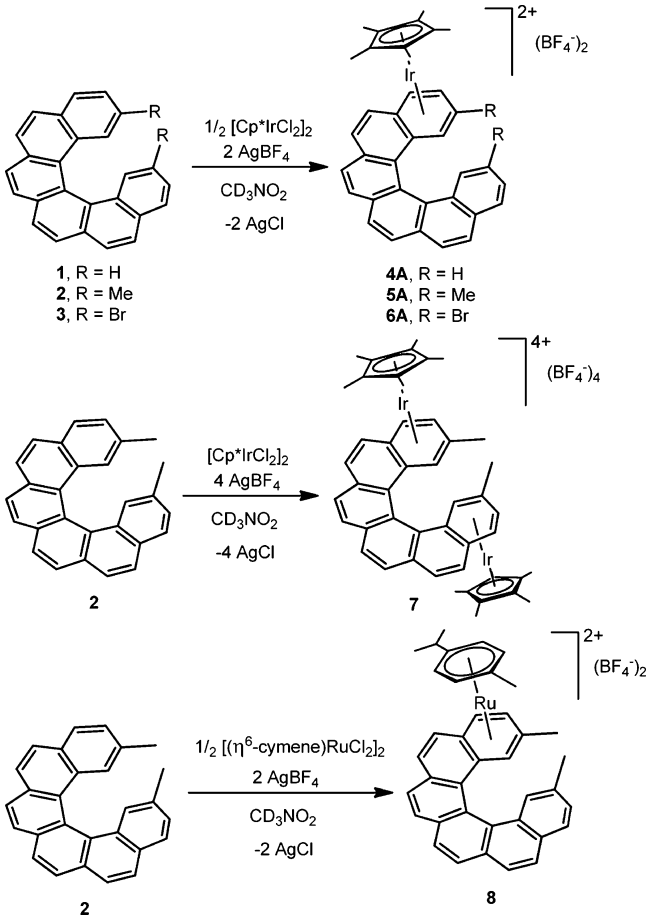

Previously, the synthesis of $[Cp^*Ir(\eta^6\text{-arene})](BF_4)_2$ complexes used the acetone solvent complex $[Cp^*Ir(OCMe_2)_3]$ as a reagent.[23] In the present work, η^6-hexalicene complexes of cyclopentadienyl–iridium have been prepared in a one-pot reaction starting from $[Cp^*IrCl_2]_2$, removing the need for synthesis of the acetone precursor. Additionally, this reaction proceeded smoothly with a solvent as weakly coordinating as nitromethane. Both facts promote a preferential binding between the cyclopentadienyl–iridium fragment and the aromatic compound, reducing the problem of competitive reactions with other potential ligands.

The reaction between $[Cp^*IrCl_2]_2$, $AgBF_4$, and **1** at room temperature under the aforementioned conditions led to preparation of **4A**. In the course of the reaction, three isomeric complexes **4A**, **4B**, and **4C** were observed by ^1H NMR (Scheme 2), two of which disappeared gradually, evolving into the single thermodynamic final product **4A**. After 15 min, the ratio between the isomers was 55:36:9 (**4A**:**4B**:**4C**). After 5 days at room temperature, the isomer **4C** had disappeared and the ratio between **4A** and **4B** was 80:20. This proportion was 93:7(**4A**:**4B**) within 10 days, and the quantitative formation of **4A** was observed after 15 days. In order to characterize these intermediates, we decided to carry out low-temperature NMR experiments. Thus, $[Cp^*IrCl_2]_2$, $AgBF_4$, and **1** were mixed in CD_3NO_2 directly into an NMR tube for study at 253 K. In the ^1H NMR spectrum acquired at that temperature, the presence of the three isomers in the ratio 27:64:9 (**4A**:**4B**:**4C**) was again observed (Figure 3).

Although none of the intermediates was isolated separately, the three isomers were characterized by NMR in CD_3NO_2 at low temperature [^1H, $^{13}C\{^1H\}$, $^1H-^1H$ correlation spectroscopy (COSY), $^1H-^1H$ nuclear Overhauser effect spectroscopy (NOESY), and $^1H-^{13}C$ heteronuclear single-quantum coherence (HSQC) NMR spectra]. The biggest challenge was to establish in which ring of the hexahelicene the metal fragment was coordinated. In the $^1H-^1H$ NOESY NMR spectrum, several cross peaks were detected between the hydrogens of the Cp* and hexahelicene ligands (see Supporting Information, Figure S9). These data showed that the $[IrCp^*]^{2+}$ metal fragment was in spatial proximity to H1, H2, H3, H4, H5, and H6 in **4A** (bonded to A ring); to H1, H2, H3, H4, H5, H6, H7, and H8 in **4B** (bonded to B ring); and to H1, H5, H6, H7, H8, H9, and H10 in **4C** (bonded to C ring) (following the labeling of Figure 2). An inspection of Cp* chemical shifts in ^1H and ^{13}C spectra of complexes **4A**, **4B**, and **4C**, summarized in Table 1, revealed several general trends. The Cp* chemical shifts are upfield for isomer **4C**, showing that the C ring has more electron density than the other two (A and B rings). Therefore, if only electronic factors are considered, the C ring of hexahelicene should form the most stable compounds for metal coordination. However, the final product is not coordinated to the C ring. The reason for this behavior is not clear, but it is probably influenced by the increase of steric hindrance from H(C1) and R (see Figure 2) as we move from ring A to ring F (Figure 2). In fact, there is no NMR evidence for the formation of cyclopentadienyl–iridium complexes coordinated to the D, E, or F rings (same face of the hexahelicene as the final product), showing the importance of steric factors in the control of the reaction.

Complex **5A** was obtained by following the procedure used for **4A**. The reaction was completed after 6 days to form compound **5A** quantitatively (see Table 2). In this case, the

Scheme 2

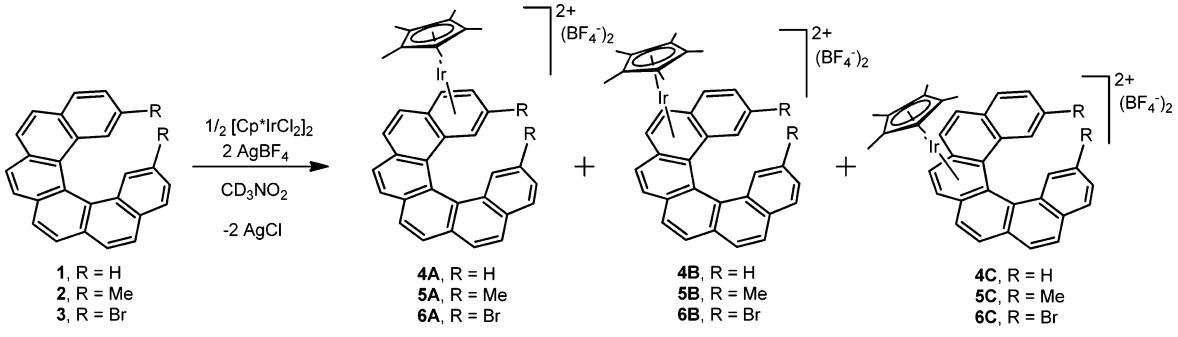

dx.doi.org/10.1021/ic300462z | Inorg. Chem. XXXX, XXX, XXX–XXX

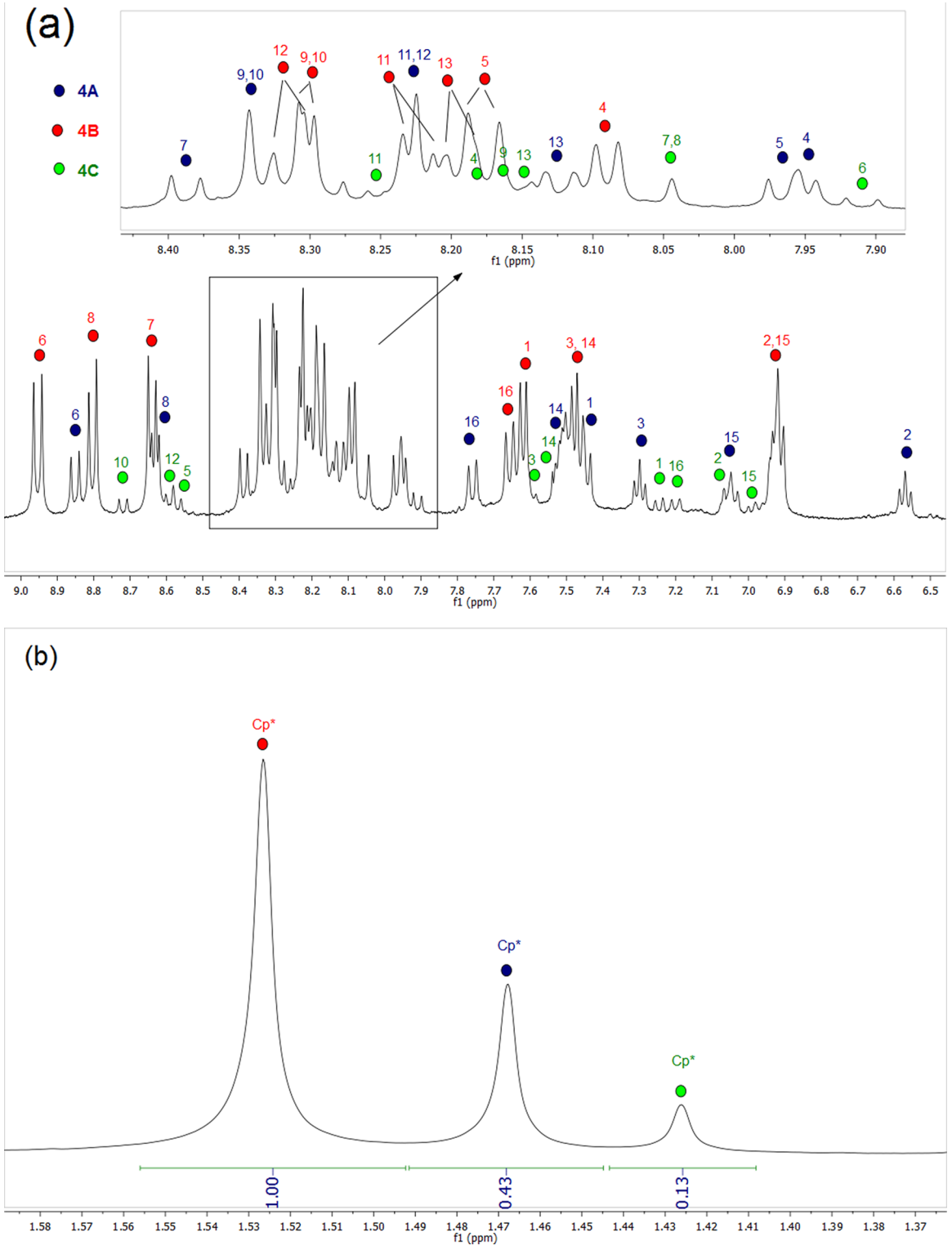

Figure 3. ^{1}H NMR spectrum at 253 K in (a) the aromatic region or (b) the cyclopentadienyl region of isomers **4A**, **4B**, and **4C** formed in the reaction between $[Cp^*IrCl_2]_2$, $AgBF_4$, and **1** in CD_3NO_2.

reaction rate was significantly higher than in the preparation of **4A**. Perhaps this is partially due to the increased stability of $[Cp^*Ir(\eta^6\text{-arene})](BF_4)_2$ complexes when the arenes are alkyl-substituted.[23] Monitoring the reaction by ^{1}H NMR spectroscopy showed the existence of two intermediates, as was observed in the case of **4A**. Although, unfortunately, none of them could be fully characterized, their spectroscopic similarities with the isomers **4B** and **4C** suggest their identification as the complexes **5B** and **5C**.

Under the same conditions, helicene **3**, $[Cp^*IrCl_2]_2$, and $AgBF_4$ reacted at room temperature to afford the complex **6A**. In the course of the reaction, two intermediates were detected. One of them was isolated and fully characterized at 253 K as complex **6C** (see Supporting Information). The ratio of the

dx.doi.org/10.1021/ic300462z | *Inorg. Chem.* XXXX, XXX, XXX−XXX

Table 1. Chemical Shifts of the Cyclopentadienyl Ligand in Isomers 4A−C[a]

	chemical shift (ppm)		
	4A	**4B**	**4C**
	^{1}H NMR		
Cp*	1.47	1.53	1.43
	^{13}C{^{1}H} NMR		
C_5Me_5	103.6	104.5	102.5
$C_5\mathit{Me}_5$	8.7	8.8	8.1

[a]In CD_3NO_2 at 253 K.

Table 2. Selected Chemical Shifts for Compounds 4A, 5A, and 6A[a]

	chemical shift (ppm)		
	4A	**5A**	**6A**
	^{1}H NMR		
Cp*	1.51	1.50	1.54
H1	7.43	7.31	7.64
H3	7.32	7.20	7.72
H4	7.96	7.87	8.06
	^{13}C{^{1}H} NMR		
C_5Me_5	105.3	104.7	106.4
$C_5\mathit{Me}_5$	8.9	8.6	8.5
C1	128.37		92.8
C2	128.43		
C3	98.14		101.6
C4	96.50		96.3

[a]In CD_3NO_2 at room temperature.

isomers **6A**:**6C** changed from 0:100 to 18:77 after 1 day at room temperature. The missing 5% was due to the presence of another isomer that could not be identified. Compound **6A** is the only product of the reaction mixture after 14 days. Isomer **6C** could be fully characterized by spectroscopic methods, since the ^{1}H NMR spectra at 253 K of complexes **4C** and **6C** display a similar pattern. The hydrogen signals for H10, H12, and H5 appear as doublets at 8.72, 8.59, and 8.57 ppm in **4C** and at 8.78, 8.65, and 8.62 ppm in **6C**. The next four signals between 8.3 and 8.1 ppm are assigned to H11, H4, H9, and H13, all showing a doublet appearance. Two signals of the C ring, H7 and H8, arise from second-order AB coupling at 8.04 ppm in **4C** and between 8.15 and 8.10 ppm in **6C**. The signal for H6 appears as a doublet at 7.91 in **4C** and at 7.99 in **6C**. Upfield signals corresponding to terminal rings of hexahelicenes could not be compared due to different substituents in 2 and 15 positions.

The availability of six rings in these systems permits the transition metal an opportunity to coordinate at more than one position. In all cases, the final products show coordination of the metal fragment to the terminal ring of the helicene. In addition, we found a clear preference for coordination to the C ring at the beginning of the reaction. This coordination is fast (less than 30 s), because free hexahelicene ligand was never observed. However, formation of the thermodynamic product occurs after several days at room temperature, which evidences a slow isomerization. This movement can occur by two ways: through a migration of metal cationic units walking over the surface or through an intermolecular dissociation/association mechanism. Recently, this migration has been observed in another nonplanar polyaromatic compound containing corannulene, $[(COE)_2Rh(\eta^6\text{-}C_{20}H_{10})]PF_6$, for which both NMR and computational data seem to demonstrate the slide as the most feasible mechanism.[17d]

The reaction between equivalent amounts of $[Cp^*IrCl_2]_2$ and **2** with an excess of $AgBF_4$ at room temperature in CD_3NO_2 solvent and under an nitrogen inert atmosphere led to formation of the homobimetallic complex $[(Cp^*Ir)_2(\mu_2\text{-}\eta^6\text{:}\eta^6\text{-}\mathbf{2})][BF_4]_4$ (**7**) (Scheme 1). The reaction was completed after 3 h to form the final compound quantitatively. This thermodynamic product **7** was isolated and fully characterized by ^{1}H, ^{13}C{^{1}H}, ^{1}H−^{1}H COSY, and ^{1}H−^{1}H NOESY NMR spectra in CD_3NO_2 (see Supporting Information). The reduced number of signals in the final ^{1}H NMR spectrum evidences the higher symmetry of this dimer, which presents the coordination of two metal fragments $[IrCp^*]^{2+}$ on the hexahelicene terminal rings. We assume that the coordination is on the exo side, since the geometry of the helicene does not permit the coordination on the endo side due to steric hindrance. The reaction rate is much higher than in the synthesis of the above monometallic complexes and could be explained by the formation of less stable intermediates. These plausible intermediates would have at least one of the two metal fragments coordinated to the internal rings. The proximity of the two rings coordinated to the metals would be disadvantageous when electronic and steric factors are considered. In addition, as already mentioned, the methyl group in the hexahelicene terminal rings favors the binding in this position. Both facts could help to promote this unusual and rapid evolution of the intermediates to afford the thermodynamic product **7**.

In an attempt to determine how many $[IrCp^*]^{2+}$ metal fragments can coordinate to 2,15-dimethylhexahelicene, an experiment was carried out in which 1 equiv of **2** and 3 equiv of $[IrCp^*]^{2+}$ were reacted under the same conditions. This reaction was monitored by ^{1}H NMR periodically over several weeks. No products with three $[IrCp^*]^{2+}$ units coordinated to **2** were observed, and the complex **7** was identified as the unique coordination product to the helicene. This reaction shows that only one $[IrCp^*]^{2+}$ metal fragment can be coordinated to each side of hexahelicene.

In order to explore the η^6-coordination of other metal fragments to hexahelicenes, we decided to study the coordination between 2,15-dimethylhexahelicene and another 12 e$^-$ metal fragment, $[(\eta^6\text{-cymene})Ru]^{2+}$. Thus, 1 equiv of $[(\eta^6\text{-cymene})RuCl_2]_2$ dimer, 2 equiv of helicene **2**, and 2 equiv of $AgBF_4$ in CD_3NO_2 solvent were reacted at room temperature to afford $[(\eta^6\text{-cymene})Ru(\eta^6\text{-}\mathbf{2})][BF_4]_2$ (**8**) in quantitative yield after 15 days (Scheme 1). During the reaction several intermediates were observed, but none could be fully characterized. The ^{1}H and ^{13}C NMR spectra of complex **8** (see Supporting Information) display a pattern similar to those observed in cymene−ruthenium compounds containing other arene ligands. For example, the proton signals for hydrogens attached to the coordinated rings are upfield relative to the free ligand, as reported for $[(\eta^6\text{-cymene})Ru(\eta^6\text{-coronene})][BF_4]_2$.[16c] The observed ^{13}C and ^{1}H chemical shifts for the *p*-cymene ligand in **8** are in agreement with those found in other Ru(II) sandwich complexes. The methyls of the isopropyl group in **8** are diasterotopic and appear as a pair of doublets. The same behavior has been found in $[(\eta^6\text{-cymene})Ru(\eta^6\text{-L})][BF_4]_2$, where L = triphenylene, 4*H*-cyclopentaphenanthrene, pyrene, 4,5-benzopyrene, 1,2:5,6-dibenzanthracene, naphthalene, phenanthrene, anthracene, fluorene, 9,10-dihy-

dx.doi.org/10.1021/ic300462z | *Inorg. Chem.* XXXX, XXX, XXX−XXX

droanthracene, *trans*-stilbene, *cis*-stilbene, coronene, chrysene, and perylene.[16]

Red crystals of complex **8** suitable for an X-ray diffraction study were obtained by layering a methylene chloride solution of the compound with diethyl ether and storing it at −20 °C overnight. In the structure of **8** the transition metal is η^6-coordinated to *p*-cymene ligand and η^6-coordinated to the terminal ring of hexahelicene. The distances between the ruthenium atom and the rings' centroid are 1.710 Å (*p*-cymene ligand) and 1.735 Å (terminal ring of hexahelicene) (Figure 4).

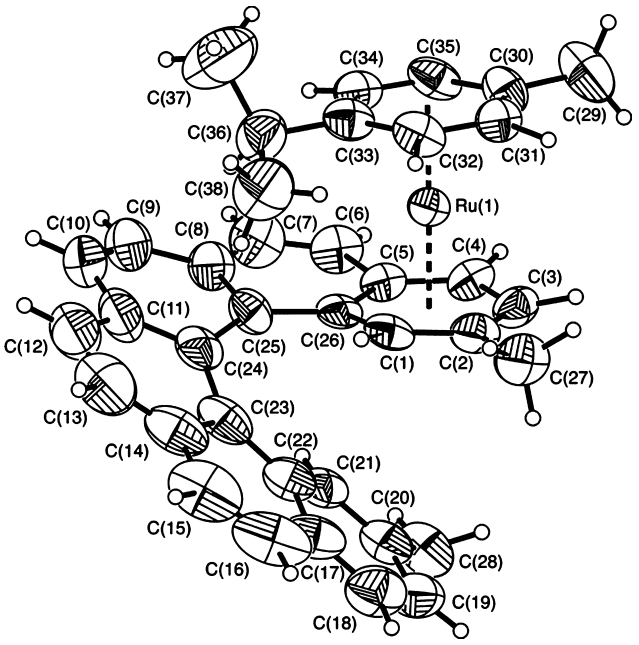

Figure 4. View of the [(η^6-cymene)Ru(η^6-**2**)][BF_4]$_2$ (**8**) structure illustrating the atomic numbering scheme. Only one of the stereo isomers is represented for clarity. Thermal ellipsoids have been drawn at the 30% probability level. The two BF_4^- counterions are not shown.

One of the parameters that can be used to describe the change of the helical structure as a consequence of the metal fragment coordination is the helical pitch, defined as the distance along the helical axis that results in one full turn of the helix. In this structure, the helical pitch measured between C2 and C20 is 3.828 Å, while in free hexahelicene the pitch is 4.576 Å.[24] These data show that the coordination of the (η^6-cymene)Ru^+ unit flattens the hexahelicene ligand.

DFT calculations were performed to gain additional information into the experimental findings. Complex **8** was examined computationally at the B3LYP/SVP (SDD for Ru) level of theory in nitromethane as solvent. The calculated structure of **8** is in reasonable agreement with the obtained X-ray crystallography structure. All bond distances in the minimized structure compare well with the experimental ones (see Supporting Information, Table S1). For example, the calculated helical pitch distance of 4.152 Å is close to the experimentally observed value of 3.828 Å, when it is taken into account that packing forces in the solid state can affect to some extent the helical pitch.

The potential energy surfaces (PES) were also simulated for the systems with cyclopentadienyl iridium coordinated to A, B, and C rings of hexahelicene (complexes **4A**, **4B**, and **4C**, respectively). If the structure of **4B** is chosen as the zero-energy reference point, the final product **4A** is lower in energy by ΔG_{298K} = −7.7 kcal/mol, while the complex **4C** has ΔG_{298K} = −2.3 kcal/mol. As expected, these energies are in good agreement with the formation of the observed structures.

DFT calculations were again performed to determine the transition states and the barriers connecting complexes **4A**, **4B**, and **4C** (Figure 5). Two new local minima (**4AB** and **4BC**) were located in the potential energy surface (PES), which correspond to η^3-C═C−C coordination of the metal between two adjacent rings. Also, four transition states were observed, all of them presenting η^2-C═C coordination. The movement of the metal center from **4C** to **4B** involves a haptotropic rearrangement from η^6-arene to η^3-C═C−C (**4C** → **4BC**) via TS(**4C**−**4BC**), followed by a new haptotropic migration from

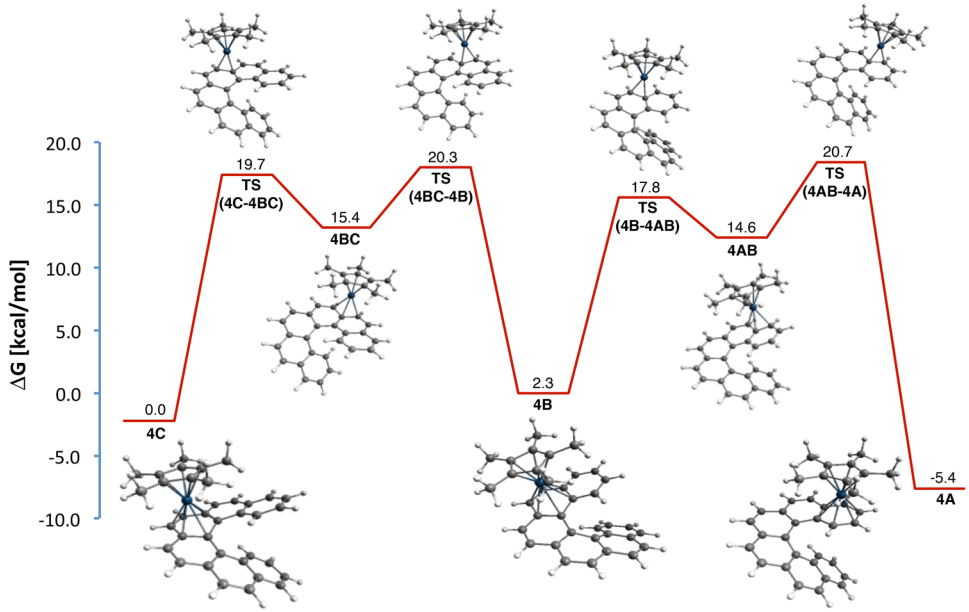

Figure 5. Reaction profile [kilocalories per mole, B3LYP/SVP (SDD for Ir)] for the ring-walking and the structures of the various complexes. (Atomic color scheme: C, gray; H, white; iridium, blue.)

dx.doi.org/10.1021/ic300462z | *Inorg. Chem.* XXXX, XXX, XXX−XXX

η^3-C=C−C to η^6-arene (**4BC** → **4B**) via TS(**4BC**−**4B**). A similar reorganization was observed to pass from **4B** to **4A**. Related findings have been observed by Solà and co-workers[25] in a previous work, where the metal fragment is tricarbonylchromium. These computational results suggest that a ring walking process through a haptotropic rearrangement is a plausible movement for this system, although dissociation could not be completely ruled out.

CONCLUSIONS

In summary, the first η^6-complexes of iridium and ruthenium coordinated to helicenes have been obtained. All of them show η^6-coordination of the metal fragment to the helicene terminal ring as manifested in the X-ray structure of complex **8**. We have also identified and fully characterized some of the intermediates in which the metal fragment is coordinated to the helicene internal rings. The first detected intermediates show the metal unit η^6-coordinated to the C ring. The subsequent migration from the C ring to the A ring (final product) is a slow process that occurs over several days. DFT calculations were performed to support a plausible reaction profile of this isomerization. In these studies, new local minima and some transition states were located and a haptotropic rearrangement seems to be the most feasible movement. In search of the maximum number of metal fragments that can be coordinated to hexahelicene, we synthesized complex **7**. This dimer involves coordination of two metal fragments $[IrCp^*]^{2+}$ on the exo side of the hexahelicene terminal rings, which is the maximum number of metal units that can be bonded.

ASSOCIATED CONTENT

Supporting Information

Additional text, 31 figures, and additional tables giving full characterization, NMR spectra (^1H, $^{13}C\{^1H\}$, COSY, NOESY, and HSQC) for compounds **4A**, **4A**/**4B**/**4C** mixture, **5A**, **6A**, **6C**, **7**, and **8**; computational details; and crystallographic data for complex **8**. This material is available free of charge via the Internet at http://pubs.acs.org.

AUTHOR INFORMATION

Corresponding Author

*E-mail: celedonio.alvarez@uva.es. Telephone: +34 983184096. Fax: +34 983423013.

Notes

The authors declare no competing financial interest.

ACKNOWLEDGMENTS

The authors wish to thank Dr. Gabriel Aullón for his help with the theoretical studies. This work was funded by the Spanish Ministerio de Ciencia e Innovación (CTQ2009-12111) and the Junta de Castilla y León (VA070A08 and GR Excelencia 125). H.B. and C.M.A. acknowledge with thanks a MEC-FPI grant and a Ramón y Cajal contract, and L.A.G.-E. thanks University of Valladolid for a Ph.D. grant.

REFERENCES

(1) (a) Urbano, A. *Angew. Chem., Int. Ed.* **2003**, *42*, 3986−3989. (b) Katz, T. J. *Angew. Chem., Int. Ed.* **2000**, *39*, 1921−1923.

(2) (a) Wigglesworth, T. J.; Sud, D.; Norsten, T. B.; Lekhi, V. S.; Branda, N. R. *J. Am. Chem. Soc.* **2005**, *127*, 7272−7273. (b) Botek, E.; Champane, B.; Turki, M.; André, J. M. *J. Chem. Phys.* **2004**, *120*, 2042−2048. (c) Nuckolls, C.; Katz, T. J.; Verbiest, T.; Van Elshotch, S.; Kuball, H. G.; Kiesewalter, S.; Lovinger, A. J.; Persoons, A. *J. Am. Chem. Soc.* **1998**, *120*, 8656−8660.

(3) (a) Furche, F.; Ahlrichs, R.; Wachsmann, C.; Weber, E.; Sobanski, A.; Vögtle, F.; Grimme, S. *J. Am. Chem. Soc.* **2000**, *122*, 1717−1724. (b) Treboux, G.; Lapstun, P.; Wu, Z.; Silverbrook, K. *Chem. Phys. Lett.* **1999**, *301*, 493−497. (c) Beljonne, D.; Shuai, Z.; Brédas, J. L.; Kauranen, M.; Verbiest, T.; Persoons, A. *J. Chem. Phys.* **1998**, *108*, 1301−1304.

(4) For recent work, see (a) Carbery, D. R.; Critall, M. R.; Rzpea, H. S. *Org. Lett.* **2011**, *13*, 1250. (b) Krausová, Z.; Sehnal, P.; Bondzic, B. P.; Chercheja, S.; Eilbracht, P.; Stará, I. G.; Šaman, D.; Starý, I. *Eur. J. Org. Chem.* **2011**, 3849. (c) Takenaka, N.; Chen, J. S.; Captain, B.; Sarangthem, R. S.; Chandrakumar, A. *J. Am. Chem. Soc.* **2010**, *132*, 4536. (d) Šámal, M.; Míšek, J.; Stará, I. G.; Starý, I. *Collect. Czech. Chem. Commun.* **2009**, *74*, 1151. (e) Chen, J. S.; Takenaka, N. *Chem.—Eur. J.* **2009**, *15*, 7268. (f) Takenaka, N.; Sarangthem, R. S.; Captain, B. *Angew. Chem., Int. Ed.* **2008**, *47*, 9708.

(5) While short helicenes are able to interconvert, it is assumed that the geometry of hexahelicenes does not permit interconversion. (a) Amabilino, D. B. *Chirality at the Nanoscale*; Wiley-VCH: Weinheim, Germany, 2009. (b) Janke, R. H.; Haufe, G.; Würthwein, E.-U.; Borkent, J. H. *J. Am. Chem. Soc.* **1996**, *118*, 6031−6035. (c) Grimme, S.; Peyerimhoff, D. *Chem. Phys.* **1996**, *204*, 411−417.

(6) For recent work, see (a) Wang, D. Z. G.; Katz, T. J. *J. Org. Chem.* **2005**, *70*, 8497. (b) Reetz, M. T.; Sostmann, S. *Tetrahedron* **2001**, *57*, 2515−2520. (c) Murguly, E.; McDonald, R.; Branda, N. R. *Org. Lett.* **2000**, *2*, 3169−3172. (d) Weix, D. J.; Drether, S. D.; Katz, T. J. *J. Am. Chem. Soc.* **2000**, *122*, 10027−10032.

(7) For recent work, see (a) Amemiya, R.; Mizutani, M.; Yamaguchi, M. *Angew. Chem., Int.Ed.* **2010**, *49*, 1995. (b) Ernst, K.-H. Z. *Phys. Chem.* **2009**, *223*, 37. (c) Ernst, K.-H. *Chimia* **2008**, *62*, 471. (d) Sugiura, H.; Amemiya, R.; Yamaguchi, M. *Chem.—Asian J.* **2008**, *3*, 244. (e) Amemiya, R.; Saito, N.; Yamaguchi, M. *J. Org. Chem.* **2008**, *73*, 7137. (f) Amemiya, R.; Yamaguchi, M. *Chem. Rec.* **2008**, *8*, 116. (g) Amemiya, R.; Yamaguchi, M. *Org. Biomol. Chem.* **2008**, *6*, 26.

(8) For recent work, see (a) Suzuki, T.; Ishigaki, Y.; Iwai, T.; Kawai, H.; Fujiwara, K.; Ikeda, H.; Kano, Y.; Mizuno, K. *Chem.—Eur. J.* **2009**, *15*, 9434. (b) Markey, M. D.; Kelly, T. R. *Tetrahedron* **2008**, *64*, 8381. (c) Kelly, T. R.; Cai, X. L.; Damkaci, F.; Panicker, S. B.; Tu, B.; Bushell, S. M.; Cornella, I.; Piggott, M. J.; Salives, R.; Cavero, M.; Zhao, Y. J.; Jasmin, S. *J. Am. Chem. Soc.* **2007**, *129*, 376. (d) Tani, Y.; Ubukata, T.; Yokoyama, Y.; Yokoyama, Y. *J. Org. Chem.* **2007**, *72*, 1639. (e) Okuyama, T.; Tani, Y.; Miyake, K.; Yokoyama, Y. *J. Org. Chem.* **2007**, *72*, 1634.

(9) For recent work, see (a) Shinohara, K.; Sannohe, Y.; Kaieda, S.; Tanaka, K.; Osuga, H.; Tahara, H.; Xu, Y.; Kawase, T.; Bando, T.; Sugiyama, H. *J. Am. Chem. Soc.* **2010**, *132*, 3778. (b) Passeri, R.; Aloisi, G. G.; Elisei, F.; Latterini, L.; Caronna, T.; Fontana, F.; Sora, I. N. *Photochem. Photobiol. Sci.* **2009**, *8*, 1574. (c) Xu, Y.; Zhang, Y. X.; Sugiyama, H.; Umano, T.; Osuga, H.; Tanaka, K. *J. Am. Chem. Soc.* **2004**, *126*, 6566.

(10) For liquid crystal applications, see (a) Vyklický, L.; Eichhorn, S. H.; Katz, T. J. *Chem. Mater.* **2003**, *15*, 3594. (b) Verbiest, T.; Sioncke, S.; Persoons, A.; Vyklický, L.; Katz, T. J. *Angew. Chem., Int. Ed.* **2002**, *41*, 3882. (c) Nuckolls, C.; Shao, R.; Jang, W. G.; Clark, N. A.; Walba, D. M.; Katz, T. J. *Chem. Mater.* **2002**, *14*, 773−776. Dye materials: (d) Ooyama, Y.; Ito, G.; Kushimoto, K.; Komaguchi, K.; Imae, I.; Harima, Y. *Org. Biomol. Chem.* **2010**, *8*, 2756. (e) Ooyama, Y.; Inoue, S.; Asada, R.; Ito, G.; Kushimoto, K.; Komaguchi, K.; Imae, I.; Harima, Y. *Eur. J. Org. Chem.* **2010**, 92. (f) Ooyama, Y.; Ito, G.; Fukuoka, H.; Nagano, T.; Kagawa, Y.; Imae, I.; Komaguchi, K.; Harima, Y. *Tetrahedron* **2010**, *66*, 7268. (g) Ooyama, Y.; Harima, Y. *Eur. J. Org. Chem.* **2009**, 2903. (h) Ooyama, Y.; Shimada, Y.; Ishii, A.; Ito, G.; Kagawa, Y.; Imae, I.; Komaguchi, K.; Harima, Y. *J. Photochem. Photobiol. A* **2009**, *203*, 177. Polymers: (i) Tagami, K.; Tsukada, M.; Wada, Y.; Iwasaki, T.; Nishide, H. *J. Chem. Phys.* **2003**, *119*, 7491. (j) Bender, T. P.; MacKinnon, S. M.; Wang, Z. Y. *J. Polym. Sci., Polym. Chem.* **2000**, *38*, 758. Langmuir−Blodgett films: (k) Feng, P.; Miyashita, T.; Okubo, H.; Yamaguchi, M. *J. Am. Chem. Soc.* **1998**, *120*,

10166. (l) Nuckolls, C.; Katz, T. J.; Verbiest, T.; Van Elshocht, S.; Kuball, H. G.; Kiesewalter, S.; Lovinger, A. J.; Persoons, A. *J. Am. Chem. Soc.* **1998**, *120*, 8656.
(11) Newman, M. S.; Lednicer, D. *J. Am. Chem. Soc.* **1956**, *78*, 4765−4770.
(12) For recent work, see (a) Aloui, F.; Hassine, B. B. *Tetrahedron Lett.* **2009**, *50*, 4321−4323. (b) Aloui, F.; El Abed, R.; Marinetti, A.; Ben Hassine, B. *C. R. Chim.* **2009**, *12*, 284. (c) El Abed, R.; Aloui, F.; Genet, J. P.; Ben Hassine, B.; Marinetti, A. *J. Organomet. Chem.* **2007**, *692*, 1156. (d) Aloui, F.; El Abed, R.; Marinetti, A.; Ben Hassine, B. *Tetrahedron Lett.* **2007**, *48*, 2017. (e) El Abed, R.; Ben Hassine, B.; Gênet, J. P.; Gorsane, M.; Marinetti, A. *Eur. J. Org. Chem.* **2004**, 1517−1522. (f) Wachsmann, C.; Weber, E.; Czugler, M.; Seichter, W. *Eur. J. Org. Chem.* **2003**, 2863. (g) de Koning, C. B.; Michael, J. P.; Rousseau, A. L. *J. Chem. Soc., Perkin Trans. 1* **2000**, 787. (h) Yano, K.; Osatani, M.; Tani, K.; Adachi, T.; Yamamoto, K.; Matsubara, H. *Bull. Chem. Soc. Jpn.* **2000**, *73*, 185−189. (i) Stammel, C.; Froehlich, R.; Wolff, C.; Wenck, H.; de Meijere, A.; Mattay, J. *Eur. J. Org. Chem.* **1999**, 1709−1718. (j) Meier, H.; Schwertel, M.; Schollmeyer, D. *Angew. Chem., Int. Ed.* **1998**, *37*, 2110−2113.
(13) For recent work, see (a) Rybáček, J.; Huerta-Angeles, G.; Kollárovič, A.; Stará, I. G.; Starý, I.; Rahe, P.; Nimmrich, M.; Kühnle, A. *Eur. J. Org. Chem.* **2011**, 853. (b) Rahe, P.; Nimmrich, M.; Greuling, A; Schütte, J.; Stará, I. G.; Rybáček, J.; Huerta-Angeles, G.; Starý, I.; Rohlfing, M.; Kühnle, A. *J. Phys. Chem. C* **2010**, *114*, 1547. (c) Songis, O.; Císek, J.; Schmid, M. B.; Kollárovie, A.; Stará, I. G.; Šaman, D.; Cisarová, I.; Starý, I. *J. Org. Chem.* **2010**, *75*, 6889. (d) Storch, J.; Sýkora, J.; Èermák, J.; Karban, J.; Císarová, I.; Rùzièka, A. *J. Org. Chem.* **2009**, *74*, 3090−3093. (e) Adriaenssens, L.; Severa, L.; Šálová, T.; Císarová, I.; Pohl, R.; Šaman, D.; Rocha, S. V.; Finney, N. S.; Pospíšil, L.; Slavícek, P.; Teplý, F. *Chem.—Eur. J.* **2009**, *15*, 1072−1076. (f) Tanaka, K.; Fukawa, N.; Suda, T.; Noguchi, K. *Angew. Chem.,Int. Ed.* **2009**, *48*, 5470. (g) Goretta, S.; Tasciotti, C.; Mathieu, S.; Smet, M.; Maes, W.; Chabre, Y. M.; Dehaen, W.; Giasson, R.; Raimundo, J. M.; Henry, C. R.; Barth, C.; Gingras, M. *Org. Lett.* **2009**, *11*, 3846. (h) Sehnal, P.; Stará, I. G.; Šaman, D.; Tichy, M.; Míšek, J.; Cvačka, J.; Rulíšek, L.; Chocholousova, J.; Vacek, J.; Goryl, G.; Szymonski, M.; Císarová, I.; Starý, I. *Proc. Natl. Acad. Sci. U.S.A.* **2009**, *106*, 13169.
(14) Shen, Y.; Chen, C.-F. *Chem. Rev.* **2012**, *112*, 1463.
(15) For reviews, see (a) Chatani, N. *Sci. Synth.* **2002**, *1*, 931−972. (b) O'Connor, J. M. *Sci. Synth.* **2002**, *1*, 617−744.
(16) (a) Porter, L. C.; Polam, J. R.; Bodige, S. *Inorg. Chem.* **1995**, *34*, 998−1001. (b) Porter, L. C.; Polam, J. R.; Mahmoud, J. *Organometallics* **1994**, *13*, 2092−2096. (c) Suravajjala, S.; Polam, J. R.; Porter, L. C. *Organometallics* **1994**, *13*, 37−42.
(17) (a) Filatov, A. S.; Petrukhina, M. A. *Coord. Chem. Rev.* **2010**, *254*, 2234−2246. (b) Petrukhina, M. A. *Angew. Chem., Int. Ed.* **2008**, *47*, 1550−1552. (c) Zhu, B.; Ellern, A.; Sygula, A.; Sygula, R.; Angelici, R. J. *Organometallics* **2007**, *26*, 1721−1728. (d) Siegel, J. S.; Baldridge, K. K.; Linden, A.; Dorta, R. *J. Am. Chem. Soc.* **2006**, *128*, 10644−10645. (e) Vecchi, P. A.; Alvarez, C. M.; Ellern, A.; Angelici, R. J.; Sygula, A.; Sygula, R.; Rabideau, P. W. *Organometallics* **2005**, *24*, 4543−4552. (f) Seiders, T. J.; Baldridge, K. K.; O'Connor, J. M.; Siegel, J. S. *Chem. Commum.* **2004**, 950−951. (g) Vecchi, P. A.; Alvarez, C. M.; Ellern, A.; Angelici, R. J.; Sygula, A.; Sygula, R.; Rabideau, P. W. *Angew. Chem., Int. Ed.* **2004**, *43*, 4497−4500. (h) Alvarez, C. M.; Angelici, R. J.; Sygula, A.; Sygula, R.; Rabideau, P. W. *Organometallics* **2003**, *22*, 624−626. (i) Seiders, T. J.; Baldridge, K. K.; O'Connor, J. M.; Siegel, J. S. *J. Am. Chem. Soc.* **1997**, *119*, 4781.
(18) (a) Haddon, R. C. *Science* **1993**, *261*, 1545. (b) Haddon, R. C. *Acc. Chem. Res.* **1988**, *21*, 243. (c) Haddon, R. C.; Scott, L. T. *Pure. Appl. Chem.* **1986**, *58*, 137.
(19) Our compounds are, as far we know, the first examples of metal coordination to "normal" [n]-helicenes. However there are a few examples of η^5-coordination in helicene derivatives capped with cyclopentadienyl groups and several studies with heterohelicenes. For η^5-Cp derivatives, see (a) Sudhakar, A.; Katz, T. J.; Yang, B. W. *J. Am. Chem. Soc.* **1986**, *108*, 2790−2791. (b) Sudhakar, A.; Katz, T. J. *J. Am. Chem. Soc.* **1986**, *108*, 179−181. (c) Dewan, J. C. *Organometallics* **1983**, *2*, 83. (d) Katz, T. J.; Pesti, J. *J. Am. Chem. Soc.* **1982**, *104*, 346−347. For metal heterohelicenes, see (e) Anger, E.; Rudolph, M.; Shen, C.; Vanthuyne, N.; Toupet, L.; Roussel, C.; Autschbach, J.; Crassous, J.; Réau, R. *J. Am. Chem. Soc.* **2011**, *133*, 3800−3803. (f) Graule, S.; Rudolph, M.; Shen, W. T.; Williams, J. A. G.; Lescop, C.; Autschbach, J.; Crassous, J.; Reau, R. *Chem.—Eur. J.* **2010**, *16*, 5976. (g) Norel, L.; Rudolph, M.; Vanthuyne, N.; Williams, J. A. G.; Lescop, C.; Roussel, C.; Autschbach, J.; Crassous, J.; Reau, R. *Angew. Chem., Int. Ed.* **2010**, *49*, 99. (h) Graule, S.; Rudolph, M.; Vanthuyne, N.; Autschbach, J.; Roussel, C.; Crassous, J.; Reau, R. *J. Am. Chem. Soc.* **2009**, *131*, 3183. (i) Aloui, F.; Hassine, B. B. *Tetrahedron Lett.* **2009**, *50*, 4321. (j) Garcia, M. H.; Florindo, P.; Piedade, M. D. M.; Maiorana, S.; Licandro, E. *Polyhedron* **2009**, *28*, 621. (k) Shen, W. T.; Graule, S.; Crassous, J.; Lescop, C.; Gornitzka, H.; Reau, R. *Chem. Commun.* **2008**, 850. (l) El Abed, R.; Aloui, F.; Genet, J. P.; Ben Hassine, B.; Marinetti, A. *J. Organomet. Chem.* **2007**, *692*, 1156.
(20) (a) Mallory, F. B.; Mallory, C. W. Photocyclization of stilbenes and related molecules. *Organic Reactions*; Wiley: Hoboken, NJ, 1984; Vol. *30*. (b) Lightner, D. A.; Hefelfinger, D. T.; Powers, T. W.; Frank, G. W.; Trueblood, K. N. *J. Am. Chem. Soc.* **1972**, *94*, 3492−3497.
(21) (a) Sato, M.; Yamamoto, K.; Sonobe, H.; Yano, K.; Matsubara, H.; Fujita, H.; Sugimoto, T.; Yamamoto, K. *J. Chem. Soc., Perkin Trans. 2* **1998**, 1909−1913. (b) Yamamoto, K.; Sonobe, H.; Matsubara, H.; Sato, M.; Okamoto, S.; Kitaura, K. *Angew. Chem., Int. Ed.* **1996**, *35*, 69−70.
(22) Yamamoto, K.; Ikeda, T.; Kitsudi, T.; Okamoto, Y; Chikamatsu, H.; Nakazaki, M. *J. Chem. Soc., Perkin Trans. 1* **1990**, 271−276.
(23) White, C.; Thompson, S. J.; Maitlis, P. M. *J. Chem. Soc., Dalton Trans.* **1977**, 1654.
(24) de Rango, C.; Tsoucaris, C.; Decclercq, J. P.; Germain, G.; Putzeys, J. P. *Cryst. Struct. Commun.* **1973**, 189.
(25) Jiménez-Halla, J. O. C.; Robles, J.; Solà, M. *Organometallics* **2008**, *27*, 5230−5240.

dx.doi.org/10.1021/ic300462z | *Inorg. Chem.* XXXX, XXX, XXX−XXX

Supporting Information

η^6-Hexahelicene Complexes of Iridium and Ruthenium. Running along the Helix

Celedonio M. Álvarez*, Héctor Barbero, Luis A. García-Escudero, José M. Martín Álvarez, Cristina Martínez-Pérez, Daniel Miguel

IU CINQUIMA/Química Inorgánica, Facultad de Ciencias, Universidad de Valladolid, E-47005, Valladolid, Spain

* To whom correspondence should be addressed. E-mail: celedonio.alvarez@uva.es.

I. Spectroscopic Characterization

II. Crystallographic Data for [(η^6-cymene)Ru(η^6-2)][BF_4]$_2$ (8).

Crystallographic Experimental Section

Selected Bond Distances and Angles

III. Computational details.

I. Spectroscopic Characterization.

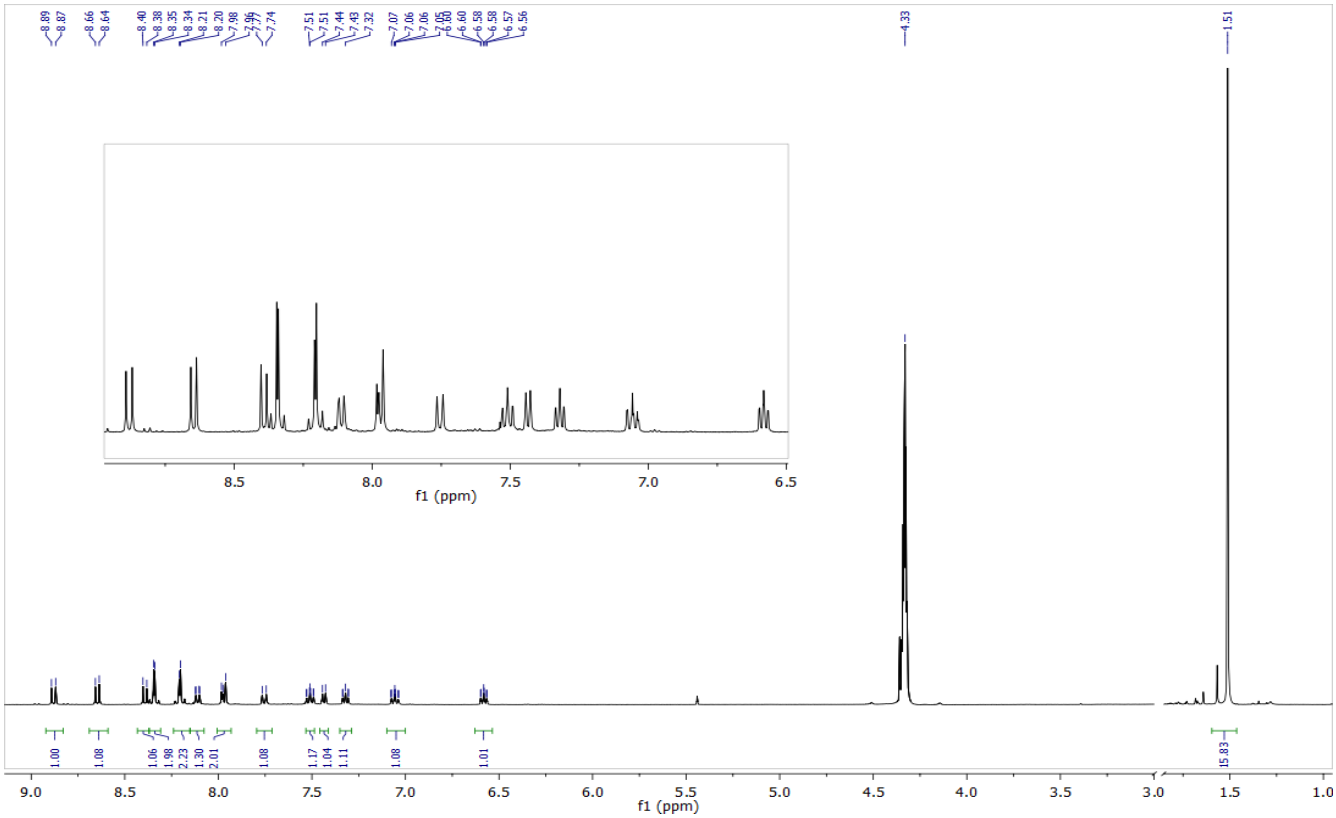

Figure S1. ^{1}H NMR spectrum of **4A** in CD_3NO_2.

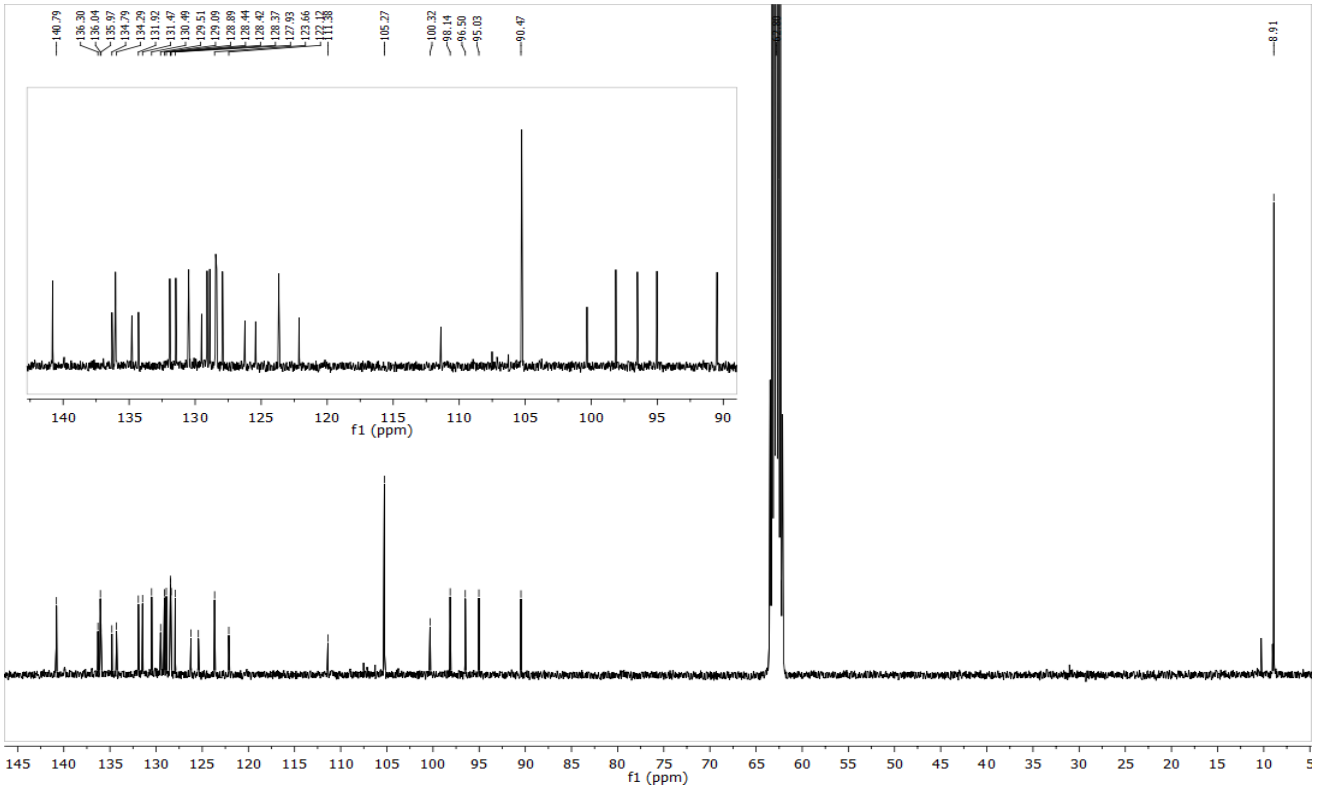

Figure S2. $^{13}C\{^{1}H\}$ NMR spectrum of **4A** in CD_3NO_2.

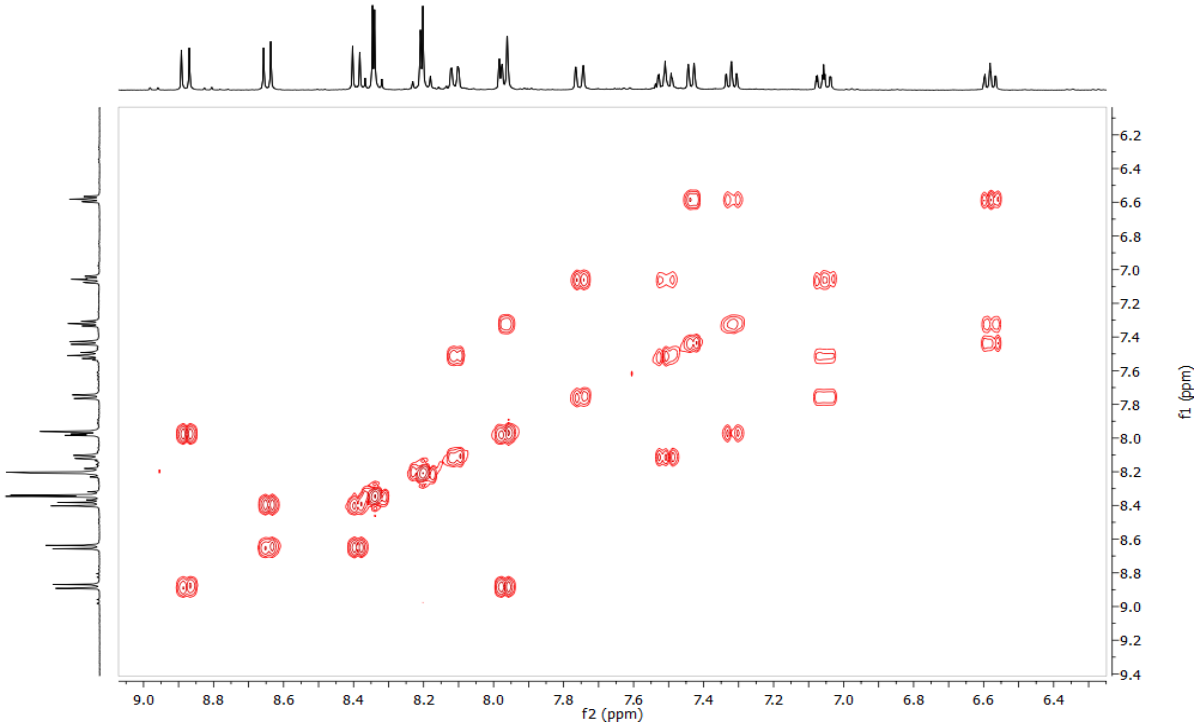

Figure S3. COSY NMR spectrum of **4A** in CD_3NO_2.

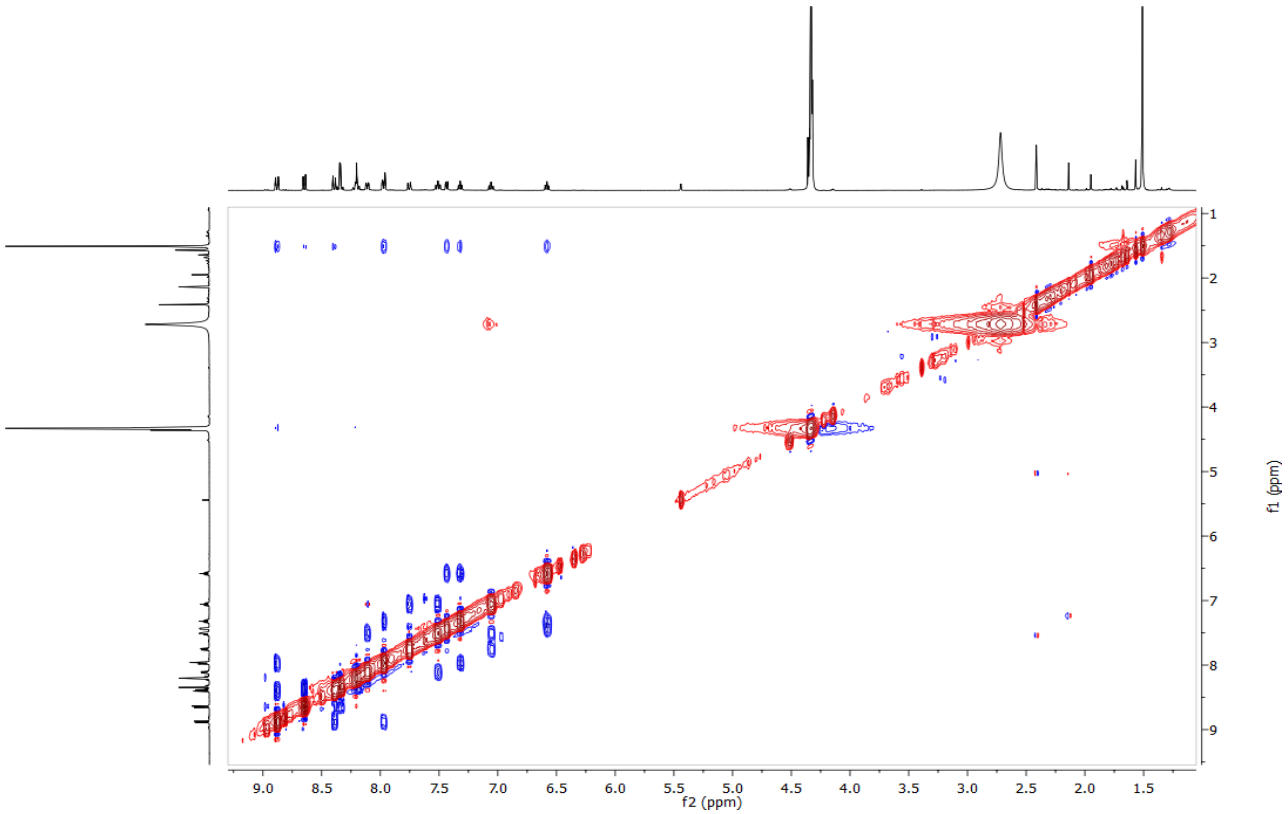

Figure S4. NOESY NMR spectrum of **4A** in CD_3NO_2.

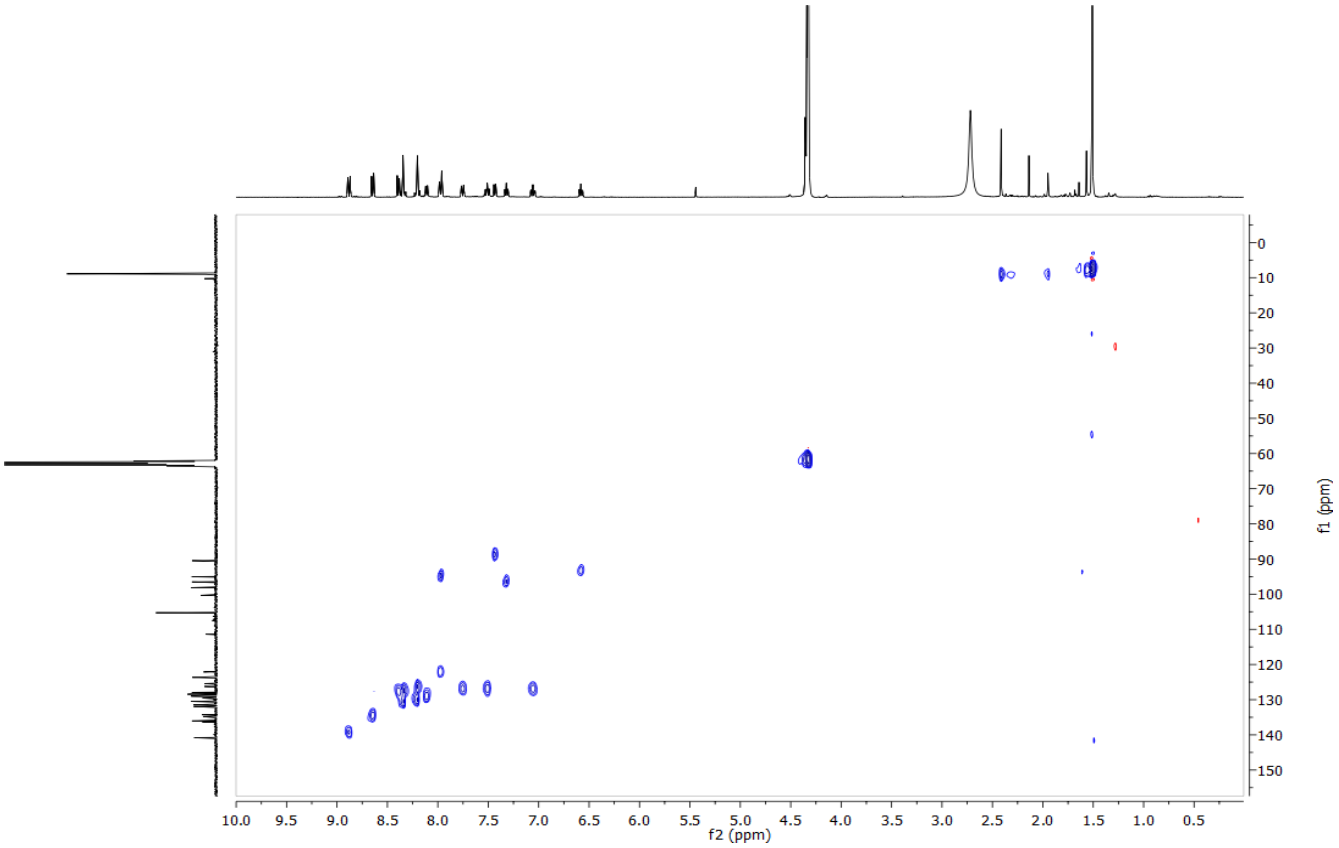

Figure S5. ^{1}H-^{13}C HSQC NMR spectrum of **4A** in CD_3NO_2.

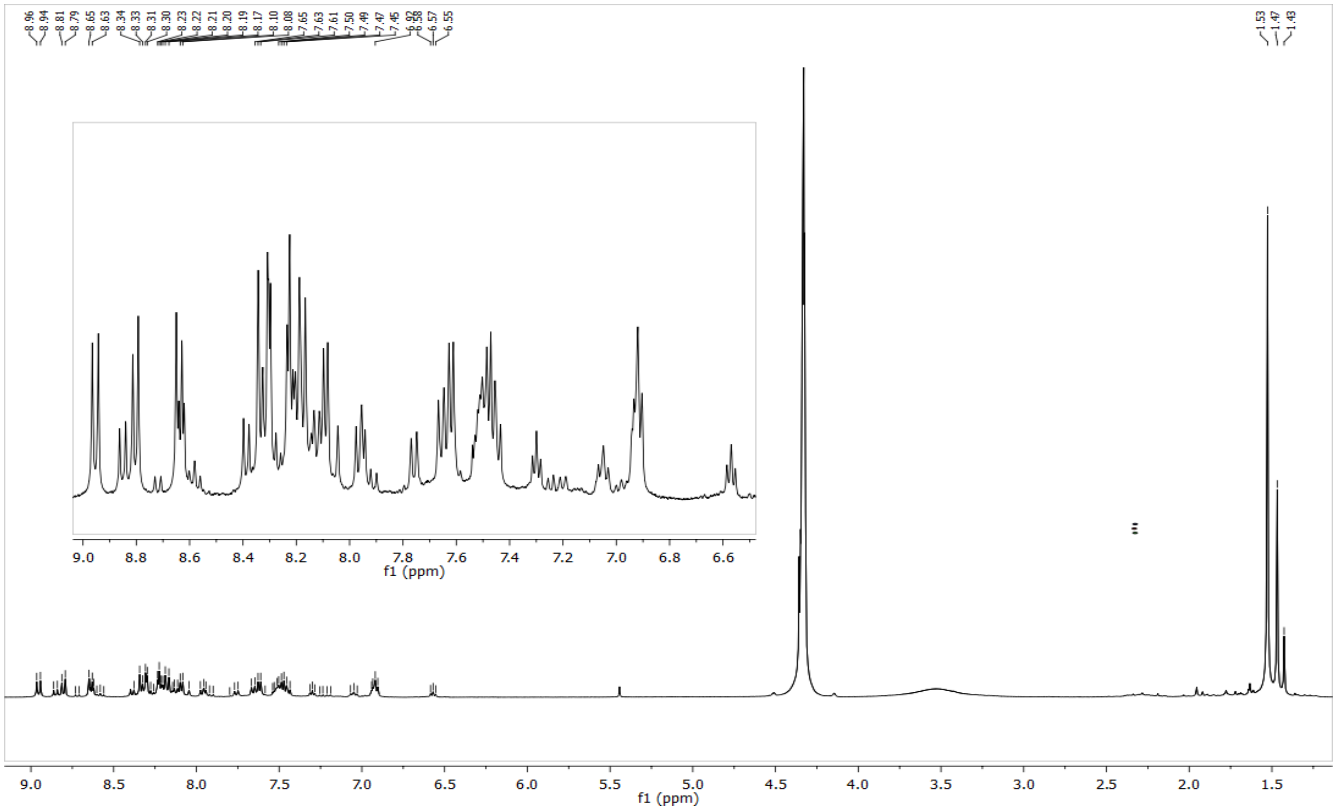

Figure S6. ^{1}H NMR spectrum of the mixture of **4A**, **4B** and **4C** in CD_3NO_2 at 253K.

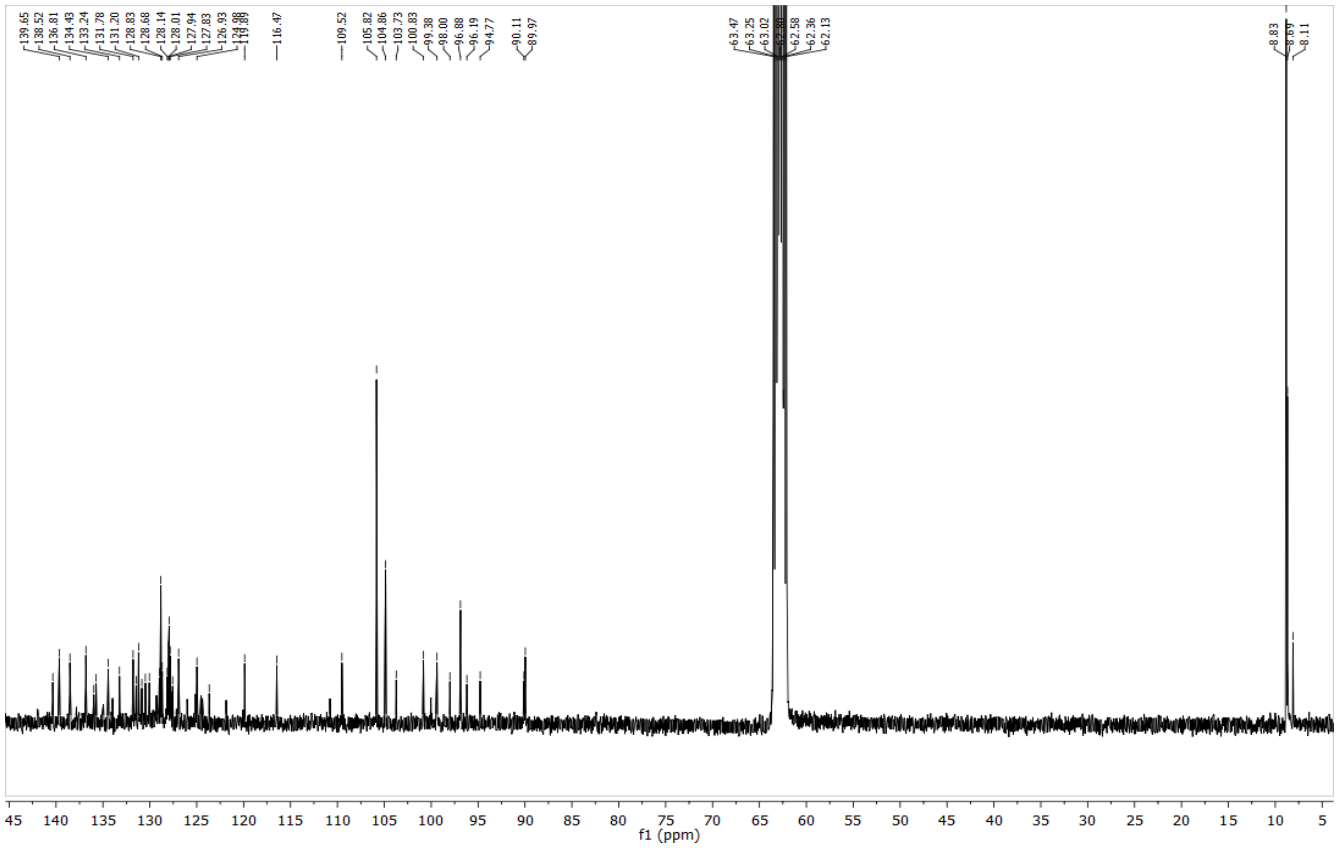

Figure S7. $^{13}C\{^{1}H\}$ NMR spectrum of the mixture of **4A**, **4B** and **4C** in CD_3NO_2 at 253K.

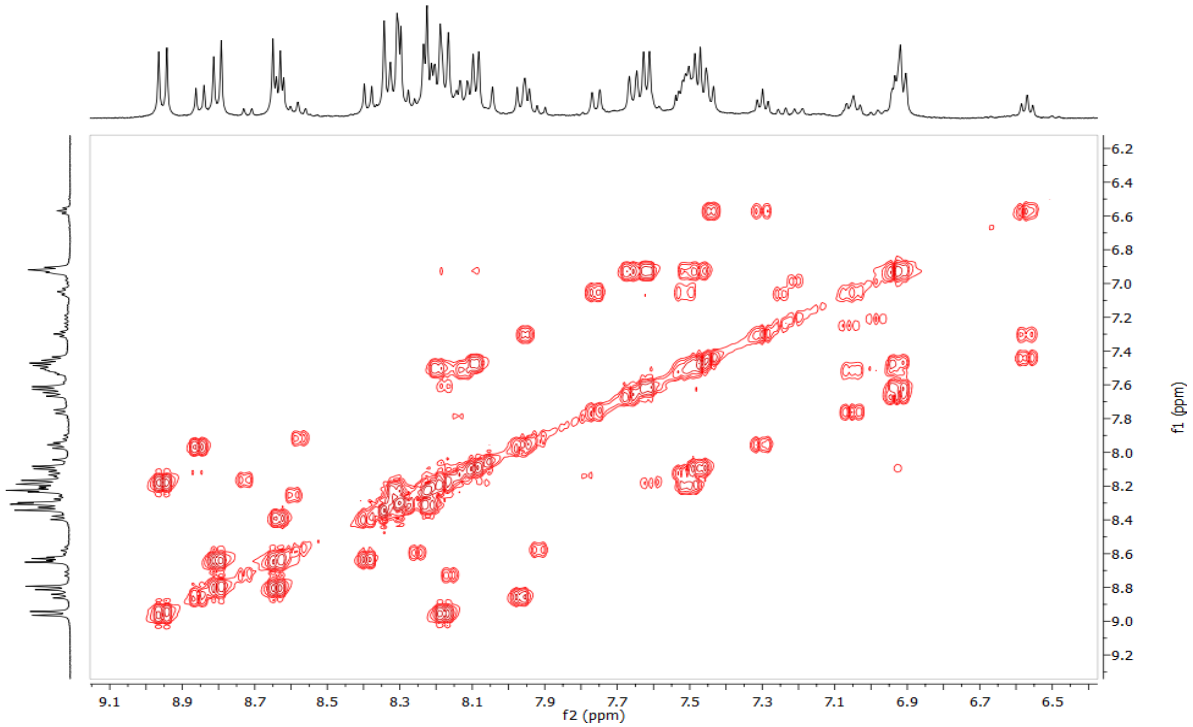

Figure S8. COSY NMR spectrum of the mixture of **4A**, **4B** and **4C** in CD_3NO_2 at 253K.

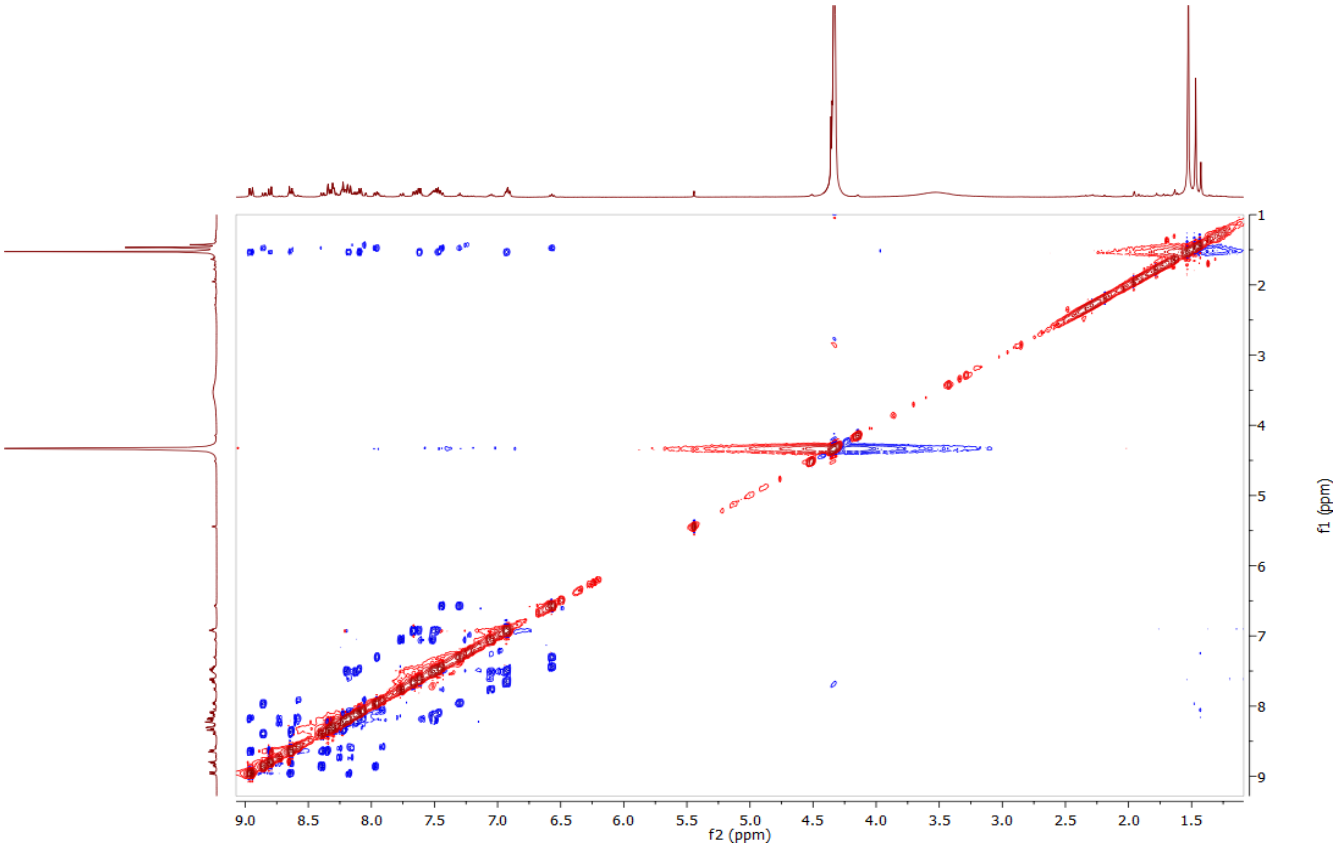

Figure S9. NOESY NMR spectrum of the mixture of **4A**, **4B** and **4C** in CD_3NO_2 at 253K.

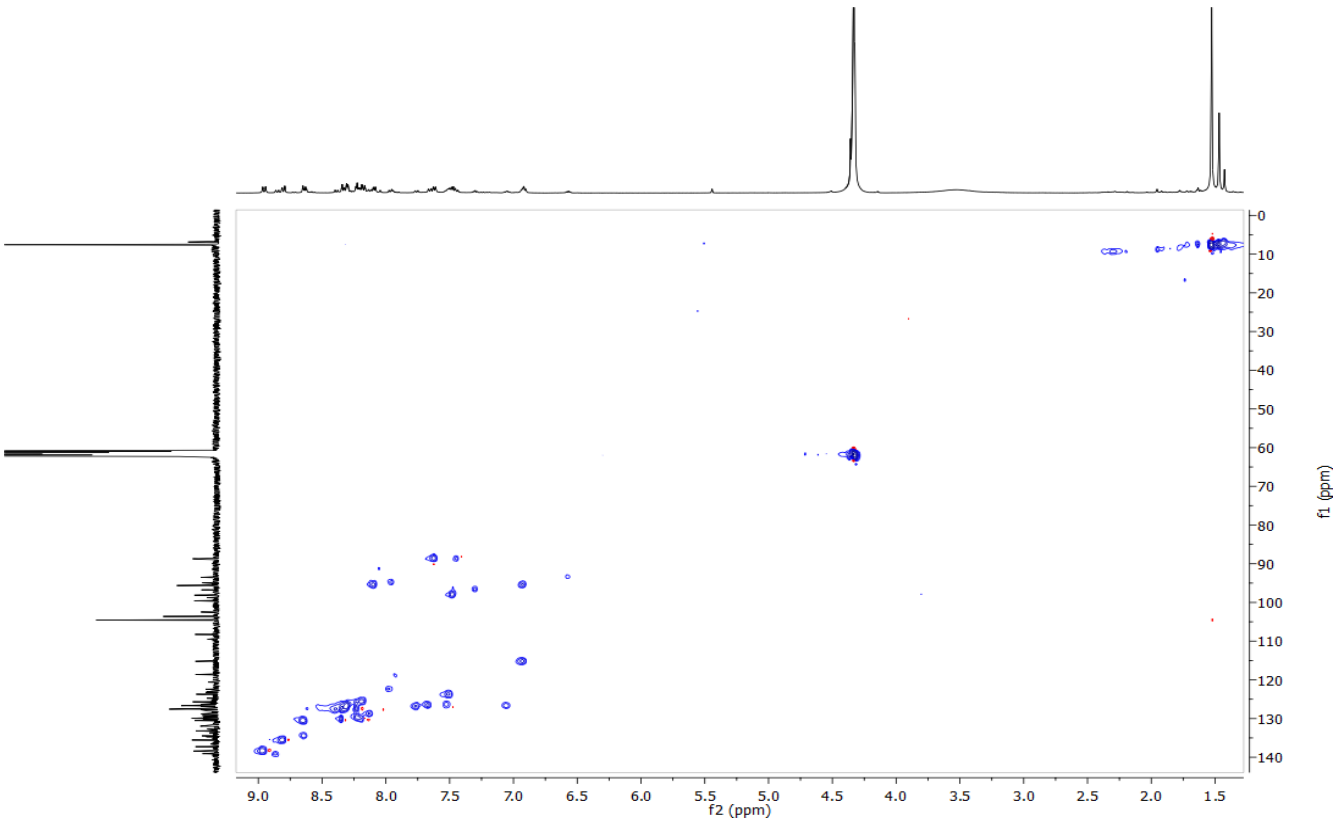

Figure S10. ^{1}H-^{13}C HSQC NMR spectrum of the mixture of **4A**, **4B** and **4C** in CD_3NO_2 at 253K.

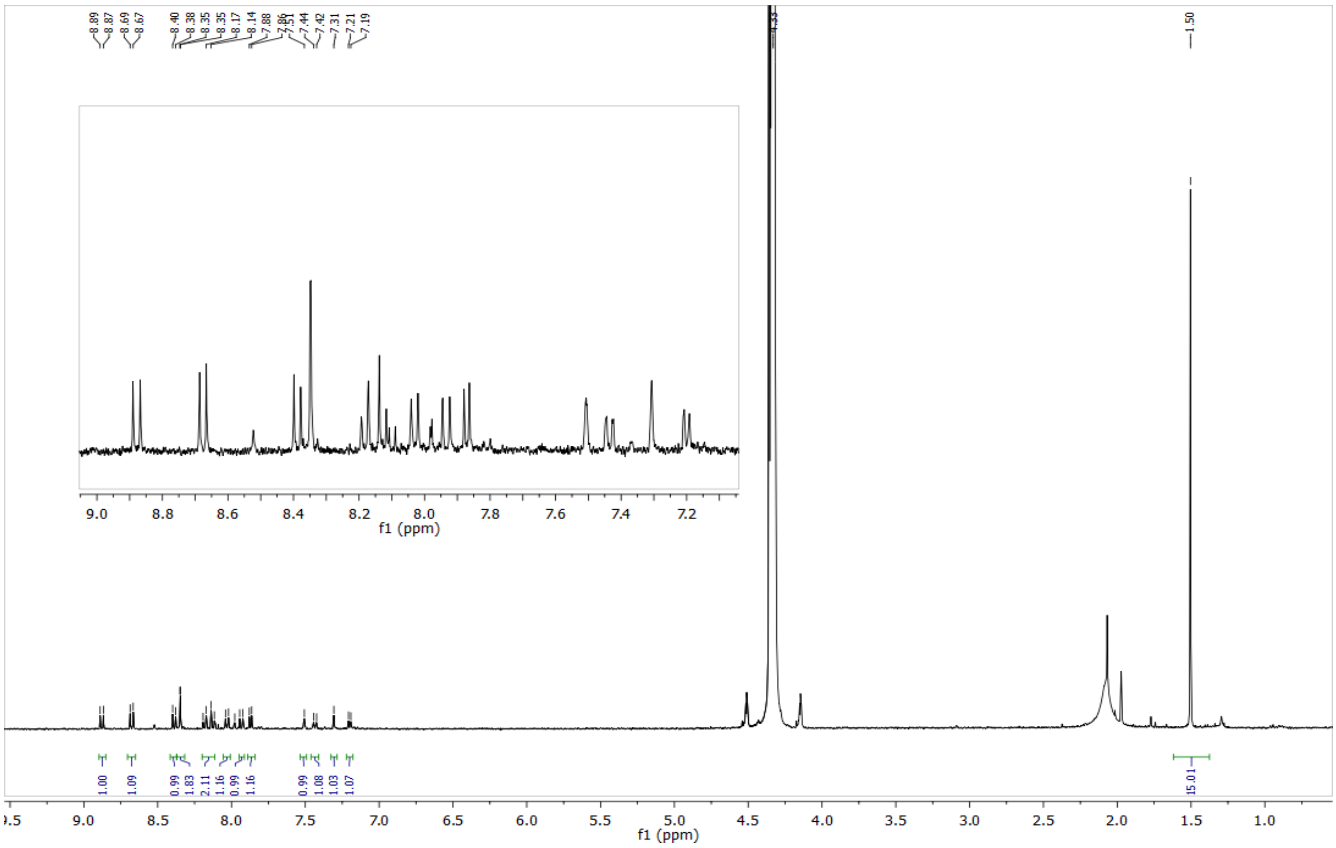

Figure S11. ^{1}H NMR spectrum of **5A** in CD_3NO_2.

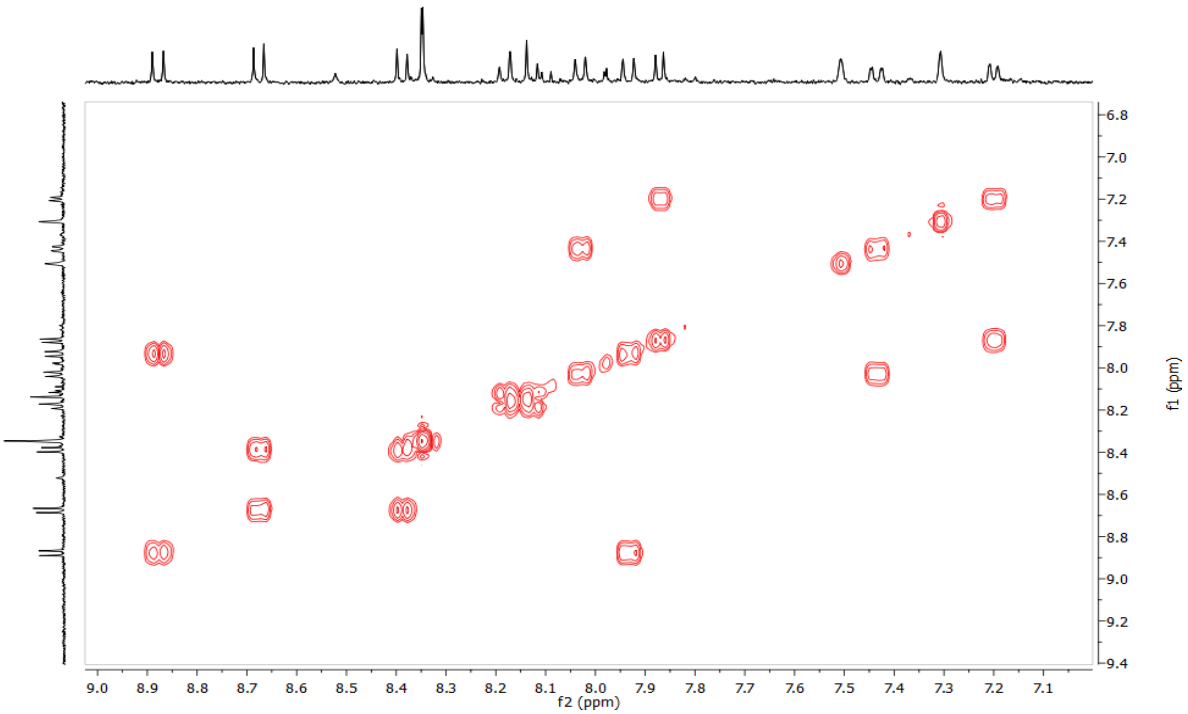

Figure S12. COSY NMR spectrum of **5A** in CD_3NO_2.

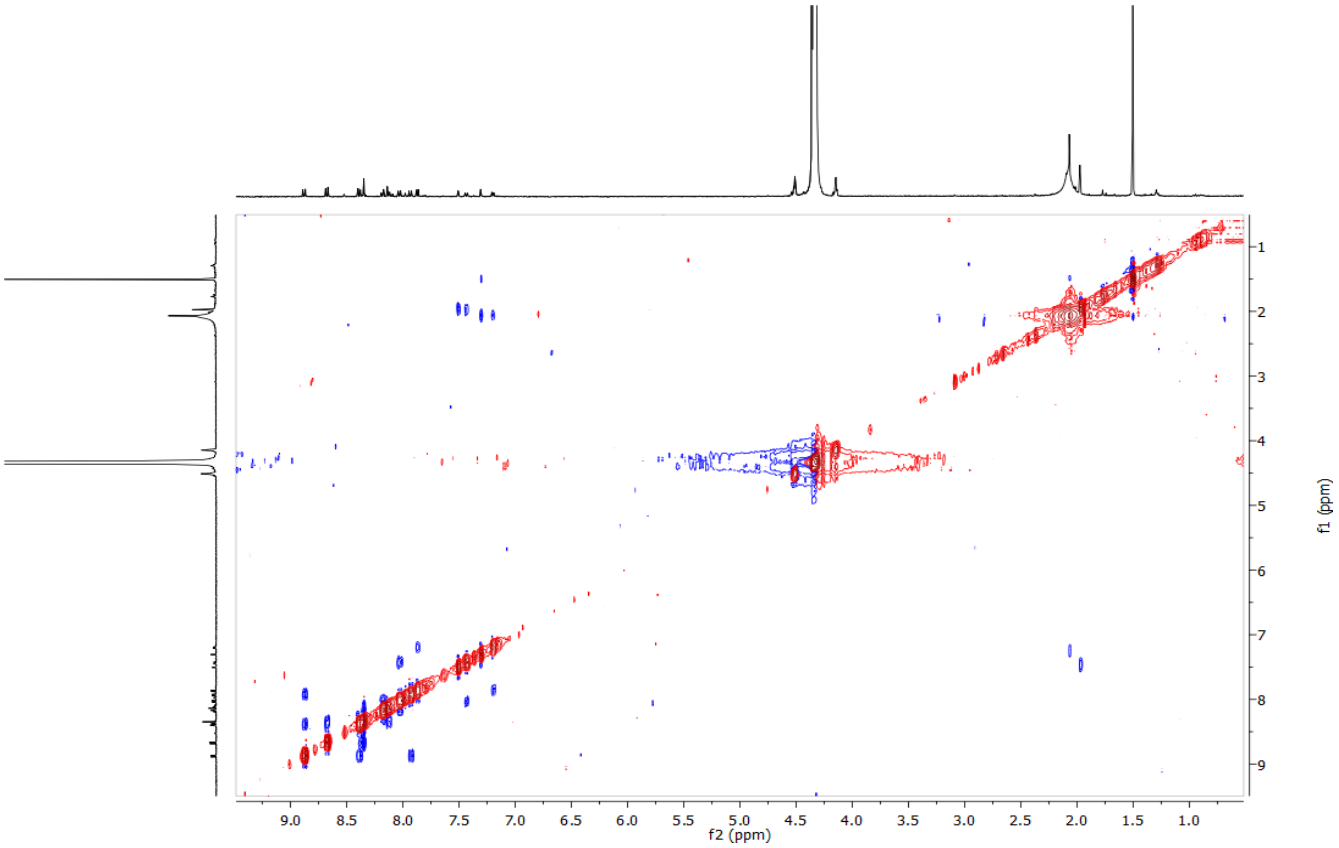

Figure S13. NOESY NMR spectrum of **5A** in CD_3NO_2.

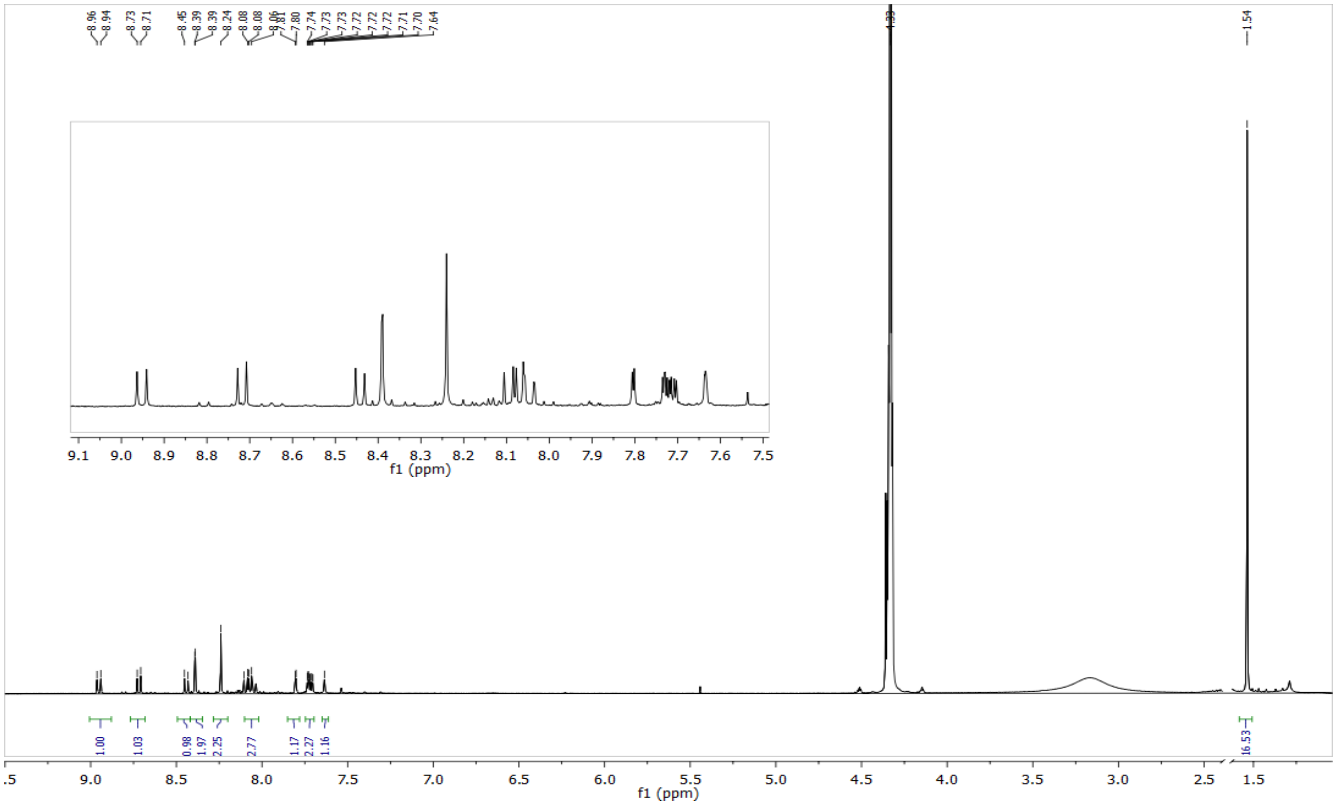

Figure S14. ^1H NMR spectrum of **6A** in CD_3NO_2.

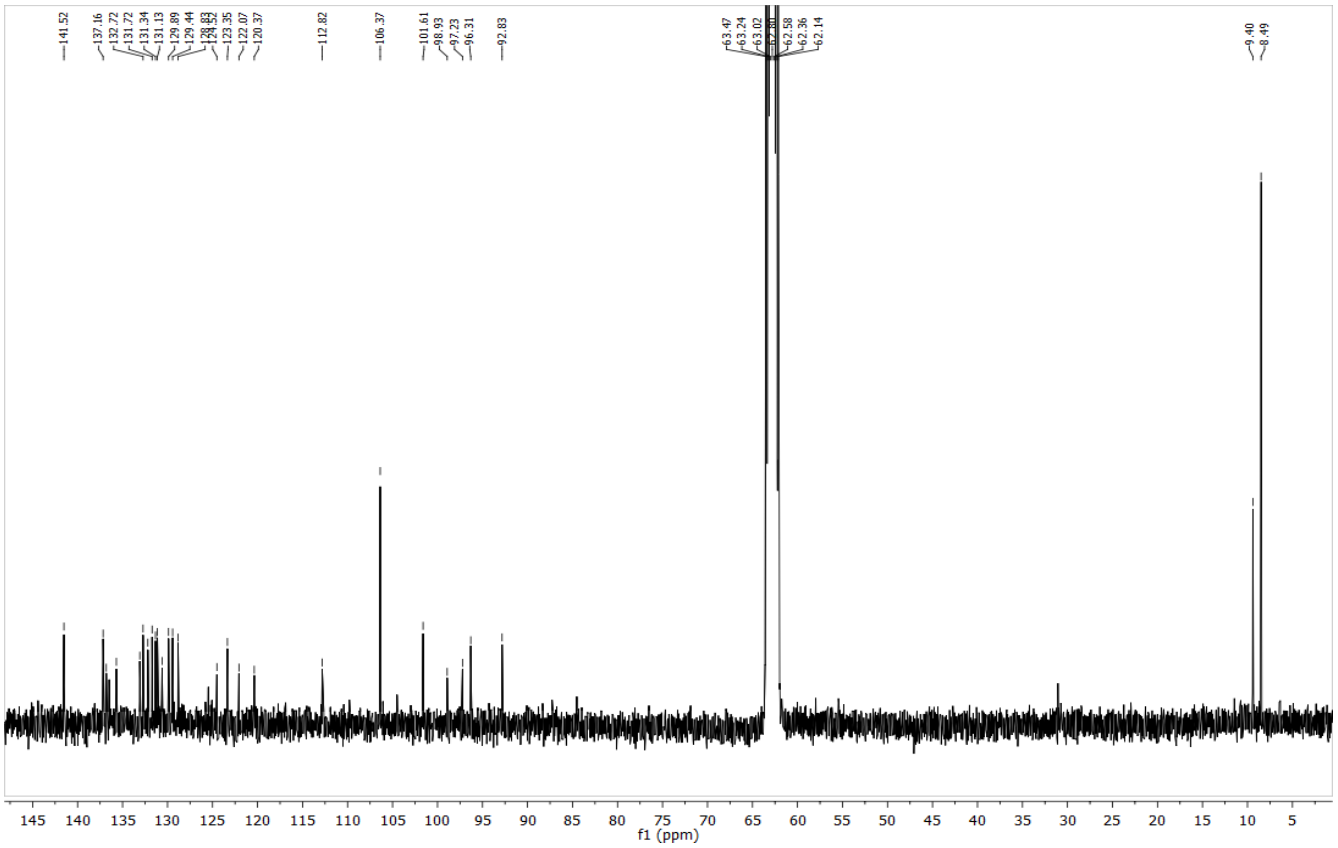

Figure S15. $^{13}C\{^{1}H\}$ NMR spectrum of **6A** in CD_3NO_2.

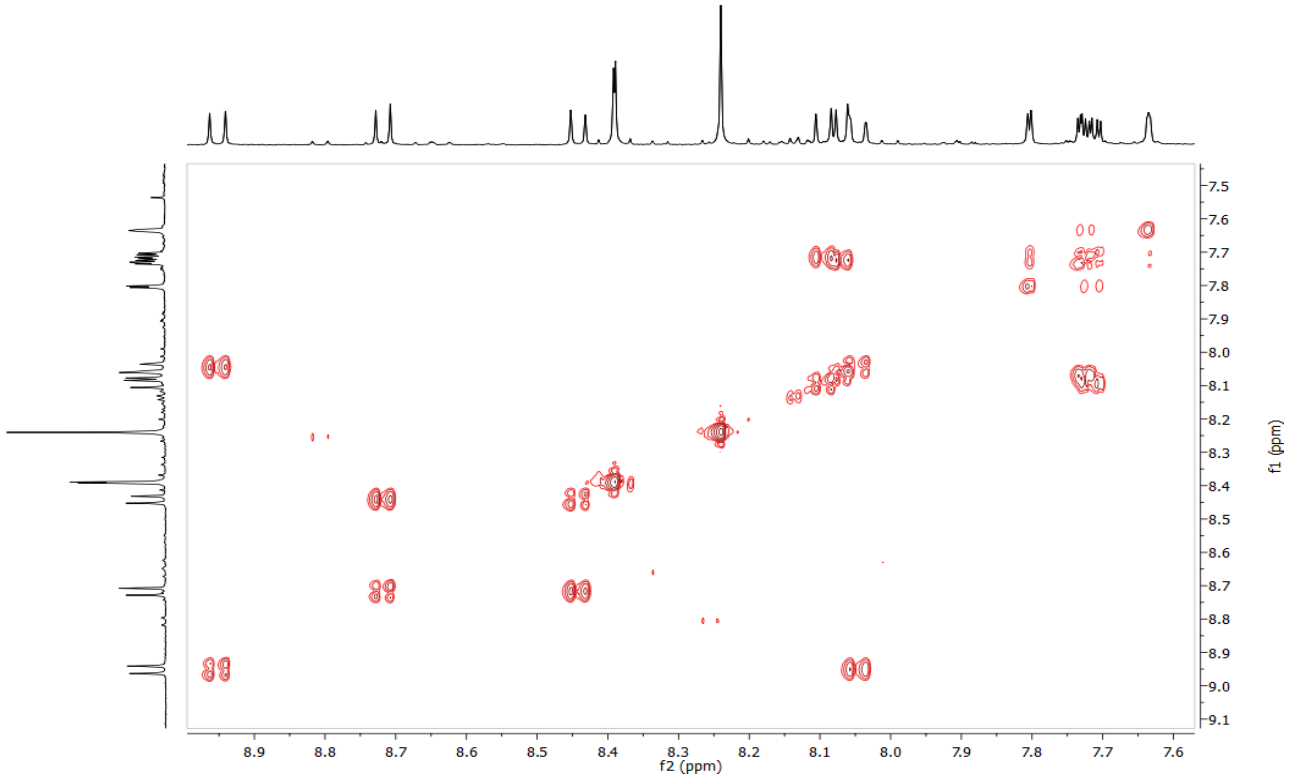

Figure S16. COSY NMR spectrum of **6A** in CD_3NO_2.

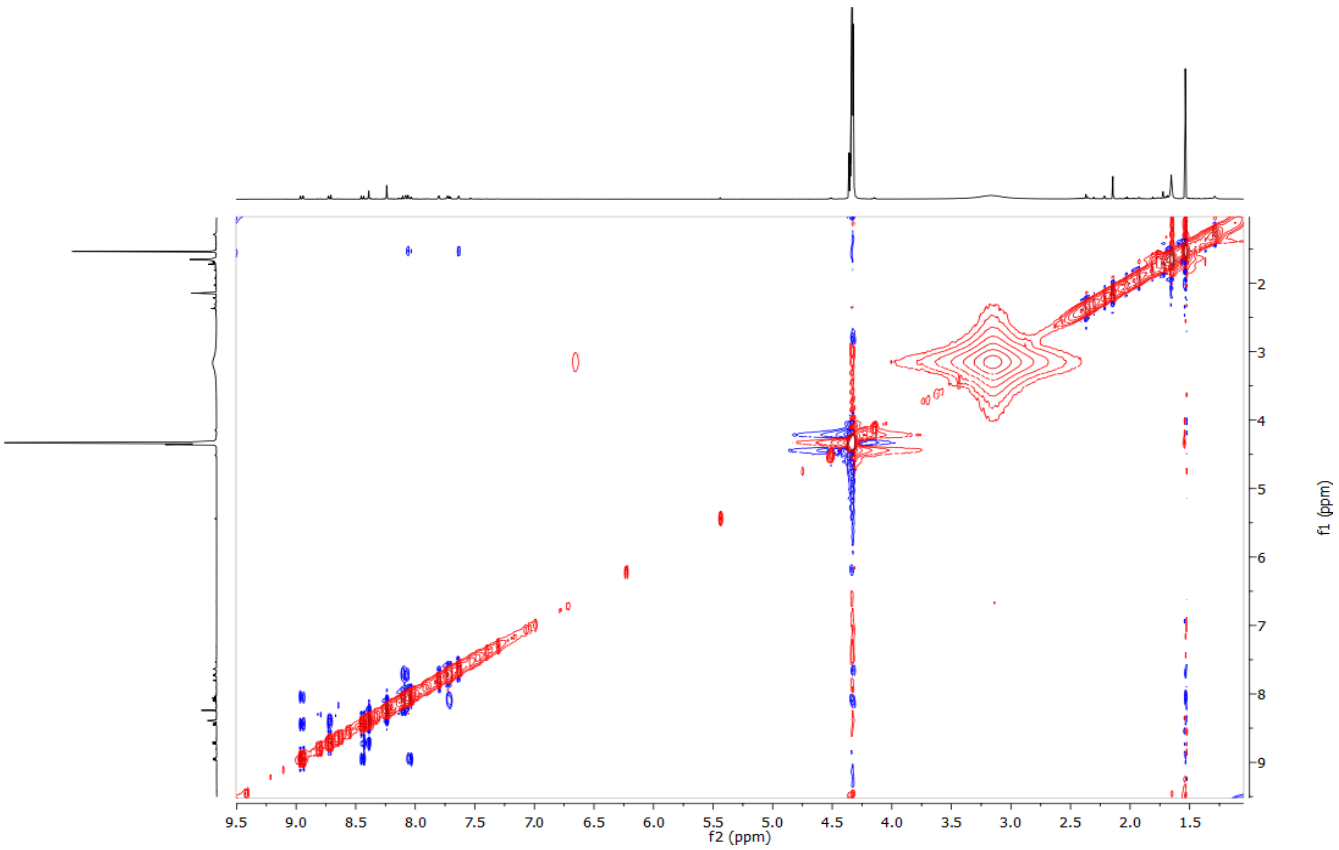

Figure S17. NOESY NMR spectrum of **6A** in CD_3NO_2.

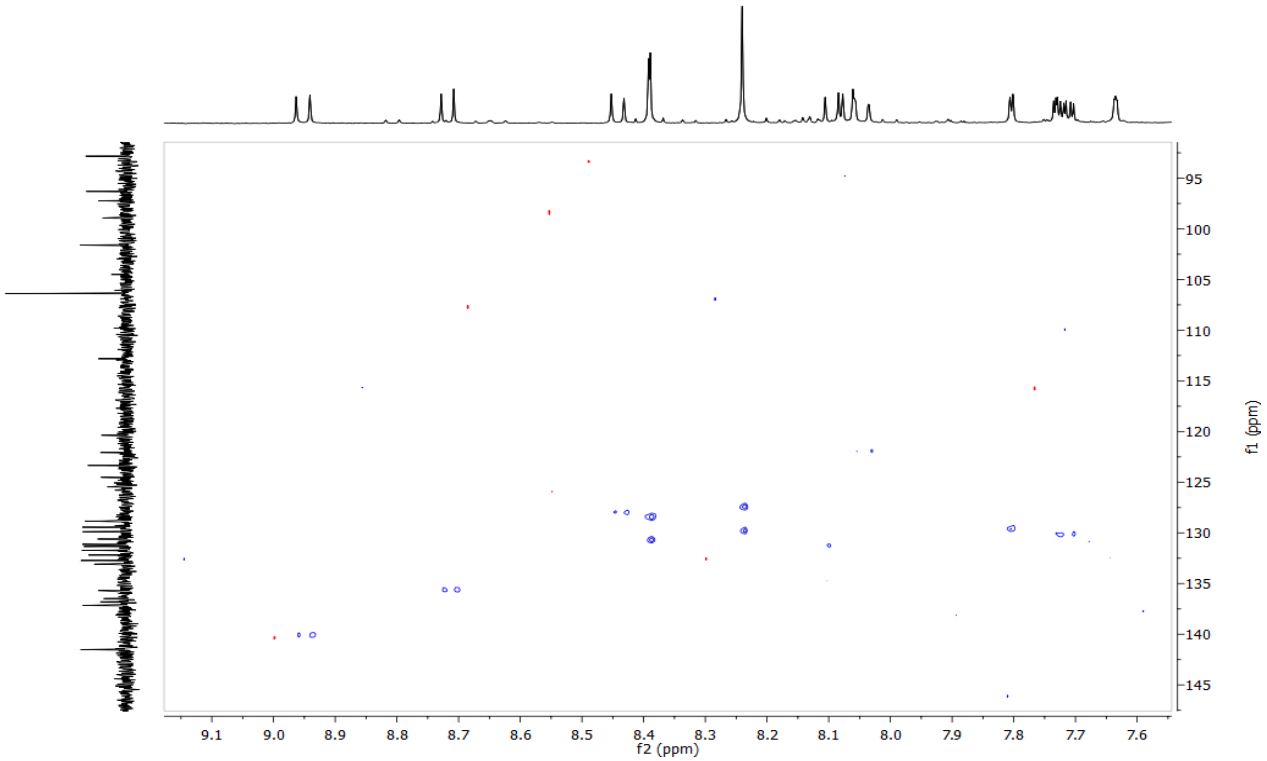

Figure S18. ^{1}H-^{13}C HSQC NMR spectrum of **6A** in CD_3NO_2.

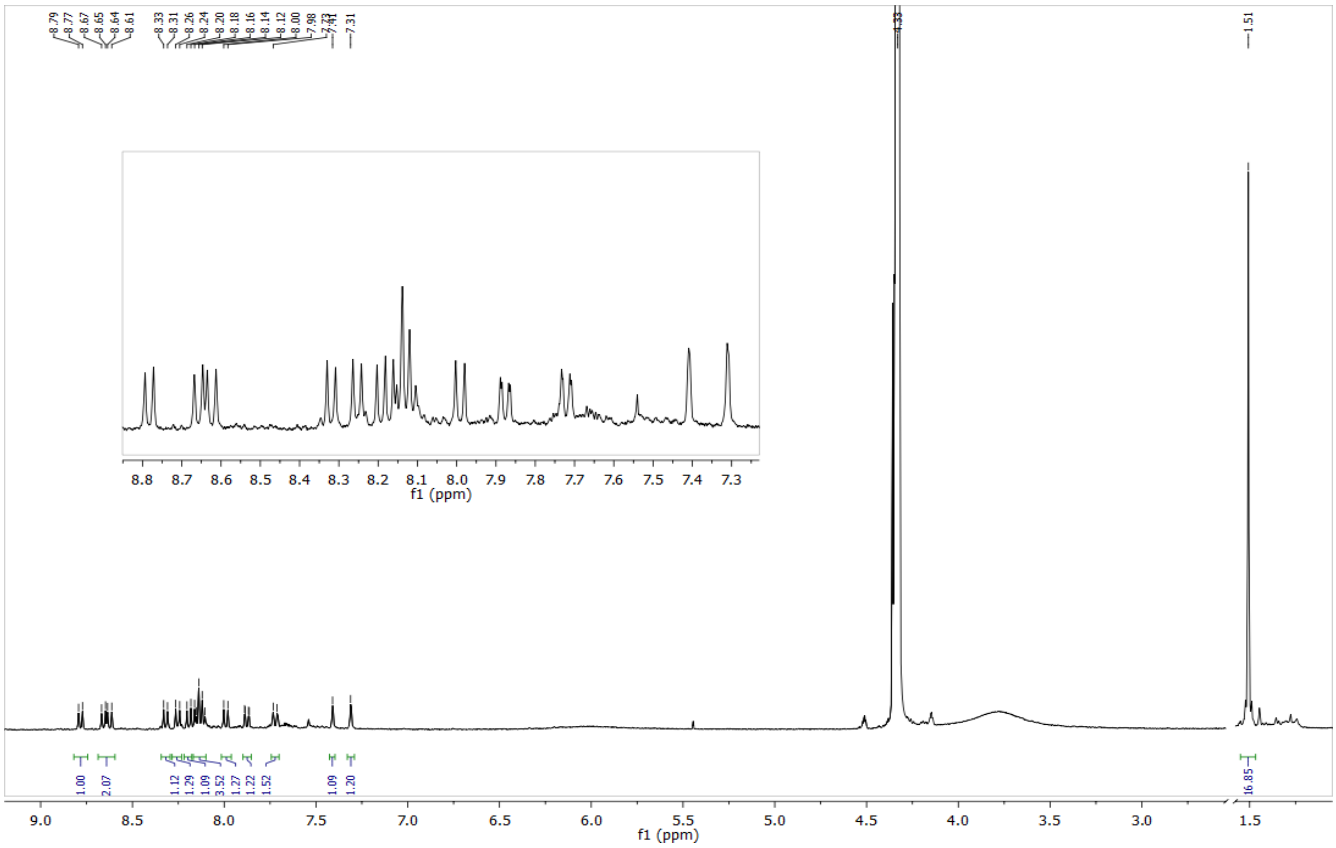

Figure S19. ^{1}H NMR spectrum of **6C** in CD_3NO_2 at 253K.

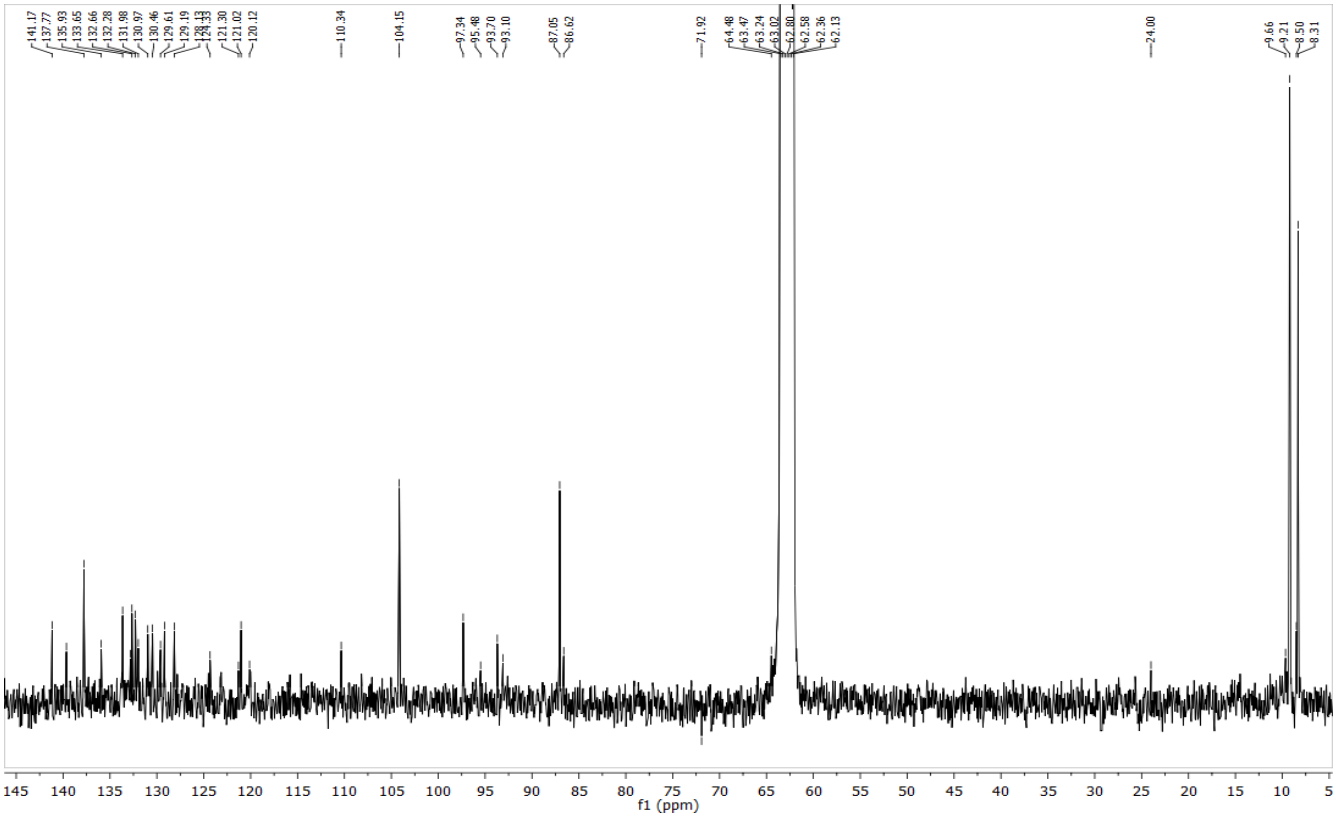

Figure S20. ^{13}C {^{1}H} NMR spectrum of **6C** in CD_3NO_2 at 253K.

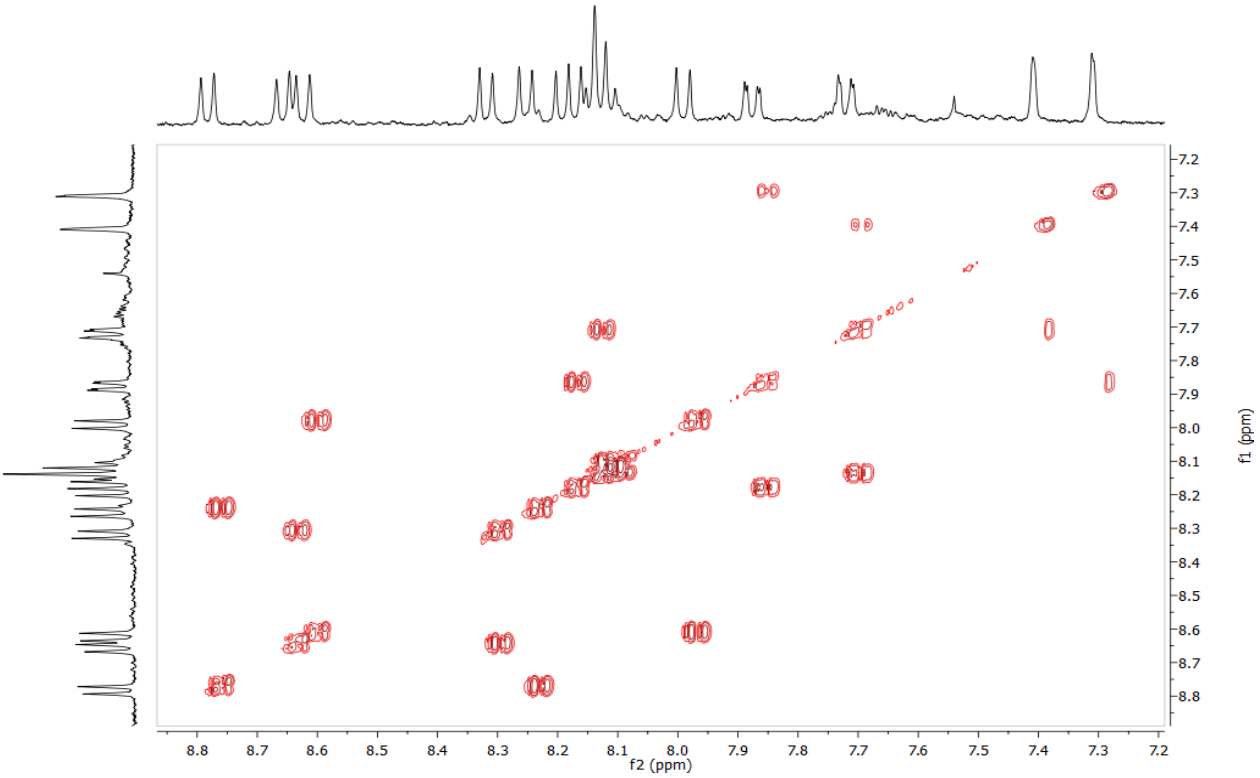

Figure S21. COSY NMR spectrum of **6C** in CD_3NO_2 at 253K.

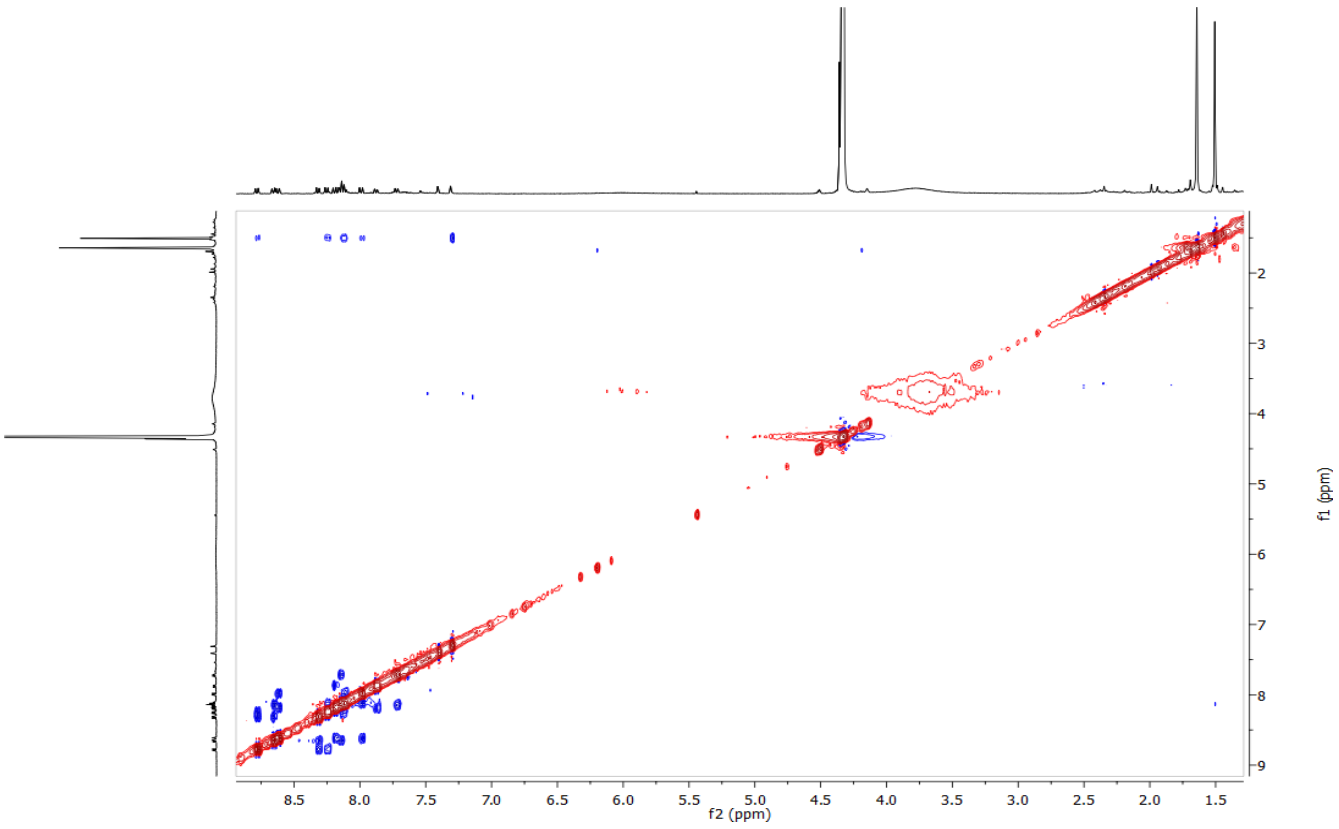

Figure S22. NOESY NMR spectrum of **6C** in CD_3NO_2 at 253K.

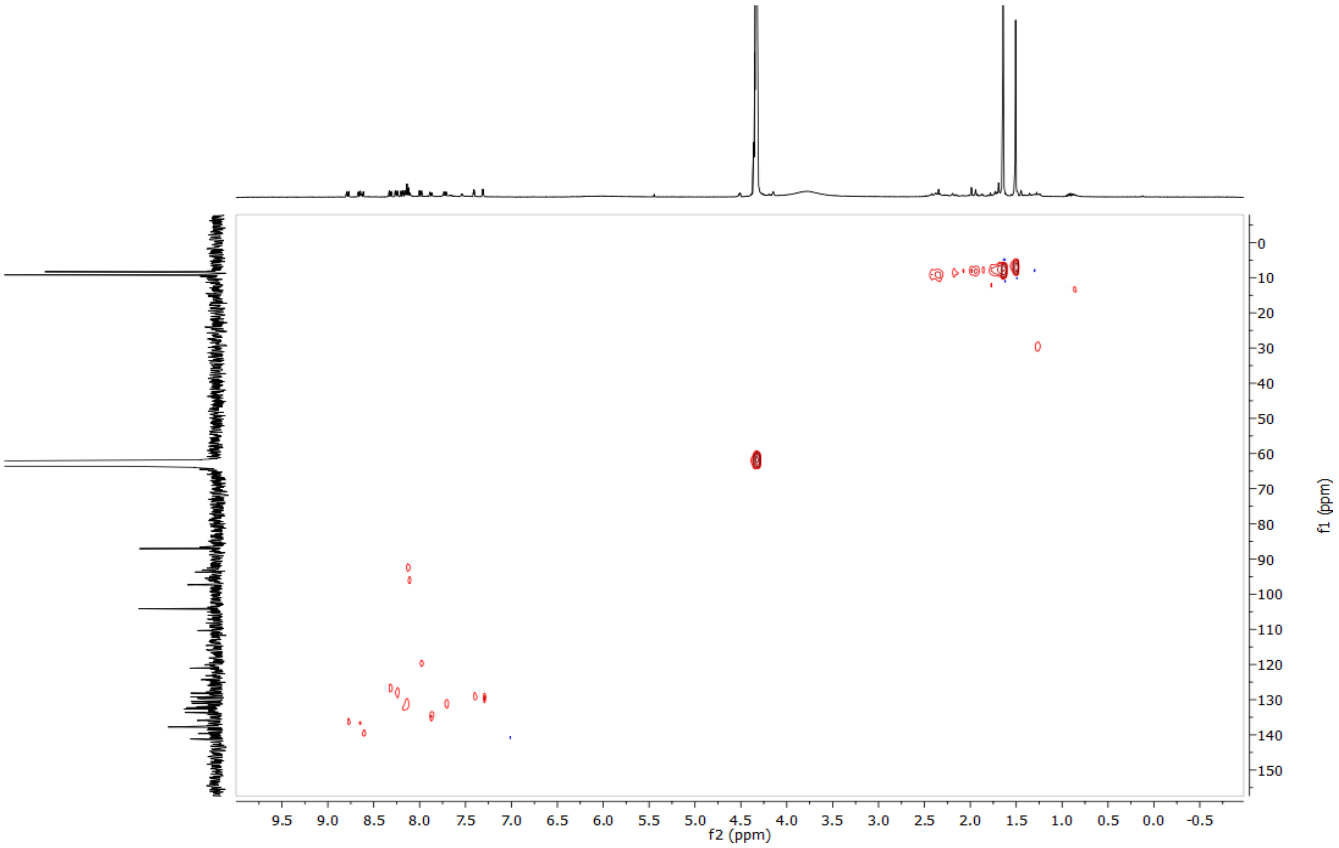

Figure S23. ^{1}H-^{13}C HSQC NMR spectrum of **6C** in CD_3NO_2 at 253K.

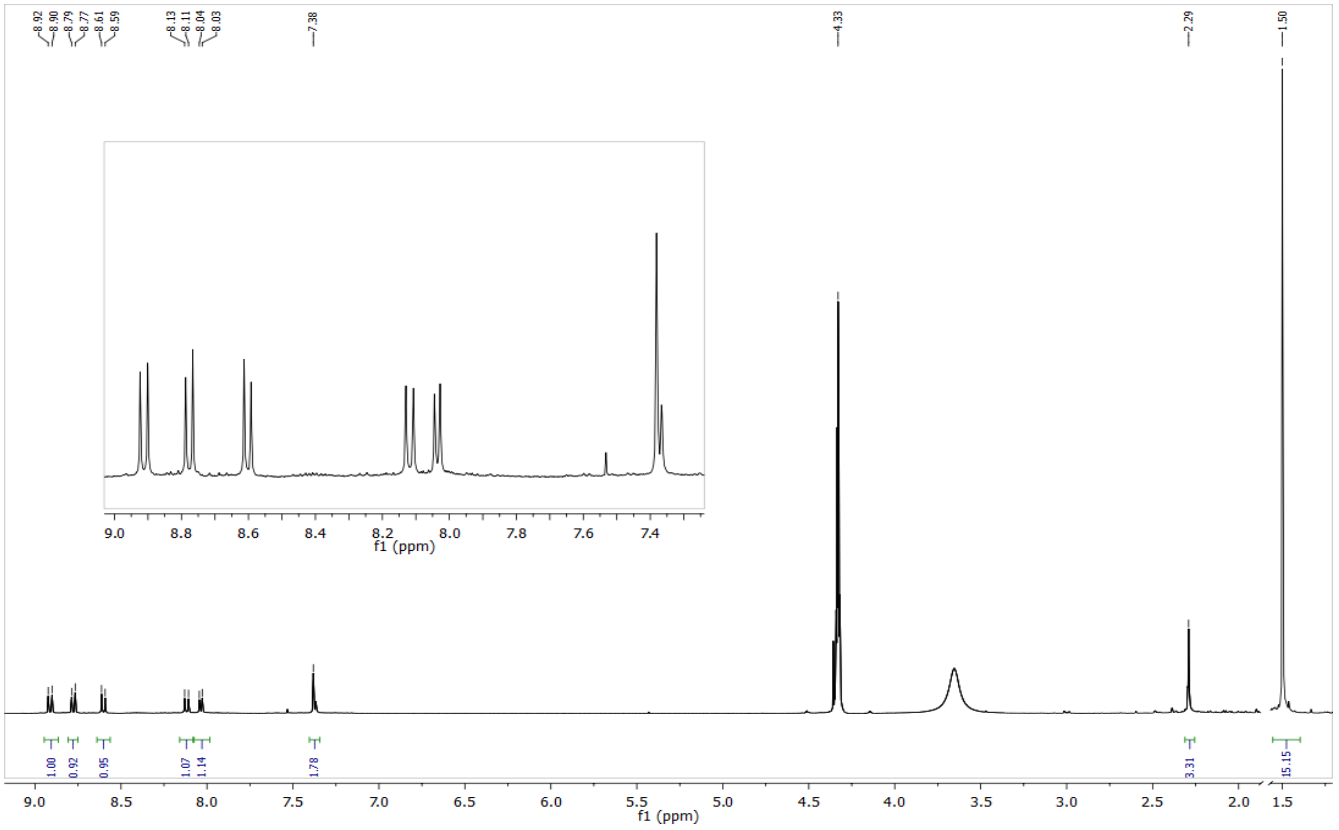

Figure S24. ^{1}H NMR spectrum of **7** in CD_3NO_2.

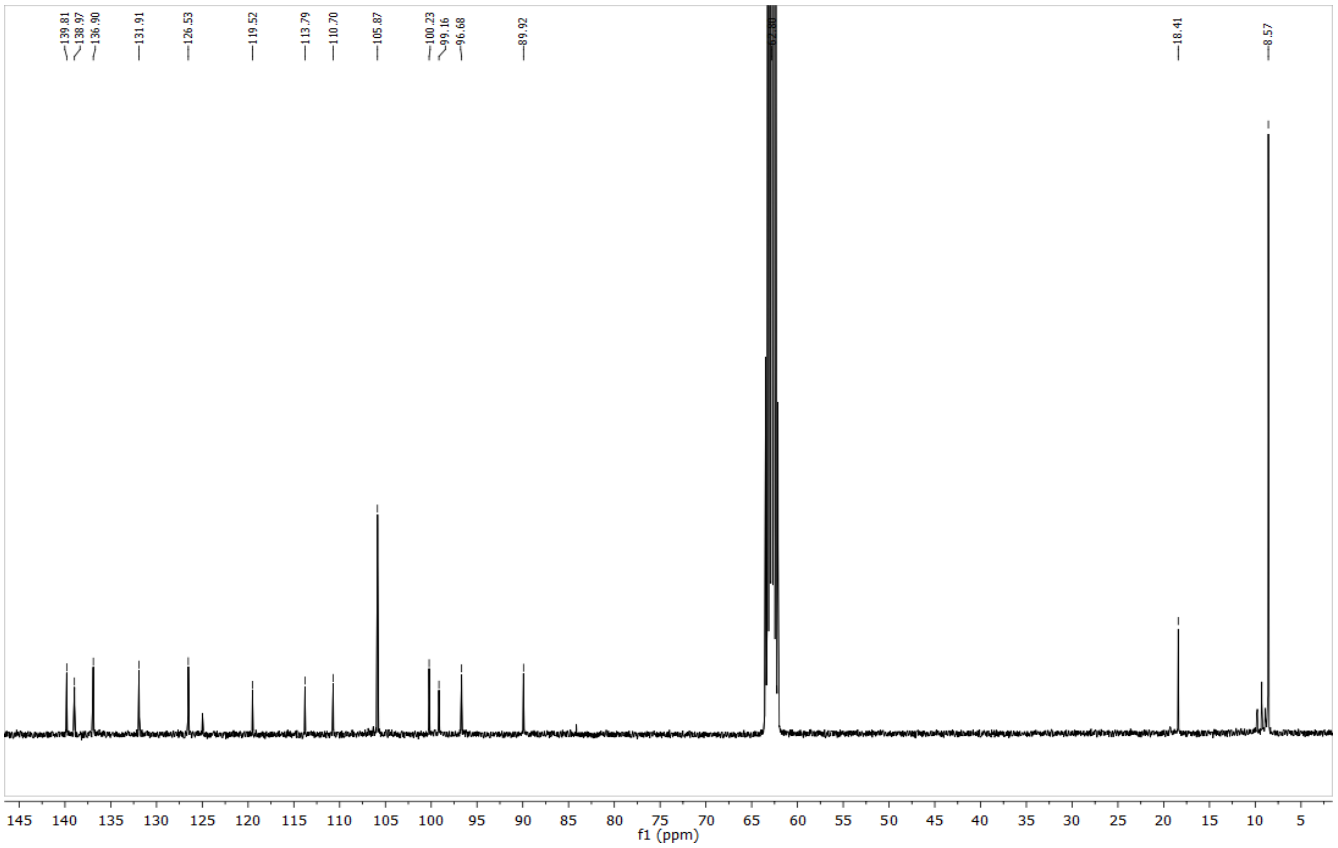

Figure S25. ^{13}C {^{1}H} NMR spectrum of **7** in CD_3NO_2.

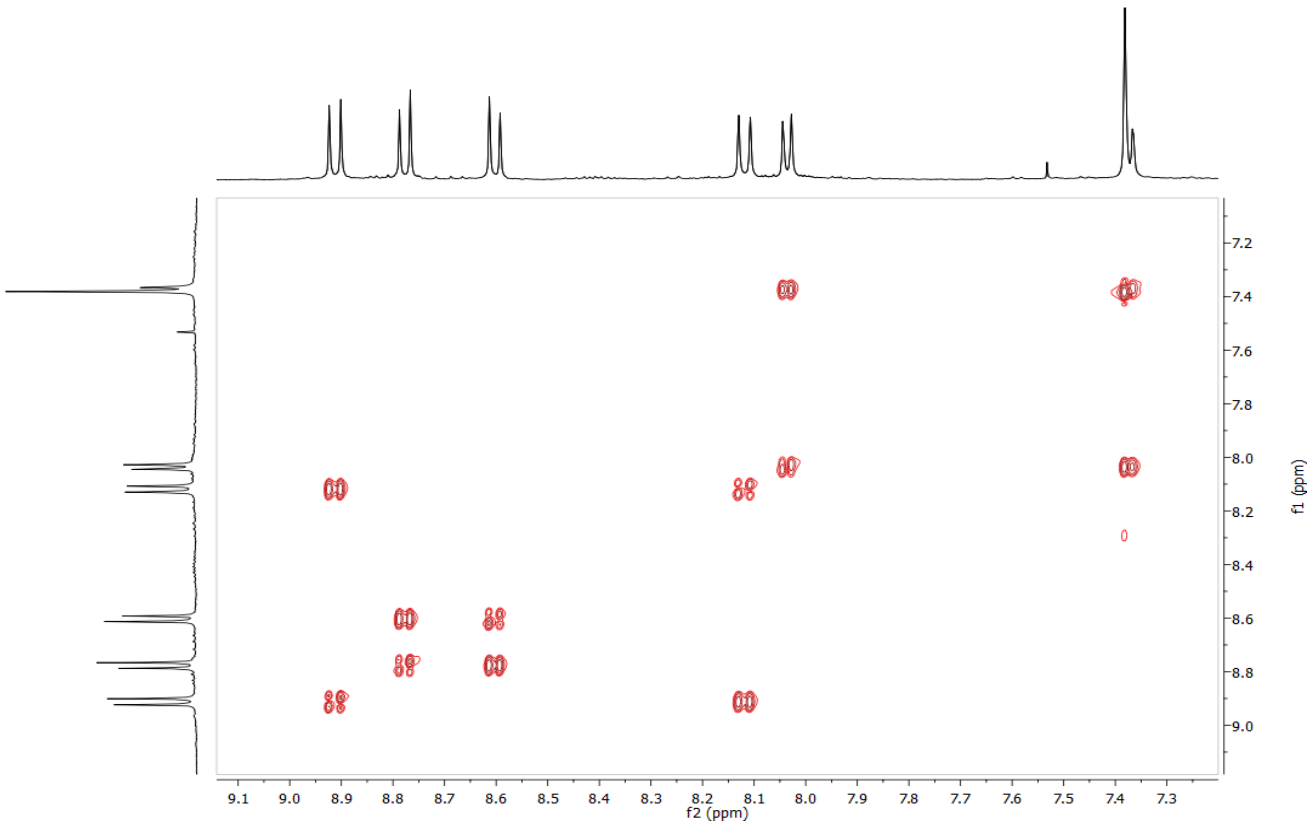

Figure S26. COSY NMR spectrum of **7** in CD_3NO_2.

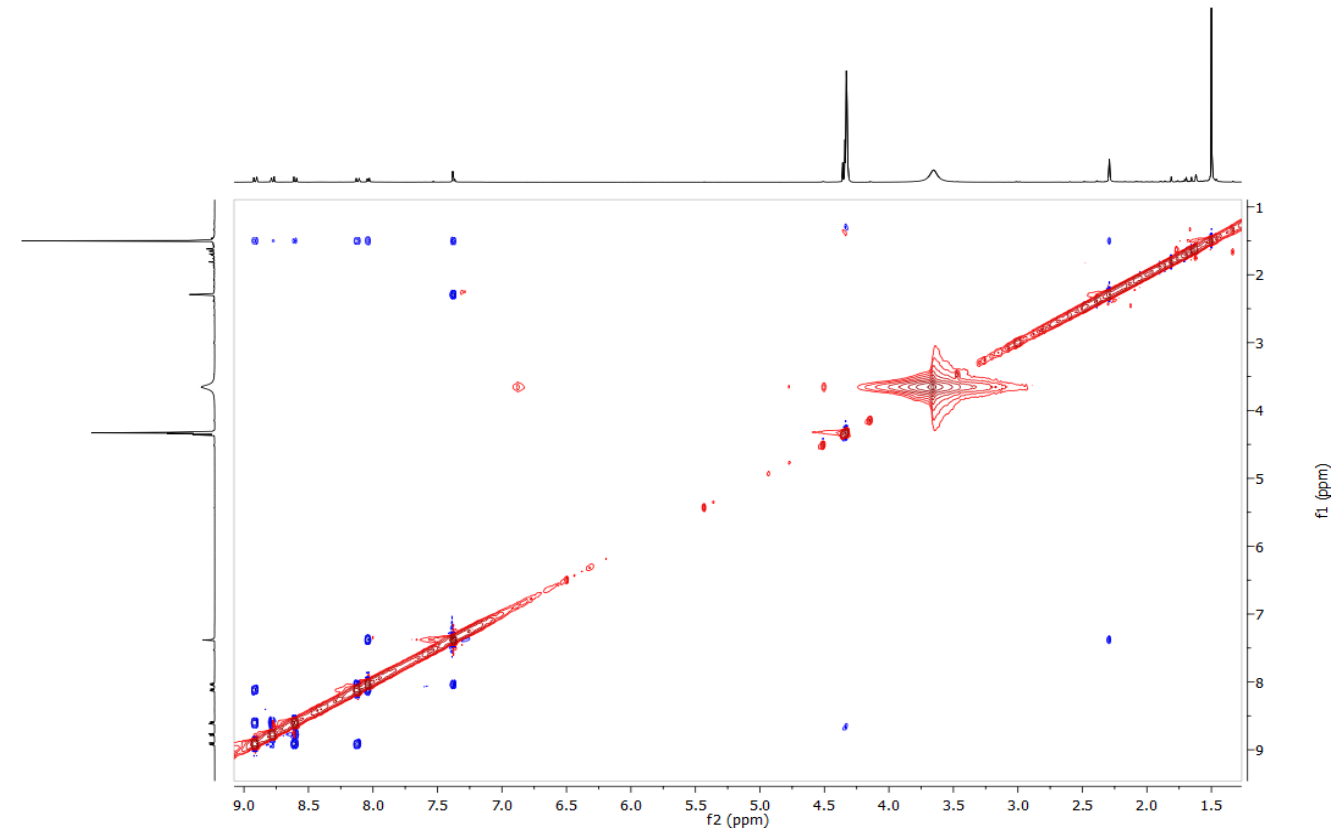

Figure S27. NOESY NMR spectrum of **7** in CD_3NO_2.

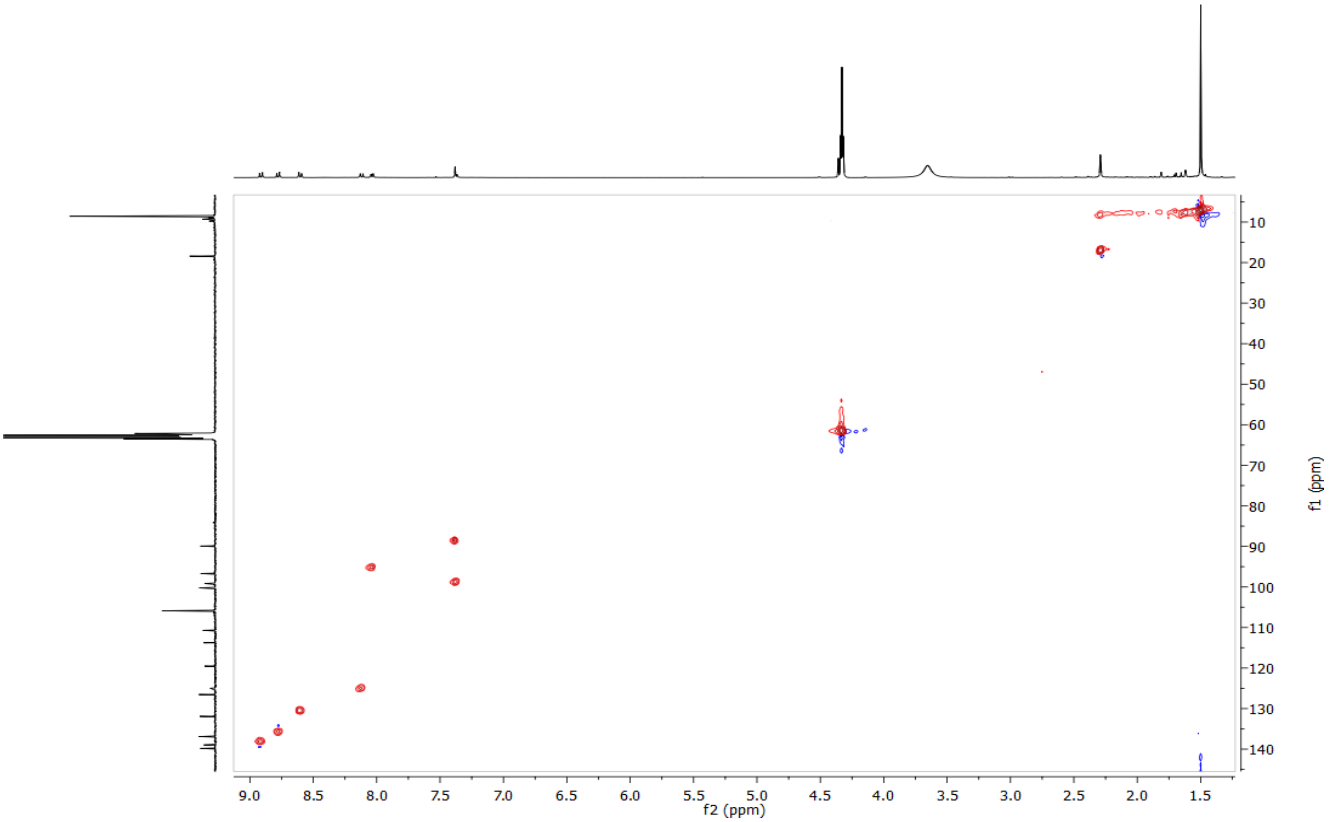

Figure S28. ^{1}H-^{13}C HSQC NMR spectrum of **7** in CD_3NO_2.

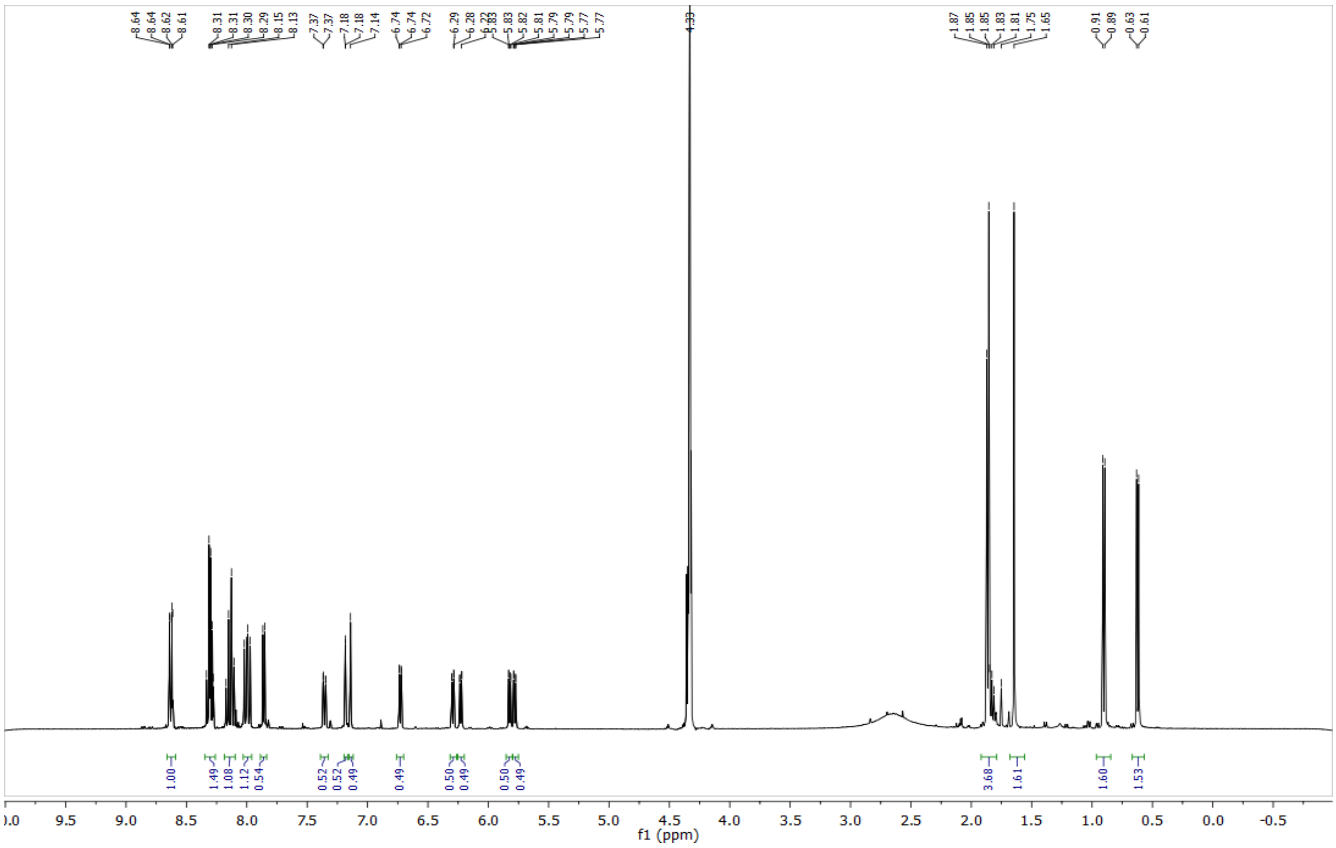

Figure S29. ^{1}H NMR spectrum of **8** in CD_3NO_2.

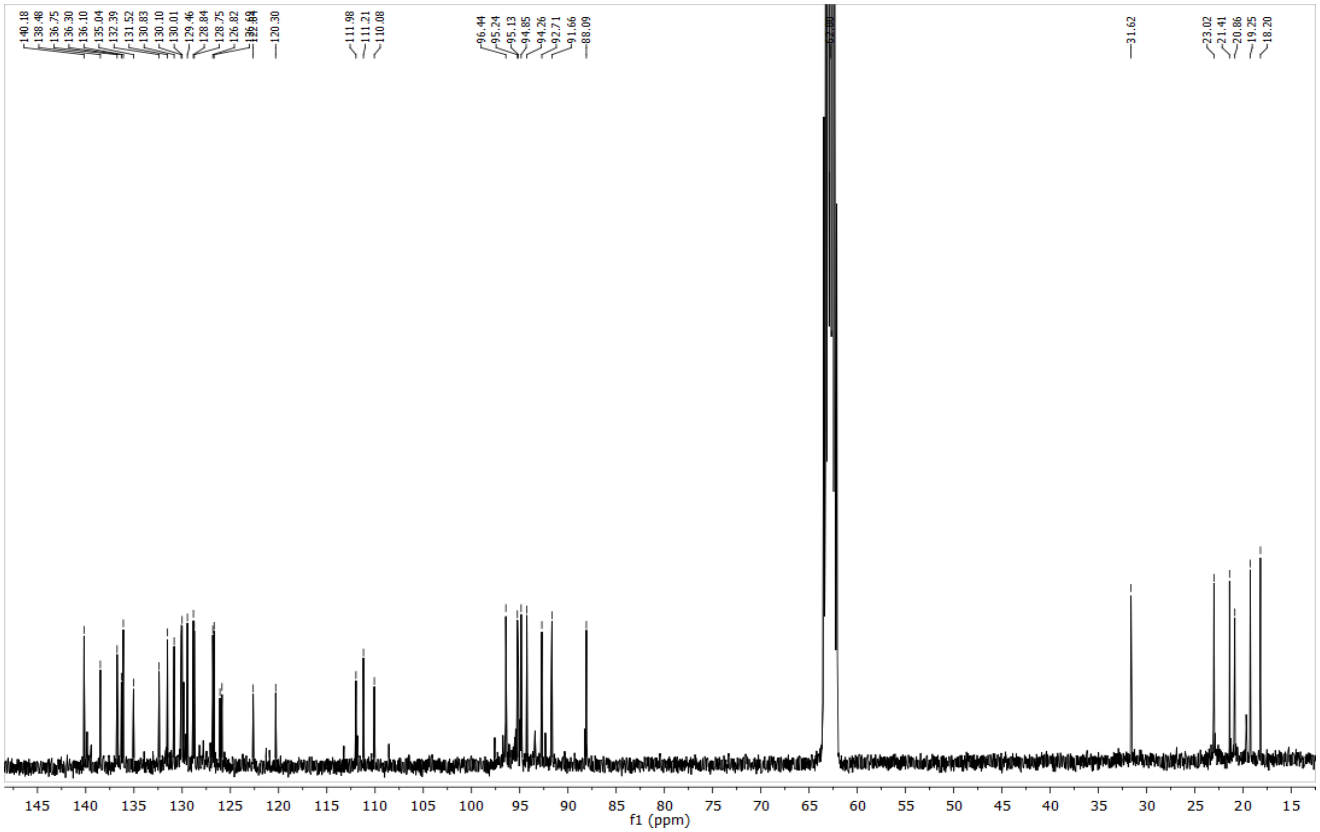

Figure S30. ^{13}C {^{1}H } NMR spectrum of **8** in CD_3NO_2.

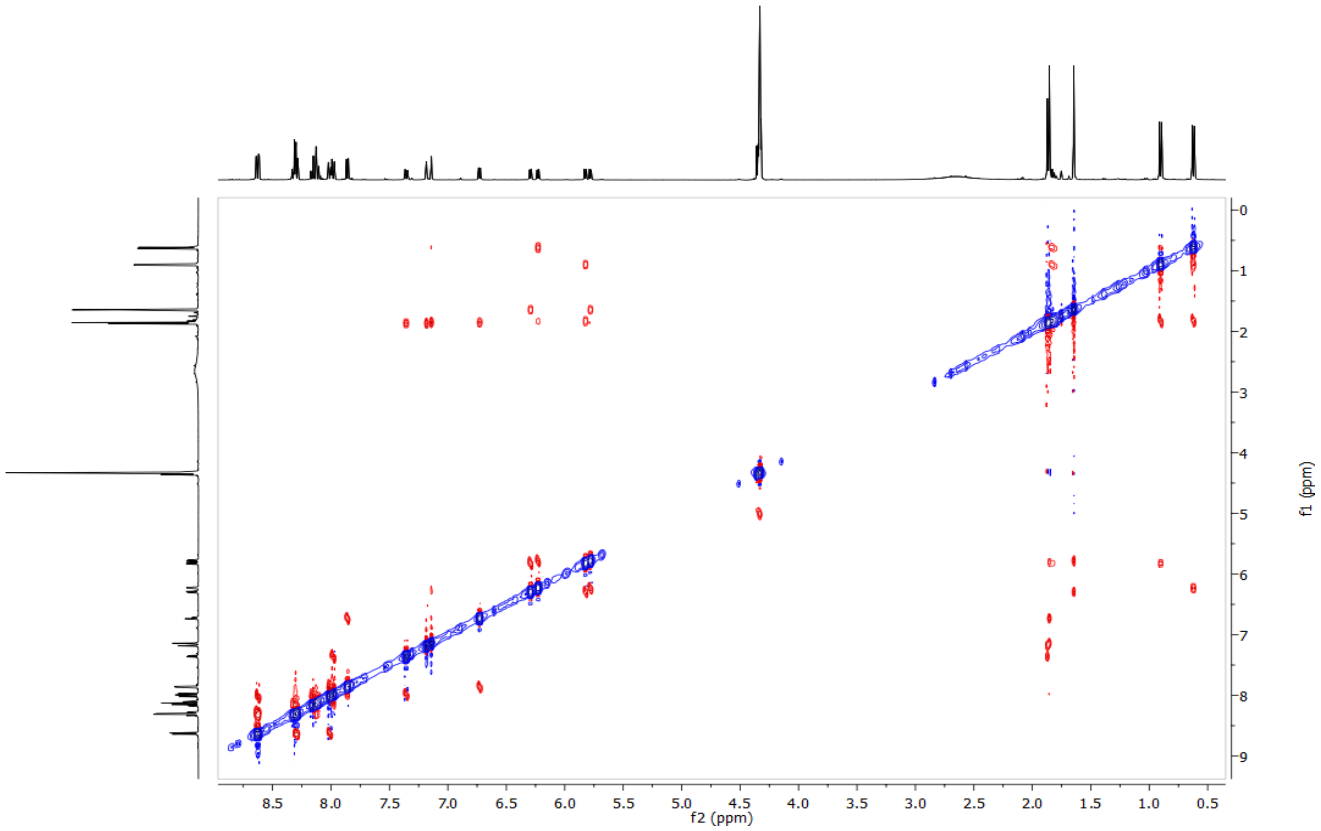

Figure S31. NOESY NMR spectrum of **8** in CD_3NO_2.

II. Crystallographic Data for [(η^6-cymene)Ru(η^6-2)][BF_4]$_2$ (8)

Empirical formula	C_{38} H_{34} B_2 F_8 Ru	
Formula weight	765.34	
Temperature	293(2) K	
Wavelength	0.71073 Å	
Crystal system	Monoclinic	
Space group	P 1 21/c 1	
Unit cell dimensions	a = 16.3654(18) Å	α = 90°.
	b = 15.8012(15) Å	β = 108.370(12)°.
	c = 14.3552(16) Å	γ = 90°.
Volume	3523.0(6) Å^3	
Z	4	
Density (calculated)	1.443 Mg/m^3	
Absorption coefficient	0.514 mm^{-1}	
F(000)	1552	
Crystal size	0.2658 × 0.1659 × 0.0888 mm^3	
Theta range for data collection	2.89 to 28.76°.	
Index ranges	-21<=h<=19, -21<=k<=17, -14<=l<=19	
Reflections collected	13233	
Independent reflections	7298 [R(int) = 0.1213]	
Completeness to theta = 25.25°	98.6 %	
Absorption correction	Analytical	
Max. and min. transmission	0.979 and 0.954	
Refinement method	Full-matrix least-squares on F^2	
Data / restraints / parameters	7298 / 222 / 478	
Goodness-of-fit on F^2	1.010	
Final R indices [I>2sigma(I)]	R_1 = 0.0936, wR_2 = 0.2243	
R indices (all data)	R_1 = 0.2321, wR_2 = 0.2588	
Largest diff. peak and hole	0.579 and -0.381 e.Å^{-3}	

Crystallographic Experimental Section

Data collection was performed with a Mo micro-focus source with multilayer optics. Data integration, scaling and empirical absorption correction was carried out using the CrysAlis Pro program package.[1] The structure was solved using direct methods and refined by Full-Matrix-Least-Squares against F^2.[2] The non-hydrogen atoms were refined anisotropically and hydrogen atoms were placed at idealised positions and refined using the riding model.

Both BF_4^- anions in the asymmetric unit were disordered. Two components were defined for each anion and all of them were treated as rigid bodies. The structure converged with these final ratios for the two components: 23-77% for components A and B for one anion and 55-45% for the other.

The crystals studied contained also disordered solvent near a special position that couldn't be modeled, therefore the SQUEEZE/PLATON programs were used to treat the solvent as a diffuse contribution to the overall scattering without specific atom positions.[3]

Selected Bond Distances and Angles

Ru(1)-C(1)	2.193(8)
Ru(1)-C(2)	2.240(9)
Ru(1)-C(3)	2.234(9)
Ru(1)-C(4)	2.190(9)
Ru(1)-C(5)	2.240(8)
Ru(1)-C(26)	2.298(8)
Ru(1)-C(30)	2.245(10)
Ru(1)-C(31)	2.216(9)
Ru(1)-C(32)	2.232(10)
Ru(1)-C(33)	2.242(11)
Ru(1)-C(34)	2.196(9)
Ru(1)-C(35)	2.203(9)
C(1)-Ru(1)-C(30)	159.6(4)
C(1)-Ru(1)-C(31)	125.5(3)
C(1)-Ru(1)-C(32)	104.3(3)
C(1)-Ru(1)-C(33)	106.1(4)
C(1)-Ru(1)-C(34)	130.7(4)
C(1)-Ru(1)-C(35)	164.8(4)
C(2)-Ru(1)-C(30)	125.7(4)
C(2)-Ru(1)-C(31)	105.1(3)
C(2)-Ru(1)-C(32)	107.0(4)
C(2)-Ru(1)-C(33)	129.5(4)
C(2)-Ru(1)-C(34)	165.4(5)

C(2)-Ru(1)-C(35)	157.6(5)
C(3)-Ru(1)-C(30)	104.5(4)
C(3)-Ru(1)-C(31)	107.4(4)
C(3)-Ru(1)-C(32)	131.3(4)
C(3)-Ru(1)-C(33)	164.6(4)
C(3)-Ru(1)-C(34)	157.0(4)
C(3)-Ru(1)-C(35)	124.1(5)
C(4)-Ru(1)-C(30)	104.8(4)
C(4)-Ru(1)-C(31)	129.7(4)
C(4)-Ru(1)-C(32)	165.7(4)
C(4)-Ru(1)-C(33)	157.8(4)
C(4)-Ru(1)-C(34)	123.4(4)
C(4)-Ru(1)-C(35)	103.0(4)
C(5)-Ru(1)-C(30)	127.8(4)
C(5)-Ru(1)-C(31)	164.2(4)
C(5)-Ru(1)-C(32)	156.5(4)
C(5)-Ru(1)-C(33)	123.7(4)
C(5)-Ru(1)-C(34)	103.0(3)
C(5)-Ru(1)-C(35)	105.2(4)
C(26)-Ru(1)-C(30)	162.3(4)
C(26)-Ru(1)-C(31)	158.7(4)
C(26)-Ru(1)-C(32)	123.6(4)
C(26)-Ru(1)-C(33)	103.2(4)
C(26)-Ru(1)-C(34)	105.9(3)
C(26)-Ru(1)-C(35)	129.2(4)

III. Computational details.

Density functional calculations were carried out by using the GAUSSIAN09 package[4]. B3LYP method (hybrid density functional) was applied.[5] A split-valence basis set with polarization functions SVP was used for C and H[6] and effective core potentials (ECP), including their associated basis set, SDD, were used for Ir and Ru.[7] Geometry optimizations were carried out on the full potential energy surface without symmetry restrictions. Transition States were predicted by the synchronous transit-guided quasi-Newton method QST3[8], were located to connect two minima and they were confirmed by vibrational analysis. Solvent effects were taken into account by single-point calculations at geometries optimized in gas-phase by using PCM algorithm with Nitromethane (e=36.562) as a solvent.[9]

	Experimental structure	Calculated structure
Ru(1)-C(1)	2.256	2.243
Ru(1)-C(2)	2.268	2.263
Ru(1)-C(3)	2.248	2.243
Ru(1)-C(4)	2.244	2.222
Ru(1)-C(5)	2.358	2.315
Ru(1)-C(26)	2.454	2.438
Ru(1)-C(30)	2.299	2.324
Ru(1)-C(31)	2.244	2.280
Ru(1)-C(32)	2.254	2.284
Ru(1)-C(33)	2.320	2.323
Ru(1)-C(34)	2.264	2.261
Ru(1)-C(35)	2.259	2.260
C(1)-Ru(1)-C(30)	161.4	160.5
C(1)-Ru(1)-C(31)	127.8	127.1
C(1)-Ru(1)-C(32)	105.9	105.4
C(1)-Ru(1)-C(33)	105.7	105.4
C(1)-Ru(1)-C(34)	127.7	127.8
C(1)-Ru(1)-C(35)	161.5	162.2

Tabla S1. Selected bond distances and angles for experimental X-ray crystallography structure and calculated structure of **8**.

(1) CrysAlisPro Software system, version 1.171.33.51, 2009, Oxford Diffraction Ltd, Oxford, UK.

(2) SHELX Software, Sheldrick, G. M. *Acta Cryst.* **2008**, *A64*, 112-122.

(3) PLATON Software, Spek, A. L. *J.Appl.Cryst.* **2003**, *36*, 7-13.

(4) Gaussian 09, Revision **A.1**, Frisch, M. J.; Trucks, G. W.; Schlegel, H. B.; Scuseria, G. E.; Robb, M. A.; Cheeseman, J. R.; Scalmani, G.; Barone, V.; Mennucci, B.; Petersson, G. A.; Nakatsuji, H.; Caricato, M.; Li, X.; Hratchian, H. P.; Izmaylov, A. F.; Bloino, J.; Zheng, G.; Sonnenberg, J. L.; Hada, M.; Ehara, M.; Toyota, K.; Fukuda, R.; Hasegawa, J.; Ishida, M.; Nakajima, T.; Honda, Y.; Kitao, O.; Nakai, H.; Vreven, T.; Montgomery, Jr., J. A.; Peralta, J. E.; Ogliaro, F.; Bearpark, M.; Heyd, J. J.; Brothers, E.; Kudin, K. N.; Staroverov, V. N.; Kobayashi, R.; Normand, J.; Raghavachari, K.; Rendell, A.; Burant, J. C.; Iyengar, S. S.; Tomasi, J.; Cossi, M.; Rega, N.; Millam, N. J.; Klene, M.; Knox, J. E.; Cross, J. B.; Bakken, V.; Adamo, C.; Jaramillo, J.; Gomperts, R.; Stratmann, R. E.; Yazyev, O.; Austin, A. J.; Cammi, R.; Pomelli, C.; Ochterski, J. W.; Martin, R. L.; Morokuma, K.; Zakrzewski, V. G.; Voth, G. A.; Salvador, P.; Dannenberg, J. J.; Dapprich, S.; Daniels, A. D.; Farkas, Ö.; Foresman, J. B.; Ortiz, J. V.; Cioslowski, J.; Fox, D. J. Gaussian, Inc., Wallingford CT, **2009**.

(5) (a) Becke, A. D. *J. Chem. Phys*. **1993**, *98*, 5648. (b) Lee, C.; Yang, W.; Parr, R. G. *Phys. Rev. B* **1988**, *37*, 785.

(6) Schaefer, A.; Horn, H.; Ahlrichs, R. *J. Chem. Phys.* **1992**, *97*, 2571-2577.

(7) Andrae, D.; Haeussermann, U.; Dolg, M.; Stoll, H. Preuss, *Theor. Chem. Acc.* **1990**, *77*, 123-141.

(8) (a) Peng, C.; Ayale, P. Y.; Schlegel, H. B.; Frisch, M. J. *J. Comput. Chem*. **1996**, *17*, 49. (b) Peng, C.; Schlegel, H. B. *Isr. J. Chem*. **1994**, *33*, 449.

(9) (a) Tomasi, J.; Persico, M.; *Chem. Rev.* **1994**, *94*, 2027. (b) Amovilli, C.; Barone, V.; Cammi, R.; Cancès, E.; Cossi, M.; Mennucci, B.; Pomelli, C. S.; Tomasi, J. *Adv. Quantum Chem.* **1998**, *32*, 227.

Artículo II.

Assembling Nonplanar Polyaromatic Units by Click Chemistry. Study of Multicorannulene Systems as Host for Fullerenes.

Assembling Nonplanar Polyaromatic Units by Click Chemistry. Study of Multicorannulene Systems as Host for Fullerenes.

Celedonio M. Álvarez*, Héctor Barbero, Luis A. García-Escudero, Cristina Martínez, Jose M. Martín-Álvarez, Daniel Miguel

GIR MIOMeT, IU CINQUIMA/Química Inorgánica, Facultad de Ciencias, Universidad de Valladolid, E-47005, Valladolid, Spain

celedonio.alvarez@uva.es

Received Date (will be automatically inserted after manuscript is accepted)

ABSTRACT

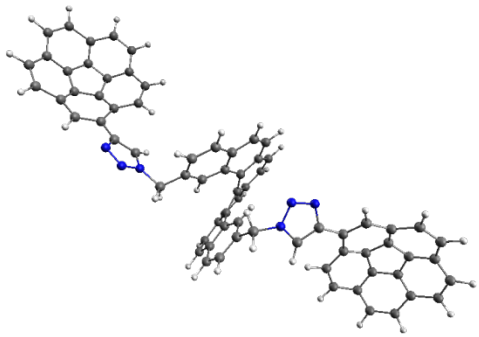

Novel compounds with two or three corannulene subunits have been obtained by "Click Chemistry". These exotic systems were synthesized in high yields using the ethynylcorannulene as common reagent. The synergistic action as receptors for fullerenes of several corannulene blocks has been evaluated. It was found that the tripod derivatives 5 and 6 showed efficient complexation abilities toward C_{60}. Furthermore, compound 7, in which two corannulene subunits are linked to a hexahelicene scaffold, has a remarkable affinity constant.

Corannulene is a non-planar polyaromatic molecule and can be considered as a fragment of fullerene C_{60}.[1] This bowl shaped π-conjugated compound has several interesting properties.[2] Corannulene has a dipole moment due to the different electronic density on its concave or convex face.[3] The excellent complementarity between the concave inner surface of corannulene and the outer convex surface of fullerene (a recent 1:1 cocrystalization between both molecules has been reported)[4] has promoted the study of several corannulene derivatives as hosts for fullerenes. [5,6] In our previous work we studied the

(1) For reviews, see: Wu, Y.-T.; Siegel, J. S. *Chem. Rev.* **2006**, *106*, 4843–4867. (b) Tsefrikas, V. M.; Scott, L. T. *Chem. Rev.* **2006**, *106*, 4868–4884.

(2) (a) Lovas, F. J.; McMahon, R. J.; Grabow, J.-U.; Schnell, M.; Mack, J.; Scott, L. T.; Kuczkowski, R. L. *J. Am. Chem. Soc.* **2005**, *127*, 4345–4349. (b) Wu, Y.-T.; Hayama, T.; Baldrige, K. K.; Linden, A.; Siegel, J. S. *J. Am. Chem. Soc.* **2006**, *128*, 6870–6884. (c) Sygula, A.; Folsom, H. E.; Sygula, R.; Abdourazak, A. H.; Marcinow, Z.; Fronczek, F. R.; Rabideau, P. W. *J. Chem. Soc., Chem. Commun.* **1994**, 2571–2572. (d) Wu, Y.-T.; Bandera, D.; Maag, R.; Linden, A.; Baldridge, K. K.; Siegel, J. S. *J. Am. Chem. Soc.* **2008**, *130*, 10729–10739.

(3) Scott, L. T.; Hashemi, M. M.; Bratcher, M. S. *J. Am. Chem. Soc.* **1992**, *114*, 1920–1921.

(4) Dawe, L. N.; AlHujran, T. A.; Tran, H.-A.; Mercer, J. I.; Jackson, E. J.; Scott, L. S.; Georghiou, P. E. *Chem. Commum.*, **2012**, *48*, 5563-5565.

(5) Alvarez, C. M.; García-Escudero, L. A.; García-Rodríguez, R.; Martín-Alvarez, J. M.; Miguel, D.; Rayón, V. M. *J. Am. Chem. Soc.*, **2012**, submitted.

(6) (a) Sygula, A.; Froncek, F. R.; Rabideau, P.; Olmstead, M. M.; *J. Am. Chem. Soc.* **2007**, *129*, 3842-3843. (b) Mück-Lichtendfeld, C.; Grimme, S.; Kobryn, L.; Sygula, A. *Phys. Chem. Chem. Phys.* **2010**, *12*, 7091-7097.(c) Sygula, R.; Sygula, A.; Sygula, R.; Ellern, A.; Rabideau, P. W. *Org. Lett.* **2003**, *5*, 2595–2597. (d) Georghiou, P. E.; Tran, A. H.; Mizyed, S.; Bancu, M.; Scott, L. T. *J. Org. Chem.* **2005**, *70*, 6158-6163. (e) Mizyed, S.; Geourghiou, P. E.; Bancu, M.; Cuadra, B.; Rai, A. K.; Cheng, P.; Scott, L. T. *J. Am. Chem. Soc.* **2001**, *123*, 12770-12774.

preparation of bis-arene(acetylide) platinum complexes of several polycyclic aromatics hidrocarbons (PAHs) such as pyrene, helicene or corannulene; evidencing that the corannulene derivative showed the most efficient association with fullerenes out of all the platinum complexes.[5] These biscorannulene tweezers present a strong π-π interaction with the fullerene. This effect had been previously found by Sygula et al. for their all-organic buckycatcher containing two corannulene units.[5a]

Considering the precedents outlined above, we decided to evaluate the ability of other multicoranulene systems as hosts for fullerenes. We reasoned that an alternative strategy to obtain corannulene-based receptors for fullerenes would be to increase the number of corannulene units in the host, where two or more corannulene moieties can interact with fullerenes simultaneously. Herein, we present the synthesis and the study of complexation with fullerene C_{60} of two tripodal triscorannulene derivatives (**5** and **6**). Additionally, we have designed and prepared a novel biscorannulene compound **7**, in which two corannulene subunits are linked to a chiral hexahelicene skeleton through triazole units.

We used copper catalyzed azide-alkyne cycloaddition (CuAAC) as a simple and practical route to prepare these compounds. Known as "click chemistry", this regioselective procedure has been used in recent years for the preparation of a wide variety of new materials.[7] Very recently, and parallel to our work, Stuparu published the synthesis of triazole-linked corannulene derivatives using CuAAC as an efficient methodology to prepare related corannulene rich materials.[8]

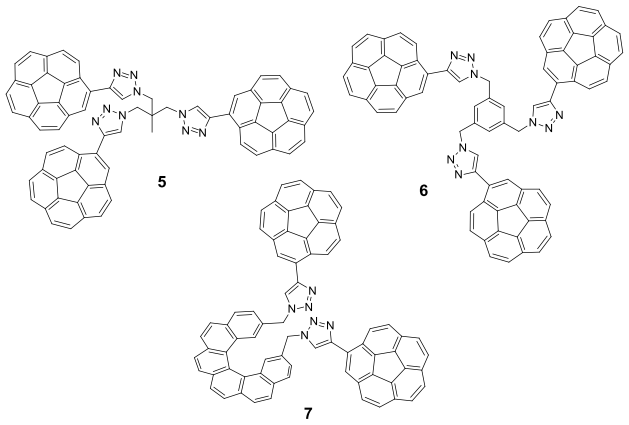

Figure 1. Structure of corannulene derivatives **5**, **6** and **7**.

The preparation of all new compounds started from ethynylcorannulene (**1**) as common alkyne reagent.[9] Subsequently, the azides α,α,α-tris(azidomethyl)ethane (**2**) and 1,3,5-tris(azidomethylbencene) (**3**) were prepared by using a reported procedure,[10] while the azide **4** was synthesized following the protocol of Scheme 1.

Scheme 1. Synthesis of 2,15-bis(azidomethyl)hexahelicene (**4**).

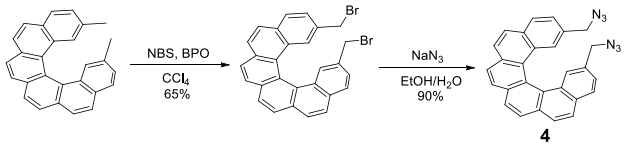

Azides **2**, **3** or **4** react with ethynylcorannulene **1**, in the presence of catalytic amounts of copper sulfate and sodium ascorbate in a mixture of 4:1 THF/H_2O to afford in good yields the expected 1,4-disubstituided 1,2,3-triazoles **5**, **6** and **7**, respectively (see supporting information for experimental details). The new corannulene compounds have been completely characterized by analytical and spectroscopic methods.

The ^{1}H NMR spectrum recorded in CD_2Cl_2 for triscorannulene derivative **5** shows the presence of a single compound of high symmetry. The protons of the three corannulene subunits appear as chemically equivalent and show a pattern consisting of a doublet at 8.38 ppm (integrating to 3H), a singlet at 8.29 ppm (integrating to 3H) and a multiplet of overlap signals between 7.82-7.70 (integrating to 21H); while the signal of the triazole appears at 8.64 ppm as a singlet. In addition, the signals of the aliphatic protons appear at 4.71 ppm as singlet (assignable as methylene protons) and at 1.16 ppm as singlet (assignable as methyl group). The integrals are in agreement with the presence of three corannulene units in the molecule. It is worth noticing that the NOESY spectrum of **5** in CD_2Cl_2 showed a NOE cross peak between the triazole and the methylene protons. However, a NOE cross peak between the methylene and the methyl group was not observed. All these results suggest that in solution the compound **5** has a structure of C_3 symmetry with the methylene protons and the methyl group in a close to *anti* orientation.

For compound **6**, the ^{1}H NMR spectral pattern at room temperature suggests that this compound again has a high degree of symmetry in solution. All the signals are relatively broad, indicating a conformational mobility. The corannulene protons on compound **6** show a characteristic signal pattern in the aromatic region consisting of one singlet, three pairs of doublets and two AB systems in the region of 8.1-7.2 ppm. Additionally, two extra singlet peaks at 7.94 and 7.28 ppm can be assigned to triazole and benzene rings, respectively. The remaining methylene protons appear at 5.54 ppm as a singlet. These results unambiguously support the tripodal structure depicted in Figure 1 for compound **6**.

Finally, compound **7** gives a very crowded ^{1}H NMR spectrum in the aromatic region in $CDCl_3$ (see Figure S7). Thirty corannulene or helicene protons appear in the

(7) Lahann J. *Click Chemistry for Biotechnology and Materials Science* Wiley-VCH Michigan, Ann Arbor, USA 2009.

(8) Stuparu, M. C. *Tetrahedron* **2012**, *68*, 3527-3531.

(9) For synthesis of ethynylcorannulene (**1**) see: Mack, J.; Vogel, P.; Jones, D.; Kavala, N.; Suttona A. *Org. Biomol. Chem*., **2007**, *5*, 2448-2452.

(10) For synthesis of α,α,α-tris(azidomethyl)ethane (**2**) see: (a) Beaufort, L.; Delaude, L.; Noels A.F. *Tetrahedron* **2007**, *63*, 7003-7007. For synthesis of 1,3,5-tris(azidomethylbencene) (**3**) see: (b) Granzhan, A.; Schowey, C.; Riis-Johannessen, T.; Scopelliti, R.; Severin, K. *J. Am. Chem. Soc*. **2011**, *133*, 7106-7115.

region of 8.2-7.6 ppm as doublets, AB systems or singlets. The triazole singlet appears at 7.27 ppm and the remaining aromatic signal corresponding to two helicene protons appears at 7.16 ppm. The diasterotopic protons of methylene appear as a pair of doublets at δ 5.17 and 4.89 ppm. The integral of the signals are in agreement with the presence of two corannulene moieties in the molecule. The $^{13}C\{^{1}H\}$ NMR spectra of all these compounds **5**-**7** are as expected for their highly symmetrical structures.

The molecular structure of compound **7** was computationally investigated at the B3LYP level. The minimum energy conformation calculated for **7** corresponds to a C_2 symmetric structure with the two corannulene subunits pointing opposite directions.

To determine the binding constant of the complexation of **5**-**7** with C_{60}, we titrated a deuterated toluene solution of either receptor with C_{60} at 25ºC. The Job plots between compounds **5**-**7** and C_{60} are all consistent with the formation of 1:1 stoichiometry. For compound **5**, the NMR titration experiment showed that, surprisingly, the most significant changes in the chemical shift were observed for the alkyl protons (see Figure 2). Although the concave surfaces of corannulene subunits should wrap nicely around the entrapped fullerene guest, this data suggests that the position of fullerene within our host is very close to the CH_2 fragment. This behavior could be explained by the formation of reasonable CH/π interactions between the methylene groups and the fullerene. There are some examples of CH/π interactions in supramolecular fullerene chemistry.[11]

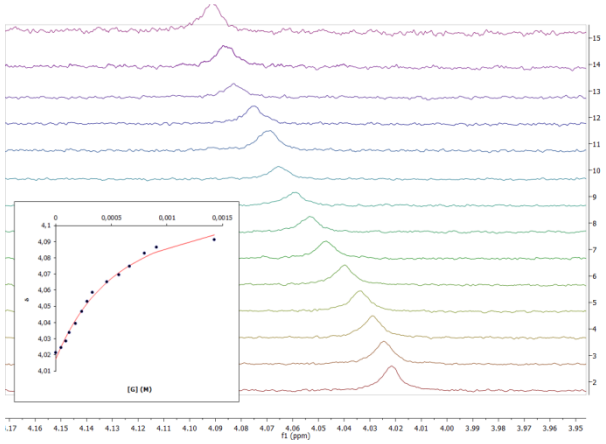

Figure 2. Methylene region of ^{1}H NMR spectra of a dilute toluene-d_8 solution of **5** (2.0×10^{-4}M) with variable concentration of C_{60}. Nonlinear curve regression for the results of the titration for methylene proton (inset, bottom left).

The binding constants (K_a) of complexes **5**⊂C_{60}, **6**⊂C_{60} and **7**⊂C_{60} in toluene-d_8 at room temperature were found to be 2152, 2192 and 2547 M^{-1} respectively. These values are among the highest reported to date for a corannulene derivative as a host for fullerene.

It is known that corannulene compounds can suffer intermolecular association among themselves. This can induce notable changes in its properties.[12] The possible self-association of compounds **5**-**7** has been studied by ^{1}H NMR spectroscopy using the analysis of proton chemical shifts changes in toluene-d_8 solution as a function of concentration. In all cases, the signals of all protons remain unchanged, evidencing the lack of self-association in the derivatives **5**-**7**. On the other hand, intramolecular association between several corannulene subunits may occur, and this fact would help to explain the comparable binding constants with fullerenes between the tris and biscorannulene derivatives.

In conclusion, we have designed and synthesized a family of fullerene receptors through combination of several corannulene fragments linked by triazole units. It was found that tripodal **5** and **6** have remarkable association constants with fullerene C_{60}. (K_a = 2152 M^{-1} and 2192 M^{-1} respectively). We have also developed a novel biscorannulene receptor **7**, which bears a chiral hexahelicene moiety, with significant abilities for binding C_{60} (K_a = 2547 M^{-1}). These findings open the possibility of utilizing the enantiomers of derivative **7**, as host molecules for recognizing and discriminating higher chiral fullerenes. This potential application in enantioselective molecular recognition is currently under investigation.

Acknowledgment. This work was funded by the Spanish Ministerio de Ciencia e Innovación (CTQ2009-12111) and the Junta de Castilla y León (VA070A08 and GR Excelencia 125). H. B. and C. M. A. wish to thank for a MEC-FPI grant and a Ramón y Cajal contract, and L. A. G.-E. thanks University of Valladolid for a Ph D grant.

Supporting Information Available: Synthetic procedure and NMR spectra for **4**-**7** compounds (^{1}H, $^{13}C\{^{1}H\}$, COSY) and complexation studies. This material is available free of charge via the Internet at http://pubs.acs.org.

(11) Suezawa, H.; Yoshida, T.; Ishihara, S.; Umezawa, Y.; Nishio, M. *Cryst. Eng. Comm.* **2003**, *5*, 514-518.

(12) (a) Miyajima, D.; Tashiro, K.; Araoka, F.; Takezoe, H.; Kim, J.; Kato, K.; Takata, M.; Aida, T. *J. Am. Chem. Soc.* **2009**, *131*, 44-45. (b) B. M. Schmidt, B. Topolinski, P. Roesch, D. Lentz *Chem. Commun.* **2012** ,*48*, 6520.

Supporting Information

Assembling Nonplanar Polyaromatic Units by Click Chemistry. Study of Multicorannulene Systems as Host for Fullerenes.

Celedonio M. Álvarez*, Héctor Barbero, Luis A. García-Escudero, Cristina Martínez, Daniel Miguel

IU CINQUIMA/Química Inorgánica, Facultad de Ciencias, Universidad de Valladolid, E-47005, Valladolid, Spain

* To whom correspondence should be addressed. E-mail: celedonio.alvarez@uva.es.

1. Experimental section.

1.1. General Methods.

Synthetic procedures were carried out under an inert atmosphere of nitrogen, in dry solvents (by passage through alumina columns in an IT Solvent Purification System and degassed with N_2), using standard Schlenk techniques, unless otherwise noted. Solution NMR spectra were obtained on a Bruker AV-400 or a Varian MR 400 spectrometers. All NMR solvents were stored over molecular sieves and degassed prior to use. Shift values are given in ppm. ^{1}H chemical shifts are referenced to solvents. Elemental analyses were performed on a Perkin-Elmer 2400B CHN analyzer. Flash chromatographic purification was performed using silica gel Merck 60 (particle size 0.040–0.063 mm); the eluting solvent for each purification was determined by thin layer chromatography (TLC). Analytical thin-layer chromatography was performed using Merck TLC silica gel 60 F254.

1.2. Synthetic procedures and characterization data.

Synthesis of 2,15-bis(azidomethyl)hexahelicene (4).

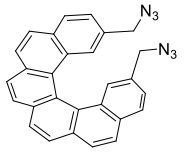

A solution of 2,15-bis(bromomethyl)hexahelicene (50 mg, 0.096 mmol) and NaN_3 (65.0 mg, 2.82 mmol) in DMF (5 mL) was stirred at room temperature for 1 h, then poured into water (25 mL) and extracted with CH_2Cl_2 (3 × 10 mL). The combined organic phases were washed with water, brine, dried over anhyd. $MgSO_4$, evaporated, and the residue was purified by column chromatography on silica gel; eluted with CH_2Cl_2/hexane = 3/2 to give **4** (38 mg, 78%) as a white solid. ^{1}H NMR ($CDCl_3$, 400MHz) δ 8.05 (d(AB system), *J* = 8.5 Hz, 2*H*), 8.01 (d(AB system), *J* = 8.5 Hz, 2*H*), 7.98 (d(AB system), *J* = 8.5 Hz, 2*H*), 7.95 (d(AB system), *J* = 8.5 Hz, 2*H*), 7.87 (d, *J* = 8.0 Hz, 2*H*), 7.52 (s, 2*H*), 7.20 (dd, *J* = 8.0 Hz and *J* = 1.5 Hz, 2*H*), 3.73 (s, 4H, -C*H*$_2$-) ; ^{13}C{^{1}H} NMR ($CDCl_3$ 100 MHz) δ 134.09, 133.37,

132.03, 131.83, 131.68, 129.77, 128.26, 127.63, 127.60, 127.56, 127.51, 127.05, 125.46, 124.07, 54.82. Anal. Calcd for $C_{28}H_{18}N_6$: C, 84.83; H, 4.58; N, 10.60. Found: C, 84.90 ; H, 4.61 ; N, 10.50.

Synthesis of compound 5.

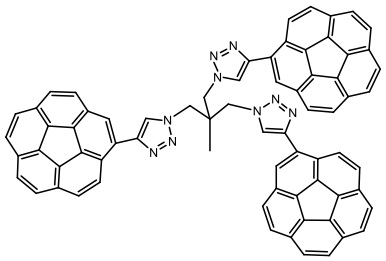

A mixture of ethynilcorannulene (0.075 g, 0.27 mmol), α,α,α-tris(azidomethyl)ethane (**2**) (0.016 g, 0.08 mmol), $CuSO_4.5H_2O$ (0.07 g, 0.026 mmol) and sodium ascorbate (0.05 g, 0.026 mmol) were reacted in 4:1 THF:water (20 mL) at 60ºC for 4 days. The compound was extracted with CH_2Cl_2 (3 × 25 mL), dried over magnesium sulfate, filtered and the volatiles removed under reduced pressure. The product was purified by column chromatography on silica gel eluted with CH_2Cl_2/methanol = 98/2 to yield **5** as a white solid. (69 mg, 85 %). ^{1}H NMR (CD_2Cl_2, 400MHz) δ 8.64 (s, 3H, trz), 8.38 (d, *J* = 8.9 Hz, 3H, cor), 8.29 (s, 3H, cor), 7.82-7.70 (m, 21H, cor), 4.71 (s, 6H, -C*H*$_2$-), 1.16 (s, 3H, -C*H*$_3$) ; ^{13}C{^{1}H} NMR (CD_2Cl_2 100 MHz) δ 146.81, 135.88, 135.77, 135.37, 135.29, 135.13, 130.93, 130.90, 130.73, 130.24, 128.84, 128.41, 127.68, 127.38, 127.30, 127.16, 127.06, 126.84, 126.78, 125.34, 124.94, 53.8, 19.73. Anal. Calcd for $C_{71}H_{39}N_9$: C, 83.76; H, 3.86; N, 12.38. Found: C, 83.85 ; H, 3.87 ; N, 12.28.

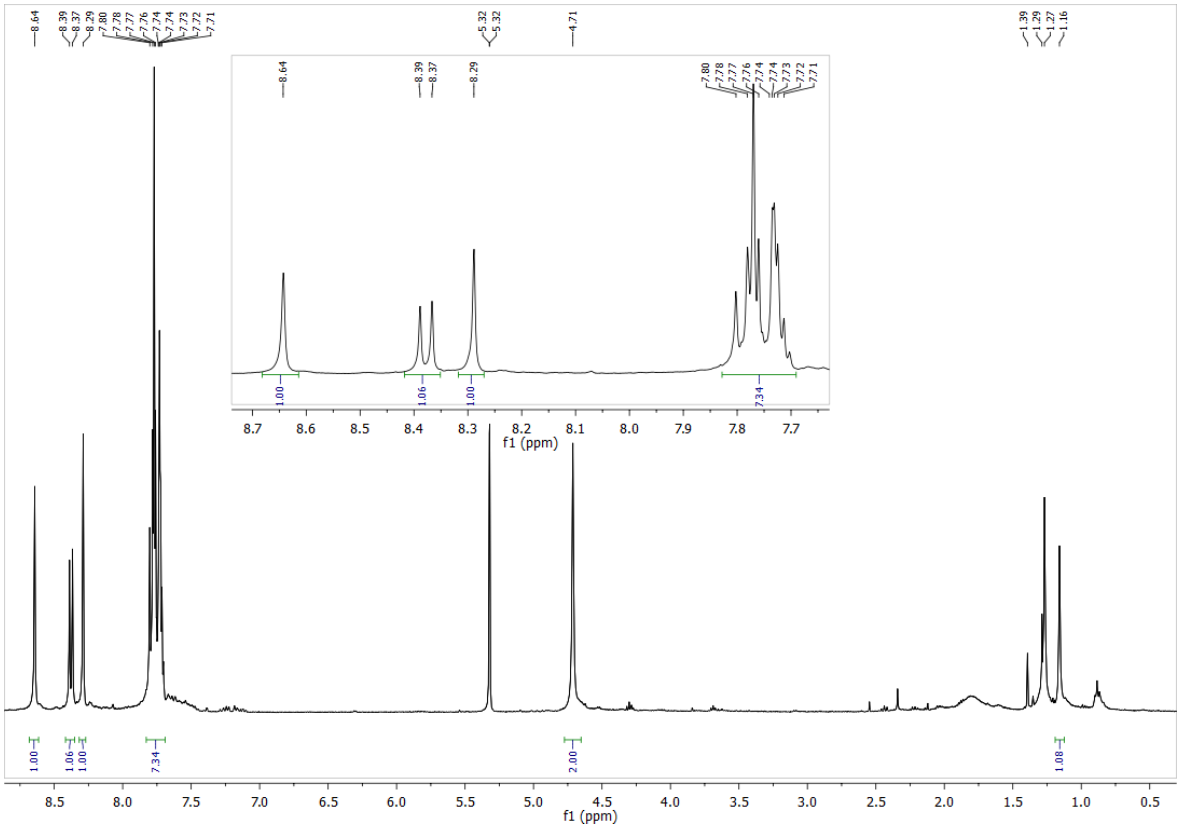

Figure S1. ^{1}H NMR spectrum of **5** in CD_2Cl_2.

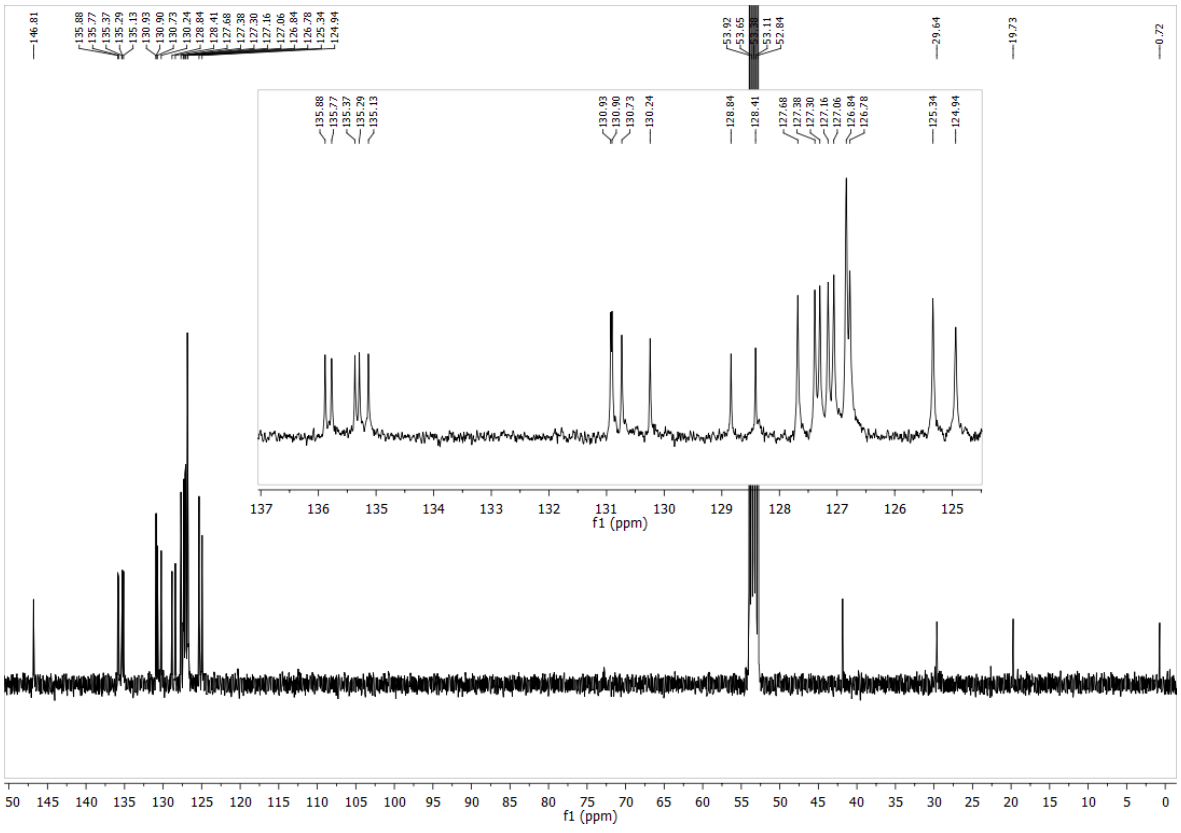

Figure S2. $^{13}C\{^{1}H\}$ NMR spectrum of **5** in CD_2Cl_2.

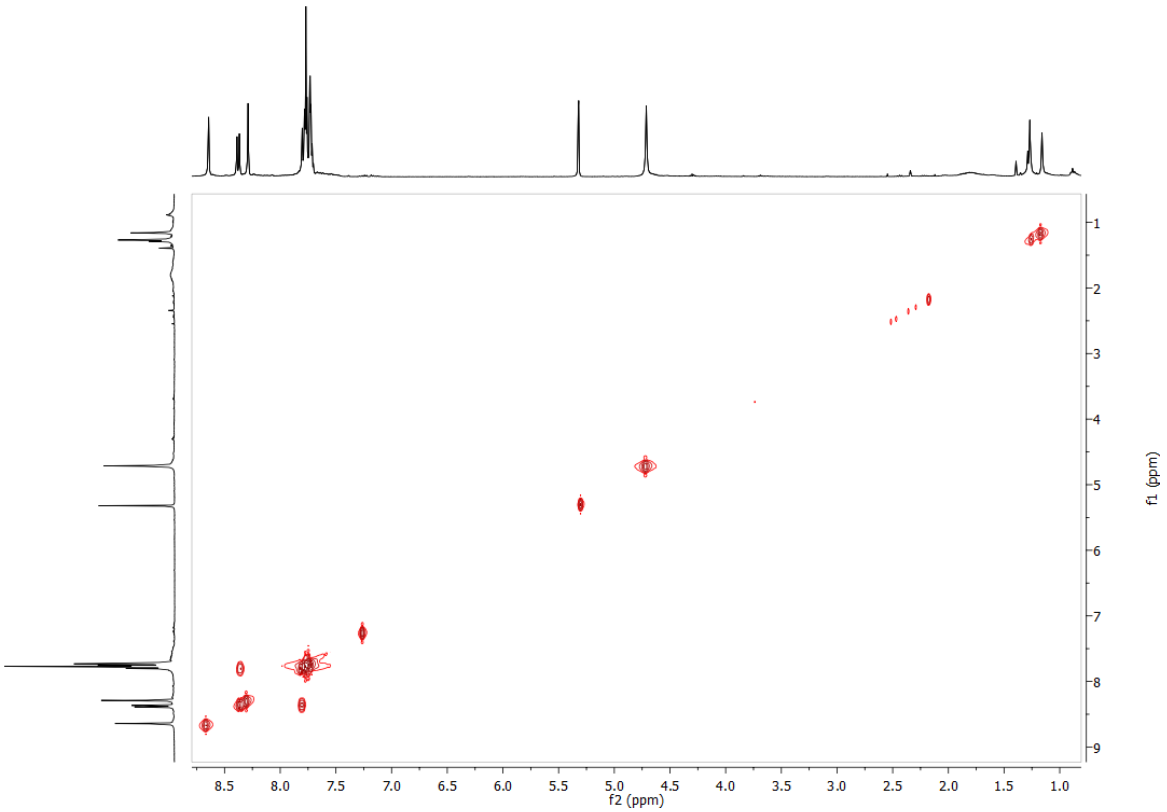

Figure S3. COSY NMR spectrum of **5** in CD_2Cl_2.

Synthesis of compound 6.

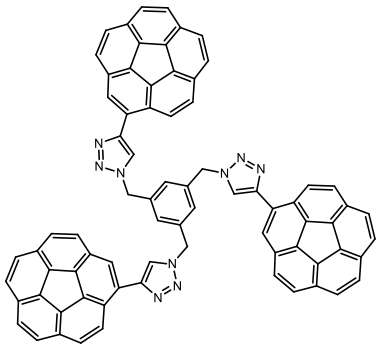

A mixture of ethynilcorannulene (0.125 g, 0.46 mmol), 1,3,5-tris(azidomethylbencene) (0.037 g, 0.152 mmol), $CuSO_4.5H_2O$ (0.012 g, 0.046 mmol) and sodium ascorbate (0.09 g, 0.046 mmol) were reacted in 4:1 THF:water (30 mL) at 60ºC for 4 days. The compound was extracted with CH_2Cl_2 (3 × 25 mL), dried over magnesium sulfate, filtered and the volatiles removed under reduced pressure. The product was purified by column chromatography on silica gel eluted with $CHCl_3$/ethylacetate = 1/1 to yield **6** as

a white solid. (134 mg, 83 %). ^{1}H NMR ($CDCl_3$, 400MHz) δ 8.07 (d, *J* = 9.0 Hz, 3H, cor), 8.99 (s, 3H, cor), 7.94 (s, 3H, trz), 7.61 (d(AB system), *J* = 8.5 Hz, 3H, cor), 7.59 (d(AB system), *J* = 8.5 Hz, 3H, cor) 7.58 (d, *J* = 8.5 Hz, 3H, cor), 7.56 (d, *J* = 8.5 Hz, 3H, cor), 7.48 (d, *J* = 8.5 Hz, 3H, cor), 7.46 (d, *J* = 8.5 Hz, 3H, cor), 7.38 (d(AB system), *J* = 8.5 Hz, 3H, cor), 7.27 (s, 3H, bencene) 5.54 (s, 6H, -CH_2-) ; ^{13}C{^{1}H} NMR ($CDCl_3$ 100 MHz) δ 147.62, 137.19, 135.72, 135.46, 135.12, 134.98, 134.88, 130.58, 130.40, 129.79, 128.49, 128.05, 127.59, 127.40, 127.12, 127.10, 126.99, 126.89, 126.66, 126.56, 126.46, 125.24, 122.06, 53.37. Anal. Calcd for $C_{75}H_{39}N_9$: C, 84.49; H, 3.69; N, 11.82. Found: C, 84.54 ; H, 3.59 ; N, 11.87.

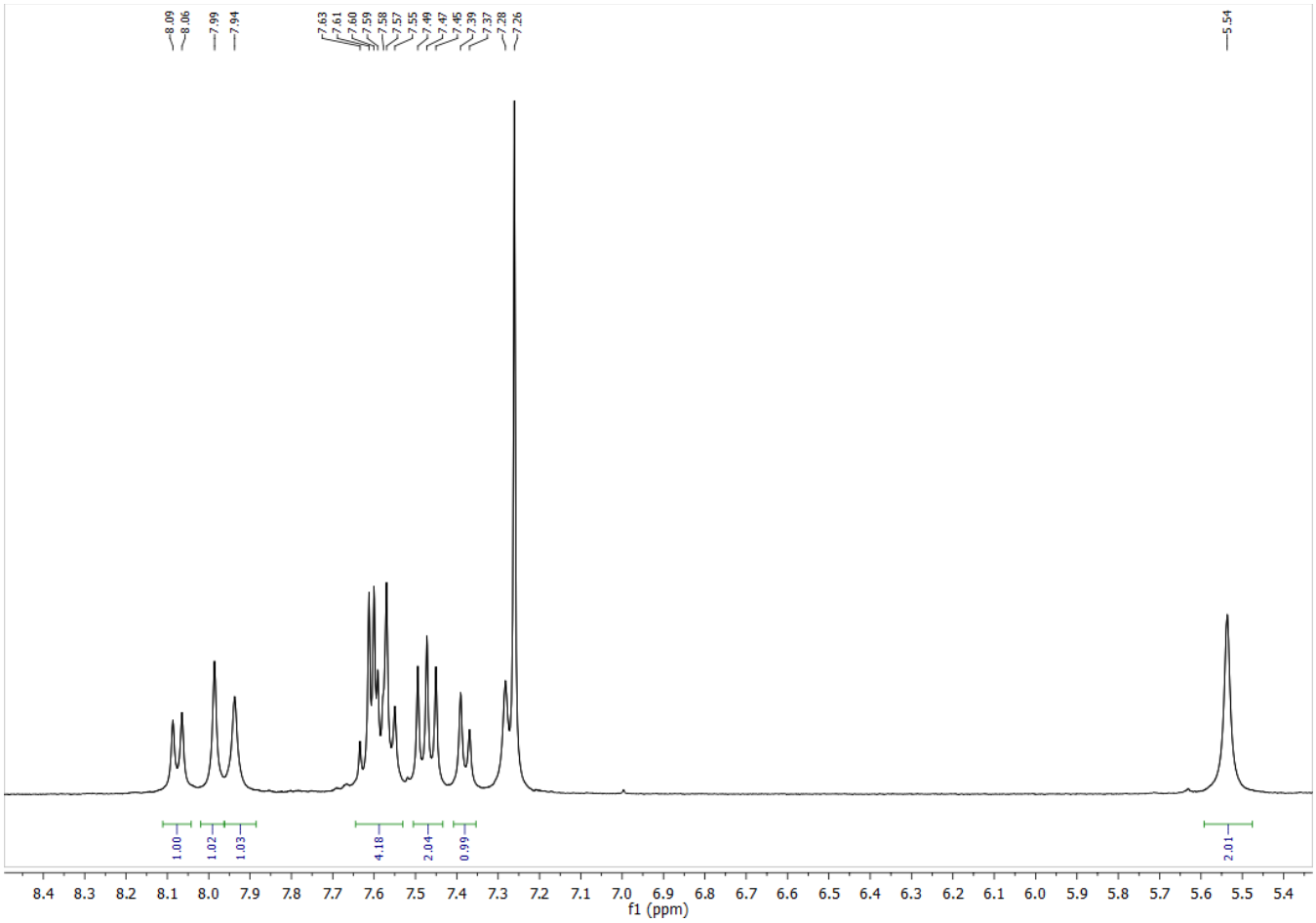

Figure S4. ^{1}H NMR spectrum of **6** in $CDCl_3$.

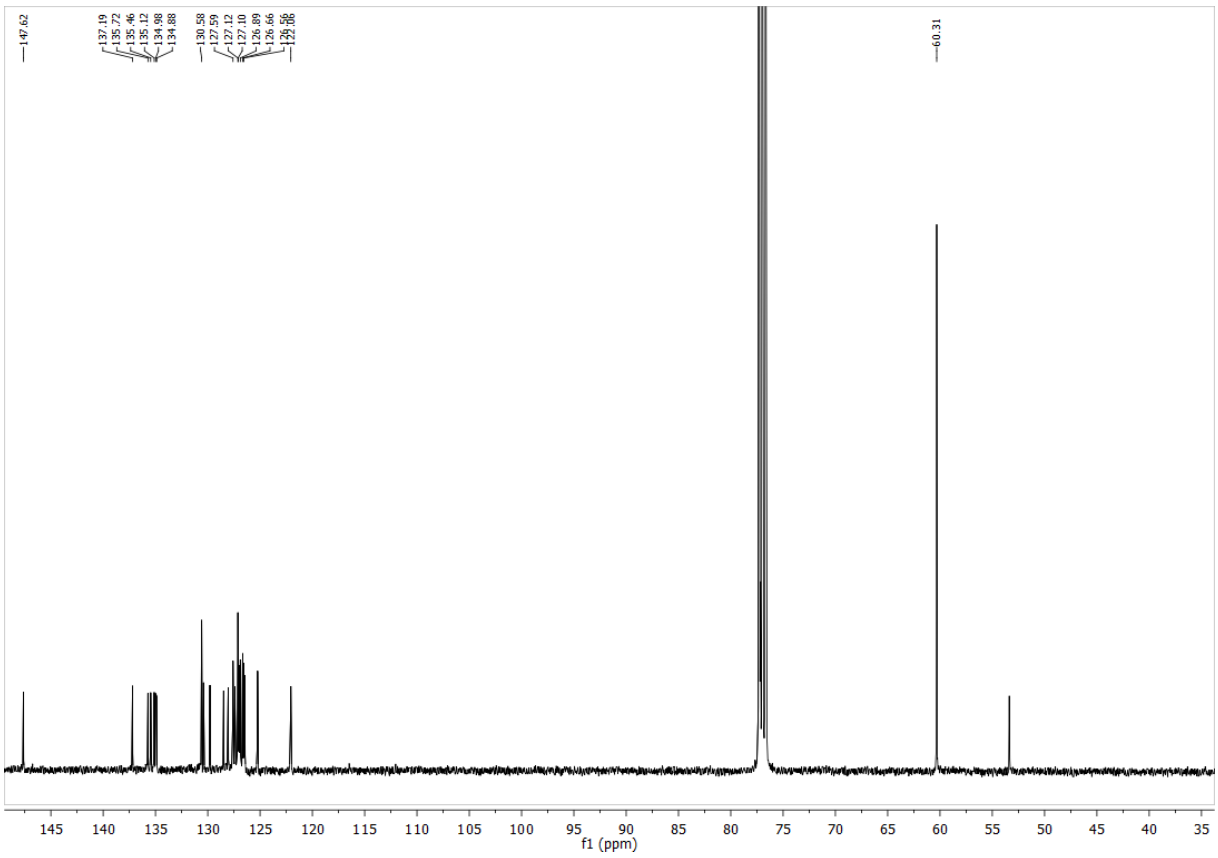

Figure S5. $^{13}C\{^{1}H\}$ NMR spectrum of **6** in $CDCl_3$.

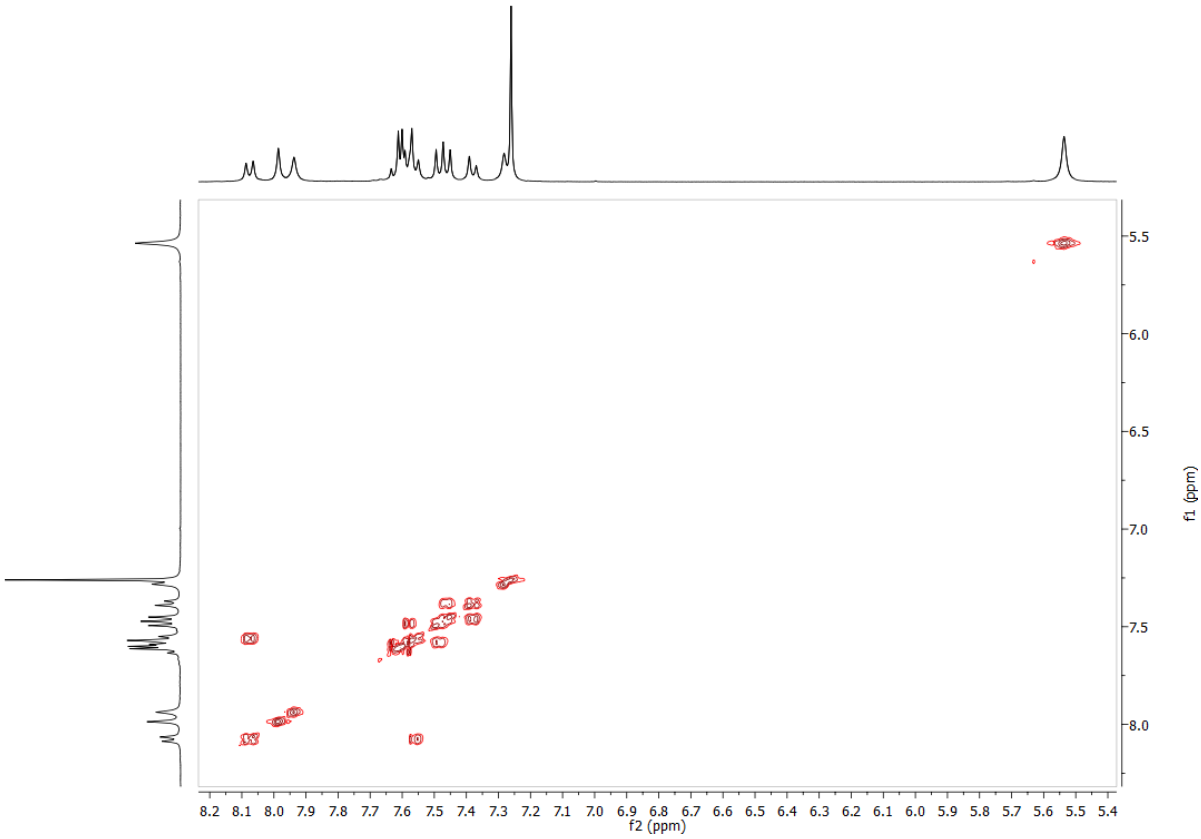

Figure S6. COSY NMR spectrum of **6** in $CDCl_3$.

Synthesis of compound 7.

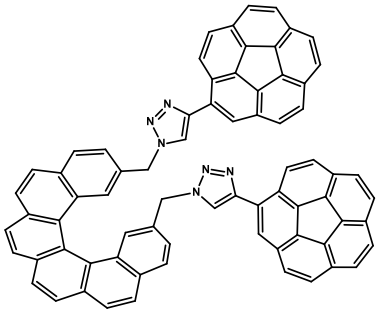

A mixture of ethynilcorannulene (0.025 g, 0.091 mmol), 2,15-bis(azidomethyl)hexahelicene (**4**) (0.020 g, 0.045 mmol), $CuSO_4.5H_2O$ (0.01 g, 0.005 mmol) and sodium ascorbate (0.01 g, 0.005 mmol) were reacted in 4:1 THF:water (15 mL) at 60ºC for 3 days. The compound was extracted with CH_2Cl_2 (3 × 25 mL), dried over magnesium sulfate, filtered and the volatiles removed under reduced pressure. The product was purified by column chromatography on silica gel eluted with CH_2Cl_2/methanol = 97/3 to yield **7** as a white solid. (33 mg, 75 %).^{1}H NMR ($CDCl_3$, 400MHz) δ 8.11 (d, *J* = 9.0 Hz, 2H, cor), 8.04 (d(AB system), *J* = 8.5 Hz, 2H, hel), 8.02 (s, 2H, cor), 7.98 (d(AB system), *J* = 8.5 Hz, 2H, hel), 7.93 (d(AB system), *J* = 8.5 Hz, 2H, hel), 7.88 (d(AB system), *J* = 8.5 Hz, 2H, hel), 7.82 (d, *J* = 8.0 Hz, 2H, hel), 7.77 (d(AB system), *J* = 8.5 Hz, 2H, cor), 7.76 (d(AB system), *J* = 8.5 Hz, 2H, cor), 7.74 (d(AB system), *J* = 8.5 Hz, 2H, cor), 7.70 (d(AB system), *J* = 8.5 Hz, 2H, cor),7.70-7.68 (m, 6H, cor(4H) and hel(2H)) 7.67 (d, *J* = 9.0 Hz, 2H, cor), 7.27 (s, 2H, trz), 7.16 (dd, *J* = 8.0 Hz and 1.5 Hz, 2H, hel),. 5.17 (d, *J* = 15.0 Hz, 2H, -C*H*$_2$-), 4.89 (d, *J* = 15.0 Hz, 2H, -C*H*$_2$-); ^{13}C{^{1}H} NMR ($CDCl_3$ 100 MHz) δ 147.20, 137.14, 135.97, 135.73, 135.40, 135.30, 135.16, 133.31, 131.75, 131.69, 131.01, 130.74, 130.61, 130.12, 129.74, 129.08, 129.01, 128.33, 127.60, 127.57, 127.52, 127.48, 127.45, 127.37, 127.30, 127.21, 127.05, 126.91, 126.85, 54.03. Anal. Calcd for $C_{72}H_{38}N_6$: C, 87.61; H, 3.88; N, 8.51. Found: C, 87.66 ; H, 3.84 ; N, 8.50.

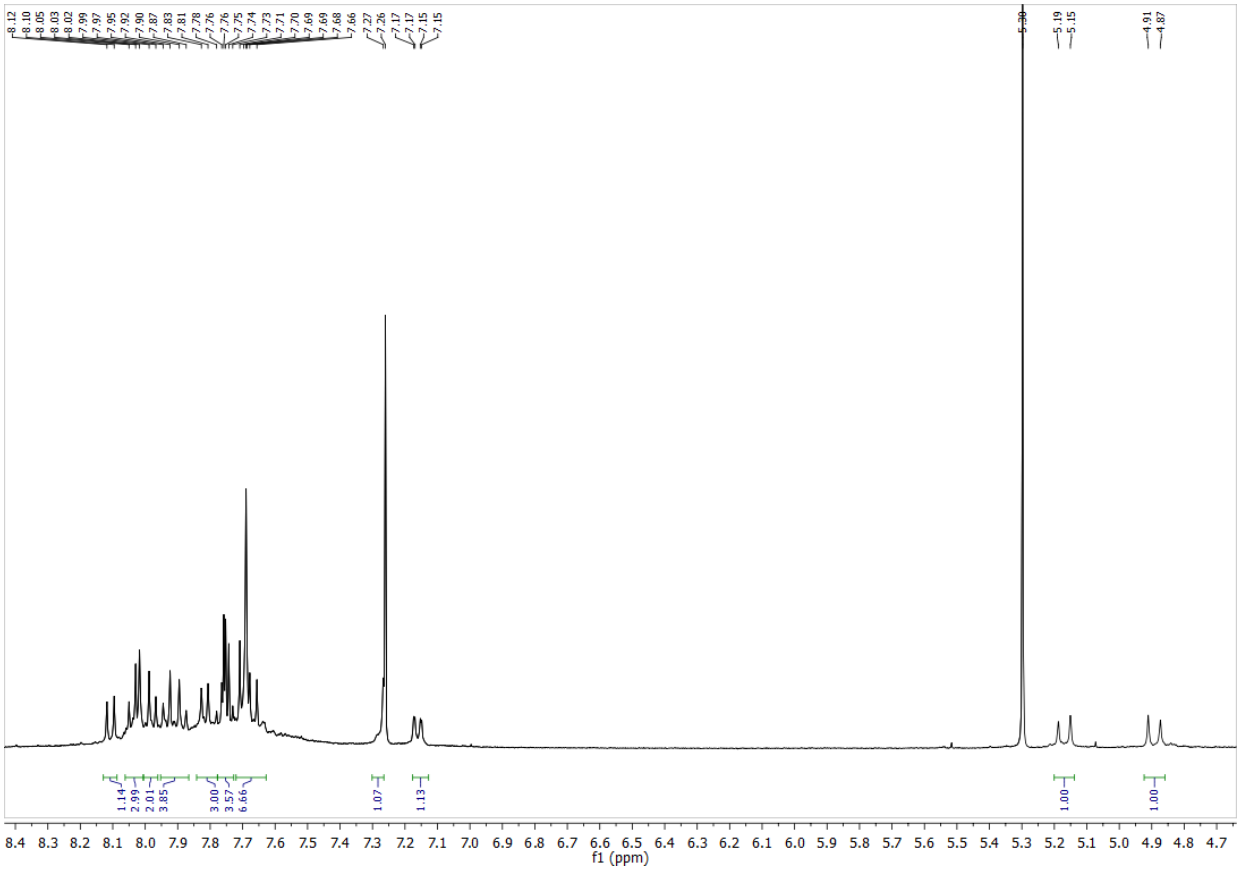

Figure S7. ^{1}H NMR spectrum of **7** in $CDCl_3$.

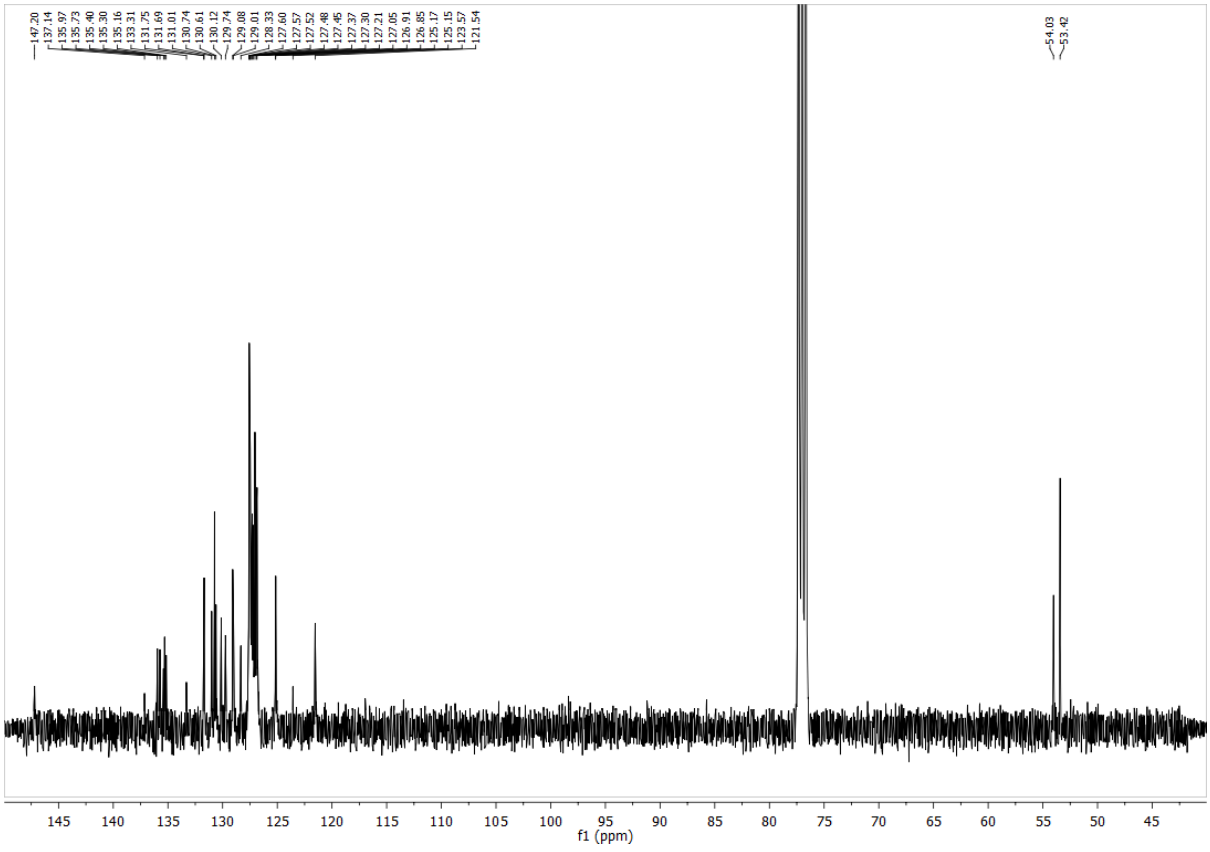

Figure S8. $^{13}C\{^{1}H\}$ NMR spectrum of **7** in $CDCl_3$.

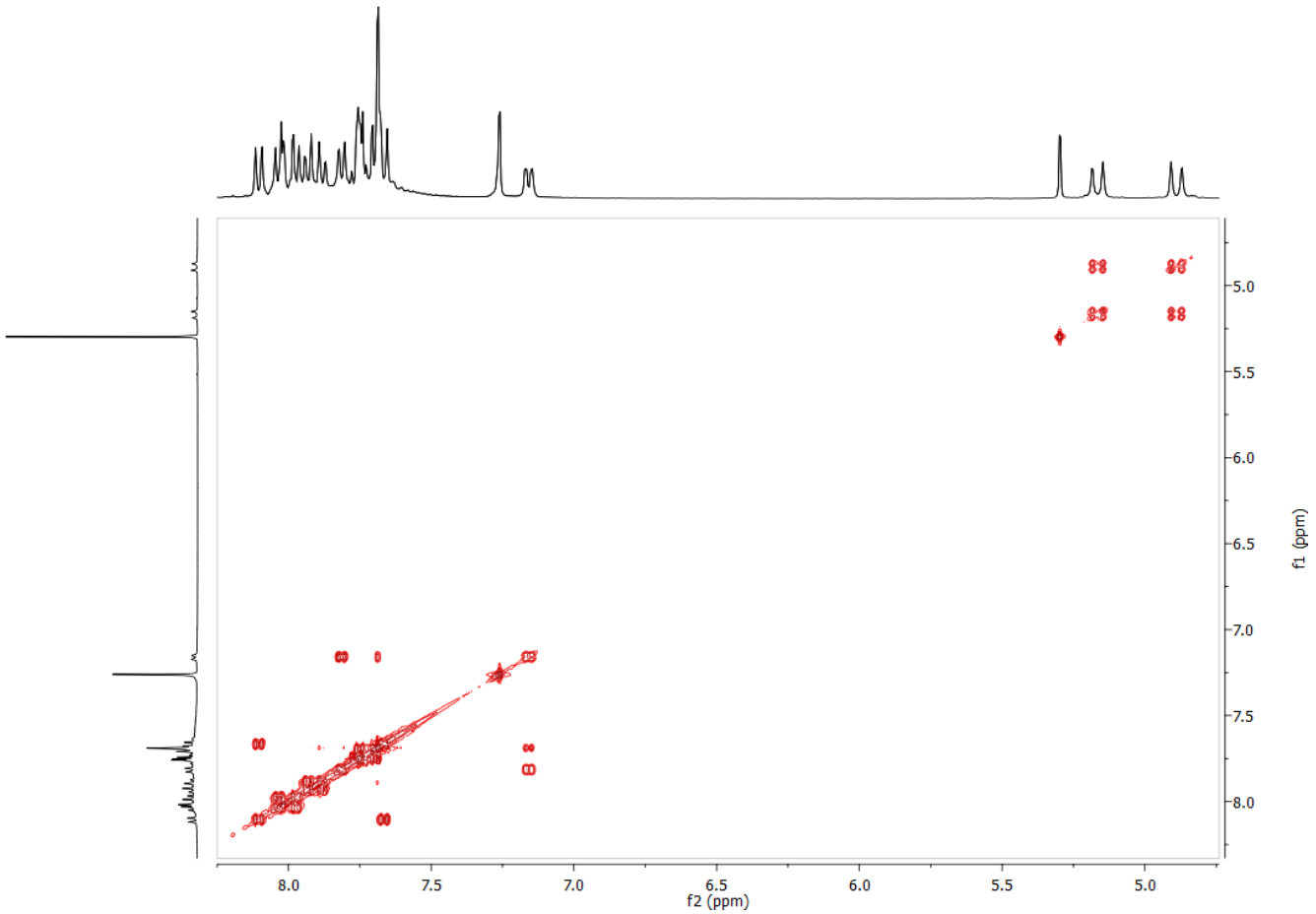

Figure S9. COSY NMR spectrum of **7** in $CDCl_3$.

2. Complexation measurements of compounds 5, 6 and 7.

To obtain the association constants (K_a) corresponding to complex formation, the changes in the chemical shifts ($\Delta\delta$) as a function of concentration of C_{60} were determined. The host compounds **5**, **6** or **7** were dissolved in toluene-d_8 (approx. 2×10^{-4}M) in an NMR tube, to which were added portions of the C_{60} solution (approx. 2×10^{-3}M). K_a was calculated from the changes of the chemical shifts of selected independent protons of the corannulene-based host **5**, **6** or **7**. K_a and L were optimized as parameters in the curve fitting. The Excel workbooks for curve-fitting NMR titration data of the Sanderson group (http://www.dur.ac.uk/j.m.sanderson/science/downloads.html) were employed for this purpose. Non linear curve regression for the results of the titration experiments of C_{60} with **5**,**6** or **7** for selected protons (binding constant (Ka) were calculated by fitting of the chemical shifts to a 1:1 binding isotherm).

The average K_a for compound **5** is 2152 M^{-1} (the estimated Ka values are 2528 M^{-1}, 1936 M^{-1}, 1797 M^{-1} and 2348 M^{-1} as calculated for selected protons in **5**).

The average K_a for compound **6** is 2192 M^{-1} (the estimated Ka values are 2220 M^{-1}, 2129 M^{-1}, 2159 M^{-1} and 2261 M^{-1} as calculated for selected protons in **6**).

The average K_a for compound **7** is 2547 M^{-1} (the estimated Ka values are 2737 M^{-1}, 2340 M^{-1}, 2603 M^{-1} and 2510 M^{-1} as calculated for selected protons in **7**).

Method of continuous variation ("Job plot") was used to determine the stoichiometry of the complexation between **5**, **6** or **7** and fullerene C_{60}. Mole ratio plot of $\Delta\delta$ versus guest-to-host molar ratios confirmed the 1:1 stoichiometry in the three cases (Figure S22).[1]

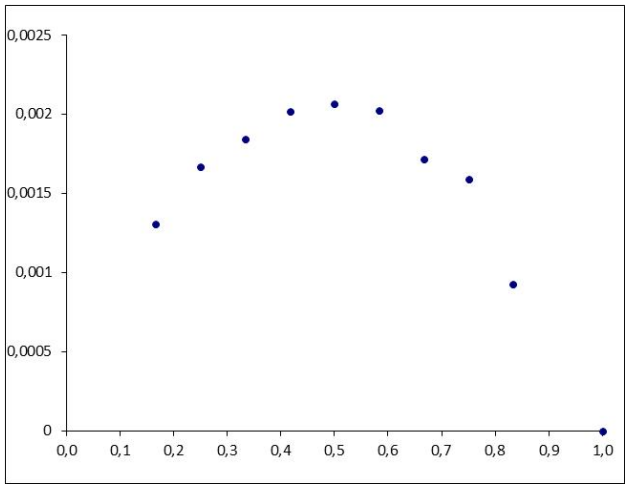

Figure S22. Job plot showing the 1:1 stoichiometry of C_{60} *vs* **5**.

([1]) Job, P. *Ann. Chim.* **1928**, *9*, 113-203.

Artículo III.

How Metals Can Induce the Right Geometry as Hosts for Fullerenes.

How Metals Can Induce the Right Geometry as Hosts for Fullerenes

Journal:	*Journal of the American Chemical Society*
Manuscript ID:	ja-2012-07002c
Manuscript Type:	Communication
Date Submitted by the Author:	17-Jul-2012

Complete List of Authors:	Alvarez, Celedonio; Universidad de Valladolid, Química Inorgánica Garcia-Escudero, Luis; Universidad de Valladolid, Martín-Alvarez, Jose; University of Valladolid, Quimica Inorganica Miguel, Daniel; Universidad de Valladolid, Quimica Inorganica Rayón, Victor; Universidad de Valladolid, Química Física García-Rodríquez, Raúl; University of Valladolid, Quimica Inorganica

How Metals Can Induce the Right Geometry as Hosts for Fullerenes

Celedonio M. Álvarez,*[,†] Luis A. García–Escudero,[†] Raúl García-Rodriguez,[†] Jose M. Martín-Alvarez,[†] Daniel Miguel,[†] Víctor M. Rayón[‡]

[†]GIR MIOMeT, IU CINQUIMA/Química Inorgánica, Facultad de Ciencias, Universidad de Valladolid, E-47005, Valladolid, Spain.

[‡]Departamento de Química Física y Química Inorgánica, Facultad de Ciencias, Universidad de Valladolid, E-47005, Valladolid, Spain

KEYWORDS. corannulene, PAHs, fullerenes, host-guest systems, supramolecular chemistry.

Supporting Information Placeholder

ABSTRACT: The geometry imposed by the coordination sphere around the metal, together with the choice of the rigid acetylide spacers can be used advantageously to build corannulene-based molecular tweezers which show great affinities for C_{60} and C_{70}, as revealed by NMR titration experiments, DFT calculations and the single crystal X-ray structural analysis of compound C_{60}⊂**1**.

The design of molecular receptors has attracted the interest of the research community during years. In particular, the syntheses of compounds that can form supramolecular aggregates by non-covalent interactions have been studied in detail.[1] In this regard, the most significant progress has been made in fullerene recognition.[2] Both size and shape are the main factors that determine the design of molecular architectures to be used to this purpose and thus cages, macrocycles or molecular tweezers are the most recurrent constructions. Looking for the right geometry, many kinds of compounds have been reported from the early calixarenes[3] or cyclotriveratrylenes (CTVs),[4] to porphyrins,[5] corannulenes,[6] tetrathiofulvalenes (TTFs),[7] cycloparaphenyleneacetylenes (CPPAs),[8] cycloparaphenylenes (CPPs),[9] or tribenzotriquenacenes.[10]

Usually, the fullerene receptors bear heteroatoms or polar substituents and, in these cases, it has been demonstrated that a high complementarity between host and guest leads to a maximization of the electrostatic interactions and induction forces that play an important role in the association of fullerenes.[2b] However, it is much more difficult to build purely carboaromatic fullerene receptors and, consequently, the number of examples that describe the formation of these supramolecular adducts is very limited. As far as we know, the onion type structures of the carbon nanorings,[8,9] and the corannulene buckycatcher of Sygula et al.[6e] are the only examples described. On the other hand, aside from porphyrin derivatives, the use of metal complexes as receptors for fullerenes has been reported for the formation of several fullerene cages.[11]

In purely carboaromatic fullerene receptors, the complementarity between host and guest should be the most important factor affecting the adduct stability. In the current work, we describe a simple procedure to prepare molecular tweezers by attaching different polycyclic aromatic hydrocarbons (PAHs) in a cis arrangement to platinum square planar complexes. The molecules prepared in this way, which have the PAHs fragments in a suitable geometry to function as fullerene receptors, while the metal atom is too far away to interact with the fullerene (therefore the receptor can be considered as purely carboaromatic), were evaluated as hosts for C_{60} and C_{70}.

Synthesis of complexes **1**-**4** was carried out in a one pot procedure by the coupling of the corresponding trimethylsilylethynylpolyaromatic derivative and [$PtCl_2$(dppe)] at room temperature in very good yields. The resulting complexes bear the well-known 1,2-bis(diphenylphosphino)ethane ligand (dppe), and the two remaining coordination positions are occupied by the two polyaromatic ethynyl units (Figure 1).

All these new compounds are air stable, can be stored as solids for several months, and were characterized by analytical and spectroscopic methods (see supporting information for experimental details and spectroscopic data).

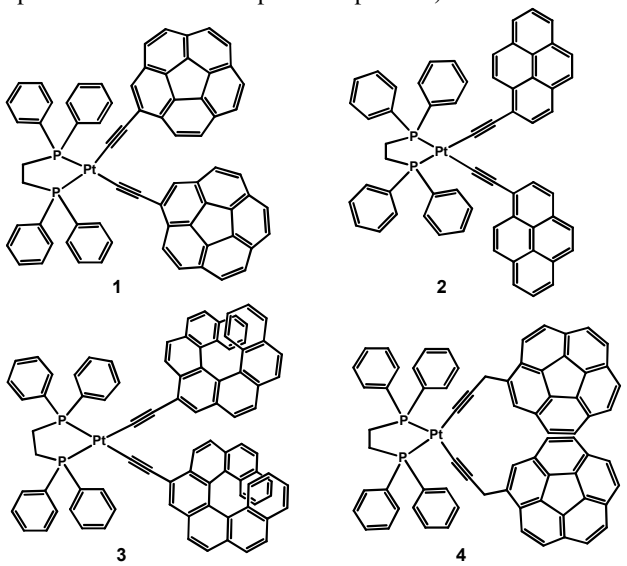

Figure 1. Square planar Platinum complexes used as molecular tweezers.

Taking advantage of the suitable arrangement of the two corannulene units in the molecular tweezers **1**, we decided to study its binding to fullerenes. The first evidence to support the formation of supramolecular association was found by

means of MALDI-TOF MS spectrum. The spectrum of a 1:1 mixture of **1** and C_{60}, showed peaks at *m/z* 1859.34 and 1860.34, corresponding to $[C_{60}\subset\mathbf{1}]^+$ and $[C_{60}\subset\mathbf{1}\text{-H}]^+$ (calcd.: 1859.24 and 1860.24).

The association of **1** and fullerenes in solution was also investigated by ^{1}H NMR titration (400 MHz, 298K) in toluene-d_8. Although toluene may lead to underestimated association constants due to host and fullerene solvation, it is the most commonly used solvent for corannulene derivatives, and therefore we used it for a better comparison with published work. Figure 2 shows NMR shift spectral changes for selected protons of corannulene in receptor **1** upon addition of C_{60} or C_{70}.

Gradual addition of fullerene to a solution of **1** in toluene-d_8 caused a corresponding change in the chemical shifts of all corannulene protons, while the signals of the dppe ligand remain unchanged. Job plots supported the 1:1 stoichiometry of the complexation in both cases (see supporting, Figure S22). The K_{assoc} constants determined for the complex $C_{60}\subset\mathbf{1}$ and $C_{70}\subset\mathbf{1}$ gave values of 4665 M^{-1} and 20708 M^{-1}, respectively, thus showing a notable increase of about four times in the binding constant value of the complex with C_{70} when compared with C_{60}. This behavior differs markedly from that of the corannulene derivative synthesized by Sygula et al. for which both association constants are similar.[6e] This interaction was also confirmed by variable temperature $^{13}C\{^1H\}$ NMR spectra (see supporting figure S25). It is worth noticing that UV-vis titration studies have been completed in PhCl at 298K, however host-guest charge transfer bands have not been observed, preventing the estimation of an association constant by this technique.

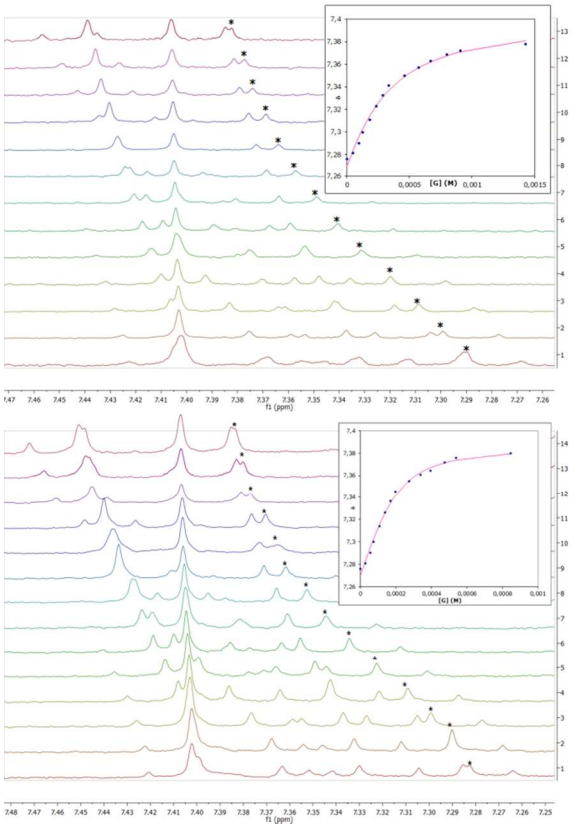

Figure 2. Selected ^{1}H NMR spectra (400 MHz, 298K, toluene-d_8) of **1** upon addition of C_{60} (a) or C_{70} (b) showing the shielding of corannulene protons. Nonlinear curve regression for the results of the titration for proton labeled (inset, top right).

Single-crystals suitable for X-ray diffraction were obtained by slow evaporation of a toluene solution of a (1:1) mixture of compound **1** and C_{60} (Figure 3). The molecular structure obtained reveals that C_{60} is embraced by the two corannulene units, showing unequivocally the inclusion of fullerene into the concave cavity formed. The depth of penetration of the C_{60} into one of the corannulene fragments is 6.92 Å, measured from the centroid of the C_{60} to the centroid of the corannulene five-membered ring, and 6.90 Å to the other corannulene. The average distance between the C_{60} cage and the inner surface of the corannulene units in **1** is roughly estimated to be 3.6 Å, which is similar to the interlinear distance in multiwalled carbon nanotubes. Unfortunately, it was not possible to obtain crystals of $C_{70}\subset\mathbf{1}$ appropriate for X-ray analysis.

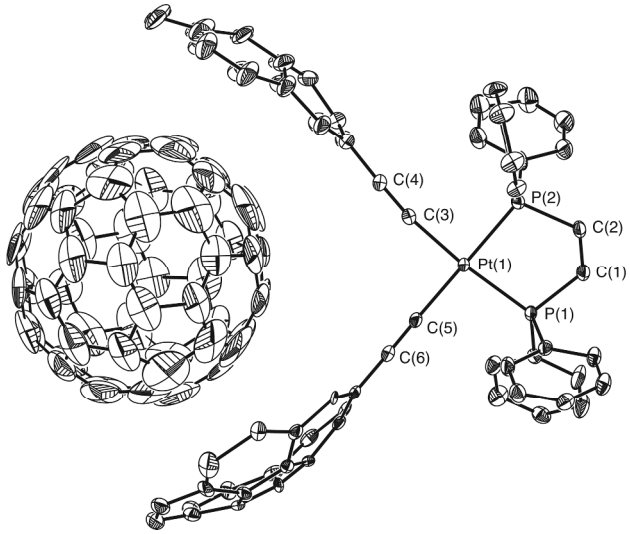

Figure 3. X-ray crystal structure of $C_{60}\subset\mathbf{1}$. Minor components of one corannulene and one phenyl ring, hydrogen atoms and toluene solvent molecules are omitted for clarity.

In order to gain additional information to experimental data, we performed DFT calculations at BLYP-D3/TZP level of theory for the supramolecular adducts of receptor **1** with C_{60} and C_{70}. These results have been summarized in Table 1 and support several empirical facts. The electronic energy of the optimized structure for the adduct with C_{70} (using the more stable conformation, $\mathbf{1}\subset C_{70}$(a), see Figure S29 in the Supporting Information) is lower than that of the complex $\mathbf{1}\subset C_{60}$ by 1.5 kcal/mol. The larger stability of the C_{70} adduct is in agreement with the empirical data and supports the ratio 4:1 in the K_{assoc} values discussed above. We additionally conducted an energy decomposition analysis for $\mathbf{1}\subset C_{60}$(a) and $\mathbf{1}\subset C_{70}$(a) in order to shed some light on the larger stability of the latter complex. The results collected in Table 1 show that the main contributor to the binding energy is the dispersion forces (E_{DISP}) whereas electrostatic forces (E_{ES}) and charge transfer/orbital interaction (E_{ORB}) are hardly significant. This behavior has been observed previously in another purely carboaromatic fragment, coranulenne derivative $C_{60}H_{28}$.[6b] The theoretical results suggest that the reason why $\mathbf{1}\subset C_{70}$(a) has a larger binding energy than $\mathbf{1}\subset C_{60}$ is twofold: a more favorable dispersion interaction in the former, on the one hand, and a smaller Pauli repulsion between the C_{70} and the catcher electronic charge densities, on the other. The energy required to deform the fragments from their equilibrium geometries is

very similar in both complexes and contributes merely 0.1 kcal/mol to the final relative energy.

	C_{60}⊂**1**	C_{70}⊂**1** (a)
E_{PAULI}	47,2	45,5
E_{ES}	-18,1	-17,3
E_{ORB}	-10,4	-10,3
E_{DFT}	18,6	18.0
E_{DSIP}	-53,1	-54.0
E_{TOT}	-34,4	-36,0
ΔE_{DEF}	-0.1	0.0
ΔE_{REL}	1,5	0,0

Table 1. Energy decomposition analysis of the adducts C_{60}⊂**1** and C_{70}⊂**1** performed with BLYP-D3/TZP. All contributions are given in kcal mol^{-1}.

To elucidate the importance of the complementarity in the concave-convex surface to the binding of fullerenes, we also studied the complexation with fullerenes in the complexes **2** and **3**, which contain pyrene or helicene acetylide pincers, respectively (Figure 1). Like corannulene, helicenes are non-planar polyaromatic compounds and good π-donors, and can form charge-transfer complexes with appropriate π-acceptors.[12] On the other hand, pyrene is a completely planar molecule and many of its derivatives have been widely used in supramolecular chemistry, mainly in studies of π-π interactions with different kinds of nanotubes.[13] In both cases, we have performed ^{1}H NMR studies of association with C_{60} in toluene-d_8 showing that the proton signals remain unchanged upon addition of fullerenes and therefore evidencing no significant formation of supramolecular associations.

Another factor that can influence the interactions between fullerenes and corannulenes is the degrees of freedom of the molecule acting as receptor. If the flexibility of the molecular tweezers arms is increased too much, the corannulene moieties can interact between them competing in fact with the fullerene and, consequently, lowering the association constant. Having that in mind, we designed a different compound with one methylene group between the acetylide and corannulene moieties (**4**, Figure 1). The presence of an extra methylene allows an increase in the distance between the corannulene pincers without allowing them to interact and, therefore, leading to a more efficient association. The ^{1}H NMR titration studies of **4** with C_{60} showed a variation in some corannulene protons, but the changes were too small for the measurement of a reliable association constant. It is assumed therefore that the association between **4** and C_{60} is barely significant. DFT calculations were again performed for this adduct, but no equilibrium structure was found. Additionally, it is worth pointing out that during the course of the optimization we observed a relatively large deformation of the acetylide groups. This would suggest that the catcher geometry has to deform significantly in order to maximize the interaction between corannulene and C_{60}. Although the theoretical calculations do not provide a conclusive answer, they suggest that an extra methylene does not yield a more efficient association in this case. This behavior could be justified by considering a plausible intramolecular interaction between the two corannulene pincers in the molecular clip **4**.

In summary, we have designed a handy platform to build molecular tweezers with different polycyclic aromatic hydrocarbons (PAHs) at the end of a rigid acetylide group. The coordination geometry about the metal center is shown to be optimal to form supramolecular host-guest complexes with fullerenes for the corannulene derivative **1** as manifested in the single crystal X-ray structural analysis of compound C_{60}⊂**1**. As far as we know, this compound is the corannulene derivative with the highest association constant for C_{70} ($K_{assoc.}$ = 20708 in toluene-d_8) and one of the best binders for C_{60} ($K_{assoc.}$ = 4665 in toluene-d_8). However, the increase in the degrees of freedom and the lack of complementarity have been shown to be critical factors to impede this association as revealed by the studies of complexation with fullerenes in compounds **2**, **3** and **4**. Additionally, the recent commercial avalaibility of corannulene [14] will facilitate its use in these and other applications.

ASSOCIATED CONTENT

Supporting Information. Full characterization, NMR spectra for all compounds (^{1}H, ^{13}C{^{1}H}, COSY, NOESY, HSQC), computational details, crystallographic data for complex C_{60}⊂**1**. This material is available free of charge via the Internet at http://pubs.acs.org

AUTHOR INFORMATION

Corresponding Author

celedonio.alvarez@uva.es

ACKNOWLEDGMENT

This work was funded by the Spanish Ministerio de Ciencia e Innovación (CTQ2009-12111) and the Junta de Castilla y León (VA070A08 and GR Excelencia 125). R. G.-R. and C. M. A. wish to thank for a MEC-FPU grant and a Ramón y Cajal contract, and L. A. G.-E. thanks University of Valladolid for a Ph D grant.

REFERENCES

(1) (a) Steed, J. W.; Turner, D. R.; Wallace, K. J. *Core Concepts in Supramolecular Chemistry and Nanochemistry*, Wiley 2007. (b) Attwood, J. L.; Steed, J. W. *Encyclopedia of Supramolecular Chemistry*, Marcel Dekker, New York, 2004. (c) Lehn, J.-M. *Supramolecular Chemistry. Concepts and Perspectives*, VCH-Wiley: Weinheim, Germany 1995.

(2) (a) Canavet, D.; Pérez, E. M. ; Martín, N. *Angew. Chem. Int. Ed.* **2011**, *50*, 2-14. (b) Pérez, E. M.; Martín, N. *Chem. Soc. Rev.* **2008**, *37*, 1512-1519. (c) Kawase, T.; Kurata, H. *Chem. Rev.* **2006**, *106*, 5250-5273.

(3) (a) Wu, J.-C.; Wang, D.-X.; Huang, Z.-T.; Wang, M.-X. *Tetrahedron Lett.* **2009**, *50*, 7209–7212. (b) Zhang, E.-X.; Wang, D.-X.; Zheng, Q.-Y.; Wang, M.-X. *Org. Lett.* **2008**, *10*, 2565–2568. (c) Haino, T.; Kukunaga, C.; Fukazawa, Y. *J. Nanosci. Nanotechnol.* **2007**, *7*, 1386-1388. (d) Liu, S.-Q.; Wang, D.-X.; Zheng, Q.-Y.; Wang, M.-X. *Chem. Commun*. **2007**, 3856–3858. (e) Haino, T.; Yanase, M.; Fukunaga, C.; Fukazawa, Y. *Tetrahedron* **2006**, *62*, 2025–2035. (f) Haino, T.; Fukunaga, C.; Fukazawa, Y. *Org. Lett.* **2006**, *8*, 3545–3548. (g) Haino, T.; Matsumoto, Y.; Fukazawa, Y. *J. Am. Chem. Soc*.**2005**, *127*, 8936–8937. (h) Haino, T.; Araki, H.; Fujiwara, Y.; Tanimoto, Y.; Fukazawa, Y. *Chem. Commun.* **2002**, 2148–2149. (i) Haino, T.; Yanase, M.; Fukazawa, Y. *Angew. Chem. Int. Ed.* **1998**, *37*, 997–998. (j) Haino, T.; Yanase, M.; Fukazawa, Y. *Angew. Chem. Int. Ed.* **1997**, *36*, 259–260. (k) Raston, C. L.; Atwood, J. L.; Nichols, P. J.; Sudria, I. B. N. *Chem. Commun.* **1996**, 2615–2616. (l) Araki, K.; Akao, K.; Ikeda, A.; Suzuki, T.; Shinkai, S. *Tetrahedron Lett.* **1996**, *37*, 73–76.

(4) (a) Yang, F.; Chen, Q.; Cheng, Q.-Y.; Yan, C.-G.; Han, B.-H. *J. Org. Chem.* **2012**, *77*, 971-976. (b) Huerta, E.; Metselaar, G. A.; Fragoso, A.; Santos, E.; Bo, C.; de Mendoza, J. *Angew. Chem. Int. Ed.* **2007**, *46*, 202–205. (c) Huerta, E.; Cequier, E.; de Mendoza, J.

Chem. Commun. **2007**, 5016–5018. (d) Rio, Y.; Nierengarten, J.-F. *Tetrahedron Lett.* **2002**, *43*, 4321–4324. (e) Felder, D.; Heinrich, B.; Guillon, D.; Nicoud, J.-F.; Nierengarten, J.-F. *Chem. Eur. J.* **2000**, *6*, 3501–3507. (f) Nierengarten, J.-F.; Oswald, L.; Eckert, J.-F.; Nicoud, J.-F.; Armaroli, N. *Tetrahedron Lett.* **1999**, *40*, 5681–5684. (g) Matsubara, H.; Shimura, T.; Hasegawa, A.; Semba, M.; Asano, K.; Yamamoto, K. *Chem. Lett.* **1998**, 1099–1100. (h) Atwood, J. L.; Barnes, M. J.; Gardiner, M. G.; Raston, C. L. *Chem. Commun*. **1996**, 1449–1450. (i) Steed, J. W.; Junk, P. C.; Atwood, J. L.; Barnes, M. J.; Raston, C. L.; Burkhalter, R. S. *J. Am. Chem.Soc.* **1994**, *116*, 10346–10347.

(5) (a) Giguere, J.-B.; Morin, J.-F. *Org. Biomol. Chem.* **2012** , *10*, 1047-1051. (b) Meng, W.; Breiner, B.; Rissanen, K.; Throburn, J. D. ;Clegg, J. K.; Nitschke, J. R. *Angew. Chem. Int. Ed.* **2011**, *50*, 3479-3483. (c) Mulholland, A. R.; Woodward, C. P.; Langford, S. J. *Chem. Commun.* **2011**, *47*, 1494. (d) Shoji, Y.; Tashiro, K.; Aida, T. *J. Am. Chem. Soc.* **2010**, *132*, 5928-5929 (e)Tashiro, K.; Aida, T. *Chem. Soc. Rev*. **2007**, 36, 189–197.

(6) (a) Petrukhina, M. A.; Scott, L. T.; *Fragments of Fullerenes and Carbon Nanotubes. Designed Synthesis, Unusual Reactions, and Coordination Chemistry*, Wiley Hoboken, New Jersey 2012. (b) Dawe, L. N.; AlHujran, T. A.; Tran, H.-A.; Mercer, J. I.; Jackson, E. A.; Scott, L. T.; Georghiou, P. E. *Chem. Commun.* **2012**, *48*, 5563-5565. (c) Mueck-Lichtenfeld, C.; Grimme, S.; Kobryn, L.; Sygula, A. *Phys. Chem. Chem. Phys.* **2010**, *12*, 7091–7097. (d) Xiao, W.; Passerone, D.; Ruffieux, P.; Aït-Mansour, K.; Gröning, O.; Tosatti, E.; Siegel, J. S.; Fasel, R. *J. Am. Chem. Soc.* **2008**, *130*, 4767-4771. (e) Sygula, A.; Fronczek, F. R.; Sygula, R.; Rabideau, P. W.; Olmstead, M. M. *J. Am. Chem. Soc.* **2007**, *129*, 3842–3843. (f) Georghiou, P. E.; Tran, A. H.; Mizyed, S.; Bancu,M.; Scott, L. T. *J. Org. Chem.* **2005**, *70*, 6158–6163. (g) Mizyed, S.; Georghiou, P.; Bancu,M.; Cuadra, B.; Rai, A. K.; Cheng, P.; Scott, L. T. *J. Am. Chem. Soc.* **2001**, *123*, 12770–12774.

(7) (a) Canavet, D.; Gallego, M.; Isla, H.; de Juan, A.; Pérez, E. M.; Martín, N. *J. Am. Chem. Soc.* **2011**, *133*, 3184-3190. (b) Isla, H.; Gallego, M.; Pérez, E. M.; Viruela, R.; Ortí, E.; Martín, N. *J. Am. Chem. Soc.* **2010**, *132*, 1772-1773. (c) Grimm, B.; Santos, J.; Illescas, B. M.; Muñoz, A.; Guldi, D. M.; Martín, N. *J. Am. Chem. Soc.* **2010**, *132*, 17387-17389. (d) Huerta, E.; Isla, H.; Pérez, E. M.; Bo, Carles, Martín, N.; de Mendoza, J. *J. Am. Chem. Soc.* **2010**, *132*, 5351-5353. (e) Gayathri, S. S.; Wielopolski, M.; Pérez, E. M.; Fernández, G.; Sánchez, L.; Viruela, R.; Ortí, E. Guldi, D. M.; Martín N. *Angew. Chem. Int. Ed.* **2009**, *48*, 815-819. (f) Fernández, G.; Pérez, E. M.; Sánchez, L.; Martín, N. *Angew. Chem. Int. Ed.* **2008**, *47*, 1094-1097. (g) Pérez, E. M.; Sierra, M.; Sánchez, L.; Torres, M. R.; Viruela, R.; Viruela, P. M.; Ortí, E.; Martín, N. *Angew. Chem. Int. Ed.* **2007**, *46*, 1847-1851. (h) Pérez, E. M.; Sánchez, L.; Fernández, G.; Martín, N. *J. Am. Chem. Soc.* **2007**, *128*, 7172-7173.

(8) (a) Kawase, T.; Kurata, H. *Chem. Rev*. **2006**, *106*, 5250–5273. (b) Kawase, T.; Tanaka, K.; Shiono, N.; Seirai, Y.; Oda, M. *Angew. Chem., Int. Ed.* **2004**, *43*, 1722–1724. (c) Kawase, T.; Fujiwara, N.; Tsutumi, M.; Oda, M.; Maeda, Y.; Wakahara, T.; Akasaka, T. *Angew. Chem., Int. Ed.* **2004**, *43*, 5060–5062. (d) Kawase, T.; Tanaka, K.; Seirai, Y.; Shiono, N.; Oda, M. *Angew. Chem., Int. Ed.* **2003**, *42*, 5597–5600.

(9) Iwamoto, T.; Watanabe, Y.; Sadahiro, T.; Haino, T.; Yamago, S. *Angew. Chem., Int. Ed.* **2011**, *50*, 8342–8344.

(10) (a) Henne, S.; Bredenkötter, B.; Dehghan Baghi, A. A.; Schmid, R.; Volkmer, D.; *Dalton Trans*., **2012**, *41*, 5995-6002. (b) Wang, T.; Li, Z.-Y.; Xie, A.-L.; Yao, X.-J.; Cao, X.-P.; Kuck, D. *J. Org. Chem.* **2011**, *76*, 3231-3238. (c) Georghiou, P. E.; Dawe, L. N.; Tran, H.-A.; Strube, J.; Neumann, B.; Stammler, H.-G.; Kuck, D. *J. Org. Chem.* **2008**, 73, 9040-9047. (d) Bredenkotter, B.; Henne, S.; Volkmer, D. *Chem. Eur. J.* **2007**, *13*, 9931-9938.

(11) (a) Inokuma, Y.; Arai, T. F.; Fujita, M. *Nat. Chem.* **2010**, *2*, 780. (b) Suzuki, K.; Takao, K. Sato, S.; Fujita, M. *J. Am. Chem. Soc.* **2010**, *132*, 2544. (c) Schmittel, M.; He, B.; Mal, P. *Org. Lett*. **2008**, *10*, 2513. (d) Kawano, M.; Fujita, M. *Coord. Chem. Rev.* **2007**, *251*, 2592. (e) Pirondini, L.; Bonifazi, D.; Cantadori, B.; Braiuca, P.; Campagnolo, M.; Zorzi, R. D.; Geremia, S.; Diederich, F.; Dalcanale, E. *Tetrahedron* **2006**, *62*, 2008. (f) Claessens, C. G.; Torres, T. *Chem. Commun.* **2004**, 1298. (g) Fox, O. D.; Drew, M. G. B.; Wilkinson, E. J. S.; Beer, P. D. *Chem.Commun.* **2000**, 391. (g) Ikeda, A.; Udzu, H.; Yoshimura, M.; Shinkai, S. *Tetrahedron* **2000**, *56*, 1825. (h) Ikeda, A.; Yoshimura, M.; Udzu, H.; Fukuhara, C.; Shinkai, S. *J. Am. Chem. Soc.* **1999**, *121*, 4296.

(12) (a) Ermer, O.; Neudörfl, J. *Helv. Chim. Acta* **2001**, *84*, 1268. (b) Brown, J. M.; Field, I. P.; Sidebottom, P. J. *Tetrahedron Lett.* **1981**, *22*, 4867. (c) Mikes, F.; Boshart, G.; Gilav, E. *J. Chem. Soc., Chem. Commun.* **1976**, 99.

(13) (a) Chen, Y.; Zhu, B.; Han, Y.; Bo, Z. *J. Mater. Chem.* **2012**, *22*, 4927-4931. (b) Liu, Y.; Yu, Z.-L.; Zhang, Y.-M.; Guo, D.-S.; Liu, Y.-P. *J. Am. Chem. Soc*. **2008**, *130*, 10431-10439. (c) Guldi, D. M.; Rahman, G. M. A.; Jux, N.; Tagmatarchis, N.; Prato, M. *Angew. Chem., Int. Ed.* **2004**, *43*, 5526-5530. (d) Lou, X.; Daussin, R.; Cuenot, S.; Duwez, A. S.; Pagnoulle, C.; Detrembleur , C.; Bailly , C.; Jérôme, R. *Chem. Mater*. **2004**, *16*, 4005. (e) Artyukhin, A. B.; Bakajin, O.; Stroeve, P.; Noy, A. *Langmuir* **2004**, *20*, 1442. (f) Nakashima, N.; Tomonari, Y.; Murakami, H.; *Chem. Lett.* **2002**, *6*, 638. (g) Chen, R.; Zhan, Y.; Wang, D.; Dai, H. *J. Am. Chem. Soc.* **2001**, *123*, 3838. (h) Liu, L.; Wang, T.; Li, J.; Guo, Z.; Dai, L.; Zhang, D.; Zhu, D. *Chem. Phys. Lett.* **2003**, *367*, 747.

(14) Butterfield, A. M.; Gilomen, B.; Siegel J. S. *Org. Process Res. Dev*. **2012**, 16, 664–676.

Supporting Information

How Metals Can Induce the Right Geometry as Hosts for Fullerenes

Celedonio M. Álvarez,[†] Luis A. García–Escudero,[†] Raúl García-Rodriguez,[†] Jose M. Martín-Alvarez,[†] Daniel Miguel,[†] Víctor M. Rayón[‡]*

[†]GIR MIOMeT, IU CINQUIMA/Química Inorgánica, Facultad de Ciencias, Universidad de Valladolid, E-47005, Valladolid, Spain.

[‡]Departamento de Química Física y Química Inorgánica, Facultad de Ciencias, Universidad de Valladolid, E-47005, Valladolid, Spain

*** To whom correspondence should be addressed. E-mail: celedonio.alvarez@uva.es.**

Table of contents.

Figure S26. MALDI-TOF isotopic pattern for C60⊂**1**.

Figure S27. Partial ^{1}H NMR titrations of [Pt(CC-Cora)$_2$(dppe)] (**1**) with C_{70} (400 MHz, 298 K, toluene-d_8).

Figure S28. Non linear curve regression for the results of the titration experiments of C_{60} with **1** for selected corannulene protons.

III. Crystallographic Data for C60⊂1.

Crystallographic Experimental Section.

Table S1. Crystal data and structure refinement for C60⊂**1**.

Table S2. Bond lengths [Å] and angles [º] for C60⊂**1**.

IV. Computational details.

Figure S29. The three posible conformations of the **1**⊂C70 adduct as obtained at the BLYP-D3/TZP level of theory.

General notes and Procedures. Synthetic procedures were carried out under an inert atmosphere of nitrogen, in dry solvents (by passage through alumina columns in an IT Solvent Purification System and degassed with N_2), using standard Schlenk techniques, unless otherwise noted. All reagents and solvents were reagent grade and were used without further purification unless otherwise specified. Flash chromatographic purification was performed using silica gel Merck 60 (particle size 0.040–0.063 mm); the eluting solvent for each purification was determined by thin layer chromatography (TLC). Analytical thin-layer chromatography was performed using Merck TLC silica gel 60 F254. Trimethylsilylethynylcorannulene,[1] methylcorannulene,[2] 1-(trimethylsilylethynyl)pyrene,[3] and 9-bromoheptahelicene [4] were prepared according to the literature procedures and the spectral data in agreement with them. Solution NMR spectra were obtained on a Bruker AV-400 or a Varian MR 400 spectrometer, using $CDCl_3$ and toluene-d_8 as the solvents, internal lock, and internal reference (δ 7.26 (^{1}H) 77.16 (^{13}C) for $CDCl_3$) and (δ 2.08 (^{1}H) 20.43 (^{13}C) for toluene-d_8). Multiplicities are given as: s (singlet), br (broad), d (doublet), t (triplet), q (quartet), dd (doublet of doublets), m (multiplet); J coupling constants are given in Hz.

Synthesis of (bromomethyl)corannulene.

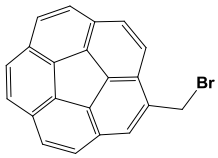

To methylcorannulene (100 mg, 0.38 mmol) in benzene (30 ml), N-bromosuccinimide (80 mg, 0.45 mmol) and benzoyl peroxide (5 mg) were added. The mixture was refluxed for 12 h. The organic layer was separated, washed with water, dried with magnesium sulphate, and evaporated. The product was purified by column chromatography on silica gel eluted with hexane/dichloromethane = 5/1 to yield (bromomethyl)corannulene as a white solid. (72 mg, 55%). ^{1}H NMR ($CDCl_3$, 400 MHz) δ 5.070 (s, 2**H**), 7.755 (d(AB system), *J* = 8.7 Hz, 1**H)**, 7.787 (d(AB system), *J* = 8.8 Hz, 1**H**), 7.804 (d(AB system), *J* = 8.7 Hz, 1**H**), 7.801 (d(AB system), *J* = 8.8 Hz, 1**H**), 7.817 (s(AB system), 2**H**), 7.830 (s, 1**H**), 7.894 (d(AB system), *J* = 9.0 Hz, 1**H**), 8.061 (d, *J* = 9.0 Hz, 1**H**). Anal. Calcd for $C_{21}H_{11}Br$: C, 73.49; H, 3.23. Found: 73.55; H 3.15.

Synthesis of [(trimethylsilylethynyl)methyl]corannulene.

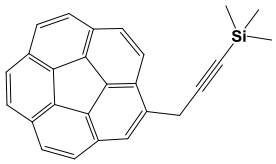

A schlenk tube was charged successively with Et_3N (30 mL), trimethylsilylacetylene (200 μL, 1.456 mmol), $Pd(PPh_3)_2Cl_2$ (20 mg, 0.028 mmol), CuI (6 mg, 0.028 mmol) and (bromomethyl)corannulene (100 mg, 0.29 mmol). The mixture was stirred vigorously at 85 ºC for 14 h., and then cooled, and the volatiles removed under reduced pressure. The product was purified by column chromatography on silica gel eluted with hexane/ethyl acetate = 20/1 to yield [(trimethylsilylethynyl)methyl]corannulene as a white solid. (89 mg, 85 %). ^{1}H NMR ($CDCl_3$, 400 MHz) δ 7.984 (d, *J* = 8.8 Hz, 1**H**), 7.855 (t, *J* = 1.0 Hz, 1**H**), 7.840 (d, *J* = 8.8 Hz, 1**H**), 7.811 (s(AB system), 2**H**), 7.801 (d(AB system), *J* = 8.8 Hz, 1**H**), 7.790 (s(AB system), 2**H**), 7.772 (d(AB system), *J* = 8.8 Hz, 1**H**), 4.176 (d, *J* = 1.0 Hz, 2**H**), 0.211 (s, 9**H**). Anal. Calcd for $C_{26}H_{20}Si$: C, 86.62; H, 5.59. Found: 86.55; H 5.60.

Synthesis of 9-(trimethylsilylethynyl)-[7]-helicene.

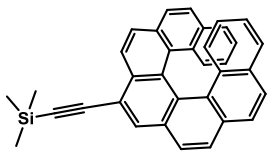

A schlenk tube was charged successively with Et_3N (15 mL), trimethylsilylacetylene (310 μL, 2.19 mmol), $Pd(PPh_3)_2Cl_2$ (31 mg, 0.044 mmol), CuI (10 mg, 0.044 mmol) and 9-bromoheptahelicene (200 mg, 0.437 mmol). The mixture was stirred vigorously at 85 ºC for 22 h., and then cooled, and the volatiles removed under reduced pressure. The product was purified by column chromatography on silica gel eluted with hexane/ethylacetate = 9/1 to yield 9-(trimethylsilylethynyl)-[7]-helicene as a white solid. (165 mg, 77 %). ^{1}H NMR ($CDCl_3$, 400 MHz) δ 8.565 (d, *J* = 8.4 Hz, 1**H**), 8.289 (s, 1**H**), 8.012 (d, *J* = 8.4 Hz, 1**H**), 7.940 (d(AB system), *J* = 8.1 Hz, 1**H**), 7.915 (d(AB system), *J* = 8.1 Hz, 1**H**), 7.751 (d, *J* = 8.6 Hz, 1**H**), 7.708 (d, *J* = 8.6 Hz, 1**H**), 7.508 (d, *J* = 8.4 Hz, 1**H**), 7.496 (d, *J* = 8.4 Hz, 1**H**), 7.300 (d, *J* = 8.6 Hz, 2**H**), 7.091 (d, *J* = 8.6 Hz, 1**H**), 7.058 (d, *J* = 8.6 Hz, 1**H**), 6.916 (t, *J* = 8.6 Hz, 1**H**), 6.908 (t, *J* = 8.6 Hz, 1**H**), 6.413 (t, *J* = 8.6 Hz, 2**H**), 0.430 (s, 9**H**). Anal. Calcd for $C_{35}H_{26}Si$: C, 88.56; H, 5.52. Found: 88.68; H 5.63.

Synthesis of Pt(dppe)(CC-Cora)$_2$ (1).

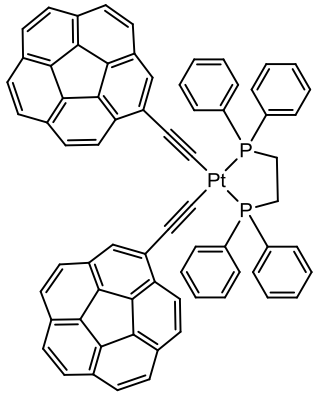

To a THF (15ml) solution of trimethylsilylethynylcorannulene (79 mg, 0.23 mmol) and $PtCl_2$dppe (73 mg 0.11 mmol) were added a solution of CuI (2mg) in acetonitrile (2 mL) and a methanol (5 mL) solution of KF (23 mg, 0.40 mmol) with stirring at room temperature for two days. The solution was concentrated by rotary evaporation to give the crude product, which was purified by silica gel column chromatography. Elution with dichlomethane – methanol (v/v = 99:1) gave a pale yellow product. (94 mg, 75%). ^{1}H NMR ($CDCl_3$, 400MHz) δ 8.07 – 8.00 (m, 8**H**, o-C_6H_5 dppe), 7.753 (d, *J* = 8.7 Hz, 2**H**, Cora), 7.751 (s, 2**H**, Cora), 7.745 (d(AB system), *J* = 8.8 Hz, 2**H**, Cora), 7.734 (s(AB system), 4**H**, Cora), 7.707 (d(AB system), *J* = 8.8 Hz, 2**H**, Cora), 7.683 (d(AB system), *J* = 8.8 Hz, 2**H**, Cora), 7.668 (d(AB system), *J* = 8.8 Hz, 2**H**, Cora), 7.640 (d, *J* = 8.7 Hz, 2**H**, Cora), 7.42 – 7.35 (m, 12**H**, m,p-C_6H_5 dppe), 2.56 – 2.36 (m, 4**H**, P(C*H*$_2$)$_2$P dppe); ^{1}H NMR (Tol-d8, 400MHz) δ 8.201 (d, *J* = 8.7 Hz, 2**H**, Cora), 8.00 - 7.92 (m, 8**H**, C_6H_5 dppe), 7.781 (s, 2**H**, Cora), 7.403 (d(AB system), *J* = 8.7 Hz, 2**H**, Cora), 7.402 (s(AB system), 4**H**, Cora), 7.355 (d(AB system), *J* = 8.7 Hz, 2**H**, Cora), 7.338 (d(AB system), *J* = 8.7 Hz, 2**H**, Cora), 7.294 (d, *J* = 8.7 Hz, 2**H**, Cora), 7.275 (d(AB system), *J* = 8.7 Hz, 2**H**, Cora), 7.05 – 6.95 (m, 12**H**, C_6H_5 dppe), 2.00 - 196 (m, 4**H**, P(C*H*$_2$)$_2$P dppe); ^{13}C{^{1}H} NMR ($CDCl_3$ 100 MHz) δ 136.08 ($C_{quaternary}$ Cora), 135.85 ($C_{quaternary}$ Cora), 135.50 ($C_{quaternary}$ Cora), 135.05 ($C_{quaternary}$ Cora), 134.05 ($C_{quaternary}$ Cora), 133.9 – 133.5 (m, C_α C_6H_5 dppe), 132.44 ($C_{quaternary}$ Cora), 131.5 – 131.3 (m, C_γ C_6H_5 dppe), 131.27 ($C_{quaternary}$ Cora), 130.77 ($C_{quaternary}$ Cora), 130.62 ($C_{quaternary}$ Cora), 130.30 ($C_{quaternary}$ Cora), 129.52 (d, $J_{P\text{-}C}$ = 55 Hz, C_{ipso} C_6H_5 dppe), 129.30 ($C_{tertiary}$ Cora), 129.1 – 128.8 (m, C_β C_6H_5 dppe), 128.27 ($C_{quaternary}$ Cora), 127.76 ($C_{tertiary}$ Cora), 126.90 ($C_{tertiary}$ Cora), 126.80 ($C_{tertiary}$ Cora), 126.76 ($C_{tertiary}$ Cora), 126.73 ($C_{tertiary}$ Cora), 126.69 ($C_{tertiary}$ Cora), 126.44 ($C_{tertiary}$ Cora), 126.34 ($C_{tertiary}$ Cora), 110.14 (dd, $J_{P\text{-}C(trans)}$ = 146 Hz, $J_{P\text{-}C(cis)}$ = 16 Hz, Pt-*C*≡C), 109.97 (d, $J_{P\text{-}C}$ = 35 Hz, Pt-C≡*C*), 29.07 – 28.45 (m, *C*H$_2$ dppe); ^{31}P{^{1}H} NMR ($CDCl_3$ 162 MHz) δ 42 (pseudo–t, $^1J_{P–Pt}$ = 2289 Hz). Anal. Calcd for $C_{70}H_{42}P_2Pt$: C, 73.74; H, 3.71. Found: 73.84; H 3.65.

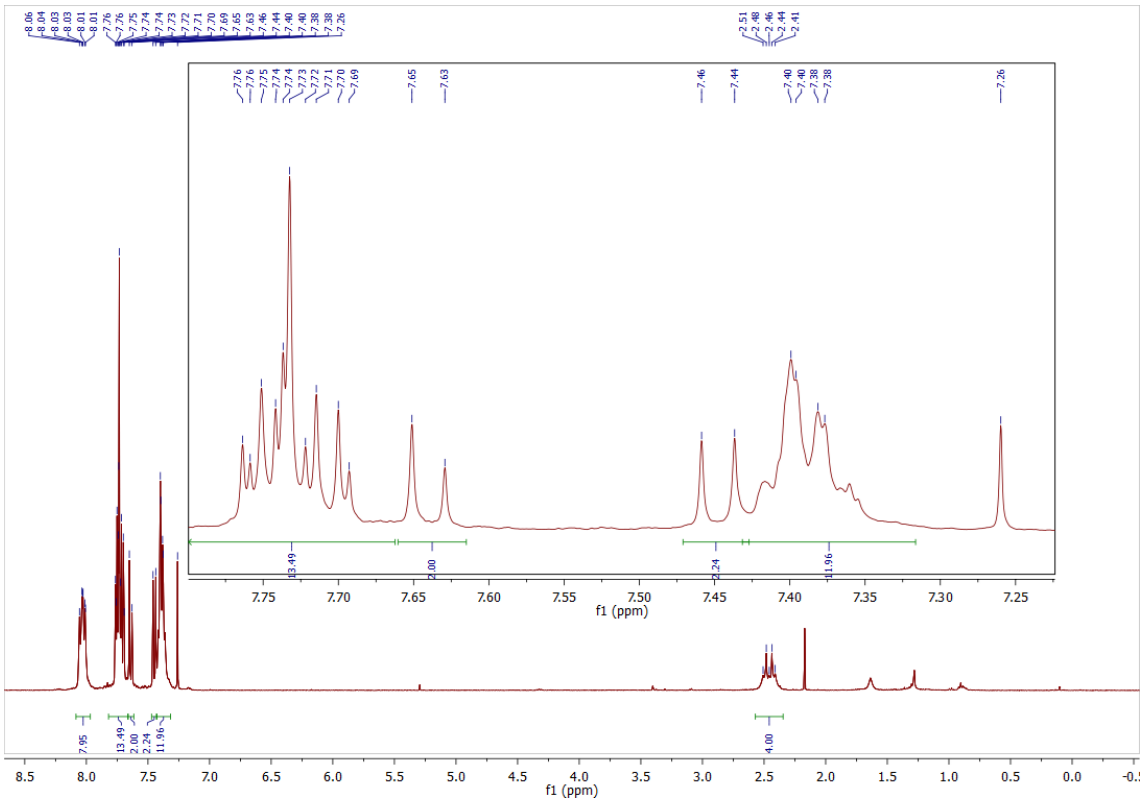

Figure S1. ^{1}H NMR spectrum of Pt(dppe)(CC-Cora)$_2$ (**1**) at 400 MHz in $CDCl_3$.

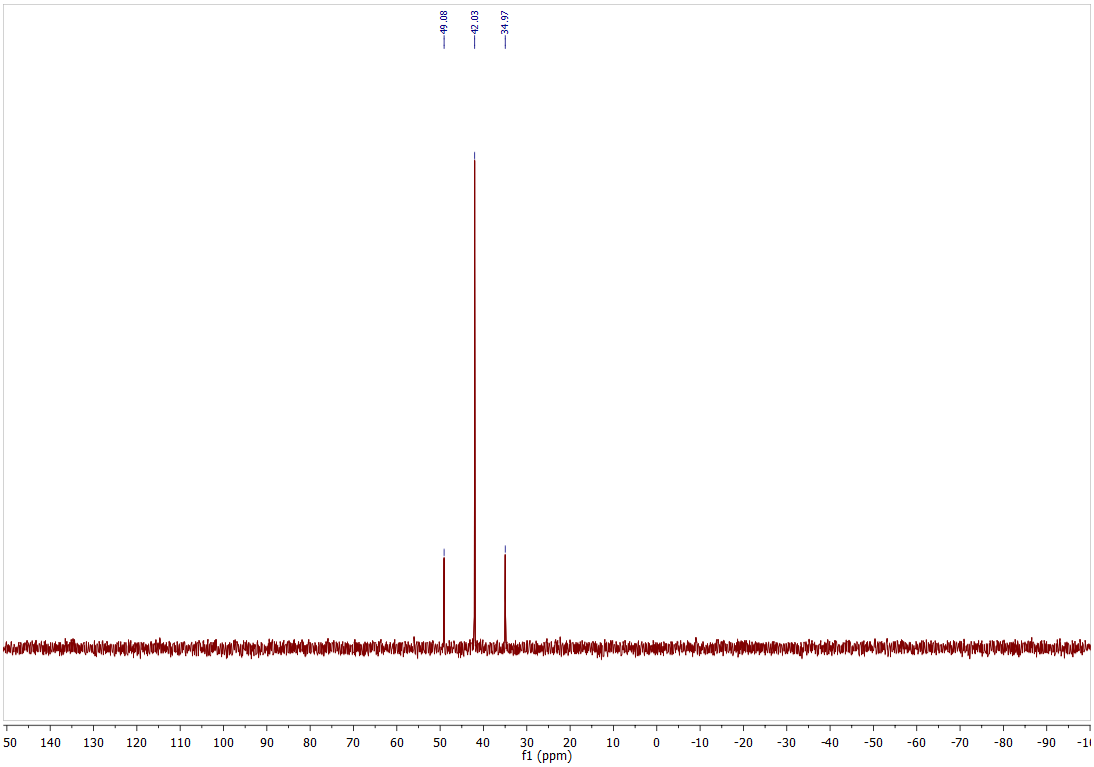

Figure S2. $^{31}P\{^{1}H\}$ NMR spectrum of Pt(dppe)(CC-Cora)$_2$ (**1**) at 162 MHz in $CDCl_3$.

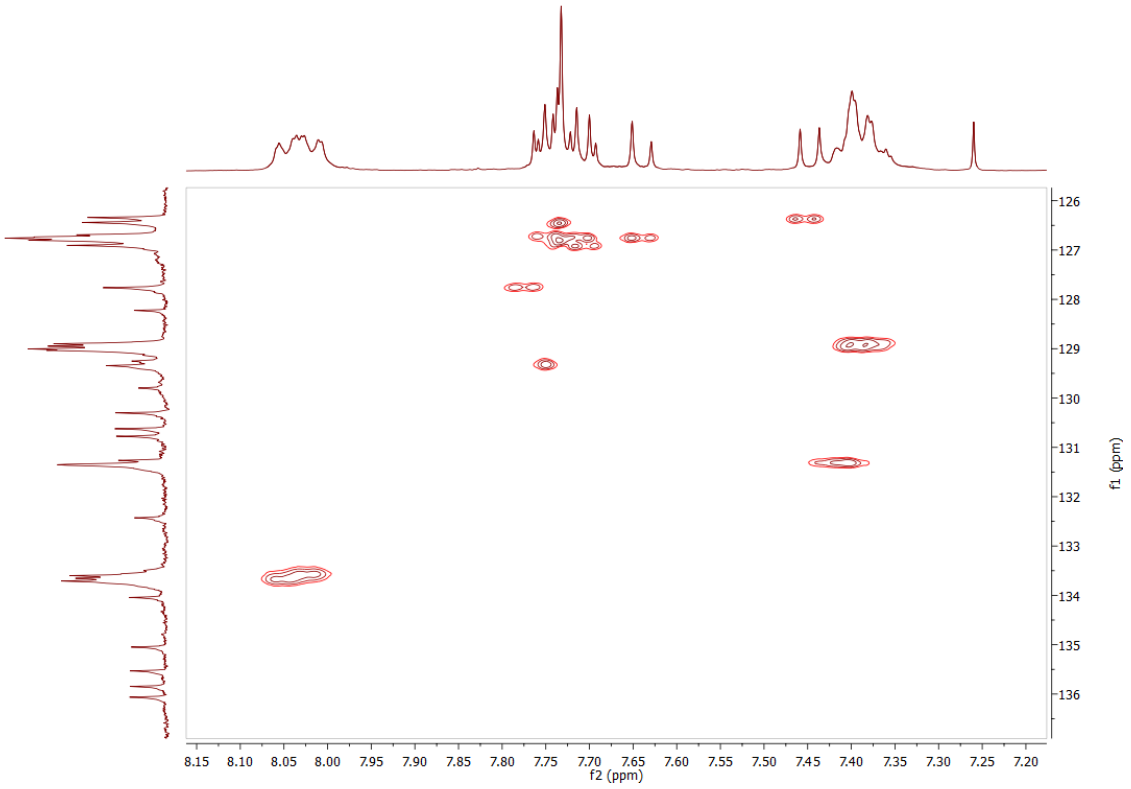

Figure S3. 2-D HSQC spectrum of Pt(dppe)(CC-Cora)$_2$ (**1**) in $CDCl_3$.

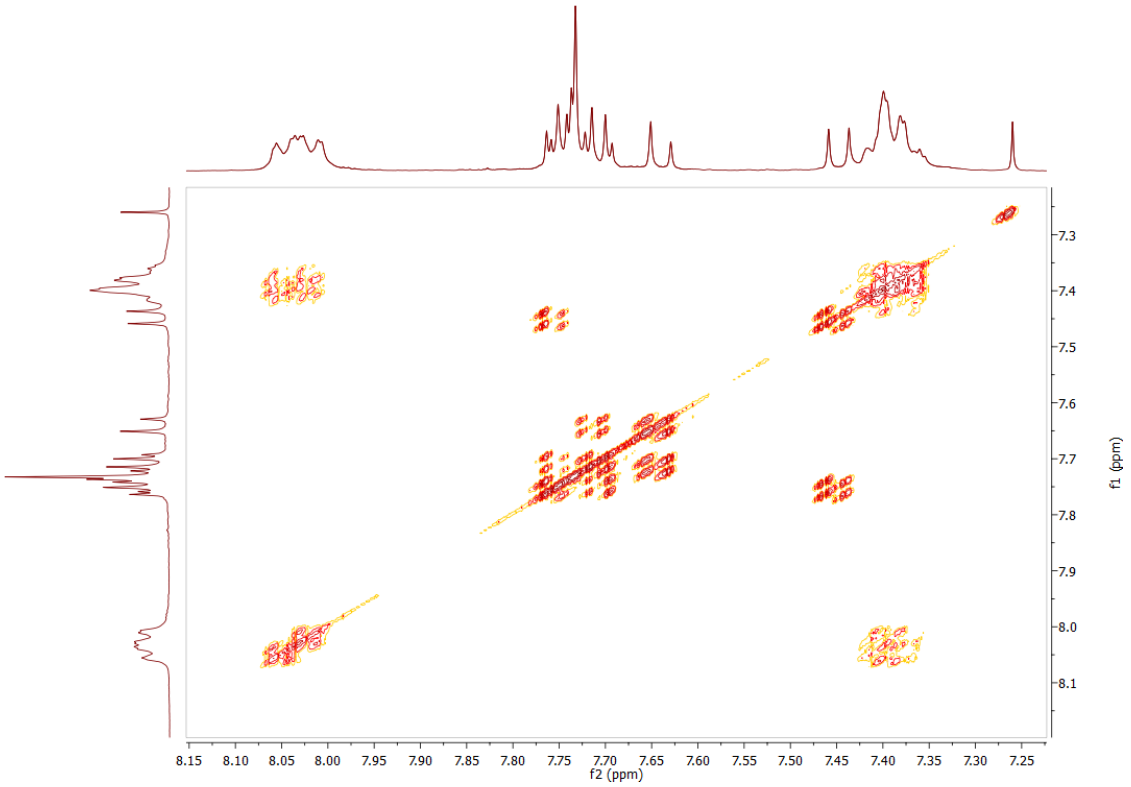

Figure S4. 2-D COSY spectrum of Pt(dppe)(CC-Cora)$_2$ (**1**) in $CDCl_3$.

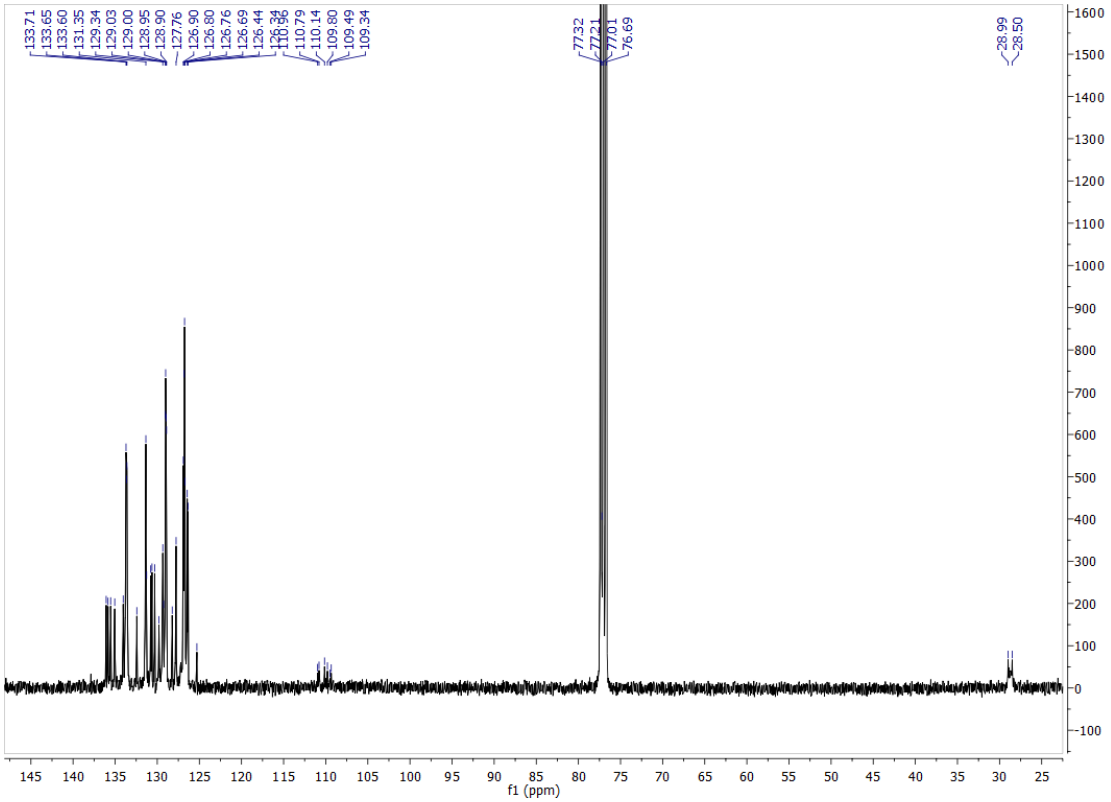

Figure S5. $^{13}C\{^{1}H\}$ NMR spectrum of Pt(dppe)(CC-Cora)$_2$ (**1**) at 100 MHz in $CDCl_3$.

Synthesis of Pt(dppe)(CC-Pyrene)$_2$ (2).

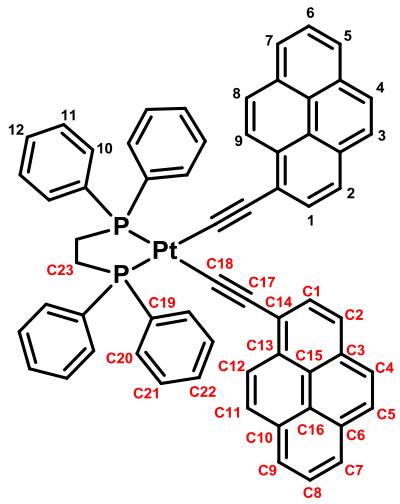

To a THF (15ml) solution of 1-(trimethylsilylethynyl)pyrene (103 mg, 0.345 mmol) and $PtCl_2$dppe (100 mg, 0.150 mmol) were added a solution of CuI (3 mg) in acetonitrile (2 mL) and a methanol (5 mL) solution of KF (32 mg, 0.54 mmol) with stirring at room temperature for five days. The solution was concentrated by rotary evaporation to give the crude product, which was purified by silica gel column chromatography. Elution with dichlomethane gave a pale yellow product. (122 mg, 80 %). ^{1}H NMR ($CDCl_3$, 400MHz) δ 8.58 (d, *J* = 9.1 Hz, 2**H**, H^9), 8.17 - 8.09 (m, 8**H**, H^{10}), 8.070 (d, *J* = 7.5 Hz, 2**H**, H^5), 8.027 (d, *J* = 7.5 Hz, 2**H**, H^7), 8.000 (d(AB system), *J* = 8.3 Hz, 2**H**, H^3 or H^4), 7.989 (d(AB system), *J* = 8.3 Hz, 2**H**, H^3 or H^4), 7.939 (d(AB system), *J* = 9 Hz, 2**H**, H^1 or H^2), 7.930 (d(AB system), *J* = 9 Hz, 2**H**, H^1 or H^2), 7.906 (pseudo-t (dd), *J* = 7.5 Hz, *J* = 7.5 Hz, 2**H**, H^6), 7.705 (d, *J* = 9.1 Hz, 2**H**, H^8), 7.53 – 7.43 (m, 12**H**, H^{11} and H^{12}), 2.64 – 2.47 (m, 4**H**, P(C*H*$_2$)$_2$P dppe); ^{13}C{^{1}H} NMR ($CDCl_3$ 100 MHz) δ 134.0 – 133.5 (m, C20), 131.84 (C13), 131.5 – 131.3 (m, C22 and C10), 130.14 (C4 or C5), 129.63 (d, *J* = 55 Hz, C19), 129.24 (C3), 129.1 – 128.8 (m, C21), 127.64 (C12), 127.39 (C1 or C2), 126.59 (C11), 126.48 (C1 or C2), 125.55 (C8), 124.63 (C6), 124.54 (C15), 124.41 (C9 and C16), 124.27 (C7), 124.23 (C4 or C5), 123.66 (C14), 111.49 (dd, *J* = 145 Hz, *J* = 15 Hz, C18), 110.90 (d, *J* = 35 Hz, C17), 29.0 – 28.4 (m, C23); ^{31}P{^{1}H} NMR (CDCl3 162 MHz) δ 42 (pseudo–t, $^1J_{P-Pt}$ = 2289 Hz). Anal. Calcd for $C_{62}H_{42}P_2Pt$: C, 71.33; H, 4.05. Found: 71.22; H 4.10.

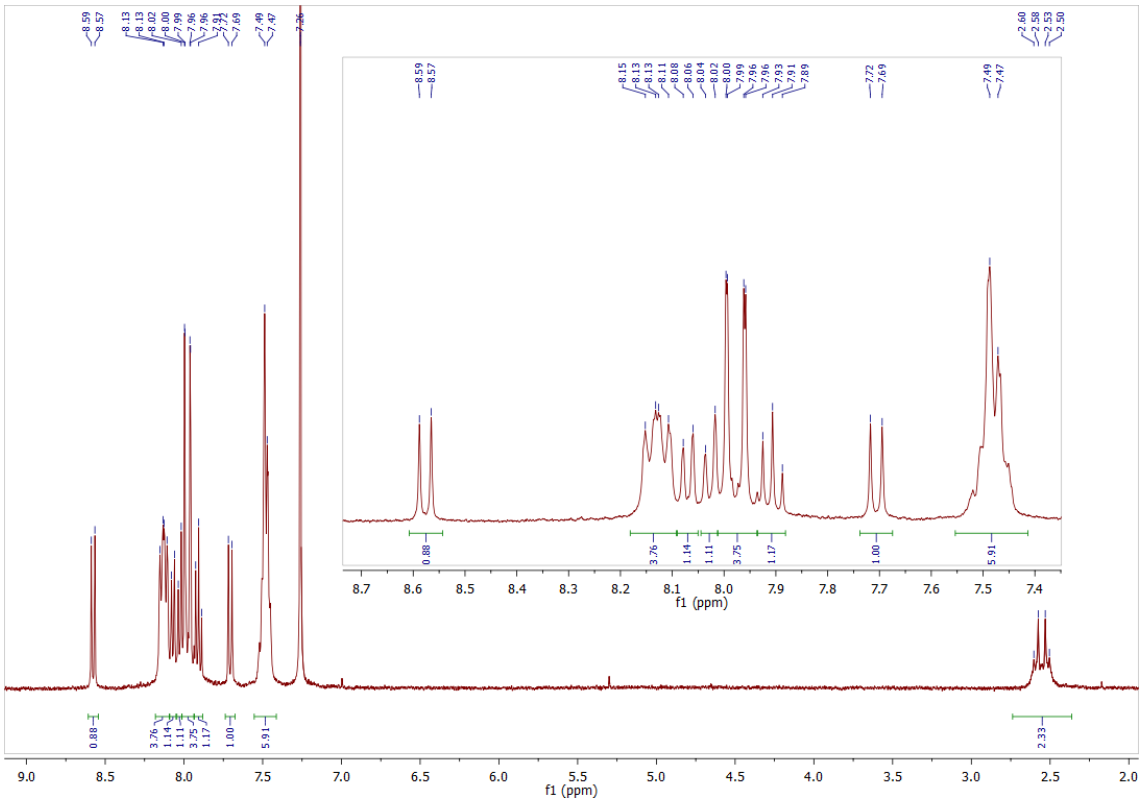

Figure S6. ^{1}H NMR spectrum of Pt(dppe)(CC-Pyrene)$_2$ (**2**) at 400 MHz in $CDCl_3$.

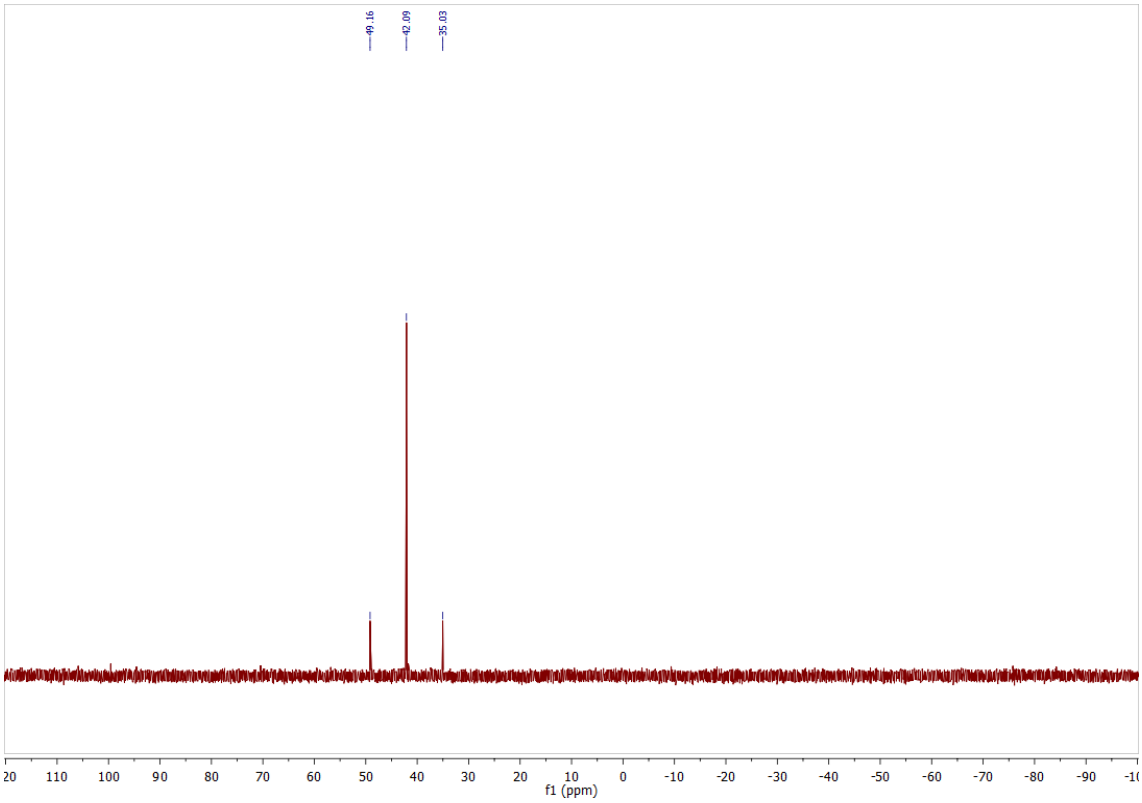

Figure S7. $^{31}P\{^{1}H\}$ NMR spectrum of Pt(dppe)(CC-Pyrene)$_2$ (**2**) at 162 MHz in $CDCl_3$.

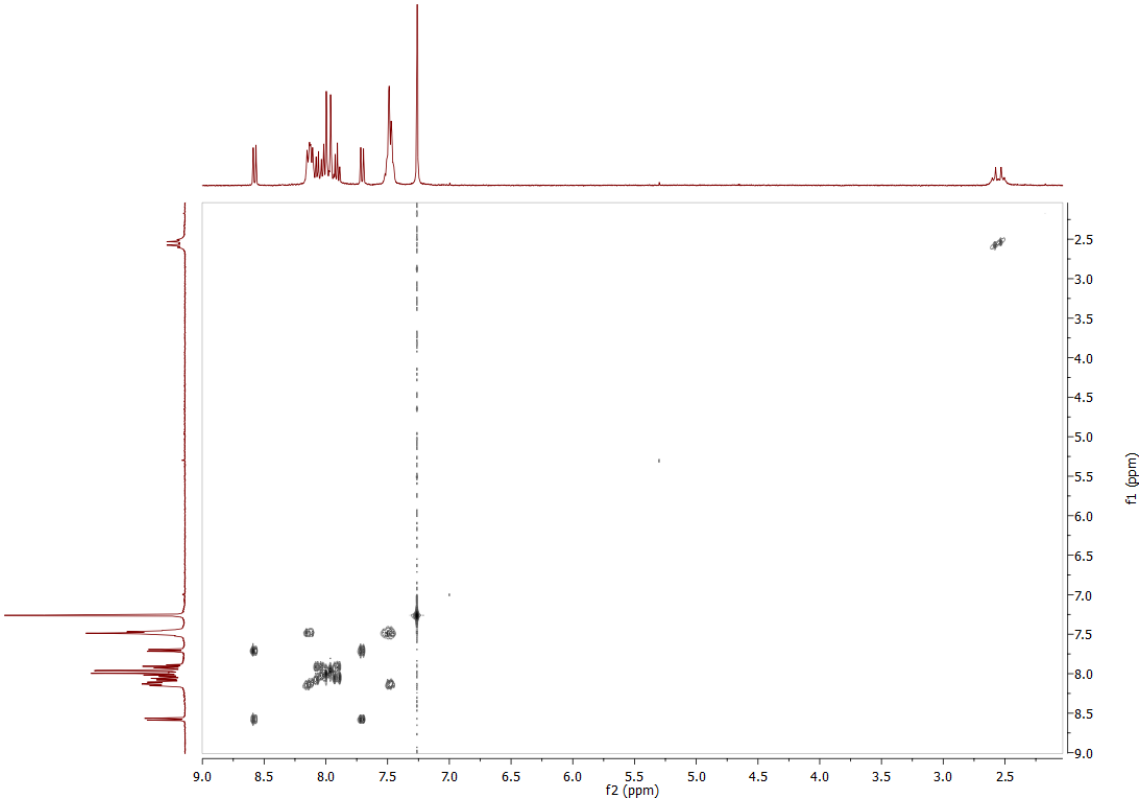

Figure S8. 2-D COSY spectrum of Pt(dppe)(CC-Pyrene)$_2$ (**2**) in $CDCl_3$.

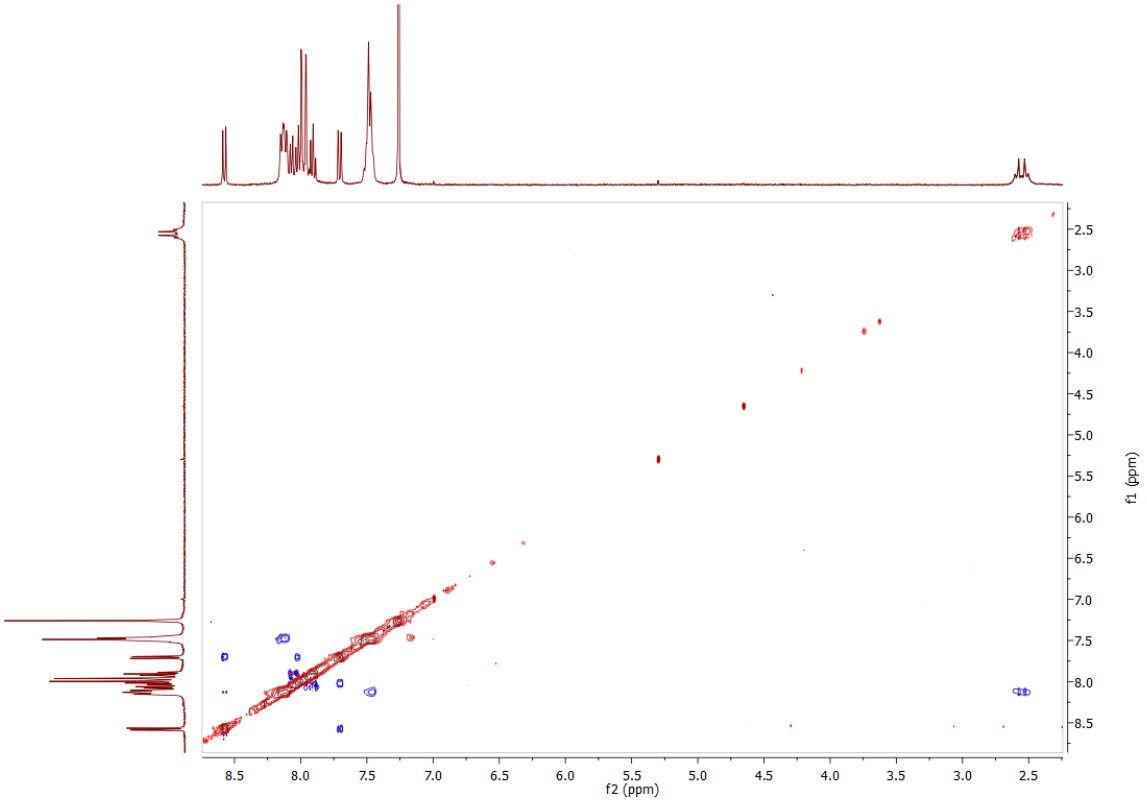

Figure S9. 2-D NOESY spectrum of Pt(dppe)(CC-Pyrene)$_2$ (**2**) in $CDCl_3$.

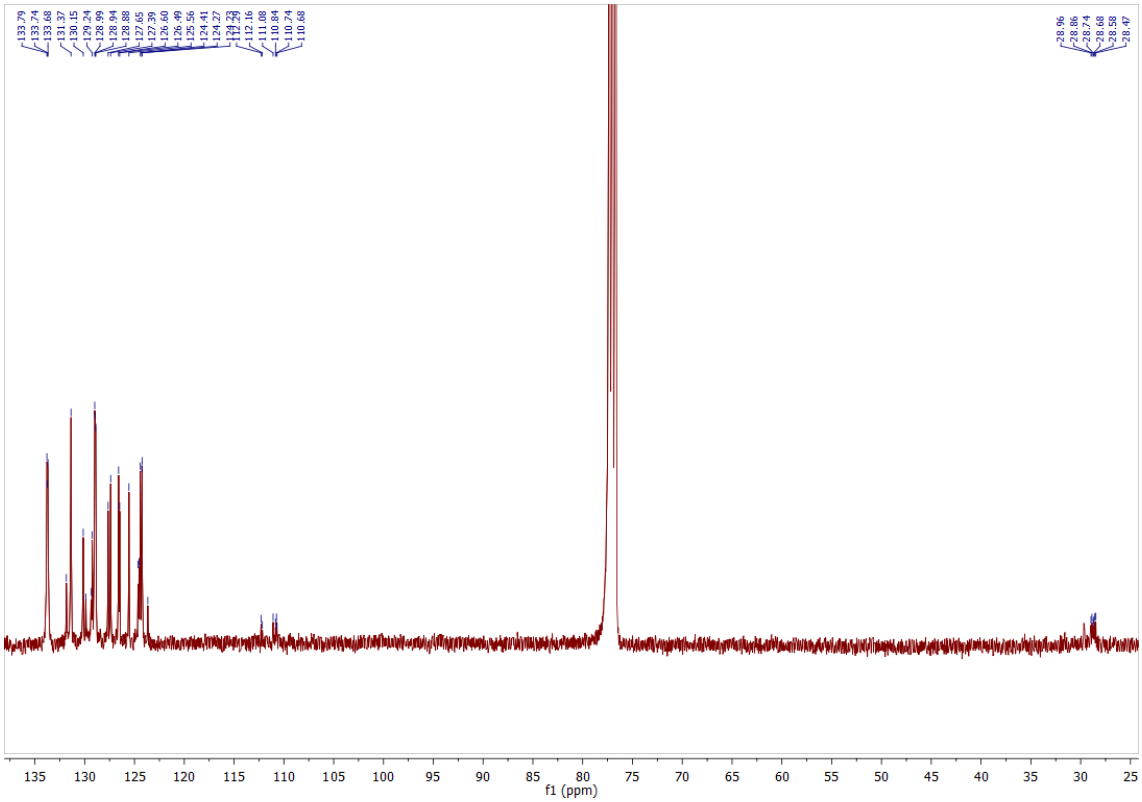

Figure S10. $^{13}C\{^{1}H\}$ NMR spectrum of Pt(dppe)(CC-Pyrene)$_2$ (**2**) at 100 MHz in $CDCl_3$.

Synthesis of Pt(dppe)(CC-hexahelicene)$_2$ (3).

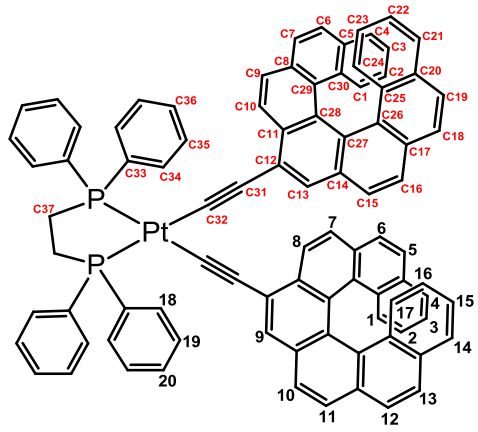

To a THF (15 ml) solution of 9-(trimethylsilylethynyl)-[7]-helicene (80 mg, 0.17 mmol) and $PtCl_2$dppe (25 mg, 0.072 mmol) were added a solution of CuI (2 mg) in acetonitrile (2 mL) and a methanol (5 mL) solution of KF (16 mg, 0.26 mmol) with stirring at room temperature for two days. The solution was concentrated by rotary evaporation to give the crude product, which was purified by silica gel column chromatography. Elution with dichlomethane gave a pale yellow product. (50 mg, 50 %). ^{1}H NMR ($CDCl_3$, 400MHz) δ 8.749 (d, *J* = 8.4 Hz, 2**H**, H^8), 8.18 - 8.10 (m, 8**H** H^{18}), 8.040 (s, 1**H**, H^9 (diastereomer A or B)), 8.034 (s, 1**H**, H^9 (diastereomer A or B)), 7.844 (d(AB system), *J* = 8.5 Hz, 2**H**, H^{10}), 7.830 (d(AB system), *J* = 8.5 Hz, 2**H**, H^{11}), 7.682 (d, *J* = 8.5 Hz, 2**H**, H^{12}), 7.592 (d, *J* = 8.6 Hz, 1**H**, H^5 or H^6 (diastereomer A or B)), 7.591 (d, *J* = 8.4 Hz, 1**H**, H^7 (diastereomer A or B)), 7.566 (d, *J* = 8.6 Hz, 1**H**, H^5 or H^6 (diastereomer A or B)), 7.565 (d, *J* = 8.4 Hz, 1**H**, H^7 (diastereomer A or B)), 7.54 – 7.48 (m, 12**H**, H^{19} and H^{20}), 7.435 (d, 8.5 Hz, 2**H**, H^{13}), 7.411 (d, *J* = 8.6 Hz, 1**H**, H^5 or H^6 (diastereomer A or B)), 7.402 (d, *J* = 8.6 Hz, 1**H**, H^5 or H^6 (diastereomer A or B)), 7.261 (d, *J* = 8.0 Hz, 4**H**, H^4 and H^{14}), 7.155 (d, *J* = 8.0 Hz, 2**H**, H^1 or H^{17}), 7.085 (d, *J* = 8.0 Hz, 1**H**, H^1 or H^{17} (diastereomer A or B)), 7.075 (d, *J* = 8.0 Hz, 1**H**, H^1 or H^{17} (diastereomer A or B)), 6.864 (pseudo-t (dd), *J* = 8.0 Hz, *J* = 8.0 Hz, 4**H**, H^3 and H^{15}), 6.376 (pseudo-t (dd), *J* = 8.0 Hz, 2**H**, H^2 or H^{16}), 6.343 (pseudo-t (dd), *J* = 8.0 Hz, 2**H**, H^2 or H^{16}), 2.62 – 2.41 (m, 4**H**, P(CH_2)$_2$P dppe); ^{13}C{^{1}H} NMR ($CDCl_3$ 100 MHz) δ 134.1 – 133.5 (m, C34), 133.04 (C11), 131.78 (C27 or C28), 131.65 (C20), 131.49 (C5), 131.4 – 131.3 (m, C36), 130.55 (C8), 130.49 (C17), 129.93 (C13), 129.72 (d, $J_{P\text{-}C}$ = 55 Hz, C33), 129.64 (C29 or C30), 129.42 (C25), 129.2 – 128.9 (m, C35), 128.40 (C26), 127.95 (C29 or C30), 127.15 (C15), 126.99 (C9), 126.97 (C6 or C7), 126.92 (C10), 126.79 (C6 or C7), 126.70 (C19), 126.60 (C16), 126.38 (C4 or C21), 126.35 (C4 or C21), 125.72 (C18 and C14), 125.19 (C12), 124.70 (C3 or C22), 124.65 (C1 or C24), 124.49 (C3 or C22), 124.37(C1 or C24), 123.89 (C27 or C28), 123.39 (C2 or C23), 123.32 (C2 or C23), 111.30 (dd, , $J_{P\text{-}C(trans)}$ = 145 Hz, $J_{P\text{-}C(cis)}$ = 15 Hz, C32), 109.88 (d, $J_{P\text{-}C}$ = 35 Hz, C31), 29.1 – 28.1 (m, C37); ^{31}P{^{1}H} NMR (CDCl3, 162 MHz) δ 42 (pseudo–t, $^1J_{P\text{–}Pt}$ = 2289 Hz); ^{31}P{^{1}H} NMR (THF-d8, 162 MHz) δ 42.33 (pseudo–t, $^1J_{P\text{–}Pt}$ = 2272 Hz, diastereomer A or B), 42.30 (pseudo–t, $^1J_{P\text{–}Pt}$ = 2272 Hz, diastereomer A or B). Anal. Calcd for $C_{62}H_{42}P_2Pt$: C, 77.41; H, 4.19. Found: 77.51; H 4.11.

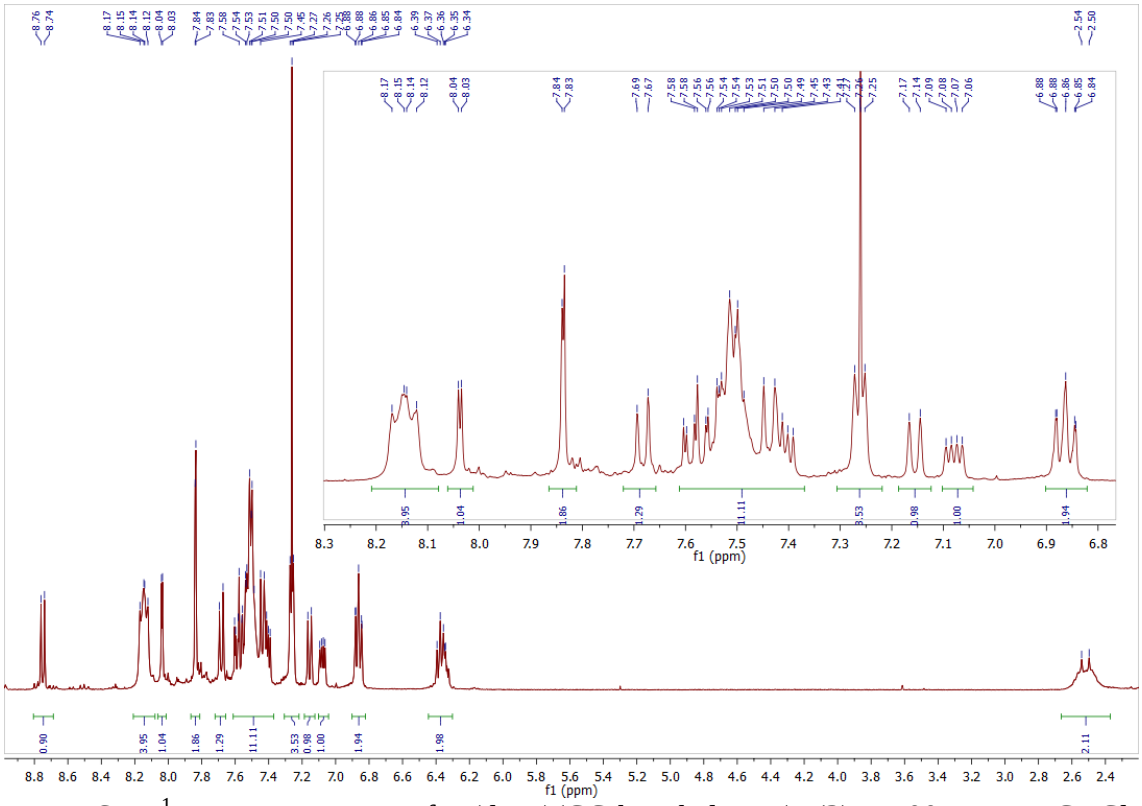

Figure S11. ^{1}H NMR spectrum of Pt(dppe)(CC-hexahelicene)$_2$ (**3**) at 400 MHz in $CDCl_3$.

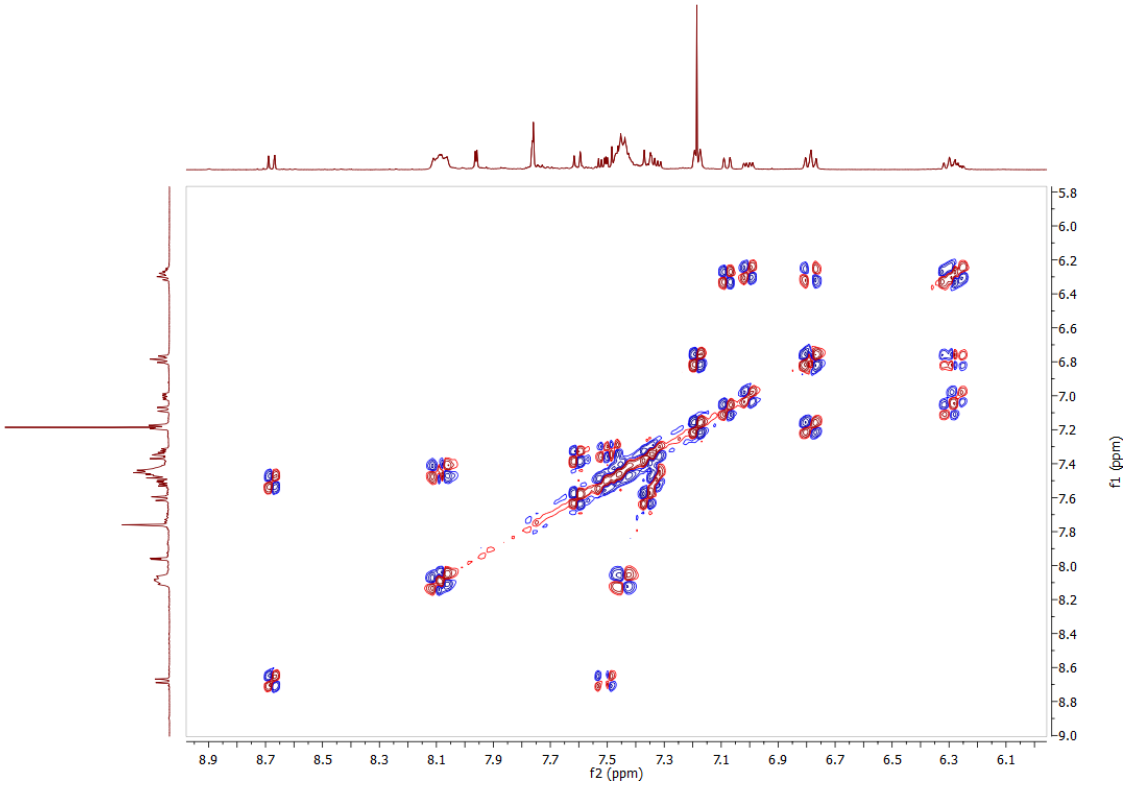

Figure S12. 2-D COSY spectrum of Pt(dppe)(CC-hexahelicene)$_2$ (**3**) in $CDCl_3$.

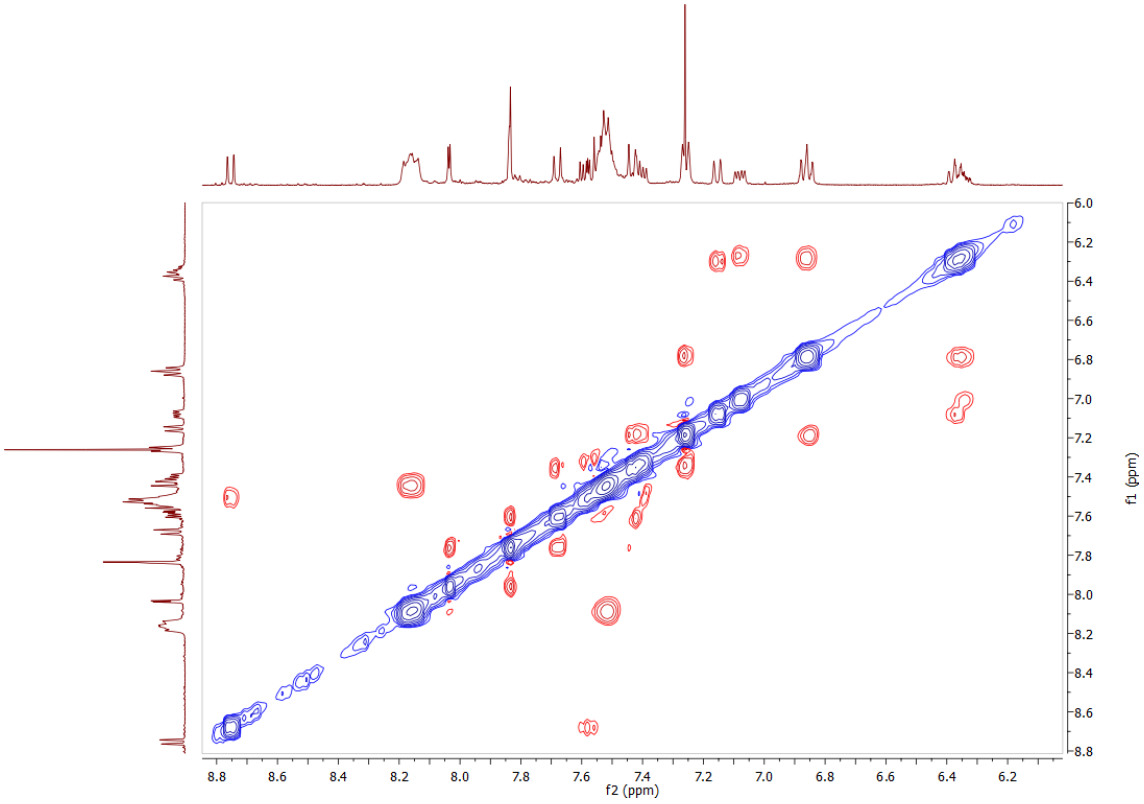

Figure S13. 2-D ROESY spectrum of Pt(dppe)(CC-hexahelicene)$_2$ (**3**) in $CDCl_3$.

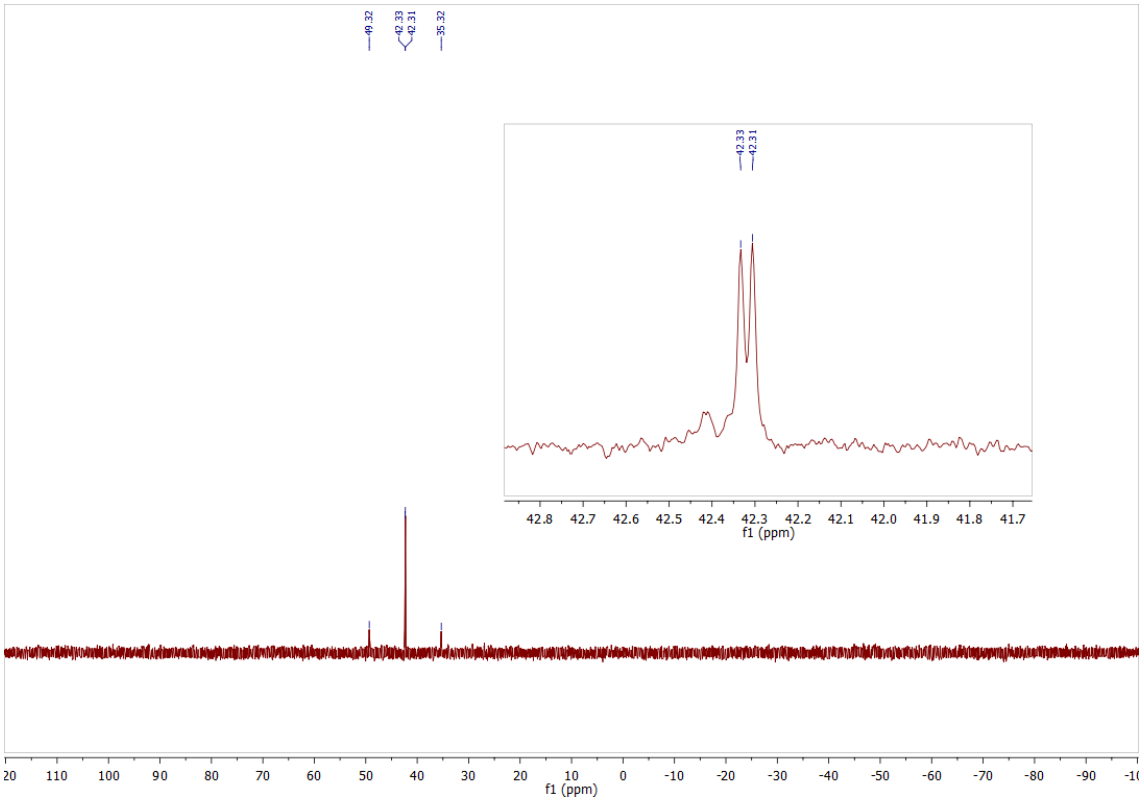

Figure S14. $^{31}P\{^1H\}$ NMR spectrum of Pt(dppe)(CC-hexahelicene)$_2$ (**3**) at 162 MHz in THF-d_8.

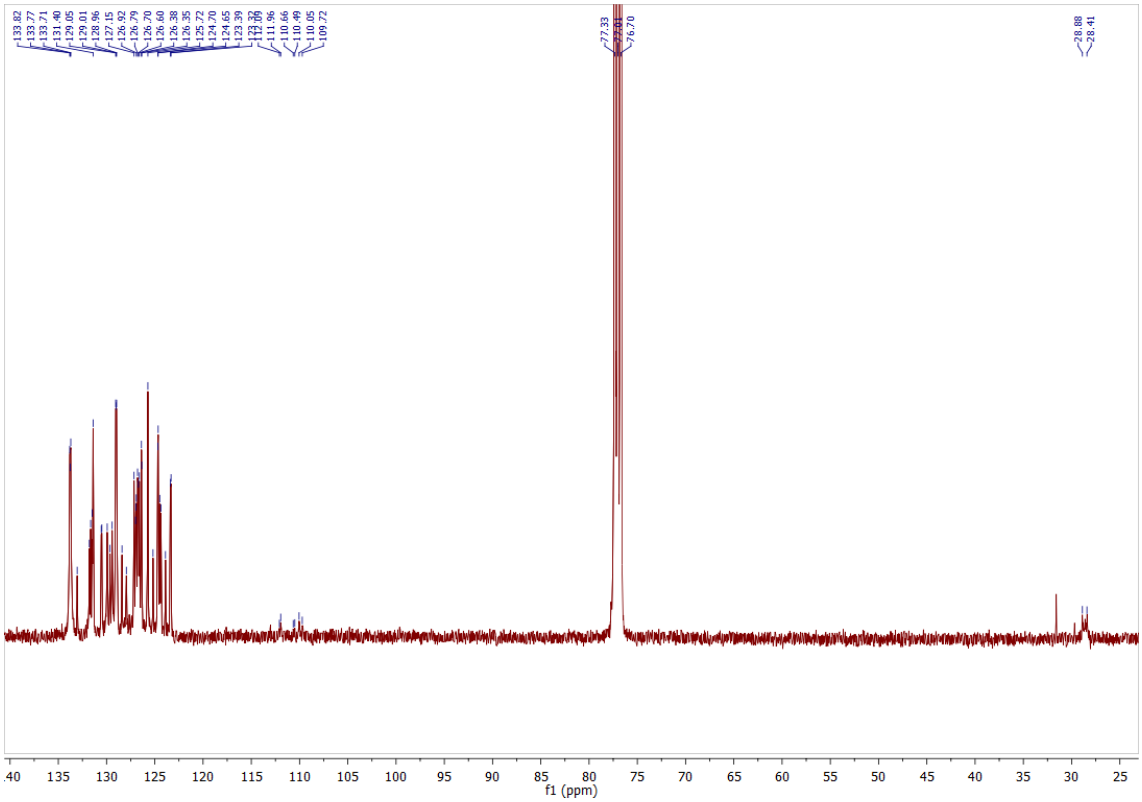

Figure S15. $^{13}C\{^{1}H\}$ NMR spectrum of Pt(dppe)(CC-hexahelicene)$_2$ (**3**) at 100 MHz in $CDCl_3$.

Synthesis of Pt(dppe)(CC-CH$_2$-Cora)$_2$ (4).

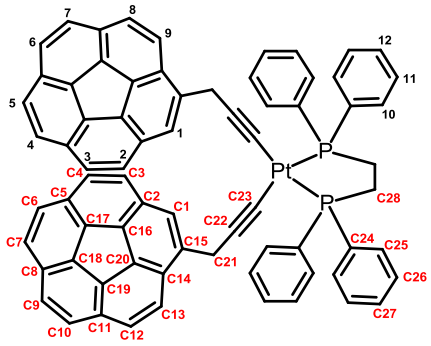

To a THF (10 ml) solution of [(trimethylsilylethynyl)methyl]corannulene (40 mg, 0.11 mmol) and PtCl$_2$dppe (32 mg, 0.048 mmol) were added a solution of CuI (1 mg) in acetonitrile (1 mL) and a methanol (2 mL) solution of KF (11 mg, 0.18 mmol) with stirring at room temperature for two days. The solution was concentrated by rotary evaporation to give the crude product, which was purified by silica gel column chromatography. Elution with dichlomethane gave a pale yellow product. (39 mg, 70 %). ^{1}H NMR ($CDCl_3$, 400MHz) δ 7.82 (d, *J* = 8.8 Hz, 2**H**; H^9), 7.76 (s(AB system), 4**H**; H^{4,5}), 7,74-7.66 (m, 8**H**; H^{10}), 7.73 (d, *J* = 8.7 Hz, 2**H**; H^6), 7.70 (t, *J* = 1.0 Hz, 2**H**; H^1), 7.64 (d, *J* = 8.8 Hz, 2**H**; H^3), 7.63 (d, *J* = 8.7 Hz, 2**H**; H^7), 7.39 (d, *J* = 8,8 Hz, 2**H**; H^2) 7.28 (d, *J* = 8.8 Hz, 2**H**; H^8), 6.90 (m, 4**H**; H^{12}), 6.81(m, 8**H**; H^{11}), 4.31 (m, 4**H**, C*H*$_2$-CC-), 2.50 (m, 4**H**, P(C*H*$_2$)$_2$P); ^{13}C{^{1}H} NMR ($CDCl_3$ 100 MHz) δ 138.59 (C15), 135.90 (C18), 135.69 (C17), 135.50 (C20), 135.28 (C19), 134.65 (C16), 133.7 – 133.0 (m, C25), 131.46 (C2), 130.7 – 130.6 (m, C27), 130.56 (C8), 130.39 (C14), 130.20 (C5 and C11), 128.93 (d, $J_{P\text{-}C}$ = 55 Hz, C24), 128.2 – 128.0 (m, C26), 127.23 (C3), 127.01 (C6 or C7), 126.85 (C10), 126.77 (C9), 126.59 (C4), 126.40 (C6 or C7), 126.33 (C12), 125.51 (C1), 1258.48 (C13), 108.24 (d, $J_{P\text{-}C}$ = 35 Hz, C22), 94.22 (dd, $J_{P\text{-}C(trans)}$ = 145 Hz, $J_{P\text{-}C(cis)}$ = 15 Hz, C23), 29.3 – 28.2 (m, C28), 25.93 (C21); ^{31}P{^{1}H} NMR (CDCl3 162 MHz) δ 41.2 (pseudo–t, $^1J_{P\text{–}Pt}$ = 2300 Hz). Anal. Calcd for $C_{72}H_{46}P_2Pt$: C, 74.03; H, 3.97. Found: 74.15; H 4.01.

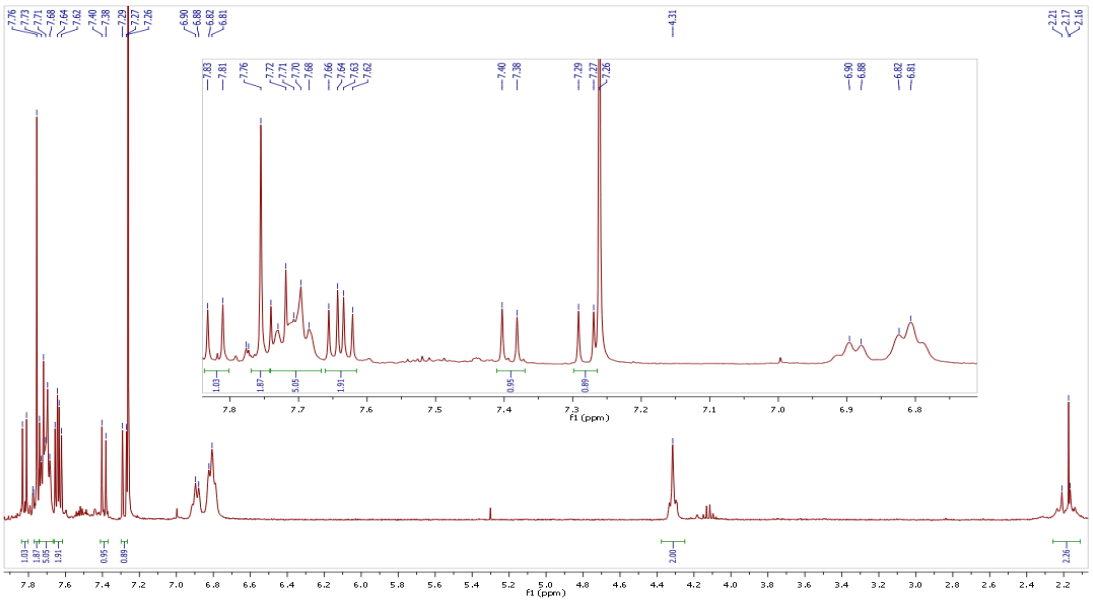

Figure S16. ^{1}H NMR spectrum of Pt(dppe)(CC-CH_2-Cora)$_2$ (**4**) at 400 MHz in $CDCl_3$.

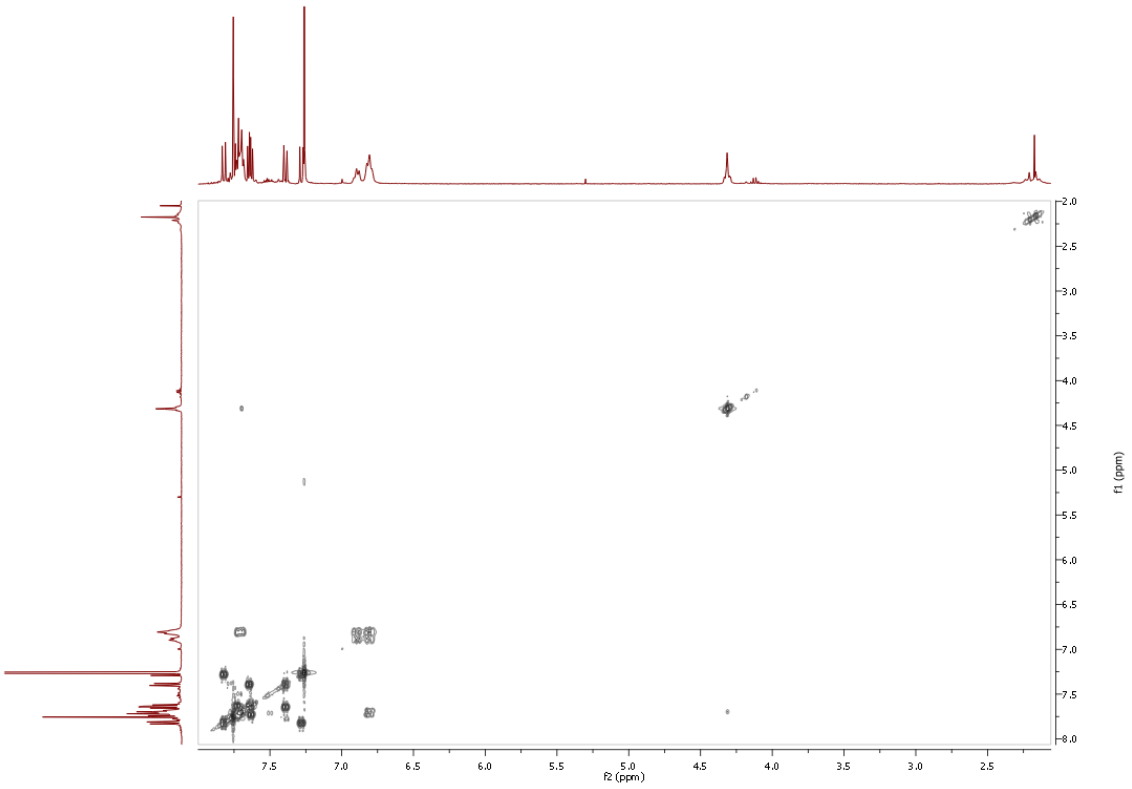

Figure S17. 2-D COSY spectrum of Pt(dppe)(CC-CH_2-Cora)$_2$ (**4**) in $CDCl_3$.

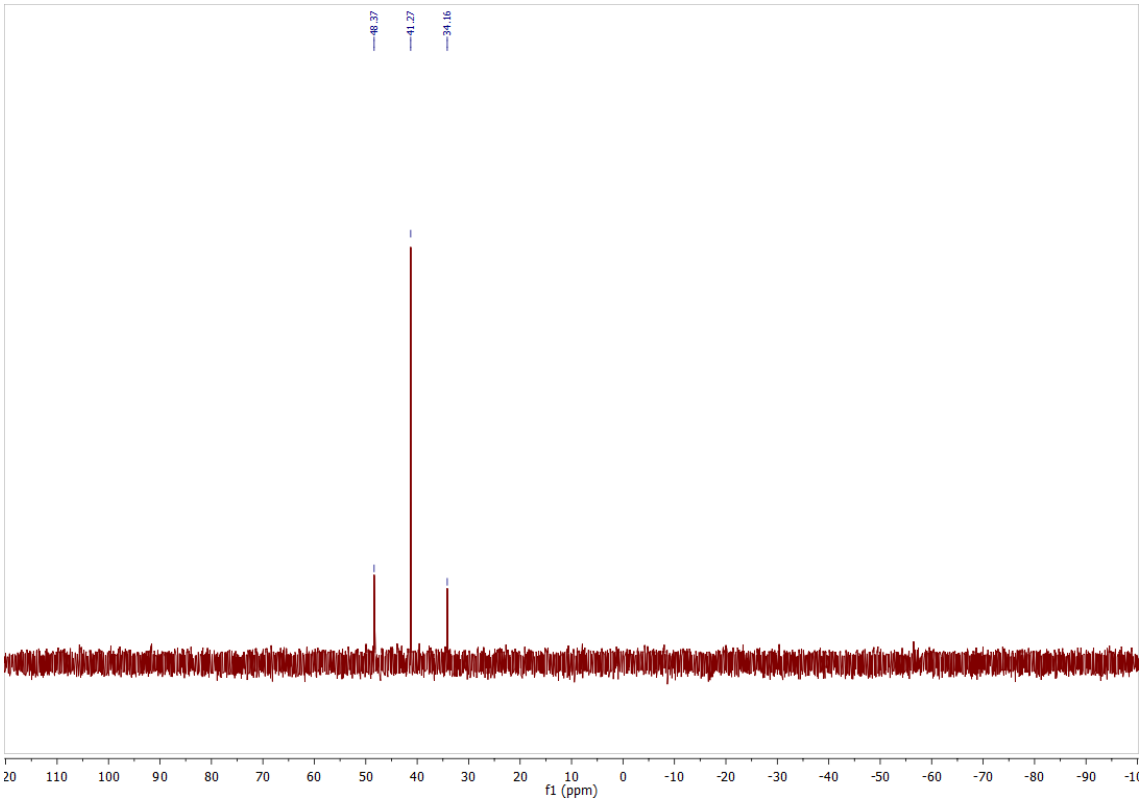

Figure S18. $^{31}P\{^{1}H\}$ NMR spectrum of Pt(dppe)(CC-CH_2-Cora)$_2$ (**4**) in $CDCl_3$ at 162 MHz.

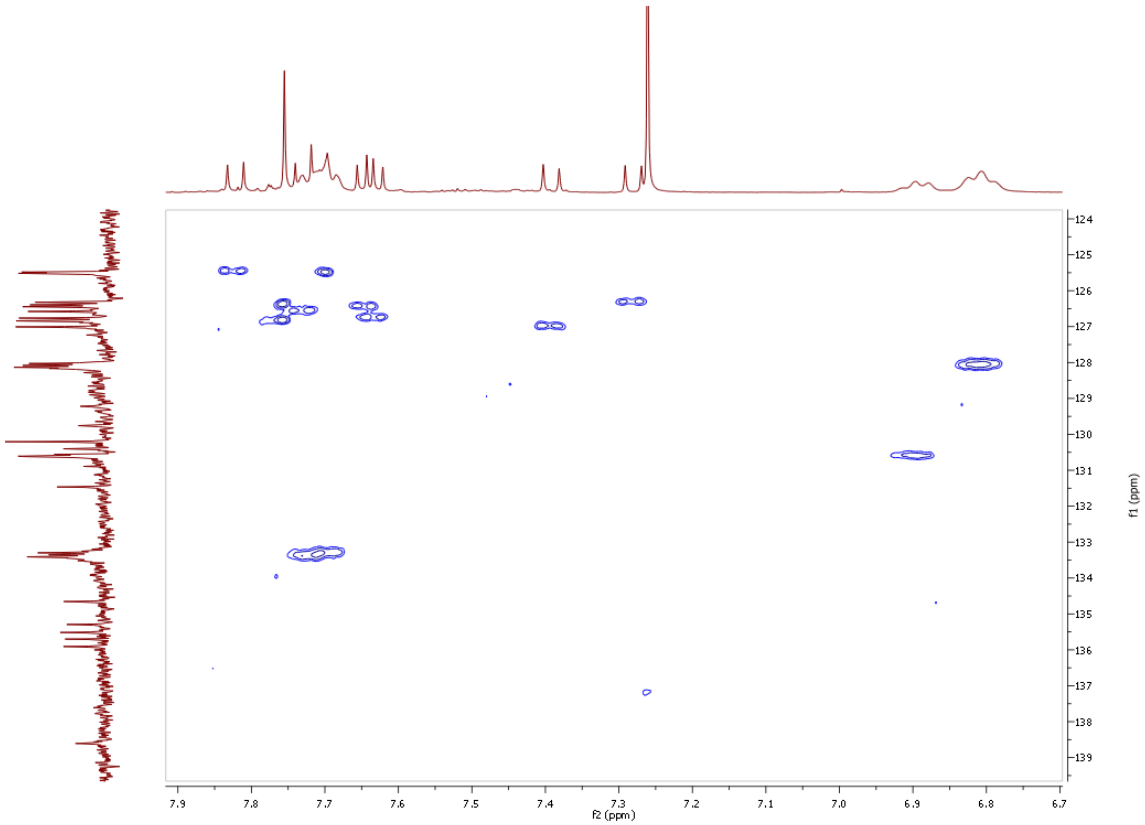

Figure S19. 2-D HSQC spectrum of Pt(dppe)(CC-CH_2-Cora)$_2$ (**4**) in $CDCl_3$.

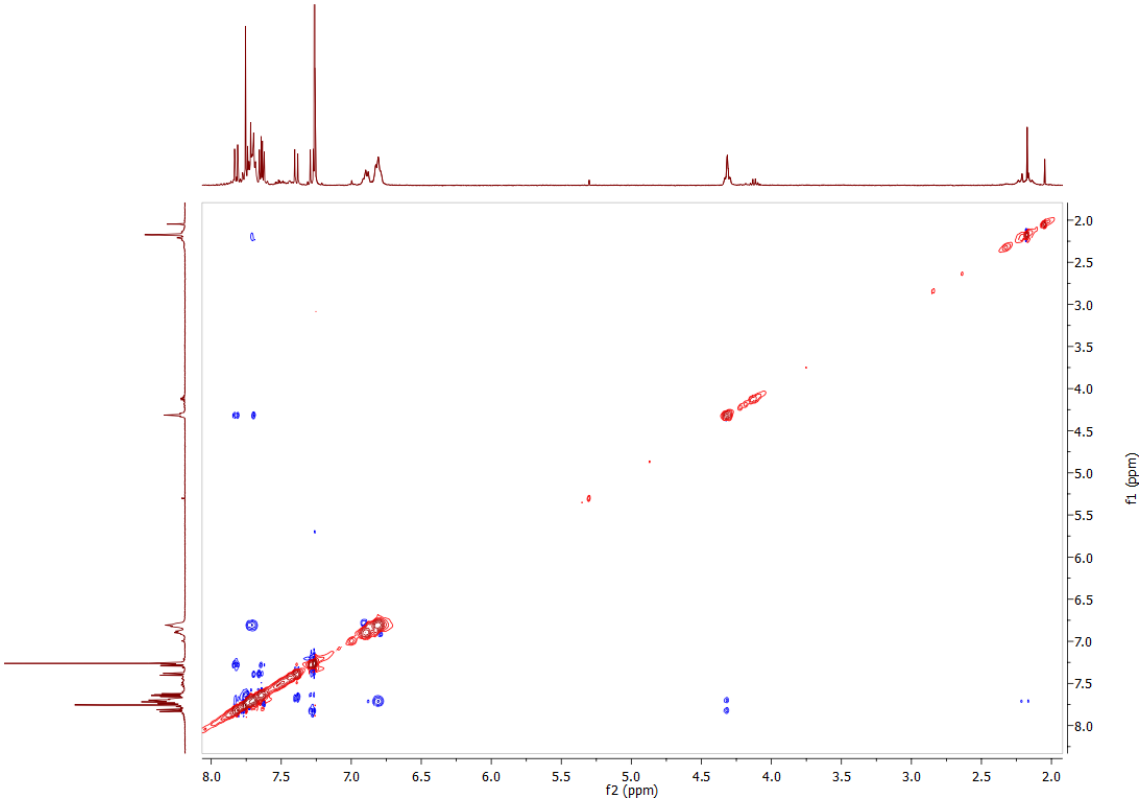

Figure S20. 2-D NOESY spectrum of Pt(dppe)(CC-CH_2-Cora)$_2$ (**4**) in $CDCl_3$.

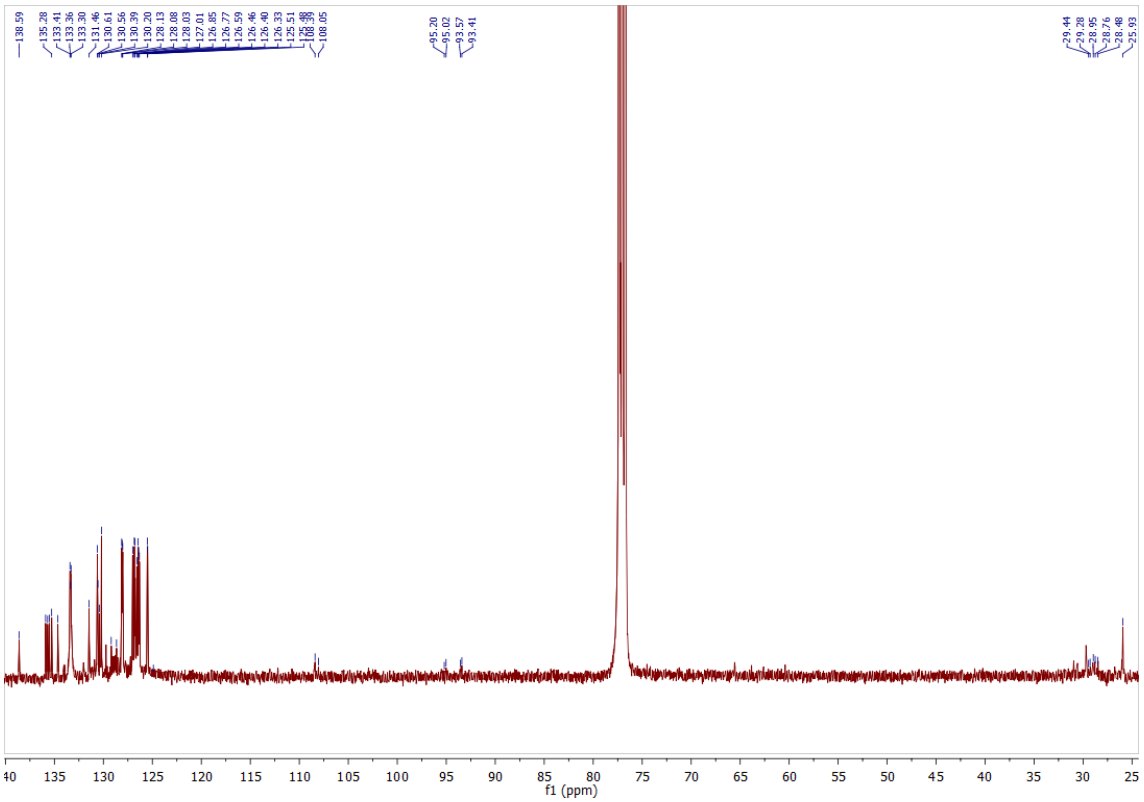

Figure S21. $^{13}C\{^1H\}$ NMR spectrum of Pt(dppe)(CC-CH_2-Cora)$_2$ (**4**) at 100 MHz in $CDCl_3$.

Job's plot experiments.

Method of continuous variation ("Job plot") was used to determine the stoichiometry of the complexation between **1** and fullerenes (C_{60} or C_{70}). Mole ratio plot of $\Delta\delta$ versus guest-to-host molar ratios confirmed the 1:1 stoichiometry in both cases (Figure S22).[5]

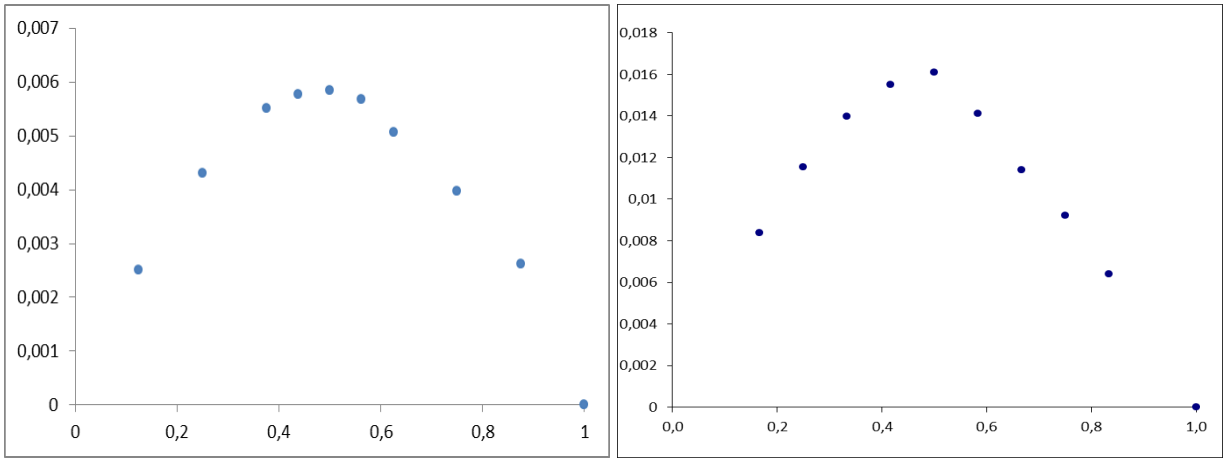

Figure S22. Job plot showing the 1:1 stoichiometry of C_{60} *vs* **1** (on the left) and C_{70} *vs* **1** (on the right).

Complexation studies of 1 with C_{60}. Titration of 1 with C60 in toluene-d_8.

The binding was investigated by ^{1}H NMR titrations. Ka was evaluated from the changes of the chemical shifts of selected independent protons of the corannulene subunits of **1**. Ka and L were optimized as parameters in the curve fitting. The Excel workbooks for curve-fitting NMR titration data of the Sanderson group (http://www.dur.ac.uk/j.m.sanderson/science/downloads.html) were employed for this purpose.

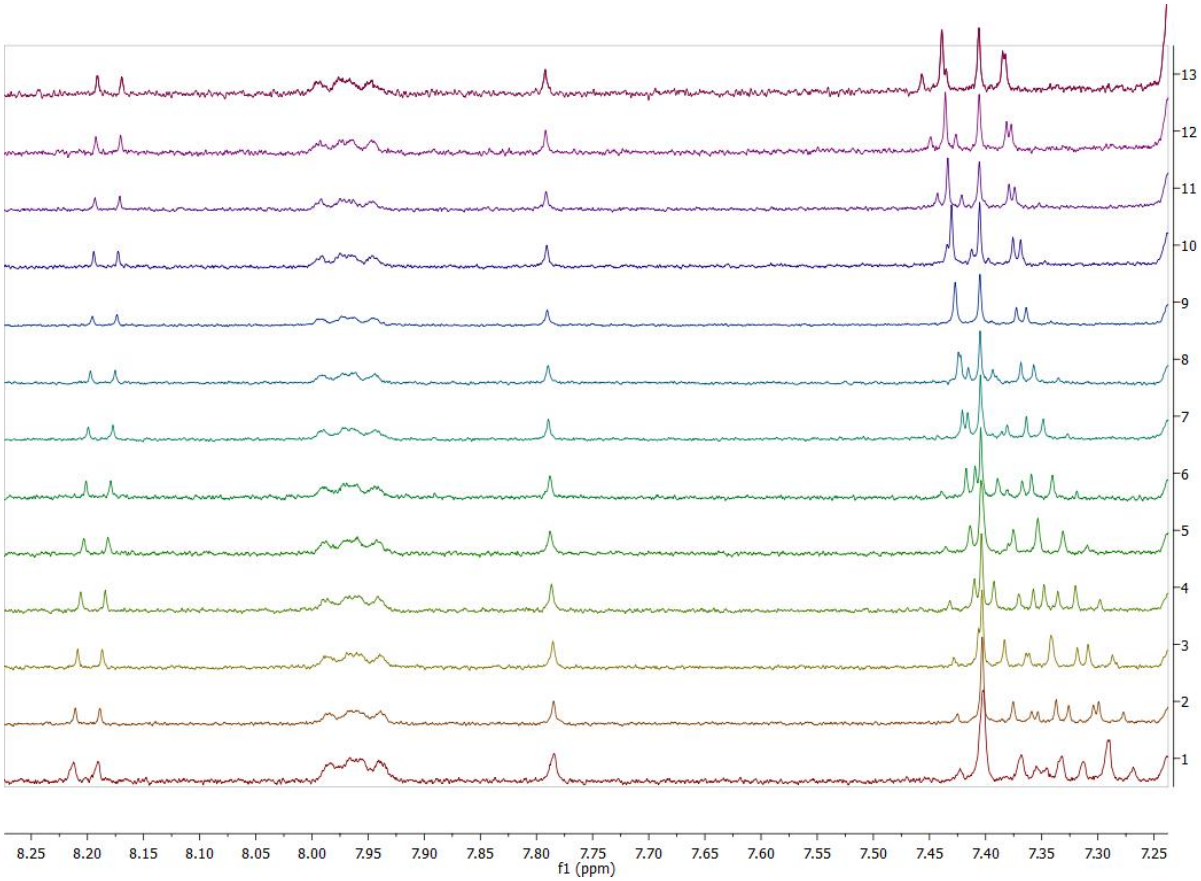

Figure S23. ^{1}H NMR titrations of [Pt(CC-Cora)$_2$(dppe)] (**1**) with C_{60} (400 MHz, 298 K, toluene-d_8).

The results of the curve-fitting for selected protons in corannulene subunits are shown below:

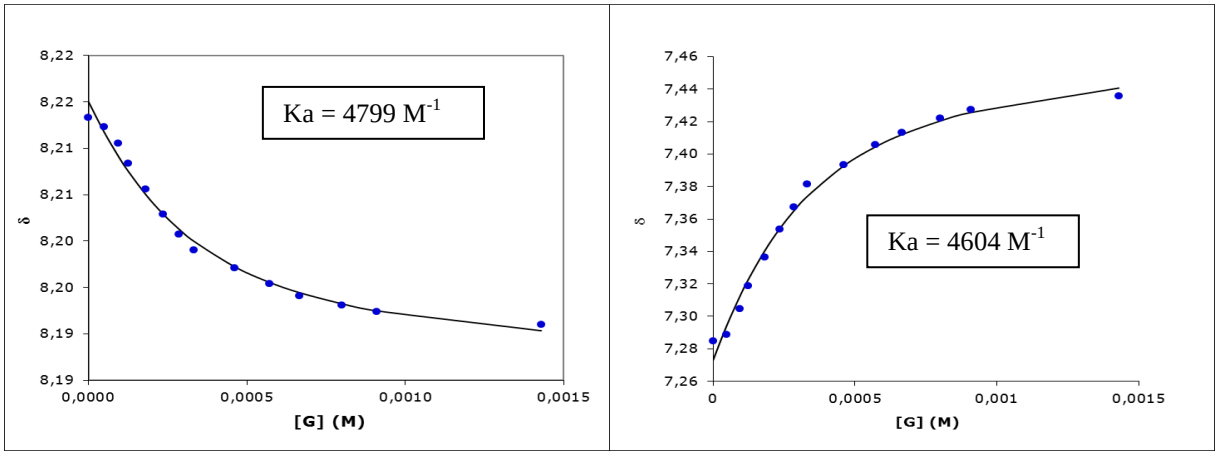

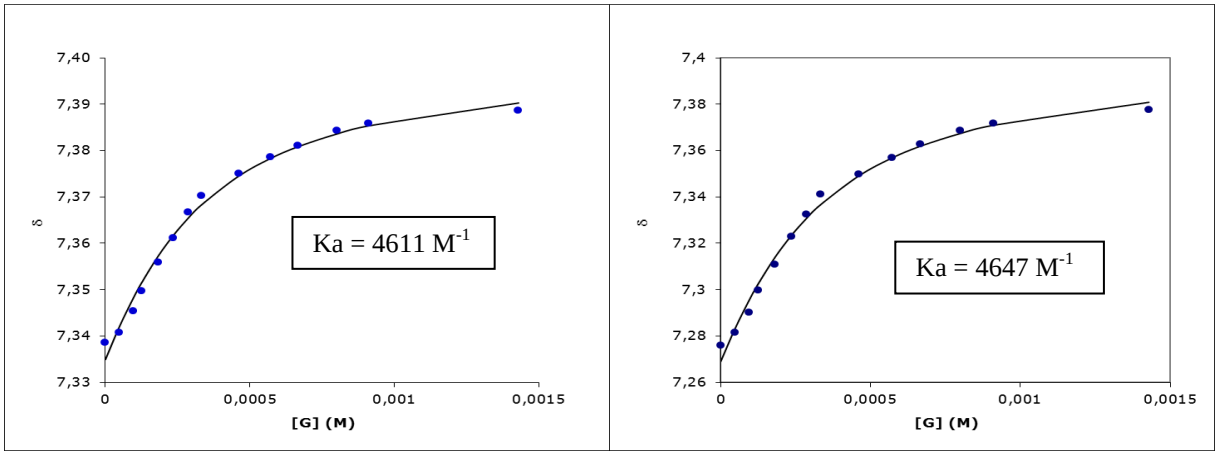

Figure S24. Non linear curve regression for the results of the titration experiments of C_{60} with **1** for selected corannulene protons (binding constant (Ka) were calculated by fitting of the chemical shifts to a 1:1 binding isotherm).

The estimated Ka values are 4799 M^{-1}, 4604 M^{-1}, 4611 M^{-1} and 4647 M^{-1} as calculated for selected corannulene protons in **1**. **The average Ka is 4665 M^{-1}**.

The binding was investigated by ^{13}C NMR spectroscopy. Figure S25 shows variable temperature ^{13}C NMR spectra for a mixture of C_{60} and **1** (1:1) in toluene-d_8. The spectra were run with sufficient number of scan to detect the signal of C_{60} only. The formation of the complex $C_{60}\subset$**1** is demonstrated by the upfield shifted of the signal of C_{60} upon cooling.

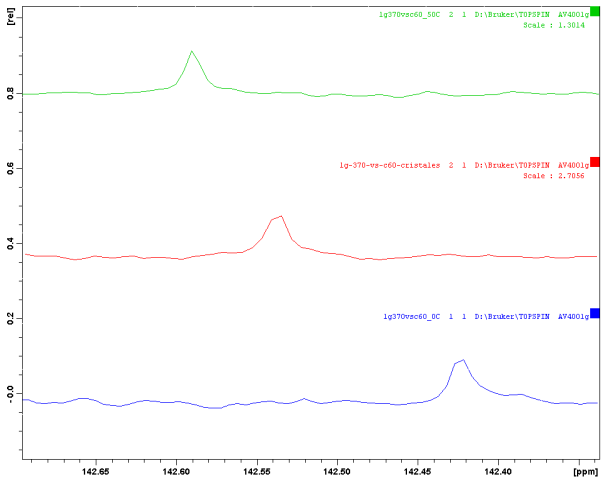

Figure S25. ^{13}C NMR (100 MHz) spectra of a mixture of C_{60} and **1** (1:1) in toluene-d_8 at several temperatures.

The molecular ion peak of inclusion complex $C_{60}\subset$**1** can be detected using MALDI-TOF mass spectrometry as can be see in Figure S26. The spectrum of a 1:1 mixture of **1** and C_{60}, showed peaks at *m/z* 1859.34 and 1860.34, corresponding to $[C_{60}\subset\mathbf{1}]^+$ and $[C_{60}\subset\mathbf{1}\text{-H}]^+$ (calcd.: 1859.24 and 1860.24).

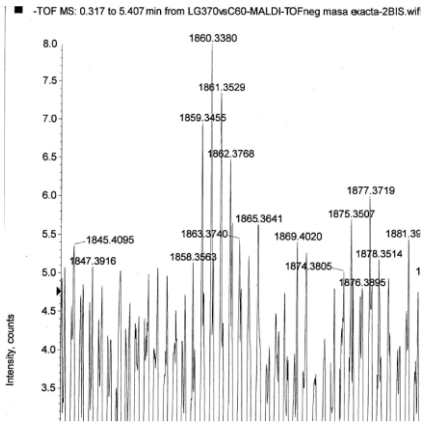

Figure S26. MALDI-TOF isotopic pattern for C60⊂**1**.

Complexation studies of 1 with C_{70}. Titration of 1 with C_{70} in toluene-d_8.

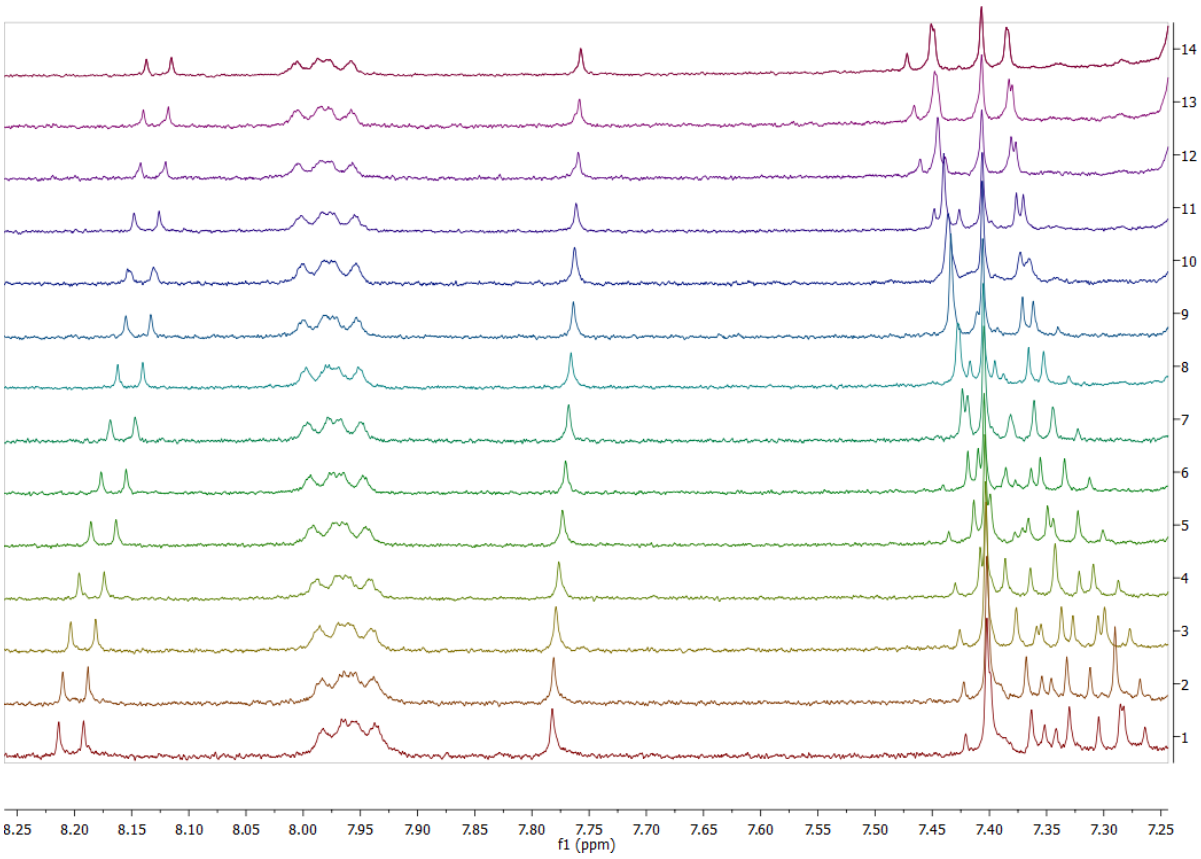

Figure S27. Partial ^{1}H NMR titrations of [Pt(CC-Cora)$_2$(dppe)] (**1**) with C_{70} (400 MHz, 298 K, toluene-d_8).

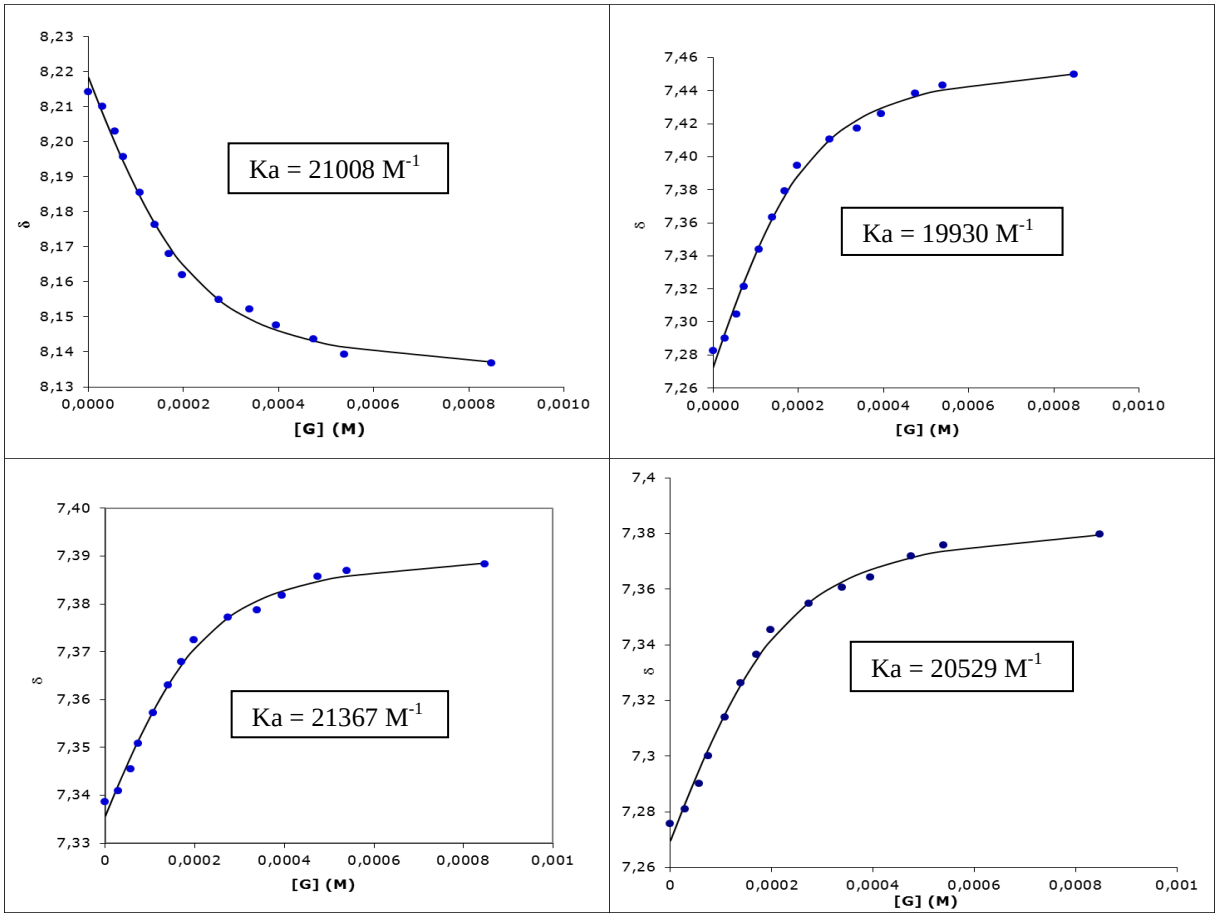

Figure S28. Non linear curve regression for the results of the titration experiments of C_{70} with **1** for selected corannulene protons (binding constant (Ka) were calculated by fitting of the chemical shifts to a 1:1 binding isotherm).

The estimated Ka values are 21008 M^{-1}, 19930 M^{-1}, 21367 M^{-1} and 20529 M^{-1} as calculated for selected corannulene protons in **1**. **The average Ka is 20708 M^{-1}**.

III. Crystallographic Data for C60⊂1.

Crystallographic Experimental Section.

Data collection was performed in an Agilent Supernova diffractometer with a Mo micro-focus source with multilayer optics. Data integration, scaling and empirical absorption correction was carried out using the CrysAlis Pro program package.[6] The structure was solved using direct methods and refined by Full-Matrix-Least-Squares against F^2.[7] The non-hydrogen atoms were refined anisotropically and hydrogen atoms were placed at idealised positions and refined using the riding model.

The C_{60} fragment was disordered but, for the sake of simplicity, it was modeled with just one component with the thermal parameters a little bit larger than usual. One phenyl ring, one corannulene and both toluene lattice solvent molecules were disordered. Two components were defined for each fragment and the structure converged with these final ratios for them: 55-45% for components A and B of the disordered phenyl ring, 51-49% for the two components of the disordered corannulene fragment, 65-35% for one toluene solvent molecule and 55-45% for the other toluene molecule.

SIMU restraints were applied to all C-C bonds in the disordered fragments, DELU restraints were applied to the C_{ipso}-C bonds in the two components of the disordered phenyl ring, and distances and angles of the two toluene solvent molecules were constrained with DFIX and DANG to achieve convergence of the structure.

Table S1. Crystal data and structure refinement for C60⊂**1**.

Empirical formula	$C_{144}\ H_{58}\ P_2\ Pt$	
Formula weight	2044.93	
Temperature	293(2) K	
Wavelength	0.71073 Å	
Crystal system	Monoclinic	
Space group	C2/c	
Unit cell dimensions	a = 56.220(11) Å	α= 90°.
	b = 17.167(3) Å	β= 101.30(3)°.
	c = 19.207(4) Å	γ = 90°.
Volume	18178(6) $Å^3$	
Z	8	
Density (calculated)	1.494 Mg/m^3	
Absorption coefficient	1.642 mm^{-1}	
F(000)	8240	
Crystal size	0.45 × 0.34 × 0.10 mm^3	
Theta range for data collection	2.89 to 28.78°.	
Index ranges	$-62 \le h \le 73$, $-20 \le k \le 23$, $-26 \le l \le 19$	
Reflections collected	36106	
Independent reflections	19052 [R_{int} = 0.0257]	
Completeness to theta = 25.25°	99.2 %	
Refinement method	Full-matrix least-squares on F^2	
Data / restraints / parameters	19052 / 1129 / 1468	
Goodness-of-fit on F^2	0.966	
Final R indices [I > 2σ (I)]	R_1 = 0.0481, wR_2 = 0.1426	
R indices (all data)	R_1 = 0.0684, wR_2 = 0.1490	
Largest diff. peak and hole	3.156 and -0.678 e.$Å^{-3}$	

Table S2. Bond lengths [Å] and angles [º] for C60⊂**1**.

Pt(1)-C(3)	2.000(5)
Pt(1)-C(5)	2.013(5)
Pt(1)-P(2)	2.2748(13)
Pt(1)-P(1)	2.2762(14)
P(1)-C(1)	1.835(5)
P(2)-C(2)	1.839(5)
C(1)-C(2)	1.517(7)
C(3)-C(4)	1.213(7)
C(4)-C(51)	1.438(7)
C(5)-C(6)	1.181(8)
C(6)-C(119)	1.477(13)
C(6)-C(138)	1.510(14)
C(3)-Pt(1)-C(5)	90.8(2)
C(3)-Pt(1)-P(2)	89.04(15)
C(5)-Pt(1)-P(2)	177.83(15)
C(3)-Pt(1)-P(1)	174.87(15)
C(5)-Pt(1)-P(1)	94.24(13)
P(2)-Pt(1)-P(1)	85.97(4)
C(2)-C(1)-P(1)	108.9(3)
C(1)-C(2)-P(2)	109.0(3)
C(4)-C(3)-Pt(1)	171.4(5)
C(3)-C(4)-C(51)	175.1(6)
C(6)-C(5)-Pt(1)	176.3(6)
C(5)-C(6)-C(119)	161.6(9)
C(5)-C(6)-C(138)	161.7(9)

IV. Computational details.

Theoretical calculations have been carried out at the BLYP/TZP level of theory including Grimme's DFT-D3 dispersion correction,[8] as implemented in ADF 2010.[9] Relativistic effects have been included using the ZORA formalism.[10] Gradients have been smoothed and converged to 1e-2 Hartree/angstrom. The energy decomposition analysis (EDA) has been carried out at the same level of theory. Details of the method can be found elsewhere (4, 5) and only a very brief account of the main concepts will be outlined here.[11,12] Within this procedure, the total interaction energy between two fragments is partitioned into three contributions: i) ΔE_{ES} is the classical electrostatic interaction energy between the fragments, calculated with a frozen electron distribution and using the geometry of the compound; ii) ΔE_{PAULI} arises from the exchange repulsion of the fragments' charge distributions; iii) ΔE_{ORB} is the stabilization due to orbital interactions (polarization and charge transfer). The sum of these three terms yields the ΔE_{DFT} interaction energy:

$$\Delta E_{DFT} = \Delta E_{PAULI} + \Delta E_{ES} + \Delta E_{ORB}$$

Inclusion of the dispersion contribution yields the total interaction energy, ΔE_{TOT}:

$$\Delta E_{TOT} = \Delta E_{DFT} + \Delta E_{DISP}$$

Finally, the total bond energy is obtained taking into account the preparation energy, ΔE_{DEF}, that is, the energy necessary to promote both fragments from their equilibrium geometry and electronic ground state to the geometry and electronic state they have in the molecule.

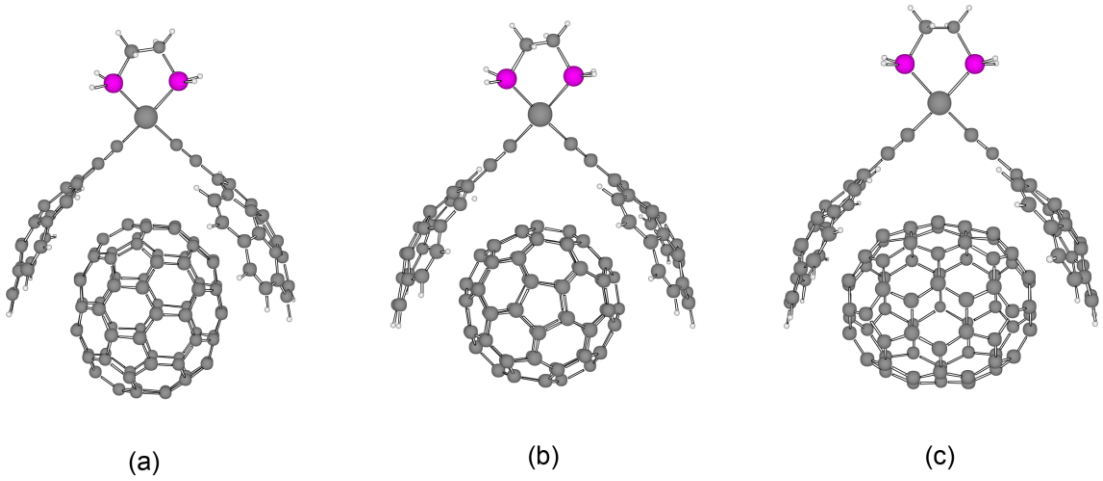

Figure S29. The three possible conformations of the **1**⊂C70 adduct as obtained at the BLYP-D3/TZP level of theory.

(1) (a) Mack, J.; Vogel, P.; Jones, D.; Kaval, N.; Sutton, A. *Org. Biomol. Chem.* **2007**, *5*, 2448-2452. (b) Jones, C. S.; Elliott, E.; Siegel, J. S. *Synlett*, **2004**, *1*, 187-191.

(2) Seiders, T. J.; Elliott, E. L.; Grube, G. H.; Siegel, J. S. *J. Am. Chem. Soc.* **1999**, *34*, 7804–7813.

(3) Maeda, H.; Maeda, T.; Mizuno, K.; Fujimoto, K.; Shimizu, H. Inouye, M. *Chem. Eur. J.* **2006**, *12*, 824–831.

(4) Sudhakar, A.; Katz, T. J. *Tetrahedron Lett.* **1986**, *20*, 2231-2234.

(5) Job, P. *Ann. Chim.* **1928**, *9*, 113-203.

(6) CrysAlisPro Software system, version 1.171.33.51, 2009, Oxford Diffraction Ltd, Oxford, UK.

(7) SHELX Software, Sheldrick, G. M. *Acta Cryst.* **2008**, *A64*, 112-122.

(8) Grimme, S.; Anthony, J.; Ehrlich, S. and Krieg, H. *J. Chem. Phys.* **2010**, *132*, 154104.

(9) ADF2010.02, Theoretical Chemistry, Vrije Universiteit, SCM, Amsterdam, The Netherlands; http://www.scm.com

(10) see van Lenthe, E.; Ehlers, A.E.; and Baerends, E.J. *J. Chem. Phys*. **1999**, *110*, 8943. and references therein.

(11) Bickelhaupt, F. M. ; Baerends, E. J. *Rev. Comput. Chem.* **2000**, *15*, 1.

(12) te Velde, G.; Bickelhaupt, F. M.; Baerends, E. J.; A. van Gisbergen, S. J.; Fonseca Guerra, C.; Snijders, J. G.; Ziegler, T. *J. Comput. Chem.* **2001**, *22*, 931.

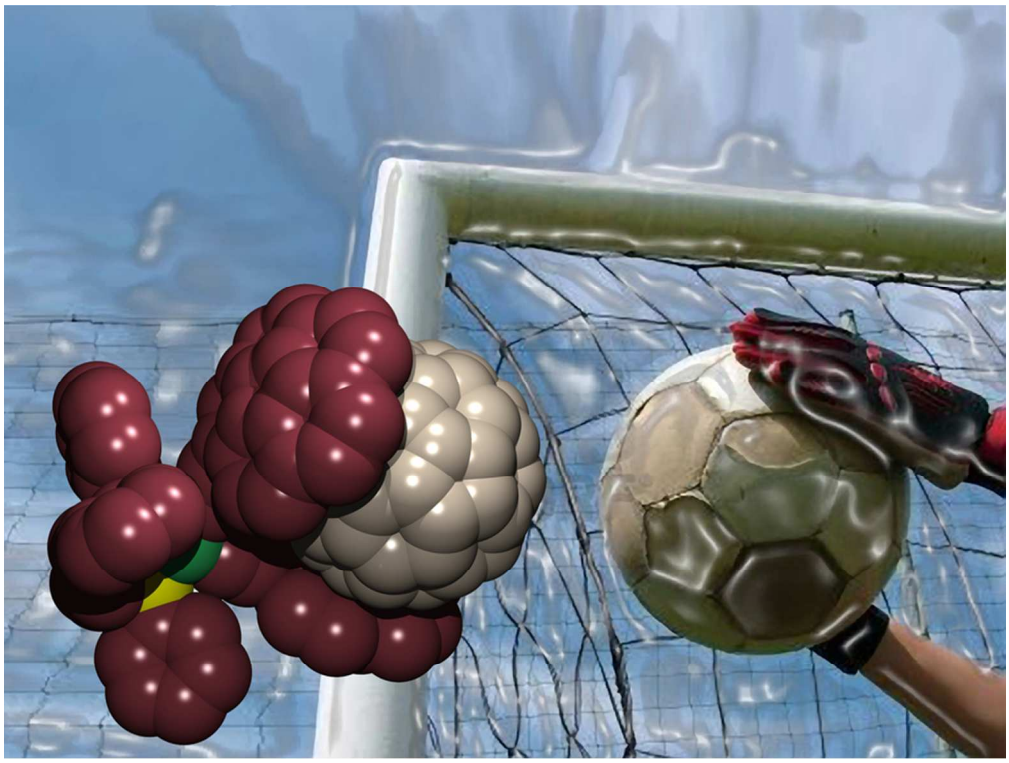

79x59mm (300 x 300 DPI)

CAPÍTULO 2

FUNCIONALIZACIÓN DE COMPLEJOS CON LIGANDOS IMINOPIRIDINA MEDIANTE *CLICK CHEMISTRY*

Artículo IV.

Schiff plus Click: One-pot Preparation of Triazole- Substituted Iminopyridines and Ring Opening of the Triazole Ring.

Cite this: DOI: 10.1039/c0xx00000x

www.rsc.org/xxxxxx

ARTICLE TYPE

Schiff plus Click: One-pot Preparation of Triazole- Substituted Iminopyridines and Ring Opening of the Triazole Ring.

Celedonio M. Álvarez, Luis A. García-Escudero, Raúl García-Rodríguez, Daniel Miguel*

Received (in XXX, XXX) Xth XXXXXXXXX 20XX, Accepted Xth XXXXXXXXX 20XX

DOI: 10.1039/b000000x

The use of Schiff condensation followed by CuAAC affords complexes containing iminopyridine ligands functionalized either with a triazole ring or with a sulfonyl amido group *via* ring opening of the unstable sulfonyl triazole.

Introduction

The use of copper azide-alkyne cycloaddition (CuAAC),[1] first reported independently by the groups of Meldal[2] and Sharpless[3] in 2002, is a well established method which is currently employed in many fields. In particular, there has been a significant increase of interest in the use of CuAAC for the derivatization of ligands which could be used in supramolecular chemistry,[4] to make polynuclear copper complexes,[5] to include a triazolide in the side arm in rhenium bipyridine complexes,[6] or to be coordinated to rhenium as pyridine-triazole[7] or as a part of a tri-coordinated chelate ligand.[8] Triazolide copper(I) intermediates have been used recently as transmetalation reagents for iridium complexes,[9] and a C-bonded triazolide ring has been incorporated in a pincer-type ligand framework in palladium complexes subsequently used as catalysts for the Heck reaction.[10]

We have recently been interested in the use of complexes containing pyridine-2-carboxaldehyde as k^2(N,O) ligands in metal complexes[11] as convenient precursors for iminopyridine complexes via Schiff condensation [12] and other reactivity studies.[13] In the course of these works we had prepared a family of 3- and 4-ethynyl-phenyliminopyridines,[14] which led us to think that succesive use of Schiff reaction and CuAAC would be a facile way to prepare triazolyl-substituted iminopyridines. Within this context we have recently reported that CuAAC between phenylacetylene and azide-functionalized iminopyridine complexes can be useful to obtain triazole complexes. In some circumstances, the use of a stoichiometric amount of the copper reagent produced *via* Cu/Re transmetalation resulted in the formation of triazolyde C-bonded to Re, which could be ultimately converted into a mesoionic C-triazolylidene carbene.[15] Herein we wish to report the use of CuAAC in the reaction of ethynylphenyliminopyridines with alkyl-, benzyl- or sulfonylazides to introduce either a triazole ring or a sulfonylamido function in the side arm of the iminopyridine ligand.

Results and discussion

We have previously shown that [$MBr(CO)_5$] reacts with ethynylphenylamine and pyridine-2-carboxaldehyde (pyca) in refluxing tetrahydrofuran to give, *fac*-[$MBr(CO)_3$(py-2-CH=N-C_6H_4-(C≡CH))] (M = Re, **2a** or **2a'**; Mn, **2b**) and the same method affords [$MoCl(\eta^3$-C_3H_4Me-2)$(CO)_2${py-2-CH=N-C_6H_4-m-(C≡CH)}] (**2c**) starting from [$MoCl(\eta^3$-C_3H_4Me-2)$(CO)_2(NCMe)_2$].[14] Alternatively, we have now found that complexes **1a-c**, bearing a chelate pyridine-2-carboxaldehyde ligand, react with ethynyl-anilines to produce the corresponding 3- or 4-ethynylphenyliminopyridine complexes **2a-c** in good yields (Scheme 1).

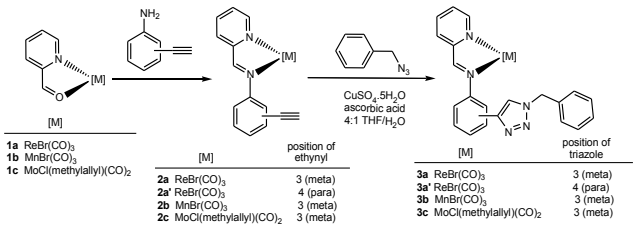

Scheme 1. Reaction of ethynyl iminopyridines with benzyl azide.

Subsequent reactions with benzylazide in the presence of Cu catalyst in CuAAC conditions produce, in good yields, the triazole derivatives **3a-c**, which have been characterized by analytical and spectroscopic methods. After the Schiff reaction from **1a-c** to **2a-c**, there is a significant change in the ν(CO) bands (among 10 to 15 cm^{-1}), evidencing the change in the metal environment from κ^2-(*N,O*) pyca to κ^2-(*N,N'*) iminopyridine. In contrast the ν(CO) bands of the new derivatives **3a-c** appear very close (within 3 cm^{-1}) to those of the precursor ethynyl complexes **2a-c** (see Experimental part), showing that the formation of the triazole ring does not produce a significant change in the electron density available at the metal for retrodonation to the carbonyl ligands. For the **3a-c** triazole derivatives, the ^{1}H NMR spectra show the expected characteristic signals corresponding to the aromatic protons of the iminopyridine, phenylene and benzyl

fragments, while the signal of triazole ring appears as a singlet between 8.48-8.53 ppm depending on the complex. The X-ray structures of **3b** and **3c** (Figure 1) confirm the formation of the 1,4-disubstituted triazole ring. Additionally, the iminopyridine ligands remain coordinated to metals through the pyridine and imine nitrogens, proving the robustness of these complexes in the CuAAC conditions. The dihedral angles between triazole and C_6H_4 rings are 5.9(4)º for **3b** and 14.5(2)º for **3c**, thus permitting some degree of delocalization between the phenyl and triazole rings. In contrast, the phenyl ring is significantly rotated with respect to the rhenium-iminopyridine system, by 44.3(2)º in **3b**, and 59.3(1)º in **3c** and, therefore no delocalization from the iminopyridine towards the phenyl or triazolyl rings is to be expected. This rotation has been commonly observed in aryliminopyridine ligands and, although it has been proposed to correlate well with the steric hindrance around the metal, the results of DFT calculations suggest that the orientation of the phenyl ring is due to electronic rather than packing forces or hydrogen bonding.[16]

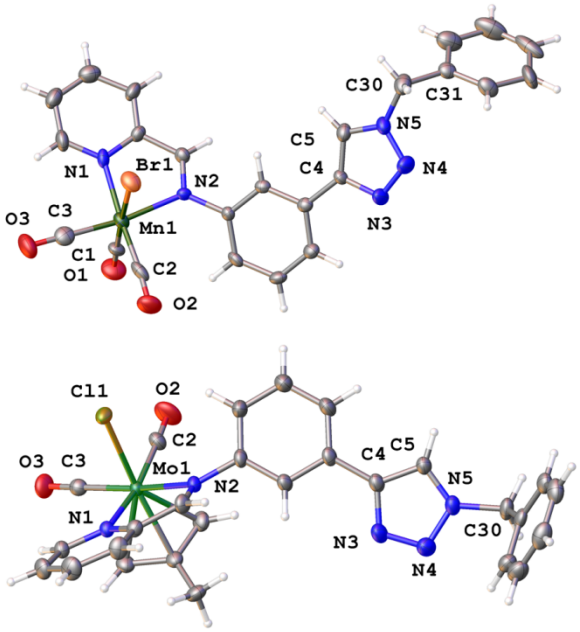

Fig. 1 Thermal ellipsoid drawings of **3a** (above) and **3c** (below) showing the atom numbering.

It is worth noticing that the steps leading from **1** to **2** (Schiff condensation) and from **2** to **3** (cycloaddition) can be performed in a one-pot fashion. Since the isolation of **2** is not required, the only by-product of the Schiff reaction is a small amount of water, and the transformation of **2** into **3** is done in THF/water. Moreover, since the Schiff reaction and the CuAAC are mutually orthogonal, it is possible to mix all the reactants at the beginning without any significant loss of yield. (See *Method B* for **3a** in experimental section).

The procedure can be extended to the preparation of other 4-substituted triazole derivatives by using the appropriate azide reagent. Thus, the reactions of *fac*-[ReBr(CO)$_3${py-2-CH=N-C_6H_4-m-(C≡CH)}] (**2a**) with 1-azidohexadecane or 1,6-diazidohexane in the presence of Cu catalyst in CuAAC conditions produce respectively the triazole derivatives **4a** and **5a** in good yields (Scheme 2). These new rhenium compounds were characterized by analysis with ^{1}H NMR and FTIR, demonstrating that this methodology can be used as a general procedure that can be applied to alkyl azides.

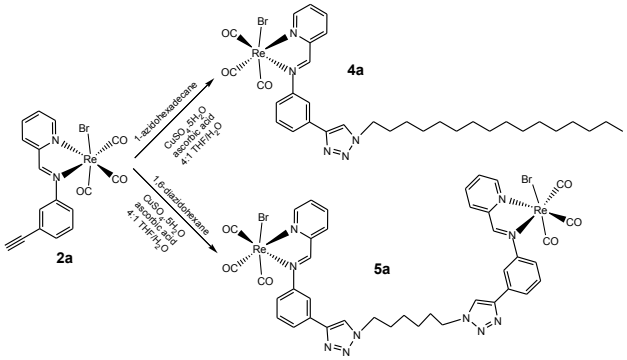

Scheme 2. Reaction of *fac*-[ReBr(CO)$_3${py-2-CH=N-C_6H_4-m-(C≡CH)}] (**2a**) with 1-azidohexadecane and 1,6-diazidohexane.

Additionally, the $CuSO_4$/sodium ascorbate system catalyzed the reaction between *fac*-[ReBr(CO)$_3${py-2-CH=N-C_6H_4-(C≡CH)}] (**2a** or **2a'**) and p-toluenesulfonyl azide to form in high yields N-acylsulfonamide derivatives **6a** and **6a'**, respectively (Scheme 3). The solid structure of **6a'** was confirmed by X-ray crystallography, showing the presence of the N-acylsulfonamide group (Figure 2). This is consistent with the presence of -C(O)-N*H*-SO_2- protons as broad singlets at 6.48 and 6.51 ppm, respectively in the ^{1}H NMR spectra of **6a** and **6a'**. Again, as in **3b** and **3c**, the phenyl group is rotated by 36.4(4)º with respect to the rhenium-iminopyridine plane in **6a'**.

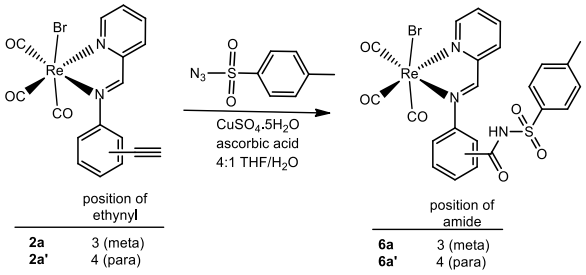

Scheme 3. Reaction of ethynyl iminopyridines with p-toluensulfonyl azide.

In the structure of **6a'** there are two crystallographically independent, but chemically equivalent, molecules in the asymmetric unit. Interestingly, the two molecules are associated by H-bonding involving the Br atom of one molecule and the amide N-H group of the other molecule, as depicted in Figure 2. In this way, a dimer is formed in which the H-bonding arrangement can be described as $R_2^2(22)$ following the graph notation of Etter.[17]

The formation of the sulfonylamide is not completely unexpected

under the reaction conditions. Although it is well known that 1,2,3-triazoles are among the most stable nitrogen heterocycles, the reaction between sulfonyl azides and alkynes using copper(I) as catalyst to form N-acylsulfonamides was first reported in 2005 by Chang.[18] Additionally, there have been later reports of the preparation of 1-sulfonyl-1,2,3-triazoles using click chemistry conditions.[19] Thus, the reaction between sulfonyl azides and alkynes using copper(I) as catalyst in the presence of water can produce either 1-sulfonyl-1,2,3-triazoles or N-acylsulfonamides. depending on a wide variety of factors such as reaction medium, catalyst, reagents employed or temperature.[20]

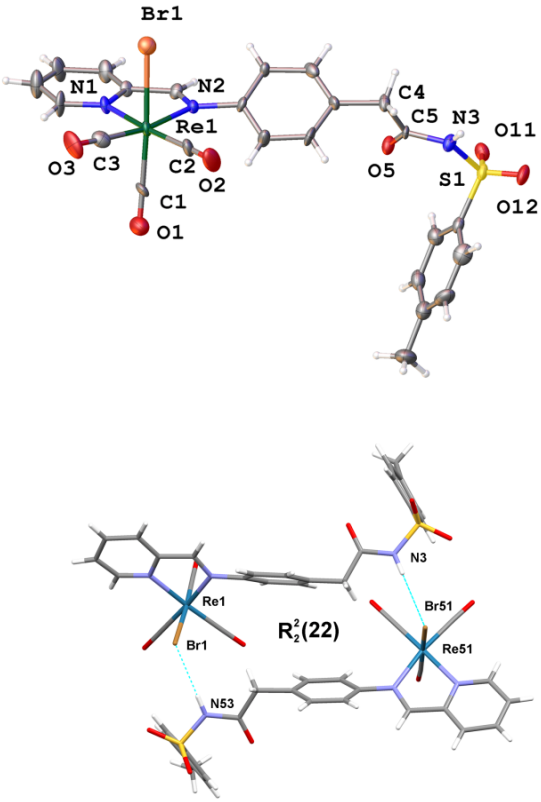

Fig. 2 (above) Thermal ellipsoid drawing of one of the two independent molecules of **6a'** showing the atom numbering. The numbering of the second molecule can be obtained by adding 50 to the number in the label of the atom in the molecule shown. The two molecules are chemically equivalent, and there are no significant differences in their geometrical parameters. (below) Mercury drawing showing the $R_2^2(22)$ H-bonding arrangement of the two molecules. Selected distances (Å) and angles (º): H(3)...Br(51) 3.340 , N(3)...Br(51) 3.240(12), N(3)-H(3)...Br(51) 174.5, H(53)...Br(1) 2.374, N(53)...Br(1) 3.404(12), N(53)-H(53)...Br(1) 178.9.

The accepted mechanism in the copper (I)-catalyzed synthesis of N-acylsulfonamides seems to proceed through a reactive ketenimine produced by ring-opening of the 1,2,3-triazolyde copper (I) intermediate.[21] The nucleophilic attack of water on the keteneimine ultimately produces the sulfonyl amido group. In the present case, the long time (5 days) needed to complete the reaction in the presence of water helps to produce the hydrolysis of the keteneimine intermediate, this being the driving force which displaces the equilibrium towards the opening of the triazole ring. The presence of small amounts of another product has been observed in the reaction mixture by ^{1}H NMR. Unfortunately, these complexes could not be characterized, impeding their identification as the plausible triazole derivatives.

Conclusions

Schiff condensation followed by CuAAC can be used to obtain functionalized iminopyridine complexes. The two reactions are compatible, and therefore they can be carried out sequentially in a one-pot fashion and even, if convenient, by mixing up the starting compounds (pyca complex + ethynylphenylamine + azide) thus performing as a three component reaction.

The outcome of the reaction depends mainly on the electronic features of the azide employed. Under the same conditions, alkyl or benzyl azides produce the expected triazole derivatives while the reaction with sulfonylazide affords sulfonylamides via opening of the intermediate triazolide ring.

Experimental section

General considerations

All operations were performed under an atmosphere of dry nitrogen using Schlenk and vacuum techniques. Dichloromethane and methanol were distilled from CaH_2. THF was distilled from Na/benzophenone. Hexane was distilled from Na. IR spectra in solution were recorded with a Perkin Elmer Spectrum RXI FT–IR instrument, using cells with CaF_2 windows. All NMR solvents were stored over molecular sieves and degassed prior to use. Solution NMR spectra were obtained on a Bruker AC300, Bruker AV-400 or a Varian MR 400 spectrometer. Shift values are given in ppm. ^{1}H chemical shifts are referenced to solvents. Elemental analyses were performed on a Perkin-Elmer 2400B CHN analyzer. Reagents were purchased and used without purification unless otherwise stated. Benzyl azide,[22] p-toluenesulfonyl azide,[22] 1-azidohexadecane,[23] 1,6-diazidohexane,[24] fac-[$ReBr(CO)_3$(pyca)] (**1a**),[11] fac-[$MnBr(CO)_3$(pyca)] (**1b**),[11] [$MoCl(\eta^3$-C_3H_4Me-2)$(CO)_2$(pyca)] (**1c**),[11] fac-[$ReBr(CO)_3${py-2-CH=N-C_6H_4-m-(C≡CH)}] (**2a**),[14] fac-[$ReBr(CO)_3${py-2-CH=N-C_6H_4-p-(C≡CH)}] (**2a'**),[14] fac-[$MnBr(CO)_3${py-2-CH=N-C_6H_4-m-(C≡CH)}] (**2b**)[14] and [$MoCl(\eta^3$-C_3H_4Me-2)$(CO)_2${py-2-CH=N-C_6H_4-m-(C≡CH)}] (**2c**)[14] were prepared according to the literature procedures and the spectral data were in agreement with them.

Synthesis of complexes

Synthesis of **3a**. *Method A*: A mixture of **2a** (0.050 g, 0.09 mmol), benzyl azide (0.012 g, 0.09 mmol), $CuSO_4.5H_2O$ (0.012 g, 0.045 mmol) and sodium ascorbate (0.09 g, 0.045 mmol) were reacted in 4:1 THF:water (20 mL) at room temperature for 5 days. The compound was extracted with CH_2Cl_2 (3 × 15 mL), dried over magnesium sulphate, filtered and evaporated to a red precipitate. The resulting solid residue was dissolved in CH_2Cl_2 and addition of hexane and slow evaporation at reduced pressure gave compound **3a** as red microcrystals. Yield: 0.050 g, 82%.

Method B: A mixture of **1a** (0.050 g, 0.11 mmol), 3-ethynylaniline (0.013 g, 0.11 mmol), benzyl azide (0.015 g, 0.11 mmol), $CuSO_4.5H_2O$ (0.013 g, 0.05 mmol) and sodium ascorbate (0.010 g, 0.05 mmol) were reacted in 4:1 THF:water (20 mL) at room temperature for 5 days. After work-up as described for method A red microcrystals of **3a** were obtained. Yield: 0.060 g, 79%. Anal. Calc. for $C_{24}H_{17}BrN_5O_3Re$: C, 41.80; H, 2.49; N, 10.16. Found: C, 41.96; H, 2.54; N, 10.22. IR (CH_2Cl_2, cm^{-1}), ν(CO): 2027 (vs), 1929 (s), 1904 (s). ^{1}H NMR (300 MHz, acetone-d_6, 298K): δ 9.39 (s, 1H, -CH=N-), 9.21 (d, J^3 = 5.5 Hz, 1H, py), 8.52-8.45 (m, 2H, py and trz), 8.41 (td, J^3 = 7.5 Hz and J^5 = 1.5 Hz, 1H, py), 8.14 (m, 1H, C_6H_4), 7.99 (m, 1H, C_6H_4), 7.92 (m, 1H, py), 7.71-7.61 (m, 2H, C_6H_4), 7.46-7.34 (m, 5H, Ph), 5.74 (s, 2H, CH_2).

Synthesis of **3a'**. A mixture of **2a'** (0.050 g, 0.09 mmol), benzyl azide (0.012 g, 0.09 mmol), $CuSO_4.5H_2O$ (0.012 g, 0.045 mmol) and sodium ascorbate (0.09 g, 0.045 mmol) were reacted in 4:1 THF:water (20 mL) at room temperature for 5 days. Work-up was as described for **3a** to give to give **3a'** as red microcrystals. Yield: 0.053 g, 85%. Anal. Calc. for $C_{24}H_{17}BrN_5O_3Re$: C, 41.80; H, 2.49; N, 10.16. Found: C, 42.03; H, 2.57; N, 10.28. IR (CH_2Cl_2, cm^{-1}), ν(CO): 2027 (vs), 1929 (s), 1905 (s). ^{1}H NMR (300 MHz, acetone-d_6, 298K): δ 9.35 (s, 1H, -CH=N-), 9.20 (d, J^3 = 5.5 Hz, 1H, py), 8.53 (s, 1H, trz), 8.46 (d, J^3 = 7.5 Hz, 1H, py), 8.40 (td, J^3 = 7.5 Hz and J^5 = 1.5 Hz, 1H, py), 8.11 (d, J^3 = 8.5 Hz, 2H, C_6H_4), 7.90 (m, 1H, py), 7.74 (d, J^3 = 8.5 Hz, 2H, C_6H_4), 7.47-7.35 (m, 5H, Ph), 5.73 (s, 2H, CH_2).

Table 1. Crystal data and structure refinement details for compounds **3b**, **3c**, and **6a'**

Compound reference	**3b**	**3c**	**6a'**
Chemical formula	$C_{25}H_{19}BrCl_2MnN_5O_3$	$C_{27}H_{24}ClMoN_5O_2$	$C_{48}H_{38}Br_2N_6O_{12}Re_2S_2$
M_f	643.20	581.90	1487.18
Crystal system	Monoclinic	Monoclinic	Triclinic
Space group	*I2/a*	*P2(1)*	$P\bar{1}$
a/Å	15.675(8)	9.130(3)	12.040(3)
b/Å	12.952(7)	9.212(4)	13.482(3)
c/Å	26.935(14)	15.212(6)	17.438(4)
α/°	90.00	90.00	71.621(4)
β/°	102.764(9)	97.672(6)	88.961(4)
γ/°	90.00	90.00	77.240(4)
Unit cell volume/Å^3	5333(5)	1268.0(8)	2615.9(10)
T/K	296(2)	298(2)	298(2)
Z	8	2	2
Absorption coefficient, μ/mm^{-1}	2.231	0.657	6.296
No. of reflections measured	11939	10815	25414
No. of independent reflections	3860	5140	12691
R(int)	0.1303	0.0323	0.0713
Final R_1 values ($I > 2\sigma(I)$)	0.0790	0.0297	0.0957
Final $wR(F^2)$ values (all data)	0.1441	0.0768	0.1896
CCDC number			

Synthesis of **3b**. A mixture of **2b** (0.100 g, 0.24 mmol), benzyl azide (0.032 g, 0.24 mmol), $CuSO_4.5H_2O$ (0.030 g, 0.12 mmol) and sodium ascorbate (0.024 g, 0.12 mmol) was reacted in 4:1 THF:water (30 mL) at room temperature for 5 days. Work-up was as described for **3a** to give **3b** as red microcrystals. Yield: 0.114 g, 87%. Anal. Calc. for $C_{24}H_{17}BrN_5O_3Mn$: C, 51.63; H, 3.07; N, 12.54. Found: C, 51.80; H, 3.13; N, 12.66. IR (CH_2Cl_2, cm^{-1}), ν(CO): 2029 (vs), 1941 (s), 1920 (s). ^{1}H NMR (300 MHz, acetone-d_6, 298K): δ 9.33 (d, J^3 = 4.0 Hz, 1H, py), 8.94 (s, 1H, -CH=N-), 8.47 (s, 1H, trz), 8.35-8.29 (m, 2H, py and C_6H_4), 8.09 (s, 1H, C_6H_4), 7.96 (d, J^3 = 6.5 Hz, 1H, py), 7.84 (m, 1H, py), 7.70-7.60 (m, 2H, C_6H_4), 7.39 (m, 5H, Ph), 5.71 (s, 2H, CH_2).

Synthesis of **3c**. A mixture of **2c** (0.083 g, 0.20 mmol), benzyl azide (0.027 g, 0.20 mmol), $CuSO_4.5H_2O$ (0.025 g, 0.10 mmol) and sodium ascorbate (0.020 g, 0.10 mmol) was reacted in 4:1 THF:water (25 mL) at room temperature for 5 days. Work-up was as described for **3a** to give **3c** as violet microcrystals. Yield: 0.092 g, 79%. Anal. Calc. for $C_{27}H_{24}ClN_5O_2Mo$: C, 55.73; H, 4.16; N, 12.03. Found: C, 55.80; H, 4.23; N, 12.0.4. IR (CH_2Cl_2, cm^{-1}), ν(CO): 1952 (vs), 1871 (s). ^{1}H NMR (300 MHz, acetone-d_6, 298K): δ 8.93 (s, 1H, -CH=N-), 8.88 (d, J^3 = 5.0 Hz, 1H, py), 8.48 (s, 1H, trz), 8.25-8.14 (m, 2H, py), 8.10 (s, 1H, C_6H_4), 7.97 (d, J^3 = 7.5 Hz, 1H, C_6H_4), 7.74 (t, J^3 = 7.5 Hz, 1H, py), 7.67 (d, J^3 = 7.5 Hz, 1H, C_6H_4), 7.53 (t, J^3 = 7.5 Hz, 1H, C_6H_4), 7.45-7.31 (m, 5H, Ph) 5.75 (s, 2H, CH_2), 2.88 (d, J^3 = 3.5 Hz, 1H, Hsyn allyl), 2.26 (d, J^3 = 3.5 Hz, 1H, Hsyn allyl), 1.37 (s, 3H, Me), 1.25 (s, 1H, Hanti allyl), 1.03 (s, 1H, Hanti allyl).

Synthesis of **4a**. A mixture of **2a** (0.100 g, 0.18 mmol), 1-azidohexadecane (0.048 g, 0.18 mmol), $CuSO_4.5H_2O$ (0.023 g, 0.09 mmol) and sodium ascorbate (0.018 g, 0.09 mmol) was reacted in 4:1 THF:water (20 mL) at room temperature for 5 days. Work-up was as described for **3a** to give **4a** as red microcrystals. Yield: 0.130 g, 88%. Anal. Calc. for $C_{33}H_{43}BrN_5O_3Re$: C, 48.11; H, 5.26; N, 8.50. Found: C, 48.20; H, 5.33; N, 8.62. IR (CH_2Cl_2, cm^{-1}), ν(CO): 2028 (vs), 1929 (s), 1905 (s). ^{1}H NMR (300 MHz, acetone-d_6, 298K): δ 9.43 (s, 1H, -CH=N-), 9.20 (d, J^3 = 5.5 Hz, 1H, py), 8.50-8.41 (m, 2H, py and trz), 8.34 (m, 1H, py), 8.19 (s, 1H, C_6H_4), 7.97 (d, J^3 = 7.5 Hz, 1H, C_6H_4), 7.89 (m, 1H, py), 7.70-7.60 (m, 2H, C_6H_4), 4.50 (t, J^3

= 7.0 Hz, 2H, NCH_2), 1.96 (m, 2H, NCH_2CH_2) 1.40-1.18 (m, 26H, CH_2), 0.88 (t, J^3 = 7.0 Hz, 3H, Me).

Synthesis of **5a**. A mixture of **2a** (0.100 g, 0.18 mmol), 1,6-diazidohexane (0.015 g, 0.09 mmol), $CuSO_4.5H_2O$ (0.023 g, 0.09 mmol) and sodium ascorbate (0.018 g, 0.09 mmol) was reacted in 4:1 THF:water (20 mL) at room temperature for 5 days. Work-up was as described for **3a** to give **5a** as red microcrystals. Yield: 0.096 g, 83%. Anal. Calc. for $C_{40}H_{32}Br_2N_{10}O_6Re_2$: C, 37.51; H, 2.52; N, 10.93. Found: C, 37.52; H, 2.67; N, 11.00. IR (CH_2Cl_2, cm^{-1}), ν(CO): 2028 (vs), 1929 (s), 1904 (s). ^{1}H NMR (300 MHz, acetone-d_6, 298K): δ 9.40 (s, 2H, -CH=N-), 9.20 (d, J^3 = 5.0 Hz, 2H, py), 8.55-8.46 (m, 4H, py and trz), 8.37 (m, 2H, py), 8.15 (s, 2H, C_6H_4), 7.97 (d, J^3 = 7.0 Hz, 2H, C_6H_4), 7.88 (m, 2H, py), 7.71-7.59 (m, 4H, C_6H_4), 4.51 (t, J^3 = 7.0 Hz, 4H, NCH_2), 1.99 (m, 4H, NCH_2CH_2) 1.42 (m, 4H, $NCH_2CH_2CH_2$).

Synthesis of **6a**. A mixture of **2a** (0.100 g, 0.18 mmol), p-toluenesulfonyl azide (0.036 g, 0.18 mmol), $CuSO_4.5H_2O$ (0.023 g, 0.09 mmol) and sodium ascorbate (0.018 g, 0.09 mmol) was reacted in 4:1 THF:water (20 mL) at room temperature for 5 days. Work-up was as described for **3a** to give **6a** as red microcrystals. Yield: 0.098 g, 73%. Anal. Calc. for $C_{24}H_{19}BrN_3O_6ReS$: C, 38.77; H, 2.58; N, 5.65. Found: C, 38.82; H, 2.67; N, 5.82. IR (CH_2Cl_2, cm^{-1}), ν(CO): 2027 (vs), 1928 (s), 1904 (s). ^{1}H NMR (300 MHz, acetone-d_6, 298K): δ 9.26 (s, 1H, -CH=N-), 9.18 (d, J^3 = 5.5 Hz, 1H, py), 8.47 (d, J^3 = 7.5 Hz, 1H, py), 8.39 (d, J^3 = 7.5 Hz, 1H, py), 7.93-7.86 (m, 3H, py and tol), 7.60 (d, J^3 = 7.5 Hz, 1H, C_6H_4), 7.49 (s, 1H, C_6H_4), 7.45 (t, J^3 = 7.5 Hz, 1H, C_6H_4), 7.37 (d, J^3 = 8.0 Hz, 2H, tol), 7.34 (d, J^3 = 7.5 Hz, 1H, C_6H_4), 6.48 (s, br, 1H, NH), 3.81 (s, 2H, CH_2), 2.40 (s, 3H, Me).

Synthesis of **6a'**. A mixture of **2a'** (0.100 g, 0.18 mmol), p-toluenesulfonyl azide (0.036 g, 0.18 mmol), $CuSO_4.5H_2O$ (0.023 g, 0.09 mmol) and sodium ascorbate (0.018 g, 0.09 mmol) was reacted in 4:1 THF:water (20 mL) at room temperature for 5 days. Work-up was as described for **3a** to give **6a'** as red microcrystals. Yield: 0.095 g, 71%. Anal. Calc. for $C_{24}H_{19}BrN_3O_6ReS$: C, 38.77; H, 2.58; N, 5.65. Found: C, 38.81; H, 2.69; N, 5.86. IR (CH_2Cl_2, cm^{-1}), ν(CO): 2027 (vs), 1928 (s), 1905 (s). ^{1}H NMR (300 MHz, acetone-d^6, 298K): δ 9.28 (s, 1H, -CH=N-), 9.19 (d, J^3 = 5.5 Hz, 1H, py), 8.48-8.34 (m, 2H, py), 7.93-7.86 (m, 3H, py and tol), 7.58 (d, J^3 = 8.5 Hz, 2H, C_6H_4), 7.46-7.36 (m, 4H, C_6H_4 and tol), 6.51 (s, br, 1H, NH), 3.79 (s, 2H, CH_2), 2.44 (s, 3H, Me).

Acknowledgements

Financial support for this work was provided by the Spanish Ministerio de Ciencia e Innovación (CTQ2009-12111) and the Junta de Castilla y León (VA070A08 and GR Excelencia 125). R. G.-R and C. M. A. wish to acknowledge a MEC-FPU grant and a Ramón y Cajal contract. L. A. G.-E. thanks the University of Valladolid for a Ph. D. grant.

Notes and references

GIR-MIOMeT-IU CINQUIMA/Química Inorgánica, Facultad de Ciencias, Universidad de Valladolid, Valladolid (Spain) . Fax: (+)34 983423013; Tel: (+)34 983184096; E-mail: dmsj@qi.uva.es

† Electronic Supplementary Information (ESI) available: Experimental procedures, spectroscopic data of all compounds and crystallographic data of and. CCDC . See DOI: 10.1039/b000000x/

1 M. Meldal and C. W. Tornoe, *Chem.Rev.* 2008, **108**, 2952.
2 C. W. Tornoe, C. Christensen and M. Meldal, *J. Org. Chem.* 2002, **67**, 3057.
3 V. V. Rostovstsev, L. G. Green, V. V. Fokin and B. K. Sharpless, *Angew. Chem., Int. Ed.* 2002, **41**, 2596.
4 T. Romero, R. A. Orenes, A. Espinosa, A. Tárraga and P. Molina, *Inorg. Chem.* 2011, **50**, 8214.
5 G. F. Manbeck, W. W. Brennessel, C. M. Evans and R. Eisenberg, *Inorg. Chem.* 2010, **49**, 2834.
6 C. Cote and R. U. Kirss, *Inorg. Chim. Acta* 2010, **363**, 2520.
7 M. Obata, A. Kitamura, A. Mori, C. Kameyama, J. A. Czaplewska, R. Tanaka, I. Kinoshita, T. Kusumoto, H. Hashimoto, M. Harada, Y. Mikata, T. Funabiki and S. Yano, *Dalton Trans.*2008, 3292.
8 H. Struthers, B. Spingler, T. L. Mindt and R. Schibli, *Chem. Eur. J.* 2008, **14**, 6173.
9 S. Liu, P. Müller, M. K. Takase and T. M. Swager, *Inorg. Chem.* 2011, **50**, 7598.
10 E. M. Schuster, M. Botoshansky and M. Gandelman, *Angew. Chem. Int. Ed.* 2008, **47**, 4555. E. M. Schuster, M. Botoshansky and M. Gandelman, *Organometallics* 2009, **28**, 7001. E. M. Schuster, G. Nisnevich, M. Botoshansky and M. Gandelman, *Organometallics* 2009, **28**, 5025.
11 C. M. Álvarez, R. García-Rodríguez and D. Miguel, *Dalton Trans*. 2007, 3546.
12 R. García-Rodríguez and D. Miguel, *Dalton Trans*. 2006, 1218. C. M. Álvarez, R. García-Rodríguez and D. Miguel, *J. Organomet. Chem.* 2007, **692**, 5717. C. M. Álvarez, R. García-Rodríguez and D. Miguel, *Inorg. Chem.* 2012, **51**, 2984. C. M. Álvarez, R. García-Rodríguez J. M. Martin-Alvarez, D. Miguel and J. A. Turiel, *Inorg. Chem.* 2012, **51**, 3938.
13 C. M. Álvarez, R. Carrillo, R. García-Rodríguez and D. Miguel, *Chem. Commun.* 2011, **47**, 12765. C. M. Álvarez, R. Carrillo, R. García-Rodríguez and D. Miguel, *Chem. Commun.* 2012, **48**, 7705. C. M. Alvarez, L. Alvarez-Miguel, R. Garcia-Rodriguez and D. Miguel, *Dalton Trans.* 2012, **41**, 7041.
14 L. A. García-Escudero, D. Miguel and J. A. Turiel, *J. Organomet. Chem.* 2006, **691**, 3434.
15 C. M. Alvarez, L. A. Garcia-Escudero, R. García-Rodríguez and D. Miguel, *Chem. Commun.*, 2012, **48**, 7209. For other examples of triazolylidene ligands see: K. J. Kilpin, U. S. D. Paul, A.-L. Lee and J. D. Crowley, *Chem. Commum.* 2011, **47**, 328. T. Nakamura, T. Terashima, K. Ogata and S. Fukuzawa, *Org. Lett*., 2011, **13**, 620. R. Saravanakumar, V. Ramkumar and S. Sankararaman, *Organometallics* 2011, **30**, 1689. S. Hohloch, C.-Y. Su and B. Sarkar, *Eur. J. Inorg. Chem.* 2011, 3067. S. Inomata, H. Hiroki, T. Terashima, K. Ogata and S. Fukuzuwa, *Tetrahedron* 2011, **67**, 7263. J. Cai, X. Yang, K. Arumugam, C. W. Bielawski and J. L. Sessler, *Organometalllics* 2011, **30**, 5033. J. Bouffard, B. K. Keitz, R. Tonner, G. Guisado-Barrios, G. Frenking, R. G. Grubbs and G. Bertrand, *Organometallics*, 2011, **30**, 2617. T. Karthikeyan and S. Sankararaman, *Tetrahedron Letters* 2009, **50**, 5834. G. Guisado-Barrios, J. Bouffard, B. Donnadieu and G. Bertrand, *Organometallics* 2011, **30**, 6017. G. Guisado-Barrios, J. Bouffard, B. Donnadieu and G. Bertrand, *Angew. Chem., Int. Ed.* 2010, **49**, 4759. E. M. Schuster, M. Botoshansky and M. Gandelman, *Dalton Trans.* 2011, **40**, 8764.
16 K. Heinze, *J. Chem. Soc. Dalton Trans.* 2002, 540. K. Heinze, V. Jacob, *J. Chem. Soc. Dalton Trans.* 2002, 2379.
17 M. C. Etter, *Acc. Chem: Res.* **1990**, *23*, 120.
18 S. H. Cho, E. J. Yoo, I. Bae and S. Chang, *J. Am. Chem. Soc.* 2005, **127**, 16406.

19 J. Raushel and V. V. Fokin, *Org. Lett.* 2010, **12**, 4952. I. Cano, M. C. Nicasio and P. J. Pérez, *Org. Biomol. Chem.* 2010, **8**, 536. F. Wang, H. Fu, Y. Jiang and Y. Zhao, *Adv. Synth. Catal.* 2008, **350**, 1830.
20 E. J. Yoo, M. Ahlquist, I. Bae, K. B. Sharpless, V. V. Fokin and S. Chang, *J. Org. Chem.* 2008, **73**, 5520.
21 M. P. Cassidy, J. Rauschel and V. V. Fokin, *Angew. Chem. Int. Ed.* 2006, **45**, 3154.
22 H. Zheng, R. McDonald and D. G. Hall, *Chem. Eur. J.* 2010, **16**, 5454.
23 M. Lamani and K. R. Prabhu, *Angew. Chem. Int. Ed.* 2010, **49**, 6622.
24 C. Romuald, E. Busseron and F. Coutrot, *J. Org. Chem.* 2010, **75**, 6516.

Artículo V.

Beyond click chemistry: spontaneous C-triazolyl transfer from copper to rhenium and transformation into mesoionic C-triazolylidene carbene.

ChemComm

Dynamic Article Links

Cite this: *Chem. Commun.*, 2012, **48**, 7209–7211

www.rsc.org/chemcomm

COMMUNICATION

Beyond click chemistry: spontaneous C-triazolyl transfer from copper to rhenium and transformation into mesoionic C-triazolylidene carbene†

Celedonio M. Álvarez, Luis A. García-Escudero, Raúl García-Rodríguez and Daniel Miguel*

Received 17th April 2012, Accepted 28th May 2012
DOI: 10.1039/c2cc32725b

The exceptional versatility of the 1,2,3-triazole ring in tridentate carbonyl rhenium complexes has been explored starting from a "click chemistry" unexpected product obtained from the spontaneous copper to rhenium transmetalation, which opens the way to successive transformation to C-triazolyl and triazolylidene mesoionic carbene.

Copper catalyzed azide–alkyne cycloaddition (CuAAC) has become ubiquitous in nearly all areas of chemistry. The reaction was first reported independently by the groups of Meldal[1] and Sharpless[2] in 2002, and it has been applied successfully in many fields.[3]

There has been increasing interest in the use of CuAAC for the derivatization of ligands.[4,5] In most cases the triazole ring is coordinated through one of the nitrogen atoms, with there being only a few examples of complexes containing C-bonded triazolyl.[6] Triazolyl copper(I) intermediates have been used recently as transmetalation reagents for iridium complexes.[7]

Albrecht and co-workers have recently reported that the methylation of the triazole ring and subsequent treatment with Ag_2O in the presence of a metal-halide complex can introduce the 1,2,3,-triazolyl-4,5-ylidene bonded through C-5 to the metal,[8] thus acting as a mesoionic carbene (MIC) pertaining to the class of *abnormal*-N-Heterocyclic Carbenes (*a*-NHCs).[9] The interest in triazolylidene ligands has expanded quickly in the last three years and a variety of complexes with different metals have been reported, some of which have been used in catalysis.[10] Bertrand *et al.* reported the preparation of stable bis-1,2,3-triazolyl-5-ylidene (i-bitz) ligands.[11] In most cases the ligands are introduced following original Albrecht's method, *i.e.* alkylation of the triazole ring followed by treatment with Ag_2O. However, Gandelman *et al.* have used an alternative route, by alkylation of a C-triazolyl ring of a pincer ligand, previously introduced by deprotonation with a base.[12]

GIR-MIOMeT-IU CINQUIMA/Química Inorgánica, Facultad de Ciencias, Universidad de Valladolid, Prado de la Magdalena, s/n 47005, Valladolid, Spain. E-mail: dmsj@qi.uva.es; Fax: +34 983423013; Tel: +34 983184096

† Electronic supplementary information (ESI) available: Experimental procedures, spectroscopic data for all compounds and crystallographic data for **2**, **5**, **6** and **7**. CCDC 867717–867720. For ESI and crystallographic data in CIF or other electronic format see DOI: 10.1039/c2cc32725b

In contrast to the well-known NHCs derived from imidazolium rings,[13] the mesoionic carbenes derived from 1,2,3-triazolylidene rings exhibit better donor properties.[11] Some interesting NHCs complexes of group 7 metals have been reported recently[14] but, as far as we know, there is no previous report of complexes of group 7 metals with 1,2,3-triazolylidene MICs.

We are currently interested in the use of complexes containing pyridine-2-carboxaldehyde as k^2(N,O) ligands in metal complexes[15] as convenient precursors for iminopyridine complexes *via* Schiff base condensation with primary amines,[16] with the aim of developing a methodology for the application of this reaction in the functionalization of amino acids and amino esters.[17] In the context of these studies it was expected that successive use of Schiff reaction and CuAAC could be a convenient method for preparation of triazolyl-substituted iminopyridines.

Herein we wish to report the use of CuAAC for the derivatization of metal carbonyl compounds to afford a new complex in which the triazolyl group acts as a bridge between Re and Cu after transmetalation. This is, as far as we know, the first example of a triazole ring acting as a ligand both through C and N. Additionally, the copper can be easily removed to give a Re triazolyl which can be converted into a mesoionic C-triazolylidene carbene.

Complex **1** containing pyridine-2-carboxaldehyde (pyca) as a chelate k^2(N,O) ligand reacts with 3-azido-1-propylamine in refluxing MeOH to give, after workup, orange microcrystals of **2** (Scheme 1), which was characterized by analytical and spectroscopic methods (see ESI† for experimental details and spectroscopic data). An X-ray determination on a crystal of **2** (see Fig. S1, ESI†) confirmed the formation of the iminopyridine ligand arising from the Schiff base condensation of the amine

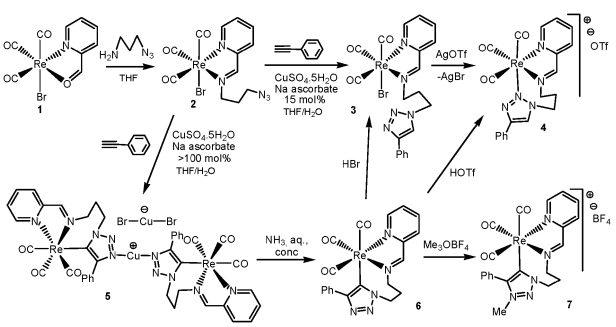

Scheme 1 Reaction schemes for the preparation of new complexes.

group with the coordinated aldehyde, and the presence of the azide group in the pendant arm of the iminopyridine.

Treatment of **2** with phenyl acetylene in the presence of $CuSO_4{\cdot}5H_2O$ and sodium ascorbate under catalytic conditions (15–20 mol%) in THF:water produced the expected complex **3** bearing a triazole ring from the [3 + 2] cycloaddition of the azide and acetylene groups. Spectroscopic data for complex **3** are in agreement with the structure depicted in Scheme 1. The coordination ability of the pendant triazole ring in **3** can be exploited to obtain cationic complexes *via* bromide abstraction with silver triflate, to afford complex **4**.[18]

In the course of the CuAAC reaction to give **3** from **2**, IR monitoring in solution revealed the presence of a small amount of an unexpected product **5** with bands at 2017 vs. 1921 s, 1904 vs. cm^{-1} (*cf.* 2026 vs. 1927 s, 1903 s, cm^{-1} for **2**). It was also observed that the addition of increasing amounts of a copper reagent led to the presence of larger amounts of **5**. Indeed when a stoichiometric amount of copper and ascorbate was added at the beginning, the reaction afforded **5** as the only product, which could be isolated as orange-red microcrystals. Better yield and shorter reaction times are obtained by using a slight excess (1.2 : 1) of Cu/ascorbate. An X-ray determination showed that the structure of **5** consists of a $CuBr_2^-$ anion and a cation in which one copper atom is bonded to two *N*-triazolyl-$(CH_2CH_2CH_2N{=}CPy)Re(CO)_3$ fragments. Both anion and cation are centrosymmetric, with the copper atoms Cu(1) and Cu(2) placed in the centres of symmetry of the anion and cation, respectively. The connectivity sequences propyl–N(3)–N(4)–N(5) and phenyl–C(4)–C(5) confirm unambiguously that the triazole ring is C-bonded to Re and N-bonded to Cu. This situation is quite unexpected since, as far as we know, there is no precedent of a triazole ring acting simultaneously as C- and N-donor.

A rationale for the process is presented in Scheme 2: the copper triazolyl resulting from the cycloaddition (**A**) transfers the triazolyl to rhenium in exchange for Br to give **B**, in which the copper atom remains bonded to the triazole ring through one N atom, followed by recombination to give the final product **5**. Similar transmetalations from Cu carbenes have been reported by Cazin and Albrecht.[19]

As shown in Fig. 1, the cation of **5** can be regarded as a copper(I) complex having two neutral N-donor ligands. To test whether the Re moiety would be stable on its own, it was deemed to be of interest to liberate the ligands. A CH_2Cl_2 solution of **5** was stirred with aqueous concentrated ammonia for 1 h. IR monitoring showed a slight change in the *ν*(CO) stretching. Subsequent workup afforded **6** as pale yellow microcrystals. An X-ray determination (Fig. 2) confirmed that **6** is the expected mononuclear rhenium tricarbonyl complex with the tridentate (N,N,C) triazolylpropyliminopyridine. The ^{13}C NMR spectrum shows the signal for the carbon

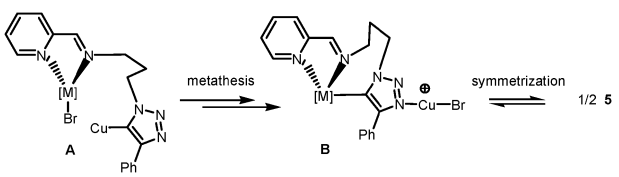

Scheme 2 Metathesis of the intermediate copper C-triazolyl and subsequent symmetrization to give the final product.

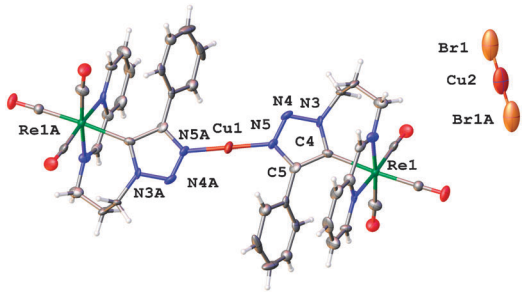

Fig. 1 Structure of **5** showing the atom numbering. Both anion and cation are centrosymmetric, with only one-half of each contained in the asymmetric unit.

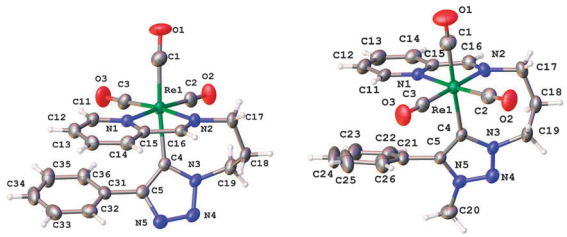

Fig. 2 Structures of **6** (left) and the cation of **7BF$_4$** (right), showing the atom numbering. Only one of the two independent molecules of 7 is shown. The geometrical parameters of the other molecule are not significantly different from the one shown.

bonded to rhenium at 153.5 ppm, slightly shifted from that of the parent **5** (153.8 ppm).

The steps leading from **1** to **2** (Schiff base condensation) and from **2** to **5** (cycloaddition and triazolyl transfer) were performed in a sequential one-pot fashion, since the isolation of **2** is not required, as the only by-product of the Schiff reaction is a small amount of water, and the transformation of **2** into **3** or **5** is done in THF/water (see ESI†).

Upon addition of trimethyloxonium tetrafluoroborate to a solution of **6** the IR spectra show a change in the *ν*(CO) absorptions from 2012 vs. 1912 s, 1899 s, cm^{-1} to 2023 vs. 1923 s, 1905 s cm^{-1}, which is consistent with the formation of the cationic complex **7** (Scheme 1). An X-ray determination (Fig. 2) confirmed the methylation of the nitrogen in position 3, converting the triazolyl ring into a triazolylidene. This heterocyclic structure formally contains a positive and a negative charge in the same ring and can thus be regarded as a mesoionic carbene. The geometry of the triazole ring is not significantly changed upon going from **6** to **7**. The Re–C distance is shortened from 2.202(6) Å in **6** to 2.175(7) and 2.173(7) Å in **7BF$_4$**, and the NMR signal for the carbon bonded to Re changes from 153.5 ppm in **6** to 162.1 ppm in **7**, all of which are consistent with the change from an anionic triazolyl to a carbene-like triazolylidene.

Treatment of triazolyl complex **6** with acid produces instantaneous protonation of the nitrogen, which can be reverted by treatment with Na_2CO_3. When **6** was heated with a slight excess of HBr (aq.) for 2 h, it was quantitatively converted into the bromo complex **3**, according to IR and NMR data. Similarly, heating **6** with HOTf in THF (4 h) produced the triflate salt of the cation **4**.

In conclusion, the successive use of Schiff base condensation and CuAAC on the pyca complex is a convenient way to

obtain triazolyl-functionalized iminopyridines, which can be used upon halide abstraction to produce cationic complexes with the triazole ligand acting as (N,N,N) tridentate. When the copper reagent used for the cycloaddition is added in a stoichiometric amount, a triazolyl transfer produces a cationic complex in which the triazolyl ring is C-bonded to Re and N-bonded to Cu. This is an unprecedented coordination mode for the triazolyl ligand. Thus, choosing stoichiometric *vs.* catalytic conditions directs the C or N coordination of the triazole ring. The copper can be extracted with aqueous ammonia, leaving a mononuclear neutral Re complex with the triazolylpropyliminopyridine acting as a (N,N,C) anionic tridentate ligand. Reaction with trimethyloxonium tetrafluoroborate yields a cationic complex in which the triazolylidene ring acts as a mesoionic carbene. To close the cycle, protonolysis of the Re–C-triazolyl produces complexes with uncoordinated or N-coordinated triazole depending on the counter anion used.

This work was funded by the Spanish Ministerio de Ciencia e Innovación (CTQ2009-12111) and Junta de Castilla y León (VA070A08 and GR Excelencia 125). R. G.-R. and C. M. A. wish to thank for a MEC-FPU grant and a Ramón y Cajal contract, and L. A. G.-E. thanks University of Valladolid for a PhD grant.

Notes and references

1 C. W. Tornoe, C. Christensen and M. Meldal, *J. Org. Chem.*, 2002, **67**, 3057.
2 V. V. Rostovstsev, L. G. Green, V. V. Fokin and B. K. Sharpless, *Angew. Chem., Int. Ed.*, 2002, **41**, 2596.
3 For leading references see: M. Meldal and C. W. Tornoe, *Chem. Rev.*, 2008, **108**, 2952; J. E. Hein and V. V. Fokin, *Chem. Soc. Rev.*, 2010, **39**, 1302. For new applications in polymer and materials science: W. H. Binder and R. Sachsenhofer, *Macromol. Rapid Commun.*, 2007, **28**, 15; C. Le Droumaguet, C. Wang and Q. Wang, *Chem. Soc. Rev.*, 2010, **39**, 1233. Supramolecular chemistry: K. Hanni and D. A. Leigh, *Chem. Soc. Rev.*, 2010, **39**, 1240; Y. Hua and A. M. Flood, *Chem. Soc. Rev.*, 2010, **39**, 1262.
4 H. Struthers, T. L. Mindt and R. Schibli, *Dalton Trans.*, 2010, **39**, 675; T. Romero, R. A. Orenes, A. Espinosa, A. Tárraga and P. Molina, *Inorg. Chem.*, 2011, **50**, 8214; G. F. Manbeck, W. W. Brennessel, C. M. Evans and R. Eisenberg, *Inorg. Chem.*, 2010, **49**, 2834; C. Cote and R. U. Kirss, *Inorg. Chim. Acta*, 2010, **363**, 2520; M. Obata, A. Kitamura, A. Mori, C. Kameyama, J. A. Czaplewska, R. Tanaka, I. Kinoshita, T. Kusumoto, H. Hashimoto, M. Harada, Y. Mikata, T. Funabiki and S. Yano, *Dalton Trans.*, 2008, 3292; H. Struthers, B. Spingler, T. L. Mindt and R. Schibli, *Chem.–Eur. J.*, 2008, **14**, 6173; D. V. Partika, J. B. Updegraff III, M. Zeller, A. D. Hunter and T. D. Gray, *Organometallics*, 2007, **26**, 183.
5 D. Urankan, B. Pinter, A. Pevec, F. De Proft, I. Turel and J. Kosmrlj, *Inorg. Chem.*, 2010, **49**, 4820.
6 D. V. Partika, L. Gao, T. S. Teets, J. B. Updegraff III, N. Deligonul and T. G. Gray, *Organometallics*, 2009, **28**, 6171; E. M. Schuster, M. Botoshansky and M. Gandelman, *Angew. Chem., Int. Ed.*, 2008, **47**, 4555; E. M. Schuster, M. Botoshansky and M. Gandelman, *Organometallics*, 2009, **28**, 7001; M. Schuster, G. Nisnevich, M. Botoshansky and M. Gandelman, *Organometallics*, 2009, **28**, 5025; C. Nolte, P. Mayer and B. F. Straub, *Angew. Chem., Int. Ed.*, 2007, **46**, 2101.
7 S. Liu, P. Müller, M. K. Takase and T. M. Swager, *Inorg. Chem.*, 2011, **50**, 7598.
8 M. Paulson, A. Neels and M. Albrecht, *J. Am. Chem. Soc.*, 2008, **130**, 13534; R. Lalrempuia, N. D. McDaniel, H. Müller-Bunz, S. Bernhard and M. Albrecht, *Angew. Chem., Int. Ed.*, 2010, **49**, 9765; A. Poulain, D. Canseco-Rodriguez, R. Hynes-Roche, H. Müller-Bunz, O. Schuster, H. Stoeckli-Evans, A. Neals and M. Albrecht, *Organometallics*, 2011, **30**, 1021; A. Prades, E. Peris and M. Albrecht, *Organometallics*, 2011, **30**, 1162; L. Bernet, R. Lalrempuia, W. Ghattas, H. Müller-Bunz, L. Vigara, A. Llobet and M. Albrecht, *Chem. Commun.*, 2011, **47**, 8058.
9 For the first examples of the C5-bonded imidazole ring see: S. Gründemann, A. Kovacevic, M. Albrecht, J. W. Faller and R. H. Crabtree, *Chem. Commun.*, 2001, 2274; S. Gründemann, A. Kovacevic, M. Albrecht, J. W. Faller and R. H. Crabtree, *J. Am. Chem. Soc.*, 2005, **127**, 16299. For other *a*NHCsB. Schulze, D. Escudero, C. Friebe, R. Siebert, H. Görls, U. Köhn, E. Altuntas, A. Baumgaertel, M. D. Hager, A. Winter, B. Dietzek, J. Popp, L. González and U. S. Schubert, *Chem.–Eur. J.*, 2011, **17**, 5494; D. G. Gusev, *Organometallics*, 2009, **28**, 6458; R. Tonner, G. Frenking, O. Schuster, L. Yang, H. G. Raubenheimer and M. Albrecht, *Chem. Rev.*, 2009, **109**, 3445.
10 K. J. Kilpin, U. S. D. Paul, A.-L. Lee and J. D. Crowley, *Chem. Commun.*, 2011, **47**, 328; T. Nakamura, T. Terashima, K. Ogata and S. Fukuzawa, *Org. Lett.*, 2011, **13**, 620; R. Saravanakumar, V. Ramkumar and S. Sankararaman, *Organometallics*, 2011, **30**, 1689; S. Hohloch, C.-Y. Su and B. Sarkar, *Eur. J. Inorg. Chem.*, 2011, **3067**; S. Inomata, H. Hiroki, T. Terashima, K. Ogata and S. Fukuzuwa, *Tetrahedron*, 2011, **67**, 7263; J. Cai, X. Yang, K. Arumugam, C. W. Bielawski and J. L. Sessler, *Organometallics*, 2011, **30**, 5033; J. Bouffard, B. K. Keitz, R. Tonner, G. Guisado-Barrios, G. Frenking, R. G. Grubbs and G. Bertrand, *Organometallics*, 2011, **30**, 2617; T. Karthikeyan and S. Sankararaman, *Tetrahedron Lett.*, 2009, **50**, 5834.
11 G. Guisado-Barrios, J. Bouffard, B. Donnadieu and G. Bertrand, *Organometallics*, 2011, **30**, 6017; G. Guisado-Barrios, J. Bouffard, B. Donnadieu and G. Bertrand, *Angew. Chem., Int. Ed.*, 2010, **49**, 4759.
12 E. M. Schuster, M. Botoshansky and M. Gandelman, *Dalton Trans.*, 2011, **40**, 8764.
13 For recent reviews, see: M. Melaimi, M. Soleilhavoup and G. Bertrand, *Angew. Chem.*, 2010, **122**, 8992 (*Angew. Chem., Int. Ed.*, 2010, **49**, 8810); S. Díaz-González, N. Marion and S. P. Nolan, *Chem. Rev.*, 2009, **109**, 3612; P. de Frémont, N. Marion and S. P. Nolan, *Coord. Chem. Rev.*, 2009, **253**, 862; F. E. Hahn and M. C. Jahnke, *Angew. Chem.*, 2008, **120**, 3166 (*Angew. Chem., Int. Ed.*, 2008, **47**, 3122).
14 D. Canella, S. J. Hock, O. Hiltner, E. Herdtweck, W. A. Herrmann and F. E. Kuehn, *Dalton Trans.*, 2012, **41**, 2110; M. Brill, J. Díaz, M. A. Huertos, R. López, J. Perez and L. Riera, *Chem.–Eur. J.*, 2011, **17**, 8584; M. Batool, T. A. Martin, M. Abu Naser, M. W. George, S. A. MacGregor, M. F. Mahon and M. K. Whittlesey, *Chem. Commun.*, 2011, **47**, 11225; T. A. Martin, C. E. Ellul, M. F. Mahon, M. E. Warren, D. Allan and M. K. Whittlesey, *Organometallics*, 2011, **30**, 2200; J. Ruiz, L. García, B. F. Perandones and M. Vivanco, *Angew. Chem., Int. Ed.*, 2011, **50**, 3010; M. A. Huertos, J. Perez, L. Riera, J. Díaz and R. López, *Angew. Chem., Int. Ed.*, 2010, **49**, 6409; M. Toganoh, T. Hihara and H. Furuta, *Inorg. Chem.*, 2010, **49**, 8182; M. A. Huertos, J. Perez, L. Riera, J. Diaz and R. Lopez, *Chem.–Eur. J.*, 2010, **16**, 8495; O. Kaufhold, A. Stasch, T. Pape, A. Hepp, P. G. Edwards, P. D. Newman and F. E. Hahn, *J. Am. Chem. Soc.*, 2009, **131**, 306; M. A. Huertos, J. Perez, L. Riera and A. Menendez-Velazquez, *J. Am. Chem. Soc.*, 2008, **130**, 13530; M. A. Huertos, J. Perez and L. Riera, *J. Am. Chem. Soc.*, 2008, **130**, 5662.
15 C. M. Álvarez, R. García-Rodríguez and D. Miguel, *Dalton Trans.*, 2007, 3546.
16 L. A. García-Escudero, D. Miguel and J. A. Turiel, *J. Organomet. Chem.*, 2006, **691**, 3434; C. M. Álvarez, R. Carrillo, R. García-Rodríguez and D. Miguel, *Chem. Commun.*, 2011, **47**, 12765.
17 R. García-Rodríguez and D. Miguel, *Dalton Trans.*, 2006, 1218; C. M. Álvarez, R. García-Rodríguez and D. Miguel, *J. Organomet. Chem.*, 2007, **692**, 5717; C. M. Álvarez, R. García-Rodríguez and D. Miguel, *Inorg. Chem.*, 2012, **51**, 2984.
18 The triazole ring in compound **4** is depicted tentatively as coordinated through the central N2 atom, see ESI† for explanation.
19 M. R. L. Furst and C. S. J. Cazin, *Chem. Commun.*, 2010, **46**, 6924; G. Venkatachalam, M. Heckenroth, A. Neels and M. Albrecht, *Helv. Chim. Acta*, 2009, **92**, 1034.

Electronic Supplementary Material (ESI) for Chemical Communications

Electronic Supporting Information (ESI) for the manuscript

Beyond Click Chemistry: Spontaneus C-triazolyl Transfer from Copper to Rhenium and Transformation into Mesoionic C-triazolylidene Carbene

*Celedonio M. Álvarez, Luis A. García-Escudero, Raúl García-Rodríguez, Daniel Miguel**

Experimental section

General considerations. All operations were performed under an atmosphere of dry nitrogen using Schlenk and vacuum techniques. Dichloromethane and methanol were distilled from CaH_2. THF was distilled from Na/benzophenone. Hexane was distilled from Na. IR spectra in solution were recorded with a Perkin Elmer Spectrum RXI FT–IR instrument, using cells with CaF_2 windows. All NMR solvents were stored over molecular sieves and degassed prior to use. Solution NMR spectra were obtained on a Bruker AC300, Bruker AV-400, Varian MR 400 or a Varian MR 500 spectrometers. Shift values are given in ppm. ^{1}H chemical shifts are referenced to solvents. Elemental analyses were performed on a Perkin-Elmer 2400B CHN analyzer. Reagents were purchased and used without purification unless otherwise stated. 3-Azidopropan-1-amine,[1] *fac*-$[ReBr(CO)_3(pyca)]$ (**1**),[2] were prepared according to the literature procedures.

Synthesis of *fac*-[ReBr(CO)$_3${py-2-CH=N-(CH$_2$)$_3$-N$_3$}] (**2**). Compound **1** (0.200 g, 0.44 mmol) and 3-azidopropan-1-amine (0.044 g, 0.44 mmol) were refluxed in MeOH (25 ml) for 1 h. The solvent was evaporated *in vacuo*, and the resulting solid residue was dissolved in CH_2Cl_2 and filtered through kieselguhr. Addition of hexane and slow evaporation at reduced pressure gave compound **2** as orange microcrystals. Yield: 0.220 g, 93%. Anal. Calc. for $C_{12}H_{11}BrN_5O_3Re$: C, 26.72; H, 2.06; N, 12.98. Found: C, 27.03; H, 2.12; N, 13.22. IR (CH_2Cl_2, cm^{-1}), ν(N_3): 2105 (w); ν(CO): 2026 (vs), 1927 (s), 1903 (s). ^{1}H NMR (300 MHz, acetone-d_6, 298K): δ 9.24 (s, 1H, C*H*=N), 9.11 (d, J^3 = 5.5 Hz, 1H, py), 8.34-8.28 (m, 2H, py), 7.83 (m, 1H, py), 4.29 (t, J^3 = 6.5 Hz, 2H, CH_2), 3.58 (t, J^3 = 6.5 Hz, 2H, CH_2), 2.34 (m, 2H, $CH_2CH_2CH_2$).

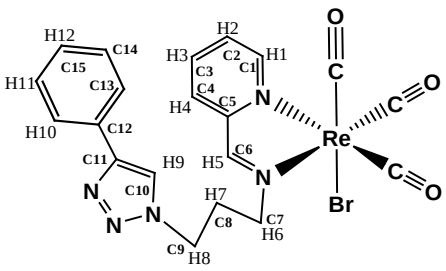

Synthesis of 3. *Method A.* A mixture of **2** (0.100 g, 0.19 mmol), phenylacetylene (0.019 g, 0.19 mmol), $CuSO_4.5H_2O$ (0.005 g, 0.02 mmol) and sodium ascorbate (0.004 g, 0.02 mmol) were reacted in 4:1 THF:water (20 ml) at room temperature for 5 days. The compound was extracted with CH_2Cl_2 (3 × 15 mL), dried over magnesium sulfate, filtered and evaporated to a red precipitate. The resulting solid residue was dissolved in CH_2Cl_2 and addition of hexane and slow evaporation at reduced pressure gave compound **3** as red microcrystals. Yield: 0.095 g, 80 %. *Method B.* To a flask containing **6** (0.067 g, 0.12 mmol) in THF (15 ml) was added concentrated aqueous hydrobromic acid (0.05 ml, excess). The reaction mixture was stirred for 2 hours at reflux temperature. The solvent was evaporated *in vacuo*, and the resulting solid residue was dissolved in CH_2Cl_2. The solution was stirred with solid Na_2CO_3 (0.5 g) to neutralize the excess acid and to ensuring deprotonation of the triazole ring, dried over magnesium sulphate and filtered. Addition of hexane and slow evaporation at reduced pressure gave compound **3** as orange microcrystals. Yield: 0.072 g, 94%. Anal. Calc. for

[1] V. Novakova, P. Zimcik, M. Miletin, K. Kopecky, J. Ivincova, *Tetrahedron Lett.* **2010**, *51*, 1016–1018.

[2] C. M. Álvarez, R. García-Rodríguez, D. Miguel, *Dalton Trans.* **2007**, 3546–3554.

$C_{20}H_{17}BrN_5O_3Re$: C, 37.45; H, 2.67; N, 10.92. Found: C, 37.56; H, 2.60; N, 11.01. IR (CH_2Cl_2, cm^{-1}), ν(CO): 2026 (vs), 1926 (s), 1904 (s). ^{1}H NMR (500 MHz, acetone-d_6, 298K): δ 9.22 (s, 1H, H5), 9.12 (d, J^3 = 5.0 Hz, 1H, H1), 8.45 (s, 1H, H9), 8.35-8.30 (m, 2H, H3 and H4), 7.88 (d, J^3 = 7.5 Hz, 2H, H10), 7.83 (m, 1H, H2), 7.43 (t, J^3 = 7.5 Hz, 2H, H11), 7.33 (t, J^3 = 7.5 Hz, 1H, H12), 4.76-4.61 (m, 2H, H8), 4.34-4.26 (m, 2H, H6), 2.81 (m, 1H, H7), 2.70 (m, 1H, H7). ^{13}C {^{1}H} NMR (125 MHz, acetone-d_6, 298 K): δ 197.2 (CO), 196.9 (CO), 186.8 (CO), 170.0 (C6), 155.2 (C5), 153.2 (C1), 147.2 (C11), 140.0 (C3 or C4), 131.3 (C12), 129.2 (C4 or C3), 128.9 (C2), 128.7 (C14), 127.7 (C15), 125.3 (C13), 120.8 (C10), 62.2 (C7), 47.1 (C9), 30.1 (C8).

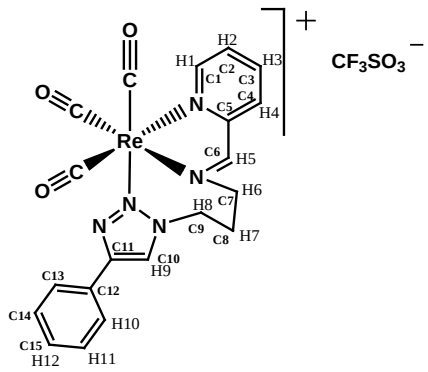

Synthesis of 4. *Method A.* To a flask containing **3** (0.070 g, 0.11 mmol) in CH_2Cl_2 (20 ml) was added AgOTf (0.028 g, 0.11 mmol). The reaction mixture was stirred for 4 hours at room temperature, and the AgBr precipitate was removed by filtration. Addition of hexane and slow evaporation at reduced pressure gave compound **4** as yellow microcrystals. Yield: 0.064 g, 83 %. *Method B.* To a flask containing **6** (0.067 g, 0.12 mmol) in THF (15 ml) was added trifluoromethanesulfonic acid (0.05 ml, excess). The reaction mixture was heated for 4 hours at reflux temperature. The solvent was evaporated *in vacuo*, and the resulting solid residue was dissolved in CH_2Cl_2. The solution was stirred with solid Na_2CO_3 (0.5 g) to neutralize the excess acid and to ensuring deprotonation of the triazole ring, dried over magnesium sulphate and filtered. Addition of hexane and slow evaporation at reduced pressure gave compound **4** as orange microcrystals. Yield: 0.077 g, 90%. Anal. Calc. for $C_{21}H_{17}N_5O_6F_3SRe$: C, 35.49; H, 2.41; N, 9.85. Found: C, 35.49; H, 2.50; N, 9.77. IR (CH_2Cl_2, cm^{-1}), ν(CO): 2038 (vs), 1936 (s), 1922 (s). ^{1}H NMR (500 MHz, acetone-d_6, 298K): δ 9.47 (d, J^3 = 5.5 Hz, 1H, H1), 9.35 (s, 1H, H5), 8.83 (s, 1H, H9), 8.40-8.36 (m, 1H, H3), 8.21 (d, J^3 = 5.5 Hz, H4), 8.07-8.03 (m, 1H, H2), 7.69-7.65 (m, 2H, H10), 7.43-7.34 (m, 3H, H11 and H12), 5.30-5.16 (m, 2H, H8), 4.93-4.86 (m, 1H, H6), 4.83-4.75 (m, 1H, H6), 2.89-2.81 (m, 1H, H7), 2.48-2.36 (m, 1H, H7). ^{13}C {^{1}H} NMR (125 MHz, acetone-d_6, 298 K): δ 195.7 (CO), 194.5 (CO), 190.0 (CO), 174.3 (C6), 155.3 (C5), 154.3 (C1), 148.3 (C11), 141.4 (C3), 130.3 (C2), 129.2 (C4), 129.1 (C15), 129.0 (C14), 128.6 (C12), 127.3 (C10), 125.4 (C13), 64.1 (C9), 51.7 (C7), 32.6 (C8).

The triazole ring in compound **4** is depicted tentatively as coordinated through the central N2 atom, whereas in compound **5** it is found to be coordinated through N3. An inspection with molecular models showed that coordination through N3 in **4** would lead to a highly tensioned arrangement. On the other hand, coordination through the central N2 have been found in related complexes with triazole tethered through N1 (see compounds in ref 5) while coordination through N3 is usually found in triazole tethered through one of the carbon atoms. Unfortunately, despite many attempts, it has not been possible to grow a crystal of **4** suitable for X-ray crystallography.

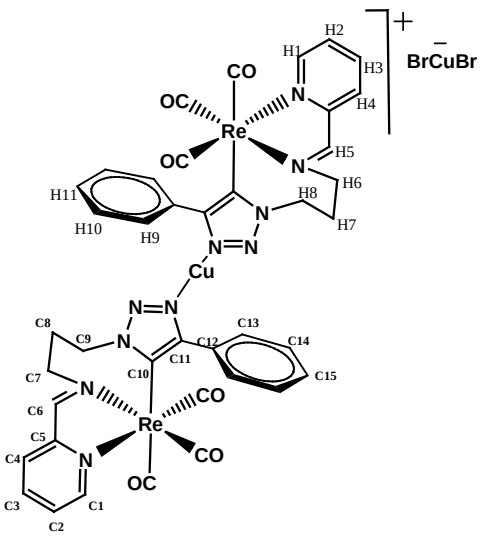

Synthesis of 5. *Method A.* A mixture of **2** (0.100 g, 0.18 mmol), phenylacetylene (0.023 g, 0.22 mmol), $CuSO_4.5H_2O$ (0.055 g, 0.22 mmol) and sodium ascorbate (0.043 g, 0.22 mmol) were reacted in 4:1 THF:water (25 ml) at reflux temperature for 1 hour. The compound was extracted with CH_2Cl_2 (3 × 25 ml), dried over magnesium sulphate, filtered and evaporated to an orange precipitate. The resulting solid residue was dissolved in CH_2Cl_2 and addition of hexane and slow diffusion gave compound **5** as yellow-orange microcrystals. Yield: 0.089 g, 79%. *Method B.* A mixture of **1** (0.050 g, 0.11 mmol), and 3-azidopropan-1-amine (0.011 g, 0.11 mmol), was refluxed in THF (20 ml). IR monitoring showed the formation of **2** after 2h. To the solution were then added phenylacetylene (0.014 g, 0.13 mmol), $CuSO_4.5H_2O$ (0.032 g, 0.13 mmol), sodium ascorbate (0.026 g, 0.13 mmol) and water (5 ml) and the mixture was heated at reflux temperature for 1 hour and then evaporated under vacuum. The orange residue was extracted with CH_2Cl_2 (3 × 15 ml) and dried over magnesium sulphate. Addition of hexane and slow evaporation gave compound **5** as yellow-orange microcrystals. Yield: 0.050 g, 72%. Anal. Calc. for $C_{28}H_{22}Cu_2Br_2N_{10}O_6Re_2$: C, 26.82; H, 1.77; N, 11.17. Found: C, 26.96; H, 1.83; N, 11.27. IR (CH_2Cl_2, cm^{-1}), ν(CO): 2017 (vs), 1921 (s), 1904 (s). ^{1}H NMR (300 MHz, acetone-d_6, 298K): δ 9.00 (s, 1H, H5), 8.06-7.99 (m, 2H, H3 and H4), 7.97 (d, J^3 = 5,5 Hz, 1H, H1), 7.40 (t, J^3 = 7.0 Hz, 1H, H11), 7.28 (t, J^3 = 7.0 Hz, 2H, H10), 7.12 (d, J^3 = 7.0 Hz, 2H, H9),7.09-7.05 (m, 1H, H2), 5.15-4.98 (m, 2H, H8), 4.75-4.58 (m, 2H, H6), 2.74-2.55 (m, 1H, H7) 2.05-1.96 (m, 1H, H7). ^{13}C {^{1}H} NMR (125 MHz, acetone-d_6, 298 K): δ 200.4 (CO), 198.6 (CO), 191.6 (CO), 170.2 (C6), 155.5 (C12), 155.4 (C5), 153.9 (C1), 153.8 (C10), 139.7 (C3 or C4), 135.8 (C11), 130.7 (C13), 129.5 (C4 or C3), 129.1 (C14), 128.7 (C2), 128.5 (C15), 65.5 (C7), 52.0 (C9), 35.2 (C8).

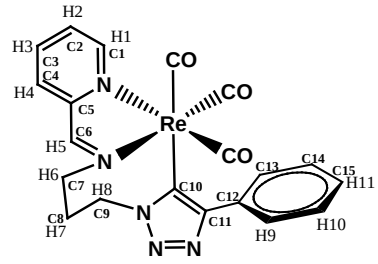

Synthesis of 6. To a flask containing **5** (0.100 g, 0.18 mmol) in CH_2Cl_2 (15 mL) was added concentrated ammonia solution (10 ml). The reaction mixture was stirred for 3 hours at room temperature. The compound was extracted with CH_2Cl_2 (3 × 10 ml), the organic layers were combined, dried over magnesium sulphate and filtered. Addition of hexane and slow evaporation at reduced pressure gave compound **6** as orange microcrystals. Yield: 0.084 g, 94%. Anal. Calc. for $C_{20}H_{16}N_5O_3Re$: C, 42.85; H, 2.88; N, 12.49. Found: C, 43.00; H, 2.80; N, 12.54. IR (CH_2Cl_2, cm^{-1}), ν(CO): 2012 (vs), 1912 (s), 1899 (s). ^{1}H NMR (500 MHz, acetone-d_6, 298K): δ 8.91 (s, 1H, H5), 8.00 (d, J^3 = 5.5 Hz, 1H, H1), 7.98-7.91 (m, 2H, H3 and H4), 7.29-7.24 (m, 1H, H11), 7.22-7.17 (m, 2H, H10), 7.15-7.11 (m, 2H, H9), 7.00-6.95 (m, 1H, H2), 5.00-4.90 (m, 2H, H8), 4.67-4.55 (m, 2H, H6), 2.63-2.55 (m, 1H, H7), 2.01-1.91 (m, 1H, H7). ^{13}C {^{1}H} NMR (125 MHz, acetone-d_6, 298 K): δ 201.2 (CO), 199.3 (CO), 191.8 (CO), 169.5 (C6), 156.2 (C12), 155.4 (C5), 153.8 (C1), 153.5 (C10), 139.4 (C3 or C4), 138.6 (C11), 130.3 (C13), 129.1 (C4 or C3), 128.5 (C14), 127.9 (C2), 127.1 (C15), 65.5 (C7), 50.7 (C9), 35.7 (C8).

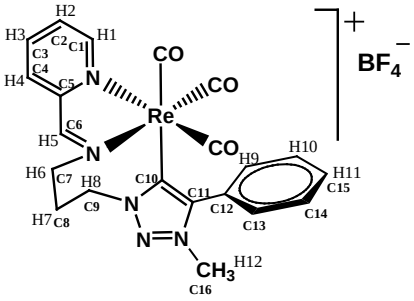

Synthesis of 7. To a flask containing **6** (0.067 g, 0.12 mmol) in CH_2Cl_2 (15 ml) was added trimethyloxonium tetrafluoroborate. (0.018 g, 0.12 mmol). The reaction mixture was stirred for 15 minutes at room temperature. Addition of hexane and slow evaporation at reduced pressure gave compound **7** as orange microcrystals. Yield: 0.070 g, 89%. Anal. Calc. for $C_{21}H_{19}BF_4N_5O_3Re$: C, 38.08; H, 2.89; N, 10.57. Found: C, 38.12; H, 2.83; N, 10.67. IR (CH_2Cl_2, cm^{-1}), ν(CO): 2023 (vs), 1923 (s), 1905 (s). ^1H NMR (500 MHz, CD_2Cl_2, 298K): δ 8.84 (s, 1H, H5), 8.01 (d, J^3 = 7.5 Hz, 1H, H4), 7.89 (td, J^3 = 7.5 Hz and J^4 = 1.5 Hz, 1H, H3), 7.67 (d, J^3 = 5.5 Hz, 1H, H1), 7.54 (t, J^3 = 7.5 Hz, 1H, H11), 7.51-7.23 (s, br, 4H, H9 and H10), 6.92-6.87 (m, 1H, H2), 5.21-5.13 (m, 1H, H8), 5.03-4.95 (m, 1H, H8), 4.63-4.47 (m, 1H, H6), 3.71 (s, 3H, H12) 2.61-2.32 (m, 2H, H7). ^{13}C {^1H} NMR (125 MHz, CD_2Cl_2, 298 K): δ 198.3 (CO), 196.9 (CO), 190.1 (CO), 171.2 (C6), 162.1 (C10), 155.2 (C5), 152.5 (C1), 148.9 (C11), 138.9 (C3), 130.6 (C15), 130.0 (C4), 129.43 (C13 and C14), 128.0 (C2), 127.2 (C12), 64.7 (C7), 53.9 (C9), 36.8 (C16), 32.8 (C8).

Crystallographic data of compounds 2, 5, 6, and 7.

Intensities measurements for **2**, **6**, and **7** were made with a Oxford Diffraction Super Nova diffractometer with graphite monochromatized Mo Kα X-radiation and a CCD area detector. Compound Data collection and integration, and phase indexing absorption corection were done with the program CrysAlisPro.[3] The crystal of **5** was measured with a Bruker AXS SMART 1000 diffractometer with graphite monochromatized Mo Kα X-radiation and a CCD area detector. Raw frame data were integrated with the SAINT program.[4] A semi-empirical absorption correction was applied with the program SADABS.[5]

The structures were solved by direct methods with SIR2002,[6] under WINGX,[7] and refined against F^2 with SHELXTL.[8] All non-hydrogen atoms were refined anisotropically unless otherwise stated. Calculations were made with SHELXTL and PARST,[9] and graphics were made with SHELXTL and MERCURY.[10]

[3] CrysAlisPro-Data collection and integration software. Oxford Diffraction Ltd. **2009**.
[4] SAINT+. SAX area detector integration program. Version 6.02. Bruker AXS, Inc. Madison, WI, 1999.
[5] G. M. Sheldrick, SADABS, Empirical Absorption Correction Program. University of Göttingen: Göttingen, Germany, 1997.
[6] Burla, M. C.; Camalli, M.; Carrozzini, B.; Cascarano, G. L.; Giacovazzo, C.; Polidory, G.; Spagna, R. *SIR2002, A program for automatic solution and refinement of crystal structures. J. Appl. Cryst.* **2003**, *36*, 1103.
[7] Farrugia, L.J. *J. Appl. Cryst.*, **1999**, *32*, 837-838.
[8] Sheldrick G. M *Acta Cryst.* **2008**, *A64*, 112-122. Sheldrick, G. M. SHELXTL, An integrated system for solving, refining, and displaying crystal structures from diffraction data. Version 5.1. Bruker AXS, Inc. Madison, WI, **1998**.
[9] *(a)* Nardelli, M. *Comput. Chem.*, 1983, **7**, 95-97. *(b)* Nardelli, M. *J. Appl. Crystallogr.*, **1995**, *28*, 659.
[10] MERCURY: a) Bruno, I. J.; Cole, J. C.; Edgington, P. R.; Kessler, M. K.; Macrae, C. F.; McCabe, P.; Pearson, J.; Taylor, R. *Acta Crystallogr*., 2002, **B58**, 389-397. b) Macrae, C. F.; Edgington, P. R.; McCabe, P.; Pidcock, E.; Shields, G. P.; Taylor, R.; Towler, M.; van de Streek, J. *J. Appl. Crystallogr.*, **2006**, *39*, 453-457.

Table S1. Crystallographic data for compounds 2, 5, 6 and 7.

Compound reference	Compound 2	Compound 5	Compound 6	Compound 7
Chemical formula	$C_{12}H_{11}BrN_5O_3Re$	$C_{20}H_{16}BrCuN_5O_3Re$	$C_{20}H_{16}N_5O_3Re$	$C_{22}H_{21}BCl_2F_4N_5O_3Re$
Formula Mass	539.37	704.03	560.58	747.35
Crystal system	Monoclinic	Triclinic	Triclinic	Monoclinic
a/Å	13.9080(11)	8.833(4)	7.2895(5)	33.0420(7)
b/Å	9.1333(5)	9.312(4)	9.7173(7)	13.0010(2)
c/Å	13.1805(7)	14.440(7)	15.3974(10)	27.7310(7)
α/°	90.00	71.824(9)	73.505(6)	90.00
β/°	101.093(6)	77.963(9)	86.389(5)	113.570(3)
γ/°	90.00	78.790(10)	70.454(6)	90.00
Unit cell volume/Å^3	1642.99(18)	1092.9(9)	984.90(11)	10918.8(4)
Temperature/K	293(2)	298(2)	293(2)	293(2)
Space group	$P2_1/c$	$P\bar{1}$	$P\bar{1}$	$C2/c$
No. of formula units per unit cell, *Z*	4	2	2	16
No. of reflections measured	8215	5006	6327	21036
No. of independent reflections	3863	3106	3906	10871
R_{int}	0.0459	0.0697	0.0422	0.0328
Final R_1 values ($I > 2\sigma(I)$)	0.0455	0.0734	0.0393	0.0456
Final $wR(F^2)$ values ($I > 2\sigma(I)$)	0.0917	0.1618	0.0931	0.1157
Final R_1 values (all data)	0.0650	0.1302	0.0439	0.0670
Final $wR(F^2)$ values (all data)	0.1061	0.1890	0.0984	0.1310
Goodness of fit on F^2	1.040	0.981	1.083	1.046
CCDC number	867717	867718	867719	867720

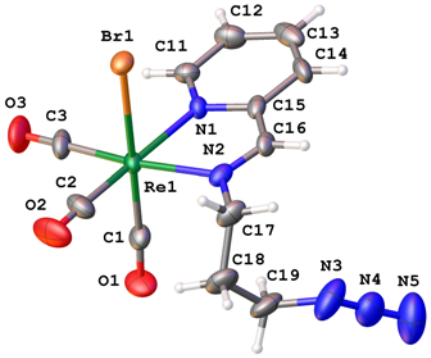

Figure S1. Perspective view of **2**, showing the atom numbering.

ANEXOS

Artículo VI.

Carbonyl complexes of manganese, rhenium and molybdenum with ethynyliminopyridine ligands.

Available online at www.sciencedirect.com
SCIENCE DIRECT
Journal of Organometallic Chemistry 691 (2006) 3434–3444
Journal of Organometallic Chemistry
www.elsevier.com/locate/jorganchem

Carbonyl complexes of manganese, rhenium and molybdenum with ethynyliminopyridine ligands

Luis A. García-Escudero, Daniel Miguel *, José A. Turiel

Quimica Inorgánica, Facultad de Ciencias, Universidad de Valladolid, C/ Prado de la Magdalena s/n, E-47071 Valladolid, Spain

Received 21 December 2005; received in revised form 21 April 2006; accepted 21 April 2006
Available online 29 April 2006

Dedicated to Prof. Víctor Riera on the occasion of his 70th birthday.

Abstract

[$MBr(CO)_5$] reacts with *m*-ethynylphenylamine and pyridine-2-carboxaldehyde in refluxing tetrahydrofuran to give, *fac*-[$MBr(CO)_3$(py-2-CH=N-C_6H_4-*m*-(C≡CH))] (M = Mn, **1a**; Re, **2a**). The same method affords the tetracarbonyl [$Mo(CO)_4${py-2-CH=N-C_6H_4-*m*-(C≡CH)}] (**3a**) starting from [$Mo(CO)_4$(piperidine)$_2$]; and the methallyl complex [$MoCl(\eta^3$-C_3H_4Me-2)$(CO)_2${py-2-CH=N-C_6H_4-*m*-(C≡CH)}] (**4a**) from [$MoCl(\eta^3$-C_3H_4Me-2)$(CO)_2(NCMe)_2$]. The use of *p*-ethynylphenylamine gives the corresponding derivatives (**1b**, **2b**, **3b**, and **4b**) with the ethynyl substituent in the *para*-position at the phenyl ring of the iminopyridine. All complexes have been isolated as crystalline solids and characterized by analytical and spectroscopic methods. X-ray determinations, carried out on crystals of **1a**, **1b**, **2a**, **2b**, **3b**, **4a**, and **4b**, reveals the same structural type for all compounds with small variations due mainly to the different size of the metal atoms. The reaction of complexes **1a** or **2a** with dicobalt octacarbonyl affords the tetrahedrane complexes [$MBr(CO)_3${py-2-CH=N-C_6H_4-*m*-{(μ-C≡CH)$Co_2(CO)_6$}}] (M = Mn, **5**; Re, **6**), the structures of which have been confirmed by an X-ray determination on a crystal of compound **5**.

Keywords: Ethynyliminopyridines; Carbonyl complexes; π-acetylene

1. Introduction

Complexes with diimine ligands are object of current interest because of their potentially useful electrochemical, spectroscopic or photochemical properties [1]. Among these, iminopyridines derived from the condensation of pyridine-2-carboxaldehyde with a primary amine are attractive because of their electronic properties which are intermediate between those of the more classic, ubiquitous bipyridine or phenanthroline [2], and the more flexible diazabutadienes [3]. Imino pyridines have been employed recently as multidentate ligands [4], and to prepare polynuclear complexes [5]. There is also interest in the use of iminopyridine ligands having additional functions such as ester [6] or hydroxo [7], capable to anchor them to polymers [8] or biological molecules [9]. On the other hand, more classic complexes of Mn(II), Ni (II) and Fe(II) and other cations with functionalized iminopyridines have been reported to exhibit very interesting properties such as spin crossover [10], second order non-linear optical properties [11], luminescence [12], or mesogenic behavior [13]. Complexes of ions having d^6 configuration such as Mn(I), Re(I) or Mo(0); or d^4, such as Mo(II) containing chelate N-donors such as bipy or phen have proved to undergo interesting reactivity in insertion of unsaturated molecules into metal alcoxo and metal-amido bonds [14]. We considered interesting to explore the chemistry of these metals with iminopyridines, and we have reported recently the preparation of molybdenum complexes with chelating iminopyridines bearing an additional carboxylate function

* Corresponding author. Tel.: +34 983 184096; fax: +34 983 423013.
E-mail address: dmsj@qi.uva.es (D. Miguel).

0022-328X/$ - see front matter © 2006 Elsevier B.V. All rights reserved.
doi:10.1016/j.jorganchem.2006.04.024

capable to establish supramolecular interactions in the solid state [15]. The availability of commercial *meta*- and *para*-ethynylanilines prompted us to explore its use to introduce an additional ethynyl function. We report here the preparation of Mn, Re, and Mo complexes containing iminopyridine ligands functionalized with an additional ethynyl group, and their reactivity towards dicobalt octacarbonyl.

2. Results and discussion

Manganese and rhenium complexes containing *meta*-ethynyl-phenyliminopyridine ligands were obtained by one-pot reactions by heating $[M(CO)_5Br]$ (M = Mn, Re) with equimolar quantities of pyridine-2-carboxaldehyde and *m*-ethynylphenylamine in THF at reflux temperature (Scheme 1).

After workup, complexes *fac*-$[M(CO)_3\{py\text{-}2\text{-}CH{=}NC_6H_4\ m\text{-}(C{\equiv}CH)\}]$ [M = Mn (**1a**), Re (**2a**)] were isolated as red solids in good yields (see Section 3). Similarly, the tetracarbonyl complex $[Mo(CO)_4\{py\text{-}2\text{-}CH{=}NC_6H_4\text{-}m\text{-}(C{\equiv}CH)\}]$ (**3a** in Scheme 1) can be obtained from $[Mo(CO)_4(pip)_2]$ via replacement of two piperidine ligands; and the dicarbonyl complex $[Mo(CO)_2Cl(\eta^3\text{-}C_3H_4\text{-}Me\text{-}2)\{py\text{-}2\text{-}CH{=}NC_6H_4\text{-}m\text{-}(C{\equiv}CH)\}]$ (**4a** in Scheme 1) by substitution of two acetonitrile ligands from $[MoCl(\eta^3\text{-}C_3H_4\text{-}Me\text{-}2)(NCMe)_2]$. Starting from *p*-ethynylaniline, the same method afforded the corresponding compounds **1b**, **2b**, **3b** and **4b**, containing *p*-ethynyliminopyridine, as summarized in Scheme 1.

The new complexes were characterized by analytical and spectroscopic methods and their structures were determined by X-ray crystallography for **1a**–**b**, **2a**–**b**, **3b**, and **4a**–**b**. Crystal data and refinement details are collected in Table 1, and thermal ellipsoid plots are presented in Figs. 1–4.

Table 2 summarizes the relevant distances and angles for all complexes together for a better comparison. Bromotricarbonyl compounds **1a** (M = Mn) and **2a** (M = Re) bearing 3-ethynylphenyliminopyridine are isostructural, as can be noticed from the plots in Fig. 1, and from the geometrical parameters in Table 2.

The same occurs to the pair **1b** and **2b** containing *p*-ethynylphenyliminopyridine (see Fig. 2). In fact the coordination environments of the metals in the four complexes are quite similar. The main distortion from the ideal octahedral geometry arises from the small bite angle N(1)–M–N(2) of the iminopyridine which falls in the range 74.5(2)–78.47(16)°. They all display the expected *facial*-tricarbonyl arrangement, with the chelate iminopyridine and bromo ligands in the opposite face of the octahedron. This geometry derives from the *cis*-labilization effect of Br directing the substitution of carbonyl ligands from $[MnBr(CO)_5]$ [16].

The structure of the tetracarbonyl molybdenum complex **3b** (Fig. 3) is very close to those of the tricarbonyls **1a**–**b** and **2a**–**b**, with the Mo atom in an octahedral environment in which the main distortion is again the small bite angle of the iminopyridine ligand [72.48(7)°]. Methallyldicarbonyl molybdenum complexes **4a**–**b** display pseudooctahedral coordination geometry, with the distortions imposed by the diimine and the methallyl ligands (Fig. 4).

There is a consistent and significant variation of the M–X, M–N, and M–C distances on passing from Mn to Re and (where applicable) to Mo complexes. This pattern has been observed for other families of complexes [17], and correlates well with the size of the metal center, estimated from their metallic radii (Mn 1.18 Å, Re 1.28 Å, Mo 1.30 Å [18]).

The spectroscopic properties of the complexes in solution correlate well with their solid state structures. IR spectra in dichloromethane display (see Table 3) the expected patterns of three active *ν*(CO) normal modes for the tricarbonyls **1a**–**b**, and **2a**–**b**; four active *ν*(CO) normal modes for the tetracarbonyls **3a**–**b**, and two active *ν*(CO) normal modes for the dicarbonyls **4a**–**b** [19].

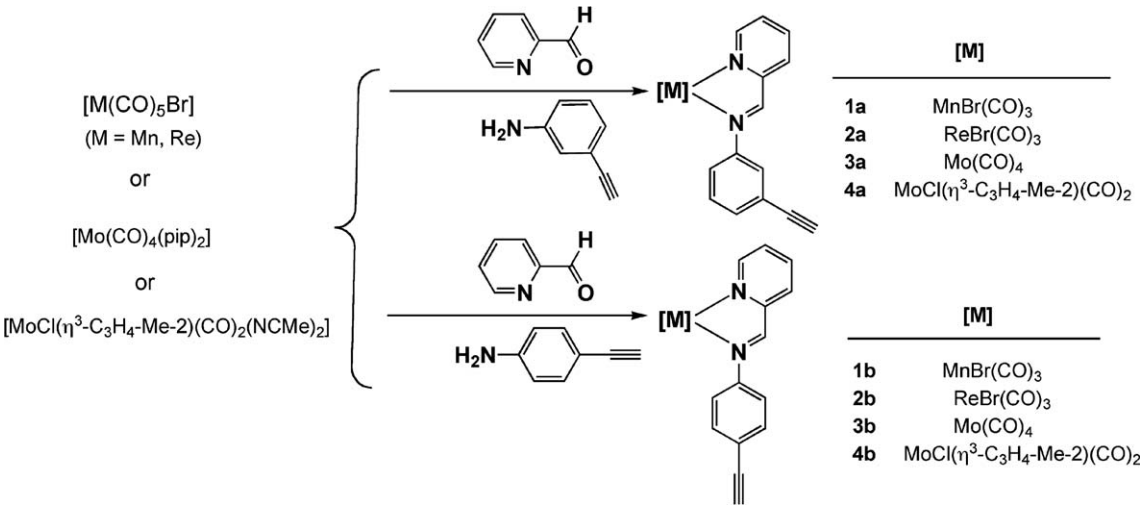

Scheme 1.

Table 1
Crystal data and refinement details for **1a**, **1b**, **2a**, and **2b**; **3b**, **4a**, **4b** and **5**

	1a	**1b**	**2a**	**2b**	**3b**	**4a**	**4b**	**5**
Empirical formula	$C_{17}H_{10}BrMnN_2O_3$ 0.5 CH_2Cl_2	$C_{17}H_{10}BrMn$ N_2O_3	$C_{17}H_{10}BrReN_2O_3$. 0.5 CH_2Cl_2	$C_{17}H_{10}BrN_2O_3Re$	$C_{18}H_{10}MoN_2O_4$	$C_{20}H_{17}ClMoN_2O_2$. CH_2Cl_2	$C_{20}H_{17}ClMoN_2O_2$	$C_{27}H_{18}BrMn$ $Co_2N_2O_{10}$
Formula weight	467.58	425.12	598.84	556.38	414.22	533.67	448.75	783.14
Crystal system	Triclinic	Triclinic	Triclinic	Triclinic	Monoclinic	Monoclinic	Triclinic	Triclinic
Space group	$P\bar{1}$	$P\bar{1}$	$P\bar{1}$	$P\bar{1}$	$P2(1)/c$	$P2(1)/n$	$P\bar{1}$	$P\bar{1}$
a (Å)	9.192(7)	8.964(3)	9.154(5)	9.034(5)	9.782(2)	11.4078(17)	8.011(4)	11.253(7)
b (Å)	9.388(7)	9.120(4)	9.461(5)	9.050(5)	10.657(2)	14.508(2)	11.384(5)	12.026(8)
c (Å)	12.477(10)	10.883(4)	12.556(6)	10.800(6)	17.011(3)	14.154(2)	12.254(6)	12.243(8)
α (°)	68.28(1)	82.172(7)	68.841(8)	75.537(9)	90	90	62.951(8)	83.856(11)
β (°)	73.35(1)	74.695(6)	72.998(9)	83.16(1)	103.023(4)	102.665(3)	82.117(9)	89.404(12)
γ (°)	81.80(2)	86.211(7)	83.020(9)	86.21(1)	90	90	77.247(8)	71.855(13)
V Å^3	957.5(13)	849.7(5)	969.6(8)	848.4(8)	1727.8(6)	2285.5(6)	969.8(8)	1565.0(17)
Z	2	2	2	2	4	4	2	2
T (K)	296(2)	296(2)	293(2)	293(2)	296(2)	296(2)	293(2)	296(2)
D_{calc} (g cm^{-3})	1.622	1.662	2.051	2.178	1.592	1.551	1.537	1.662
F(000)	462	420	562	520	824	1072	452	776
λ(Mo Kα) (Å)	0.71073	0.71073	0.71073	0.71073	0.71073	0.71073	0.71073	0.71073
Crystal size (mm); color	0.07 × 0.11 × 0.23; orange-red	0.14 × 0.06 × 0.05; red	0.19 × 0.10 × 0.05; red	0.16 × 0.09 × 0.05; red	0.13 × 0.19 × 0.34; dark red	0.23 × 0.19 × 0.09; black	0.27 × 0.17 × 0.12; black	0.45 × 0.14 × 0.07; dark red
μ(Mo Kα) (mm^{-1})	2.933	3.144	8.482	9.533	0.783	0.944	0.830	2.776
Collection range (°)	$1.82 \leqslant \theta \leqslant 23.33$	$1.96 \leqslant \theta \leqslant 23.32$	$1.81 \leqslant \theta \leqslant 23.35$	$1.96 \leqslant \theta \leqslant 23.28$	$2.14 \leqslant \theta \leqslant 23.26$	$2.04 \leqslant \theta \leqslant 23.29$	$1.87 \leqslant \theta \leqslant 23.37$	$1.79 \leqslant \theta \leqslant 23.47$
Correction factors (SADABS) min/max	0.5803	0.6940	0.6137	0.5662	0.7120	0.827023	0.7741	0.587066
Reflections collected	4275	3895	4415	3875	7208	9913	4352	7110
Independent reflections [R_{int}]	2696 [0.0237]	2433 [0.0694]	2793 [0.0233]	2403 [0.0465]	2460 [0.0196]	3287 [0.0294]	2755 [0.0152]	4506 [0.0169]
Reflections observed, $I > 2\sigma(I)$	2007	1026	2406	1696	2235	2544	2496	3568
GOF on F^2	1.010	0.843	1.010	1.016	1.068	1.012	1.046	1.007
Number of parameters	241	217	226	217	227	263	236	388
Residuals R, wR_2(all)	0.0453, 0.1215	0.0583, 0.0786	0.0326, 0.0760	0.0516, 0.1004	0.0218, 0.0583	0.0369, 0.0937	0.0233, 0.0641	0.0334, 0.0933

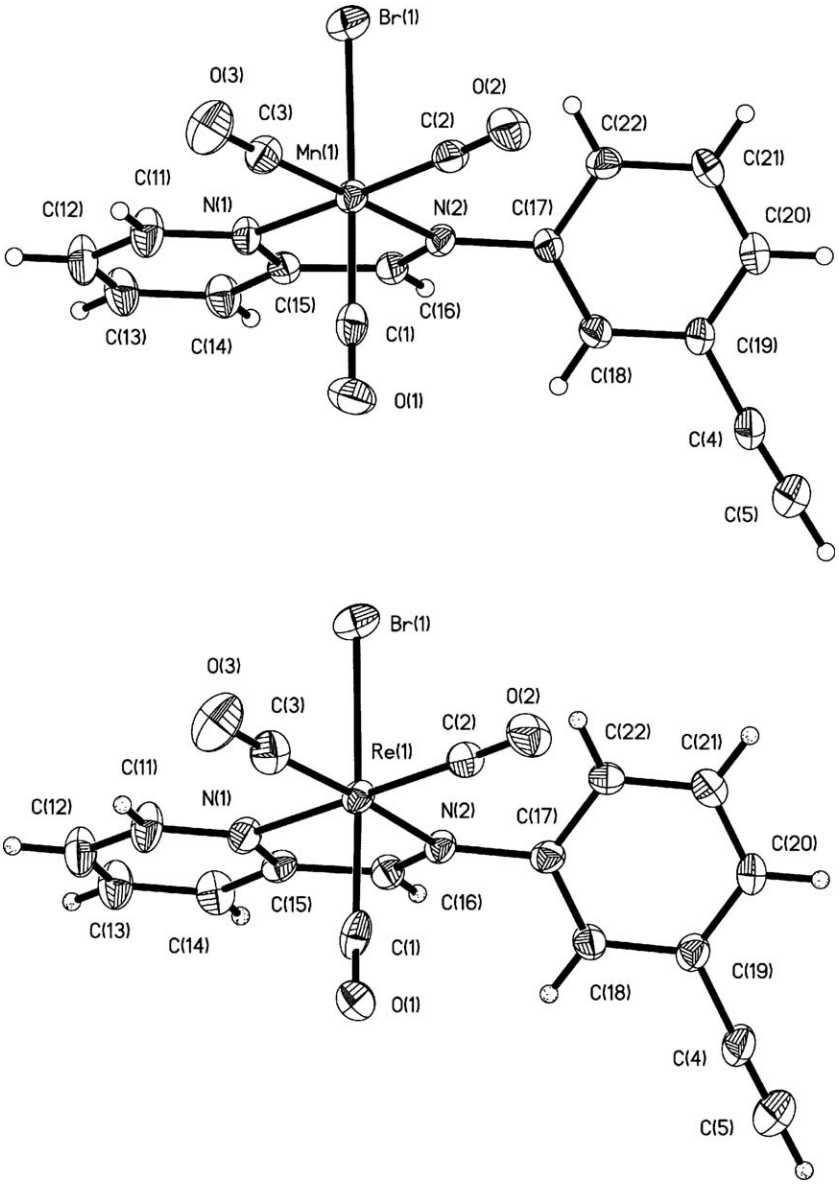

Fig. 1. ORTEP plot (30% ellipsoid probability) of compounds **1a** (above) and **2a** (below) showing the atom numbering.

As it can be seen in Table 3, the ν(CO) bands appear very close (within 1 cm^{-1}) for each pair of complexes containing the ethynyl group in *meta*- or *para*-position. Moreover, there is a very small change when compared with the corresponding complexes such as [$MBr(CO)_3$(pyCH=N-C_6H_4-*p*-CH_3)] containing a methyl group in *para*-. On the other hand, the position of the ν(CO) bands is shifted slightly but consistently to higher energy on passing from bipy (or phen) [20] to iminopyridine complexes.

In the ^{1}H NMR spectra in acetone-d_6, the signal of the imine proton appears for all complexes as an easily identifiable singlet in the range δ 9.34–8.55 ppm, shifted upfield from the signal of the starting aldehyde at δ 9.99 ppm, while the terminal acetylene proton appears as a singlet in the range δ 3.79–3.83 ppm.

The ^{1}H NMR spectra in solution of complexes **4a**–**b** in solution are consistent with the solid state structure depicted for them in Fig. 4. The usual disposition of the allyl and chloride ligands on opposite sides of the equatorial plane defined by the two carbonyls and the two nitrogen atoms [21], with the open face of the allyl ligand directed towards the two carbonyls, is maintained in solution, and thus the *syn* protons of the allyl terminus exhibit two different signals coupled to each other. Two separate signals are also observed for the *anti* protons which are also inequivalent. This implies that the inequivalency of the two allyl *termini* is maintained in solution at room temperature. Nevertheless this would be compatible with the existence of a trigonal twist involving the "triangular" face formed by the η^3-methallyl and the two carbonyls [22]. This concerted rotation would maintain the relative orientation of the allyl and carbonyl ligands, keeping the inequivalency of the two allyl halves.

All the complexes exhibit a common feature: the planarity of the pyridine ring is extended to the imine system but

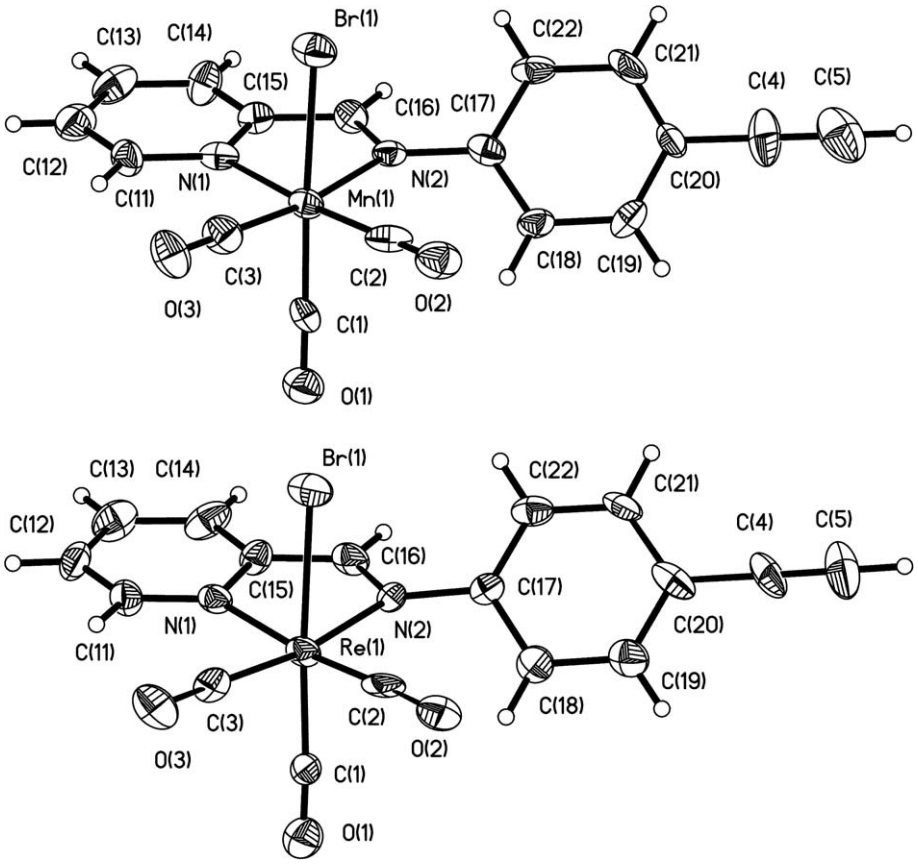

Fig. 2. ORTEP plot (30% ellipsoid probability) of compounds **1b** and **2b** showing the atom numbering.

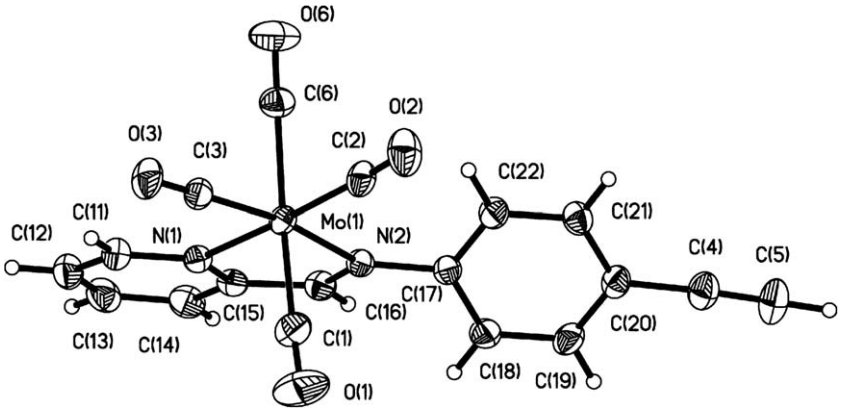

Fig. 3. ORTEP plot (30% ellipsoid probability) of compound **3b** showing the atom numbering.

this planarity does not extend to the phenyl ring which is rotated significantly with respect to the iminopyridine plane, the dihedral angles ranging from 35.7° (for **4b**) to 50.5° (for **1a**) as summarized in Table 4. The torsion is a common feature of the phenyliminopyridine ligands, and appears to correlate well with the steric hindrance around the metal [7], although electronic factors can not be ruled out. The results of DFT calculations led Heinze to conclude that the orientation of the phenyl ring is an intrinsic property of the molecules, not influenced by packing forces or hydrogen bonding [7a].

As a preliminary exploration of the alkynyl group reactivity, compounds **1a** and **2a** were made to react with dicobalt octacarbonyl in dichloromethane to afford the tetrahedrane complexes **5** and **6** which were isolated in good yield in crystalline form (Scheme 2). The presence of five bands in the ν_{CO} region of their IR spectra in THF (ν(CO) for **5**: 2096m, 2059s, 2031vs, 1947s, 1926s, cm^{-1}; ν(CO) for **6**: 2096m, 2059s, 2028vs, 1931s, 1906s, cm^{-1}) clearly pointed to their polynuclear nature. All the bands can be assigned by comparison with those of the starting compounds and related tetrahedranes. Six ν(CO)

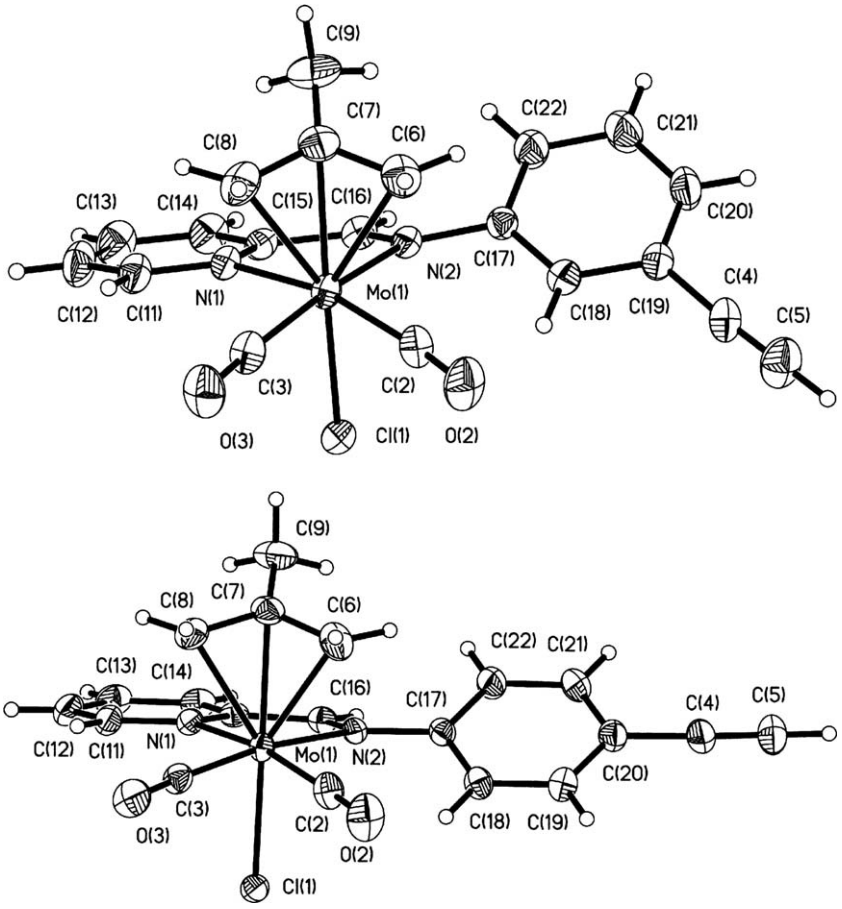

Fig. 4. ORTEP plot (30% ellipsoid probability) of compounds **4a** and **4b** showing the atom numbering.

Table 2
Selected distances (Å) and angles (°) for ethynyliminopyridine compounds

	1a (X = Br, M = Mn)	**2a** (X = Br, M = Re)	**1b** (X = Br, M = Mn)	**2b** (X = Br, M = Re)	**3b**, (X = CO, M = Mo)	**4a** (X = Cl, M = Mo)	**4b** (X = Cl, M = Mo)
M–X	2.531(2)	2.620(2)	2.502(2)	2.598(2)	2.048(3)	2.502(2)	2.502(1)
M–N(1)	2.062(5)	2.188(6)	2.030(8)	2.14(1)	2.247(2)	2.235(3)	2.234(2)
M–N(2)	2.070(4)	2.186(6)	2.032(7)	2.17(1)	2.284(2)	2.272(3)	2.286(2)
M–C(1)	1.860(7)	2.00(1)	1.809(9)	1.90(2)	2.023(3)	–	–
M–C(2)	1.834(7)	1.917(9)	1.78(1)	1.78(2)	1.966(3)	1.967(5)	1.966(3)
M–C(3)	1.807(6)	1.92(1)	1.78(1)	1.91(2)	1.948(3)	1.956(5)	1.952(3)
C(4)–C(5)	1.123(8)	1.10(1)	1.15(2)	1.10(2)	1.168(4)	1.111(7)	1.167(5)
N(1)–M–N(2)	78.5(2)	74.5(2)	77.9(4)	75.3(4)	72.48(7)	73.1(1)	73.11(8)

bands can be observed for $[Co_2(CO)_6(PhC{\equiv}CH)]$ at 2095w, 2058s, 2032s, 2028(sh), 2016w, and 2001(sh) cm^{-1} [23]. The two at lower frequencies are very weak and often can not be observed in other tetrahedranes [24]. In the case of **5**, the two bands at upper frequencies (2095m and 2059s, cm^{-1}) can be assigned to ν(CO) vibrations of the dicobalt hexacarbonyl moiety, only slightly shifted from those of the phenylacetylene analogue. Consistently with this assignment, the position of these two upper bands do not change in the rhenium complex **6**. The strongest band of **5**, at 2031 cm^{-1}, can be considered to be the envelope of the highest band of $Mn(CO)_3$, overlapped with the two bands of the $\{Co_2(CO)_6\}$ unit. The corresponding band appears at 2028 cm^{-1} for the Re complex **6**. The bands of compound **5** at 1947s and 1926s cm^{-1} clearly correspond to the lower ν(CO) vibrations of $Mn(CO)_3$ shifted to 1931s and 1906s cm^{-1} for the rhenium complex **6**. It is worth to notice that while the bands of $Co_2(CO)_6$ do not change significantly from those of $[Co_2(CO)_6(PhC{\equiv}CH)]$, the bands attributable to $Mn(CO)_3$ and $Re(CO)_3$ fragments are shifted to higher frequencies from those of the parent compounds **1a** and **2a**.

The most salient feature of the ^1H NMR spectra of **5** and **6** is the significant shift of the signal corresponding to the acetylenic proton, from ca δ 3.8 ppm in the starting **1a** and **2a** to about δ 6.9 ppm in **5** and **6**. This well precedented

Table 3
Carbonyl stretching frequencies (cm^{-1}, THF solution)[a] for complexes **1a**–**b**, **2a**–**b**, **3a**–**b** and **4a**–**b**, and their analogues with bipy and phen

	ν_1(s)	ν_2(s)	ν_3(s)
(N–N) in [Mn(CO)$_3$Br(N–N)]			
(pyCH=NC$_6$H$_4$-*m*-C≡CH) (**1a**)	2026	1944	1919
(pyCH=NC$_6$H$_4$-*p*-C≡CH) (**1b**)	2026	1944	1919
(pyCH=NC$_6$H$_4$-*p*-CH$_3$)	2026	1942	1917
bipy	2023	1935	1915
phen	2024	1936	1915
(N–N) in [Re(CO)$_3$Br(N–N)]			
(pyCH=NC$_6$H$_4$-*m*-C≡CH) (**2a**)	2024	1927	1901
(pyCH=NC$_6$H$_4$-*p*-C≡CH) (**2b**)	2024	1927	1900
(pyCH=NC$_6$H$_4$-*p*-CH$_3$)	2023	1925	1899
bipy	2020	1920	1896
phen	2021	1920	1897

	ν_1(m)	ν_2(s)	ν_3(m,sh)	ν_4(m)
(N–N) in [Mo (CO)$_4$(N–N)]				
(pyCH=NC$_6$H$_4$-*m*-C≡CH) (**3a**)	2013	1906	1892	1851
(pyCH=NC$_6$H$_4$-*p*-C≡CH) (**3b**)	2013	1905	1892	1851
bipy	2013	1901	1883	1842
phen	2012	1901	1884	1842

	ν_1(s)	ν_2(s)
(N–N) in MoCl(methallyl)(CO)$_2$(N–N)]		
(pyCH=NC$_6$H$_4$-*m*-C≡CH) (**4a**)	1952	1877
(pyCH=NC$_6$H$_4$-*p*-C≡CH) (**4b**)	1953	1877
bipy	1950	1871
phen	1950	1872

[a] For a more accurate comparison, the spectra of the complexes with bipy and phen have been taken in the same solvent and measured with the same instrument.

Table 4
Dihedral angles between the planes of the iminopyridine system and the phenyl ring

Compound	Angle (°)
1a	50.5 (2)
2a	49.3(2)
1b	47.8(3)
2b	43.4(4)
3b	38.84(8)
4a	43.4(1)
4b	35.7(1)
5	60.7(1)

[25] effect of the change from a linear sp hybridisation of the acetylenic carbon in the starting complexes to a near-tetrahedral sp^3 in **5** and **6** is in good agreement with the geometry of the molecule in solid state. An X-ray determination was carried out on a crystal of **5**, and the results are presented in Fig. 5 and Table 5. The coordination of the acetylene to the $Co_2(CO)_6$ fragment causes the expected elongation of the C(4)–C(5) distance from 1.123(8) Å in **1a** to 1.344(5) Å in **5**, and the loss of linearity of the C(Ph)–C(4)–C(5) sequence from 176.9° in **1a** to 141.4(3)° in **5**. This features are consistent with the C(4)–C(5) fragment acting as a 4e donor towards the cobalt atoms. A comparison between the geometric parameters of **1a** and **5** shows no significant change of the geometry around manganese. In contrast the torsion of the phenyl ring with respect to the plane of the iminopyridine increases from 50.5(2)° in **1a** to 60.7° in **5** (see Table 4). As discussed above, this could be attributed to the steric bulk of the $Co_2(CO)_6$ moiety.

In conclusion, we have developed a facile "one-pot" method for the preparation of a variety of complexes of Mn(I), Re(I), Mo(0) and Mo(II), with phenyliminopyridine ligands bearing an ethynyl function at *meta*- or *para*-position. The structural determinations show little variations of the geometry of the metal-iminopyridine core which can be ascribed to the different size of the metals. The ethynyl functionality can be used for further reactivity, as illustrated by its reaction with octacarbonyl dicobalt, to afford tetrahedrane clusters.

3. Experimental

3.1. Materials and general methods

All operations were performed under an atmosphere of dry dinitrogen using Schlenk and vacuum techniques. Details of the instrumentation and experimental procedures have been given elsewhere [26]. IR spectra in solution were recorded with a Perkin Elmer Spectrum RX I FT-IR instrument, using cells with CaF_2 windows. Literature procedures for the preparation of starting materials are quoted in each case. Ligands and other reagents were purchased and used without purification unless otherwise stated.

3.2. [MnBr(CO)$_3${py-2-CH=N-C$_6$H$_4$-*m*-(C≡CH)}] (**1a**)

[Mn(CO)$_5$Br] (0.1 g, 0.364 mmol), 2-pyridinecarboxaldehyde (0.039 g, 0.364 mmol) and 3-ethynylaniline (0.043 g, 0.364 mmol) were refluxed in THF (25 mL) for 3 h. The solvent was evaporated in vacuo, and the residue was taken up in CH_2Cl_2 and filtered through silica gel. The red band was collected and the solvent was evaporated in vacuo to obtain compound **1a** as a red, microcrystalline solid. Yield 0.130 g, 84%. Anal. Calc. for $C_{17}H_{10}BrMnN_2O_3$: C 48.03, H 2.37, N 6.59. Found: C 48.18, H 2.44, N 6.79. ^{1}H NMR (acetone-d_6): $\delta = 9.33$ [d(5), 1H, H^6 py], 8.92 (s, 1H, –C*H*=N–), 8.30 (m, 2H, $H^{3,4}$ py), 7.85 (m, 1H, H^5 py), 7.74 (s, 1H, H^2 Ph), 7.72 (m, 1H, H^4 Ph), 7.59 (m, 2H, $H^{5,6}$ Ph), 3.81 (s, 1H, –C≡C*H*).

3.3. [MnBr(CO)$_3${py-2-CH=N-C$_6$H$_4$-*p*-(C≡CH)}] (**1b**)

Compound **1b** was prepared as described above for compound **1a**, starting from [Mn(CO)$_5$Br] (0.275 g, 1 mmol), 2-pyridinecarboxaldehyde (0.107 g, 1 mmol) and 4-ethynylaniline (0.117 g, 1 mmol). The workup was as described for **1a** to afford compound **1b**. Yield 0.361 g, 84.9%. Anal. Calc. for $C_{17}H_{10}BrMnN_2O_3$: C 48.03, H 2.37, N 6.59. Found: C 48.12, H 2.42, N 6.70. ^{1}H NMR (acetone-d_6): $\delta = 9.32$ [d(5), 1H, H^6 py], 8.90 (s, 1H, –C*H*=N–), 8.30 (m, 2H, $H^{3,4}$ py), 7.84 (m, 1H, H^5 py), 7.68 (m, 4H, $H^{2,3,5,6}$ Ph), 3.80 (s, 1H, –C≡C*H*).

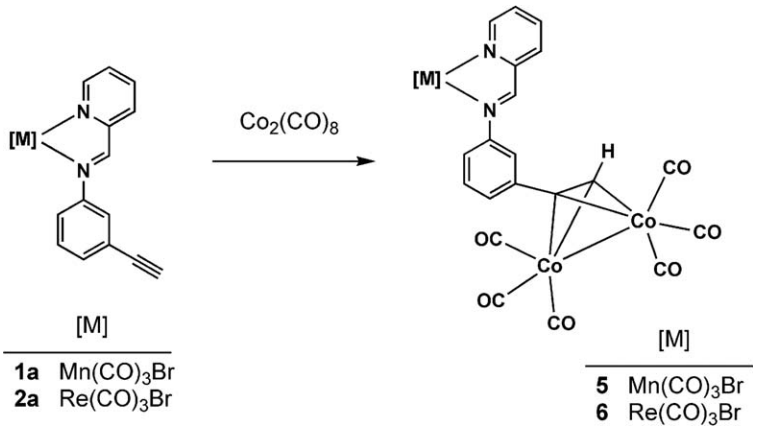

Scheme 2.

3.4. [ReBr(CO)$_3${py-2-CH=N-C$_6$H$_4$-m-(C≡CH)}] (**2a**)

[Re(CO)$_5$Br] (0.1 g, 0.246 mmol), 2-pyridinecarboxaldehyde (0.026 g, 0.246 mmol) and 3-ethynylaniline (0.029 g, 0.246 mmol) were refluxed in THF (25 mL) for 9 h. The workup was as described for **1a** to afford compound **2a**. Yield 0.109 g, 79.6%. Anal. Calc. for $C_{17}H_{10}BrReN_2O_3$: C 36.70, H 1.81, N 5.03. Found: C 36.85, H 1.89, N 5.03. ^{1}H NMR (acetone-d_6): $\delta = 9.34$ (s, 1H, –C*H*=N–), 9.19 [d(6), 1H, H^6 py], 8.45 [d(8), 1H, H^3 py], 8.39 [*pseudo*-t(8), 1H, H^4 py], 7.90 (m, 1H, H^5 py), 7.75 (s, 1H, H^2 Ph), 7.70 (m, 1H, H^4 Ph), 7.60 (m, 2H, $H^{5,6}$ Ph), 3.82 (s, 1H, –C≡C*H*).

3.5. [ReBr(CO)$_3${py-2-CH=N-C$_6$H$_4$-p-(C≡CH)}] (**2b**)

Compound **2b** was prepared as described above for compound **2a**, starting from [Re(CO)$_5$Br] (0.1 g, 0.246 mmol), 2-pyridinecarboxaldehyde (0.026 g, 0.246 mmol) and 4-ethynylaniline (0.029 g, 0.246 mmol). The workup was as described for **1a** to afford compound **2b**. Yield 0.115 g,

Table 5
Selected bond lengths (Å) and angles (°) for compound **5**

Mn(1)–Br(1)	2.5146(14)
Mn(1)–N(1)	2.071(3)
Mn(1)–N(2)	2.054(3)
Mn(1)–C(1)	1.828(5)
Mn(1)–C(2)	1.818(5)
Mn(1)–C(3)	1.808(4)
Co(1)–Co(2)	2.4851(13)
Co(1)–C(4)	1.987(4)
Co(1)–C(5)	1.949(4)
Co(2)–C(4)	1.971(4)
Co(2)–C(5)	1.975(4)
C(4)–C(5)	1.344(5)
N(1)–Mn(1)–N(2)	78.23(11)
C(1)–Mn(1)–Br(1)	178.88(12)
C(2)–Mn(1)–N(1)	174.11(15)
C(3)–Mn(1)–N(2)	173.11(14)
C(5)–Co(1)–Co(2)	51.17(11)
C(4)–Co(1)–Co(2)	50.81(10)
C(4)–Co(1)–C(5)	39.92(14)
C(4)–Co(2)–C(5)	39.84(14)
C(5)–Co(2)–Co(1)	50.24(11)
C(18)–C(4)–C(5)	141.4(3)

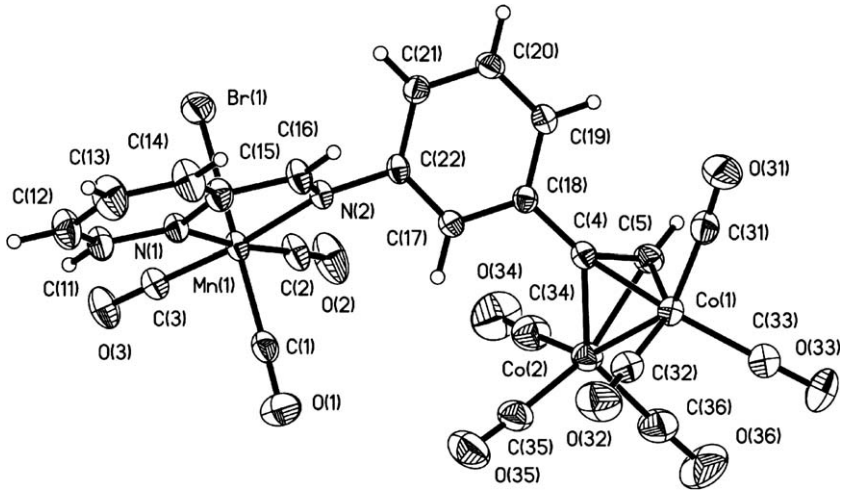

Fig. 5. ORTEP plot (30% ellipsoid probability) of compound **5** showing the atom numbering.

84%. Anal. Calc. for $C_{17}H_{10}BrReN_2O_3$: C 36.70, H 1.81, N 5.03. Found: C 36.80, H 1.87, N 5.08. ^{1}H NMR (acetone-d_6): $\delta = 9.33$ (s, 1H, –C*H*=N–), 9.18 [d(6), 1H, H^6 py], 8.46 [d(8), 1H, H^3 py], 8.39 [*pseudo*-t(8), 1H, H^4 py], 7.90 (m, 1H, H^5 py), 7.72–7.65 (m, 4H, $H^{2,3,5,6}$ Ph), 3.83 (s, 1H, –C≡C*H*).

3.6. [Mo(CO)$_4${py-2-CH=N-C$_6$H$_4$-m-(C≡CH)}] (3a)

[Mo(CO)$_4$(pip)$_2$] [27] (0.1 g, 0.264 mmol), 2-pyridinecarboxaldehyde (0.028 g, 0.264 mmol) and 3-ethynylaniline (0.031 g, 0.264 mmol) were made to react in THF (25 mL) for 2 h. The solvent was evaporated in vacuo, and the residue was taken up in CH_2Cl_2 and filtered through silica gel. The purple band was collected and the solvent was evaporated in vacuo to obtain compound **3a** as a dark purple, microcrystalline solid. Yield 0.071 g, 64.9%. Anal. Calc. for $C_{18}H_{10}MoN_2O_4$: C 52.19, H 2.43, N 6.76. Found: C 52.37, H 2.53, N 6.87. ^{1}H NMR (acetone-d_6): $\delta = 9.17$ [d(5), 1H, H^6 py], 9.01 (s, 1H, –C*H*=N–), 8.30 [d(7), 1H, H^3 py], 8.23 [*pseudo*-t(8), 1H, H^4 py], 7.78–7.67 (m, 3H, H^5 py and $H^{2,4}$ Ph), 7.56 (m, 2H, $H^{5,6}$ Ph), 3.80 (s, 1H, –C≡C*H*).

3.7. [Mo(CO)$_4${py-2-CH=N-C$_6$H$_4$-p-(C≡CH)}] (3b)

Compound **3b** was prepared as described above for compound **3a**, starting from [Mo(CO)$_4$(pip)$_2$] (0.1 g, 0.264 mmol), 2-pyridinecarboxaldehyde (0.028 g, 0.264 mmol) and 4-ethynylaniline (0.031 g, 0.264 mmol). The workup was as described for **3a** to afford compound **3b**. Yield 0.080 g, 73.2%. Anal. Calc. for $C_{18}H_{10}MoN_2O_4$: C 52.19, H 2.43, N 6.76. Found: C 52.34, H 2.50, N 6.84. ^{1}H NMR (acetone-d_6): $\delta = 9.18$ [d(5), 1H, H^6 py], 9.00 (s, 1H, –C*H*=N–), 8.29 [d(7), 1H, H^3 py], 8.23 [*pseudo*-t(7), 1H, H^4 py], 7.75 (m, 1H, H^5 py), 7.66 (m, 4H, $H^{2,3,5,6}$ Ph), 3.79 (s, 1H, –C≡C*H*).

3.8. [MoCl(η^3-C$_3$H$_4$Me-2)(CO)$_2${py-2-CH=N-C$_6$H$_4$-m-(C≡CH)}] (4a)

[MoCl(η^3-C$_3$H$_4$Me-2)(CO)$_2$(NCMe)$_2$] [28] (0.1 g, 0.308 mmol), 2-pyridinecarboxaldehyde (0.033 g, 0.308 mmol) and 3-ethynylaniline (0.036 g, 0.308 mmol) were made to react in THF (25 mL) for 15 min. The solvent was evaporated in vacuo, and the residue was washed with hexane (3 × 10 mL). The resulting solid residue was dissolved in CH_2Cl_2 and filtered through kieselguhr. Addition of hexane and slow evaporation at reduced pressure gave compound **4a** as dark blue microcrystals. Yield: 0.114 g, 82.5%. Anal. Calc. for $C_{20}H_{17}ClMoN_2O_2$: C 53.53, H 3.81, N 6.24. Found: C 53.70, H 3.90, N 6.34. ^{1}H NMR (acetone-d_6): $\delta = 8.89$ (m, 2H, H^6 py and –C*H*=N–), 8.24 (m, 2H, $H^{3,4}$ py), 7.74 (m, 3H, H^5 py and $H^{2,4}$ Ph), 7.55 (m, 2H, $H^{5,6}$ Ph), 3.80 (s, 1H, –C≡C*H*), 2.90 [d(4), 1H, H_{syn} allyl], 2.26 [d(4), 1H, H_{syn} allyl], 1.41 (s, 3H, –CH_3), 1.27 (s, 1H, H_{anti} allyl), 1.05 (s, 1H, H_{anti} allyl).

3.9. [MoCl(η^3-C$_3$H$_4$Me-2)(CO)$_2${py-2-CH=N-C$_6$H$_4$-p-(C≡CH)}] (4b)

Compound **4b** was prepared as described above for compound **4a**, starting from [MoCl(η^3-C$_3$H$_4$Me-2)-(CO)$_2$(NCMe)$_2$] (0.1 g, 0.308 mmol), 2-pyridinecarboxaldehyde (0.033 g, 0.308 mmol) and 4-ethynylaniline (0.036 g, 0.308 mmol). The workup was as described for **4a** to afford compound **4b**. Yield: 0.120 g, 86.8%. Anal. Calc. for $C_{20}H_{17}ClMoN_2O_2$: C 53.53, H 3.81, N 6.24. Found: C 53.71, H 3.90, N 6.30. ^{1}H NMR (acetone-d_6): $\delta = 8.88$ (m, 2H, H^6 py and –C*H*=N–), 8.23 (m, 2H, $H^{3,4}$ py), 7.76 (m, 1H, H^5 py), 7.65 (m, 4H, $H^{2,3,5,6}$ Ph), 3.82 (s, 1H, –C≡C*H*), 2.89 [d(3), 1H, H_{syn} allyl], 2.23 [d(3), 1H, H_{syn} allyl], 1.39 (s, 3H, –CH_3), 1.26 (s, 1H, H_{anti} allyl), 1.04 (s, 1H, H_{anti} allyl).

3.10. [MnBr(CO)$_3${py-2-CH=N-C$_6$H$_4$-m-{(μ-C≡CH)Co$_2$(CO)$_6$}}] (5)

To a solution of compound **1a** (0.155 g, 0.364 mmol) in CH_2Cl_2 (25 mL) was added $Co_2(CO)_8$ (0.124 g, 0.364 mmol), and the mixture was stirred for 30 min. The solvent was evaporated in vacuo, and the residue was washed with hexane (3 × 10 mL). The residue was taken up in toluene and filtered through kieselguhr. Addition of hexane and slow evaporation at reduced pressure gave compound **5** as red microcrystals. Yield: 0.246 g, 95%. Anal. Calc. for $C_{23}H_{10}BrMnCo_2N_2O_9$: C 38.85, H 1.42, N 3.94. Found: C 39.01, H 1.46, N 3.99. IR (THF), ν(CO): 2096m, 2059s, 2031vs, 1947s, 1926s, cm^{-1}. ^{1}H NMR (acetone-d_6): $\delta = 9.31$ (m, 1H, H^6 py), 8.93 (s, 1H, –C*H*=N–), 8.31 (m, 2H, $H^{3,4}$ py), 8.00 (s, 1H, H^2 Ph), 7.84 (m, 1H, H^5 py), 7.70 (m, 1H, H^4 Ph), 7.54 (m, 2H, $H^{5,6}$ Ph), 6.92 (s, 1H, μ-C-C*H*).

3.11. [ReBr(CO)$_3${py-2-CH=N-C$_6$H$_4$-m-{(μ-C≡CH)Co$_2$(CO)$_6$}}] (6)

Compound **6** was prepared as described above for compound **5**, from a solution of **2a** (0.137 g, 0.246 mmol) and $Co_2(CO)_8$ (0.084 g, 0.246 mmol). The workup was as described for **5** to afford compound **6**. Yield: 0.200 g, 96.5%. Anal. Calc. for $C_{23}H_{10}BrReCo_2N_2O_9$: C 32.80, H 1.20, N 3.33. Found: C 32.91, H 1.25, N 3.39. IR (THF), ν(CO): 2096m, 2059s, 2028vs, 1931s, 1906s, cm^{-1}. ^{1}H NMR (acetone-d_6): $\delta = 9.35$ (s, 1H, –C*H*=N–), 9.19 [d(5), 1H, H^6 py], 8.44 [d(7), 1H, H^3 py], 8.38 [*pseudo*-t(7), 1H, H^4 py], 8.00 (s, 1H, H^2 Ph), 7.89 (m, 1H, H^5 py), 7.73 [d(8), 1H, H^4 Ph], 7.56 (m, 2H, $H^{5,6}$ Ph), 6.91 (s, 1H, μ-C-C*H*).

3.12. X-ray crystallography

Crystals suitable for diffraction studies were grown by slow diffusion of hexane into dichloromethane solutions (for **1a**, **1b**, **2a**, **2b**, **3b**, **4a** and **4b**) or toluene (for **5**) at

−20 °C. Data were collected on a Bruker Smart 1000 CCD diffractometer (graphite-monochromatized Mo Kα radiation, $\lambda = 0.71073$ Å). Crystallographic data and experimental details for the structures are summarized in Table 1. Raw frame data were integrated with SAINT [29]. A semi-empirical absorption correction was applied with SADABS [30]. The structures were solved by direct methods with SIR 2002 [31] under WINGX [32] and refined against F^2 with SHELXTL [33]. All non-hydrogen atoms were refined anisotropically. Hydrogen atoms were set in calculated positions and refined as riding atoms, with a common thermal parameter. Graphics were made with SHELXTL. Additional calculations were made with PARST [34].

Acknowledgements

We thank MCYT (BQU2002-03414), JCyL (VA052/03, VA012C05) for financial support, and Universidad de Valladolid for a grant (to J.A.T).

Appendix A. Supplementary material

Crystallographic data have been deposited with the Cambridge Crystallographic Data Centre, CCDC nos. 292598 (compound **1a**), 292599 (**1b**), 292600 (**2a**), 292601 (**2b**), 292602 (**3b**), 292603 (**4a**), 292604 (**4b**) and 292605 (**5**). Copies of the data may be obtained free of charge from The Director, CCDC, 12 Union Road, Cambridge CB2 1EZ, UK (fax: +44 1223 336033; e-mail: deposit@ccdc.cam.ac.uk or www: http://www.ccdc.cam.ac.uk). Supplementary data associated with this article can be found, in the online version, at doi:10.1016/j.jorganchem.2006.04.024.

References

[1] A. Vlcek Jr, Coord. Chem. Rev. 230 (2002) 225.
[2] C. Kaes, A. Katz, M.W. Hosseini, Chem. Rev. 100 (2000) 3553.
[3] (a) G. Van Koten, K. Vrieze, Adv. Organomet. Chem. 21 (1982) 151;
(b) N. Feiken, P. Schreuder, R. Siebenlist, H.W. Frühauf, K. Vrieze, H. Kooijman, N. Veldman, A.L. Spek, J. Fraanje, K. Goubitz, Organometallics 15 (1996) 2148.
[4] N. Bréfuel, C. Lepetit, S. Shova, F. Dahan, J.P. Tuchagues, Inorg. Chem. 44 (2005) 8916.
[5] (a) K. Heinze, J.D.B. Toro, Angew. Chem. Int. Ed. 42 (2003) 4533;
(b) K. Heinze, V. Jacob, Eur. J. Inorg. Chem. (2003) 3918;
(c) K. Heinze, J.D.B. Toro, Eur. J. Inorg. Chem. (2003) 3498;
(d) P.J. Ball, T. Rarog Shtoyko, J.A. Krause Bauer, W.J. Oldham, W.B. Connick, Inorg. Chem. 43 (2004) 622.
[6] (a) R.S. Herrick, K.L. Houde, J.S. McDowell, L.P. Kizeck, G. Bonavia, J. Organomet. Chem. 589 (1999) 29;
(b) R.S. Herrick, C.J. Ziegler, H. Bohan, M. Corey, M. Eskander, J. Giguere, N. McMicken, I. Wrona, J. Organomet. Chem. 687 (2003) 178.
[7] (a) K. Heinze, J. Chem. Soc., Dalton Trans. (2002) 540;
(b) K. Heinze, V. Jacob, J. Chem. Soc., Dalton Trans. (2002) 2379.
[8] K. Heinze, J.D.B. Toro, Eur. J. Inorg. Chem. (2004) 3498.
[9] R.S. Herrick, I. Wrona, N. McMicken, G. Jones, C.J. Ziegler, J. Shaw, J. Organomet. Chem. 689 (2004) 4848.
[10] H. Daubric, C. Cantin, C. Thomas, J. Kliava, J.-F. Létard, O. Kahn, Chem. Phys. 244 (1999) 75.
[11] J.-B. Gaudry, L. Capes, P. Langot, S. Marcén, M. Kollmannsberger, O. Lavastre, E. Freysz, J.-F. Létard, O. Kahn, Chem. Phys. Lett. 324 (2000) 321.
[12] R.N. Dominey, B. Hauser, J. Hubbard, J. Dunham, Inorg. Chem. 30 (1991) 4754.
[13] F. Morale, R.W. Date, D. Guillon, D.W. Bruce, R.L. Finn, C. Wilson, A.J. Blake, M. Schröder, B. Donnio, Chem. Eur. J. 9 (2003) 2484.
[14] (a) L. Cuesta, D.C. Gerbino, E. Hevia, D. Morales, M.E. Navarro Clemente, J. Pérez, L. Riera, V. Riera, D. Miguel, I. del Río, S. García-Granda, Chem. Eur. J. 10 (2004) 1765;
(b) D. Morales, J. Pérez, L. Riera, V. Riera, D. Miguel, M.E.G. Mosquera, S. García-Granda, Chem. Eur. J. 9 (2003) 4132;
(c) E. Hevia, J. Pérez, V. Riera, D. Miguel, P. Campomanes, M.I. Menéndez, T.L. Sordo, S. García-Granda, J. Am. Chem. Soc. 125 (2003) 3706.
[15] R. García-Rodríguez, D. Miguel, Dalton Trans. (2006) 1218.
[16] A *mer*-disposition would place two carbonyls mutually trans to each other, thus competing for the back-donation from the metal. In fact complexes *mer*-[MnBr(CO)$_3$(diimine)] are thermally unstable, and have been observed only as intermediates in photoreactions of the fac-isomers: G.J. Stor, S.L. Morrison, D.J. Stufkens, A. Oskam, Organometallics 13 (1994) 2641.
[17] A.G. Orpen, L. Brammer, F.H. Allen, O. Kennard, D.G. Watson, R. Taylor, J. Chem. Soc., Dalton Trans. (1989) S1.
[18] M.C. Ball, A.H. Norbury, Physical Data for Inorganic Chemists, Longman, London, 1974, pp. 139–144.
[19] P.S. Braterman, Metal Carbonyl Spectra, Academic Press, New York, 1975.
[20] (a) MnBr(CO)$_3$(bipy) or (phen): E.W. Abel, G.J. Wilkinson, J. Chem. Soc. (1959) 1501;
(b) , ReBr(CO)$_3$(bipy) or (phen)L.H. Staal, A. Oskam, K. Vrieze, J. Organomet. Chem. 170 (1979) 235;
(c) , Mo(CO)$_4$(bipy) or (phen)M.B.H. Stiddard, J. Chem. Soc. (1962) 4713;
(d) , MoCl(CO)$_2$(methallyl)(bipy) or (phen)P. Powell, J. Organomet. Chem. 129 (1977) 175.
[21] M.D. Curtis, O. Eisenstein, Organometallics 3 (1984) 887.
[22] J.W. Faller, D.A. Haitko, R.D. Adams, D.F. Chodosh, J. Am. Chem. Soc. 101 (1979) 865.
[23] (a) C.M. Gordon, M. Kiszka, I.R. Dunkin, W.J. Kerr, J.S. Scott, J. Gebicki, J. Organomet. Chem. 554 (1998) 147;
(b) G. Bor, S.F.A. Kettle, P.L. Stanghellini, Inorg. Chim. Acta 18 (1976) L18.
[24] G. Várady, I. Vecsei, A. Vizi-Orosz, G. Pályi, A.G. Massey, J. Organomet. Chem. 114 (1976) 213.
[25] (a) M. Akita, M. Terada, Y. Moro Oka, Organometallics 11 (1992) 1825;
(b) M. Akita, M. Terada, M. Tanaka, Y. Moro Oka, Organometallics 11 (1992) 3468;
(c) J. Pérez, L. Riera, V. Riera, S. García-Granda, E. García-Rodríguez, D.G. Churchill, M.R. Churchill, T.S. Janik, Inorg.Chim. Acta 347 (2003) 189.
[26] G. Barrado, M.M. Hricko, D. Miguel, V. Riera, H. Wally, S. García-Granda, Organometallics 17 (1998) 820.
[27] D.J. Darensbourg, R.L. Kump, Inorg. Chem. 17 (1978) 2680.
[28] D.C. Clark, D.L. Jones, R.J. Mawby, J. Chem. Soc., Dalton Trans. (1980) 565.
[29] SAINT+, SAX Area Detector Integration Program. Version 6.02, Bruker, AXS, Madison, WI, 1999.
[30] G.M. Sheldrick, SADABS, Empirical Absorption Correction Program, University of Göttingen, Göttingen, Germany, 1977.
[31] M.C. Burla, M. Camalli, B. Carrozzini, G.L. Cascarano, C. Giacovazzo, G. Polidory, R. Spagna, SIR2002, A program for automatic

solution and refinement of crystal structures. A. Altomare, M.C. Burla, M. Camalli, G.L. Cascarano, C. Giacovazzo, A. Guagliardi, A.G.G. Moliterni, G. Polidori, R. Spagna, J. Appl. Crystallogr. 32 (1999) 115.
[32] L.J. Farrugia, J. Appl. Crystallogr. 32 (1999) 837.
[33] G.M. Sheldrick, SHELXTL, An Integrated System for Solving, Refining, and Displaying Crystal Structures from Diffraction Data. Version 5.1, Bruker AXS, Inc., Madison, WI, 1998.
[34] (a) M. Nardelli, Comput. Chem. 7 (1983) 95;
(b) M. Nardelli, J. Appl. Crystallogr. 28 (1995) 659.